Multi-way Relay Networks: Characterization, Performance Analysis and Transmission Scheme Design

Shama Naz Islam

May 2015

A thesis submitted for the degree of

Doctor of Philosophy

of The Australian National University

Australian National University

Research School of Engineering

College of Engineering and Computer Science

The Australian National University

Declaration

The contents of this thesis are the results of original research and have not been submitted for a higher degree to any other university or institution.

Much of the work in this thesis has been published or has been submitted for publication in journals or conference proceedings. These papers are:

Journal articles

J1. **S. N. Islam**, P. Sadeghi, and S. Durrani, ”Error Performance Analysis of Decode-and-Forward and Amplify-and-Forward Multi-way Relay Networks with Binary Phase Shift Keying Modulation,” *IET Commun.*, vol. 7, no. 15, pp. 1605-1616, Oct. 2013.

J2. **S. N. Islam**, S. Durrani, and P. Sadeghi, ”A Novel User Pairing Scheme for Functional Decode-and-Forward Multi-way Relay Network,” submitted to *Physical Communications*, Sep. 2014, http://arxiv.org/abs/1402.6422v3.

J3. **S. N. Islam**, S. Durrani, and P. Sadeghi, ”Lattice Code Based Multi-way Relay Networks: SER Analysis and the Impact of Imperfect Channel Estimation,” submitted to *Journal of Communications and Networks*, May 2015.

Conference papers

C1. **S. N. Islam**, and P. Sadeghi, ”Error Propagation in a Multi-way Relay channel,” *in Proc. IEEE ICSPCS*, pp. 1-8, Dec. 2011.

C2. **S. N. Islam**, S. Durrani, and P. Sadeghi, ”Optimum Power Allocation for Sum Rate Improvement in AF Multi-way Relay Networks,” accepted in *IEEE ICSPCS*, Dec. 2014.

The following publications are also the results from my PhD study but not included in this thesis:

J4. **S. Islam**, ”Optimal User Pairing to Improve the Sum Rate of a Pairwise AF Multi-way Relay Network,” *IEEE Wireless Commun. Lett.*, Feb. 2015.

C3. **S. N. Islam**, P. Sadeghi, and S. Durrani, ”A Novel Pairing Scheme to Reduce Error Propagation in an Amplify and Forward Multi-way Relay Network,” *in Proc. IEEE SSP*, pp. 544-547, Jun. 2014.

C4. **S. Islam**, and P. Sadeghi, ”Joint decoding: Extracting the correlation among user pairs in a multi-way relay channel,” *in Proc. IEEE PIMRC*, pp. 54-59, Sep. 2012.

C5. **S. Islam**, and P. Sadeghi, ”Joint user decoding: A technique to enhance the benefits of coding in a multi-way relay channel,” *in Proc. IEEE ICSPCS*, pp. 1-7, Dec. 2012.

The research work presented in this thesis has been performed under the supervision of Dr. Parastoo Sadeghi (The Australian National University) and Dr. Salman Durrani (The Australian National University). The substantial majority of this work is my own.

Shama Naz Islam

28 May 2015

Acknowledgments

The work presented in this thesis would not have been possible without the support of a number of individuals and organizations and they are gratefully acknowledged below:

- First of all, I would like to thank Almighty Allah for allowing me the opportunity to pursue the journey towards a PhD.

- I would like to express my sincere and very special thanks to my supervisors and friends Dr. Salman Durrani, Dr. Parastoo Sadeghi and Prof. Rodney A. Kennedy for their guidance, support and encouragement throughout my PhD studies. They have always motivated me to explore new research ideas and helped a lot whenever I face some problems in research. They also allow me to discuss about my PhD and relevant research areas in detail. Moreover, I thank them for reviewing my publication drafts with great care and for all their efforts to improve my writing skills. Also, they help me learn how to present my research in a more effective way. Apart from my research studies, they have also given me great support in obtaining teaching and supervision experiences.

- I feel lucky to have the opportunity for being in the applied signal processing (ASP) group at the Research School of Engineering. I would like to thank everyone in ASP group, for whom I always felt the research environment quite friendly and relaxing. I would also like to acknowledge the assistance of administrative staff at the college of engineering and computer science (CECS). I am especially thankful to our school administrator Ms. Lesley Goldburg.

- I would like to thank the Australian National University for providing me with the PhD scholarship and supporting my conference attendances. The opportunity of studying in one of Australia's best universities will always be a remarkable experience in my life.

- I acknowledge my home country Bangladesh, where I met some wonderful teachers who motivated me towards research.

- I thank my parents for their never-ending love and support without which I would not be able to make this journey of PhD. They have always been my inspirations whenever I encounter hardships in my PhD. Special thanks to my mother for believing that a girl has the ability to perform equally well like a boy in the field of science and engineering.

- I would like to thank my husband Adnan for his immense support and motivation which inspired me a lot throughout my PhD. Without his love and sacrifices, I would not be able to manage my PhD along with a baby. I also thank my little daughter Arisha, who was born during this PhD, for allowing me to spend my time and attention towards PhD research. She always brought back my smile whenever I was stressed with the PhD. Last but not least, I thank my in-laws for their support and encouragement.

Abstract

Multi-way relay networks (MWRNs) are a growing research area in the field of relay based wireless networks. Such networks provide a pathway for solving the ever increasing demand for higher data rate and spectral efficiency in a general multi-user scenario. MWRNs have potential applications in video conferencing, file sharing in a social network, as well as satellite networks and sensor networks. Recent research on MWRNs focuses on efficient transmission protocol design by harnessing different network coding schemes, higher dimensional structured codes and advanced relaying protocols. However, the existing research misses out the characterization and analysis of practical issues that influence the performance of MWRNs. Moreover, the existing transmission schemes suffer some significant limitations, that need to be solved for maximizing the benefits of MWRNs.

In this thesis, we investigate the practical issues that critically influence the performance of a MWRN and propose solutions that can outperform existing schemes. To be specific, we characterize error propagation phenomenon for additive white Gaussian noise (AWGN) and fading channels with functional decode and forward (FDF) and amplify and forward (AF) relaying protocols, propose a new pairing scheme that outperforms the existing schemes for lattice coded FDF MWRNs in terms of the achievable rate and error performance and finally, analyze the impact of imperfect channel state information (CSI) and optimum power allocation on MWRNs.

At first, we analyze the error performance of FDF and AF MWRNs with pairwise transmission using binary phase shift keying (BPSK) modulation in AWGN and Rayleigh fading channels. We quantify the possible error events in an L-user FDF or AF MWRN and derive accurate asymptotic bounds on the probability for the general case that a user incorrectly decodes the messages of exactly k ($k \in [1, L-1]$) other users. We show that at high signal-to-noise ratio (SNR), the higher order error events ($k \geq 3$) are

less probable in AF MWRN, but all error events are equally probable in a FDF MWRN. We derive the average BER of a user in a FDF or AF MWRN under high SNR conditions and provide simulation results to verify them.

Next, we propose a novel user pairing scheme for lattice coded FDF MWRNs. Lattice codes can achieve the capacity of AWGN channels and are used in digital communications as high-rate signal constellations. Our proposed pairing scheme selects a common user with the best average channel gain and thus, allows it to positively contribute to the overall system performance. Assuming lattice code based transmissions, we derive upper bounds on the average common rate and the average sum rate with the proposed pairing scheme. In addition, considering M-ary QAM with square constellation as a special case of lattice codes, we derive asymptotic average symbol error rate (SER) of the MWRN. We show that in terms of the achievable rates and error performance, the proposed pairing scheme outperforms the existing pairing schemes under a wide range of channel scenarios.

Finally, we investigate lattice coded FDF and AF MWRNs with imperfect CSI. Considering lattice codes of sufficiently large dimension, we obtain the bounds on the common rate and sum rate. In addition, considering M-ary quadrature amplitude modulation (QAM) with square constellations, we obtain expressions for the average SER in FDF MWRNs. For AF MWRNs, considering BPSK modulation as the simplest case of lattice codes, we obtain the average BER. Moreover, we obtain the optimum power allocation coefficients to maximize the sum rate in AF MWRN. For both FDF and AF relaying protocols, the average common rate and sum rate are decreasing functions of the estimation error. The analysis shows that the error performance of a FDF MWRN is an increasing function of both the channel estimation error and the number of users, whereas, for AF MWRN, the error performance is an increasing function of only the channel estimation error. Also, we show that to achieve the same sum rate in AF MWRN, optimum power allocation requires $7-9$ dB less power compared to equal power allocation depending upon users' channel conditions.

Notations

$\lfloor \cdot \rfloor$	Integer Floor operation
$E[\cdot]$	Expectation
$\mid \cdot \mid$	Absolute value
$\arg(\cdot)$	Argument
$\mid\mid \cdot \mid\mid$	Euclidean norm
mod	Modulo operation
$\hat{(\cdot)}$	Estimate of a random variable
$\hat{\hat{(\cdot)}}$	Estimate of an estimate of a random variable
$\min(\cdot)$	Minimum
$\log(\cdot)$	Logarithm to the base two
$\oplus$	XOR operation
$\mathrm{erfc}(\cdot)$	Complementary error function
$\mathrm{erf}(\cdot)$	Error function
$\mathrm{Q}(\cdot)$	Gaussian Q function
$(\cdot)^p$	Pilot signal
$\tilde{(\cdot)}$	Estimation error
$(\cdot)^*$	Complex conjugate

Acronyms

AF Amplify and forward

AWGN Additive white Gaussian noise

BER Bit error rate

BPSK Binary phase shift keying

CF Compress and forward

CSI Channel state information

DF Decode and forward

DNC Digital network coding

FDF Functional decode and forward

MAP Maximum a posteriori

MIMO Multiple input multiple output

ML Maximum likelihood

MMSE Minimum mean square error

MWRN Multi-way relay network

PAM Pulse amplitude modulation

PNC Physical layer network coding

QAM Quadrature amplitude modulation

SER Symbol error rate

SNR Signal-to-noise ratio

TWRN Two-way relay network

4G Fourth generation

Contents

List of Figures

List of Tables

Chapter 1

Introduction

1.1 Motivation and Background

Relay networks have recently attracted significant research interest for providing spatial diversity and extended coverage with less power consumption [1, 2]. Besides this, in the presence of poor quality direct transmission link and limited transmission range of the base station, the relay networks can outperform conventional cellular networks by employing relay nodes to exploit cooperative diversity [3]. Moreover, in densely populated urban areas, these networks can serve as a feasible solution for the very high data rate requirements of fourth generation (4G) wireless systems. This is because the conventional cellular architecture would require higher power level, as well as more densely deployed base stations to achieve the data rates required by 4G systems [4, 5].

1.1.1 Types of Relay Networks

The *classical relay channel*, first introduced by Meulen [6], is a three terminal network, where the relay contributes to the successful transmission of information from the source to the destination. The performance of this unidirectional relay channel has been investigated in many works including [4, 7–11]. The unidirectional relay channel with direct links between source and destination, which allows cooperative diversity gains to enhance the spectral efficiency and throughput, has been investigated in many works, most notably [3,12–14]. The system model for unidirectional relay channel without and with direct links has been illustrated in Fig. 1.1(a) and Fig. 1.1(b), respectively.

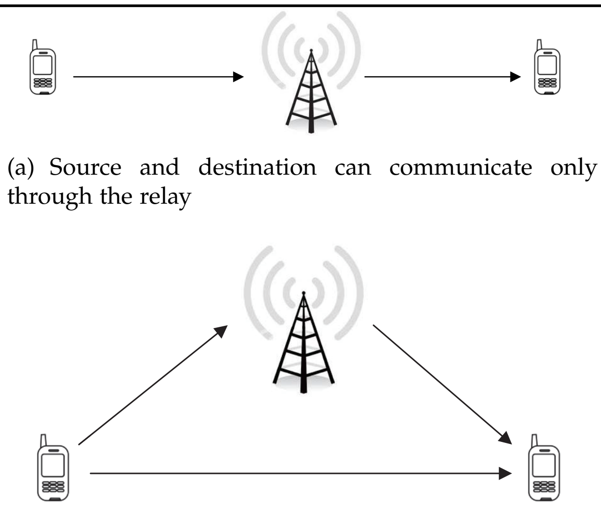

(a) Source and destination can communicate only through the relay

(b) Direct link between source and destination also exists

Figure 1.1: Unidirectional relay network.

Figure 1.2: Two-way relay network.

This unidirectional relay channel has been later extended to bidirectional or *two-way relay networks (TWRNs)* (as illustrated in Fig. 1.2) for complete exchange of information between two users [15–25].

Now-a-days, there is a growing research interest to apply the concept of relaying in scenarios involving multiple users. Thus, TWRNs can be generalized to incorporate multiple users in the form of *multi-way relay networks (MWRNs)*, in which multiple users can exchange information with the help of a single relay terminal [26–35] (as illustrated in Fig. 1.3). MWRNs have important potential applications in teleconferencing, satellite networks, data exchange in a sensor network or file sharing in a social network [36–39]. Some applications are illustrated in Figures 1.4(a) and 1.4(b).

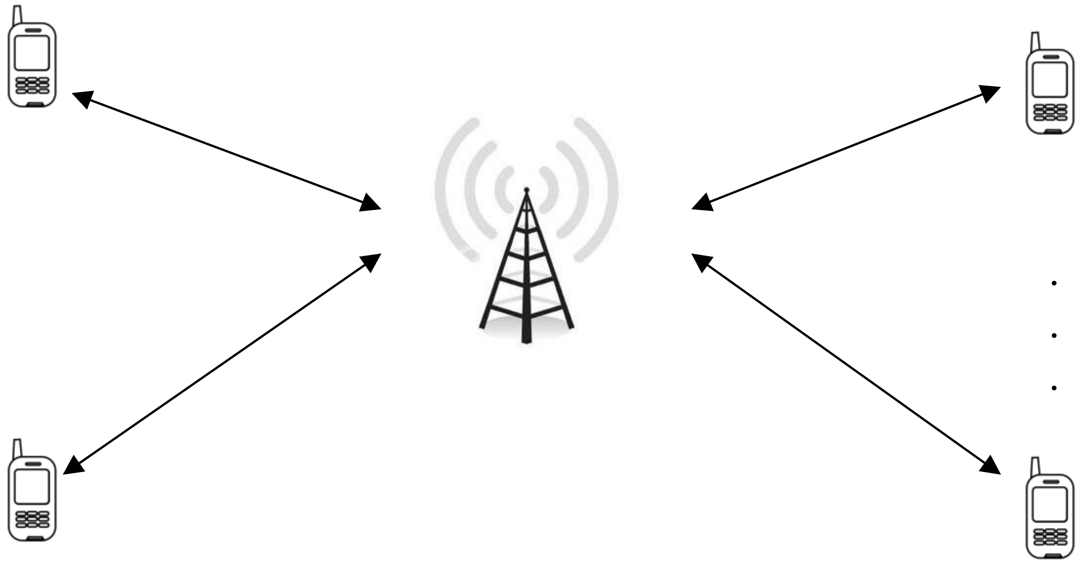

Figure 1.3: Multi-way relay network.

1.1.2 Network Coding for MWRNs

The relay networks can be designed to harness further benefits like improved energy efficiency, as well as increased throughput by means of network coding [15,40,41]. Due to the broadcast nature of wireless networks, each node in the network can overhear other nodes' transmission which are in close proximity [42]. In addition, due to superposition nature of the wireless medium, each node can receive the sum of the signals from simultaneously transmitting nodes within its range [43]. Though the broadcast and superposition nature of wireless network causes unmanaged interference leading to performance degradation, extracting the interference signals through intelligent network coding can result in higher rates [15,43]. For this reason, the application of network coding protocols like digital network coding (DNC) and physical layer network coding (PNC) in relay networks have been proposed by recent research works on cooperative relay networks.

In DNC protocol, the users transmit their messages in separate time slots and then finally, the relay broadcasts the XOR of the messages. The users perform XOR operation between their own messages and the message received from the relay to extract the other

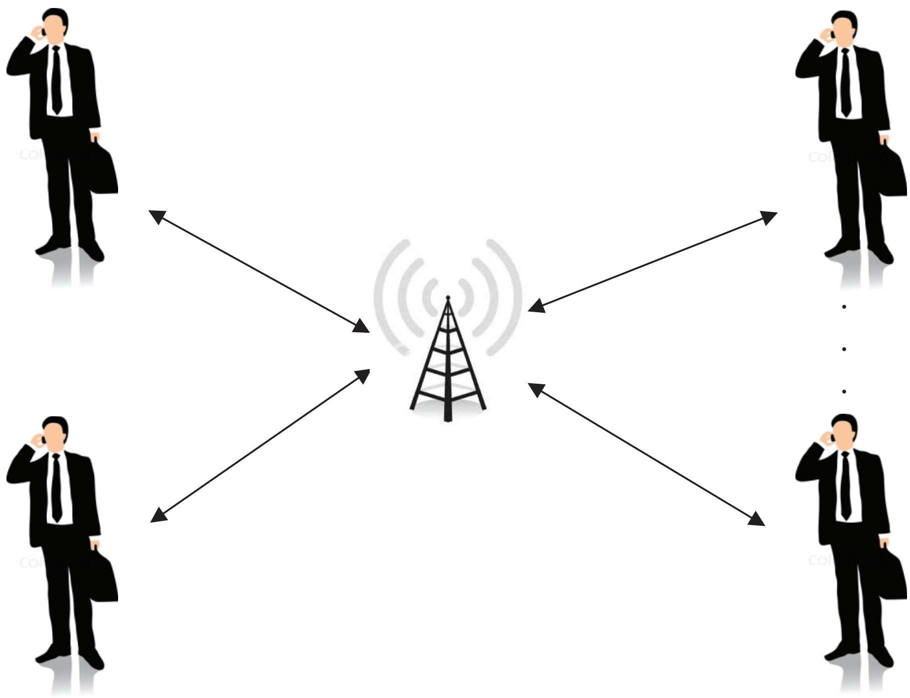

(a) Teleconferencing

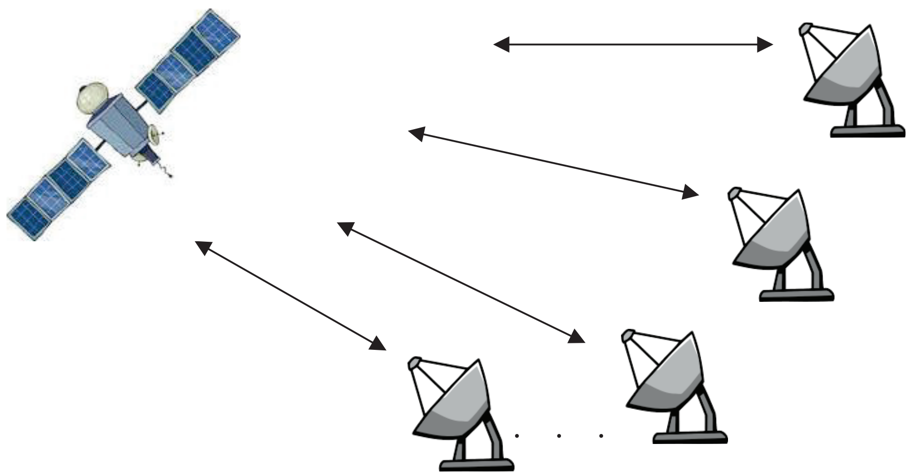

(b) Satellite Nework

Figure 1.4: Potential applications of MWRNs.

(a) user 1 transmits

(b) user 2 transmits

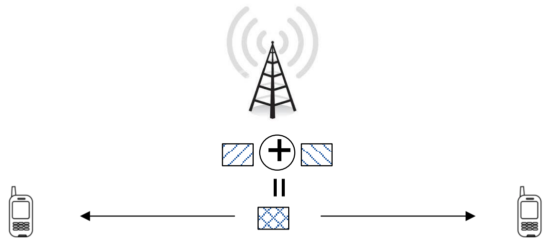

(c) relay performs XOR operation and broadcasts

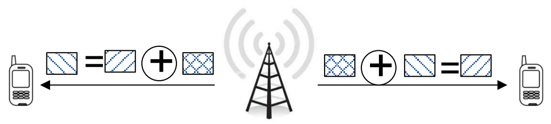

(d) users perform XOR between their own messages and the received message

Figure 1.5: Message exchange in DNC scheme, where '$\oplus$' denotes XOR operation.

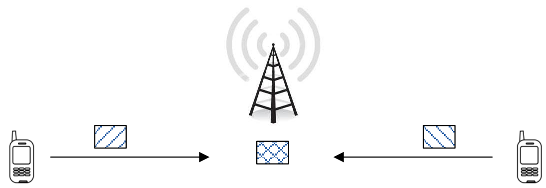

(a) the users transmit and the relay receives the sum

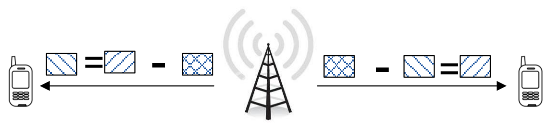

(b) the relay broadcasts the sum or a function of the sum and the users cancel self interference

Figure 1.6: Message exchange in PNC scheme, where '$-$' denotes subtraction.

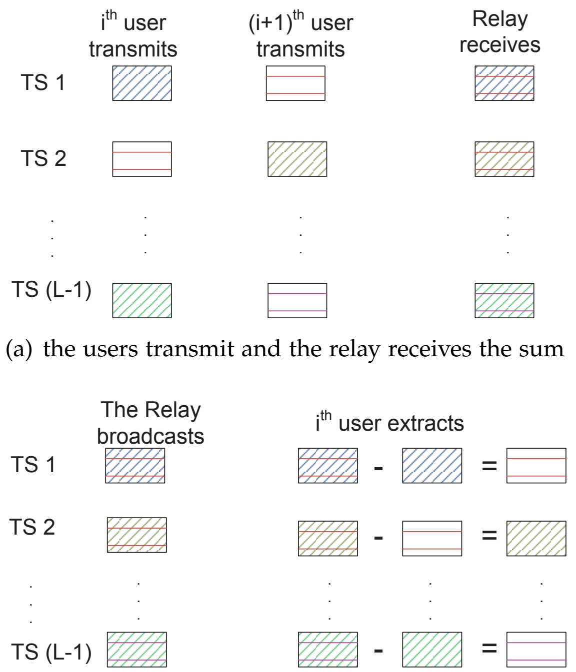

(a) the users transmit and the relay receives the sum

(b) the relay broadcasts and the users cancel self interference

Figure 1.7: Pairwise message exchange in a MWRN, where '−' denotes subtraction.

users' messages. The message exchange in DNC scheme has been illustrated in figures 1.5(a), 1.5(b), 1.5(c) and 1.5(d).

In PNC protocol, the users transmit simultaneously in the first time slot and the relay receives the sum utilizing the additive nature of physical electromagnetic waves. Then, in the next time slot, the relay broadcasts the sum or a function or combination of the signals to the users. The users then subtract self-information from the received signal and extract the messages of the other users. The message exchange in PNC scheme has been illustrated in figures 1.6(a) and 1.6(b). *Since, PNC scheme requires less time slots and achieves more throughput in a TWRN [16, 44–46], we choose to investigate PNC protocol for MWRNs in this thesis.*

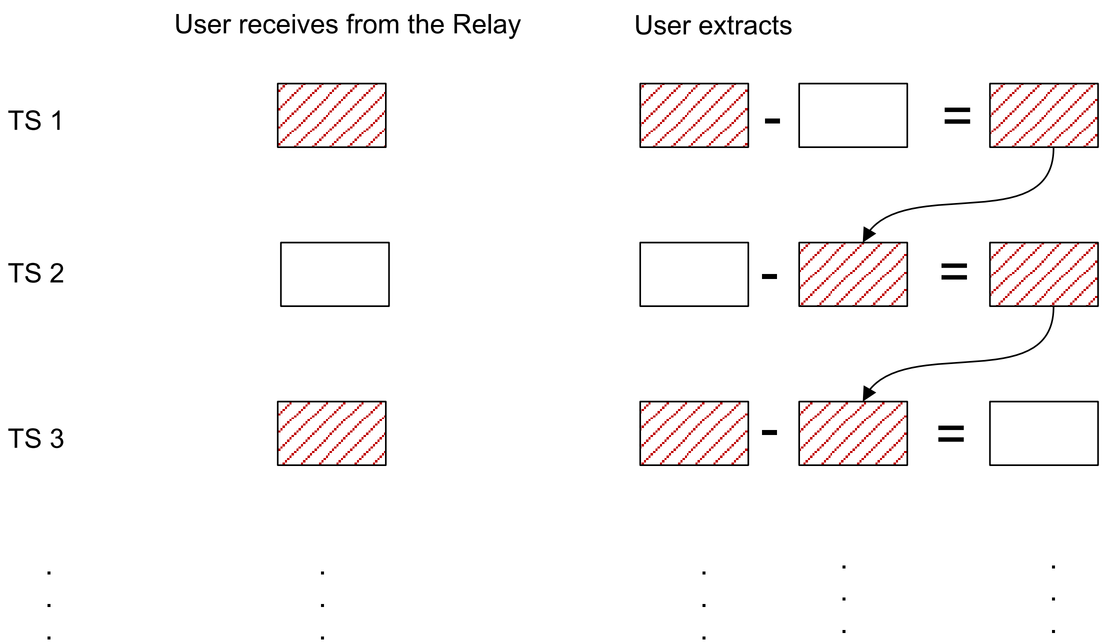

Figure 1.8: Error propagation in a MWRN. The red blocks indicate that the corresponding message is incorrectly decoded, whereas, the white blocks indicate that the message is correctly decoded.

1.1.3 Transmission Strategies for MWRNs

MWRNs can operate with pairwise, as well as non-pairwise transmission strategies. In pairwise transmission based MWRNs, the users transmit in pairs, that is, in each time slot, two users transmit simultaneously [28, 47, 48]. Each user has to decode all the user pairs' messages correctly for correct decisions about every other user's messages. *Thus, the user pair formation is a critical issue for pairwise transmission based MWRNs*. To ensure efficient usage of the transmission resources (i.e., in terms of the number of time slots or bandwidth), each user pair needs to have at least one common user with the following and the preceding user pair. The transmission mechanism for pairwise MWRNs has been illustrated in Fig. 1.7(a) and in Fig. 1.7(b).

On the other hand, for non-pairwise transmission based MWRNs, all the users transmit simultaneously and the relay broadcasts the received signal after linear precoding. In [49], it has been shown that the pairwise transmission strategy has a lower signal processing complexity at the relay, whereas, the non-pairwise transmission achieves higher spatial multiplexing gains at the cost of additional signal processing complexity. *In this thesis, we focus on pairwise transmission strategy to exploit its simpler implementation benefits.*

1.1.4 Open Problems in MWRNs

In this subsection, we discuss some open problems in the field of MWRNs, that motivate our research regarding MWRNs.

In a pairwise transmission based MWRN, the users have to correctly decode every user pair's network coded message for error free message exchange. This is because, in this strategy, the decision about each user depends on the decoded message of the previous users. This gives rise to a significant practical issue in MWRNs with pairwise data exchange, which is termed as error propagation. The error propagation in a MWRN has been illustrated in Fig. 1.8. The error propagation problem degrades the received signal-to-noise ratio (SNR) at the users and as a result, degrades the error performance of a MWRN. *Thus, the characterization of error propagation is an important open problem, which to the best of our knowledge, has not been fully studied in the literature before.*

From figures 1.7(a), 1.7(b) and 1.8, it can be identified that the error propagation problem in a MWRN is influenced by the way the users are paired. Thus, choosing the user pairs appropriately is crucial for the reliable operation of a MWRN. It can be intuitively understood that choosing the user pairs arbitrarily and independent of their channel conditions, cannot be much useful from the perspective of a pairwise MWRN. *Thus, designing a pairing scheme in a way that ensures reliable decoding of the users' messages and hence, reduce error propagation, is another important open problem for MWRNs.*

In a MWRN, each user has to subtract self interference from the received signal to obtain other users' messages. For perfect recovery of the messages, the channels need to be perfectly estimated [50, 51] at both the users and the relay. However, this is not possible in a practical system with imperfections like imperfect channel state information (CSI). Figures 1.9(a), 1.9(b) and 1.9(c) illustrate the case when perfect CSI

(a) Users in a pair transmit simultaneously

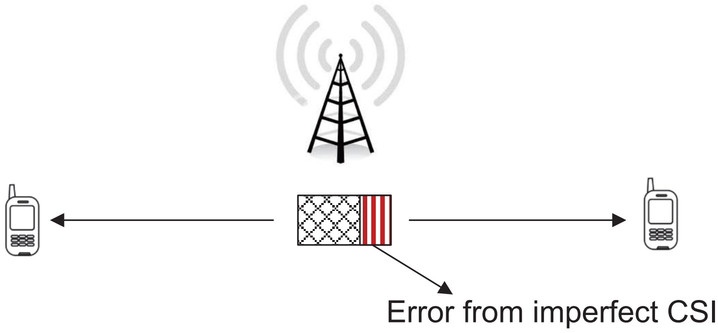

(b) Relay processes the sum of the signals using imperfect CSI and broadcasts

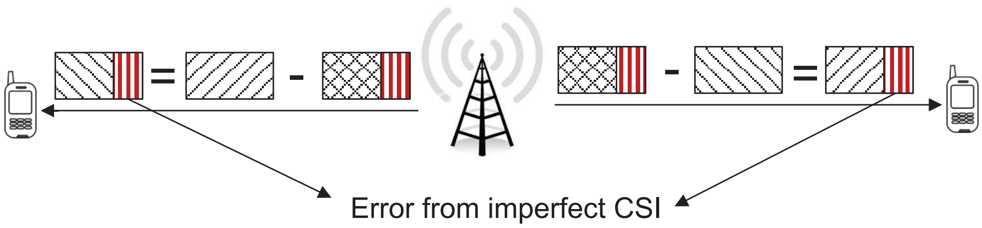

(c) Users cancel self interference

Figure 1.9: The impact of imperfect CSI on MWRNs. Note that, due to channel estimation error, the users cannot completely recover the desired messages.

is not available and hence, self interference cannot be completely cancelled. In the presence of imperfect CSI, the channel estimation error will add to the error propagation problem and worsen the error performance of a MWRN. *Analyzing the impact of imperfect CSI on MWRNs is also an important open problem.* Finally, to optimize the performance of a MWRN, *optimum power allocation* needs to be investigated. Especially, when channel estimation errors are present, the importance of the optimum power allocation between the pilot and the data signals becomes inevitable for an increased system throughput.

In this thesis, we provide solutions to the above open problems whose answers are still missing in the literature. Specifically, the main focus of this thesis is *firstly*, the characterization of pairwise transmission based MWRNs through mathematical modeling of the error propagation phenomenon, *secondly*, proposing a novel pairing scheme that can outperform existing pairing schemes in terms of the achievable rate and error performance and *thirdly*, consideration of performance limiting practical issues like imperfect CSI and how power allocation can alleviate these issues. In the remaining part of this chapter, we discuss the prior works on the performance analysis of MWRNs for background information. Finally, we present our contributions and the outline of the thesis.

1.1.5 Literature Review on MWRNs

In a MWRN, the users transmit in a half-duplex manner and do not have any direct link between them. Each of the users intend to receive messages from every other user in the network. Potential applications of MWRNs include information exchange in satellite networks, social networks and sensor networks. Another way for realizing the benefits of TWRNs in a multi-user scenario is a multi-user TWRN, consisting of multiple TWRNs, where users exchange messages with their pre-assigned partners and has been studied widely in the literature [52–56]. Note that, a multi-user TWRN is a special version of a MWRN and hence, we focus on the analysis of more generalized MWRNs in this thesis.

In a MWRN, message exchange is accomplished in two phases-multiple access and broadcast phase. In the *multiple access phase*, the users transmit messages in a pairwise manner and the relay receives the sum of the signals. In the *broadcast phase*, the relay broadcasts the messages to all the users after performing some relaying operations. The relaying operations depend on different relaying protocols which include (1) amplify and forward (AF) [57,58], (2) decode and forward (DF) [26,50], (3) compress and forward (CF) [26], (4) functional decode and forward (FDF) [28, 48, 59, 60] and (5) compute and forward [61,62] relaying protocols. Among these protocols, the first three protocols have already been considered for unidirectional and bidirectional relay networks in [63] and the last two protocols are proposed very recently for MWRNs. In the following part, we briefly discuss the relaying process for the aforementioned relaying protocols.

1. *Amplify and Forward:* In this protocol (originally termed as 'Facilitation' in [63]), the relay amplifies the received signal and broadcasts to all the users (as illustrated in Fig. 1.10(a)).

2. *Decode and Forward:* In this protocol (originally termed as 'Cooperation' in [63]), the relay decodes the received signal and broadcasts to all users (as illustrated in Fig. 1.10(b)).

3. *Compress and Forward:* In this protocol (originally termed as 'Observation' in [36]), the relay encodes a quantized version of the received signal and broadcasts to all users (as illustrated in Fig. 1.10(c)).

4. *Functional Decode and Forward:* In FDF MWRNs, the relay decodes a function of the users' messages instead of decoding the messages individually [28] (as illustrated in Fig. 1.10(d)).

5. *Compute and Forward:* In compute and forward MWRNs, the relay computes linear equations of the transmitted messages according to their observed channel coefficients [62] (as illustrated in Fig. 1.10(e)). The relay forwards these equations to the users and each user, upon receiving sufficient number of equations, can decode the messages of the other users.

Next, we discuss the prior works on MWRNs relevant to the above relaying protocols.

Amplify and Forward: For AF MWRNs, the end-to-end SNR expression and its cumulative distribution function, probability density function, as well as the moment generating function, have been derived in closed form in [57]. Moreover, in the aforementioned work, the outage probability and the average BER of an AF MWRN have been

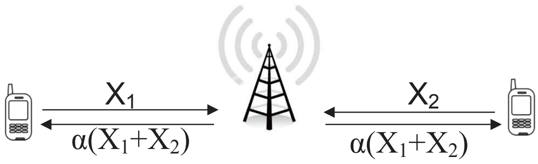

(a) AF relaying. Here α denotes amplification factor

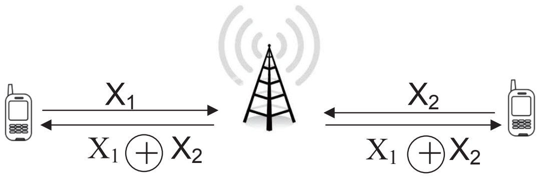

(b) DF relaying. Here $\oplus$ denotes XOR operation

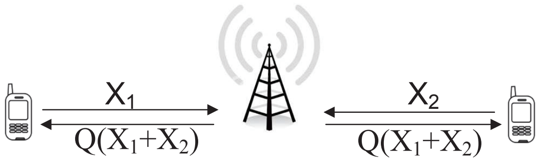

(c) CF relaying. Here $Q(\cdot)$ denotes quantization operation

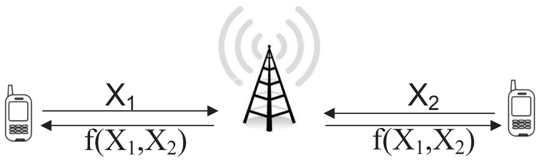

(d) FDF relaying. Here $f(\cdot)$ denotes a function

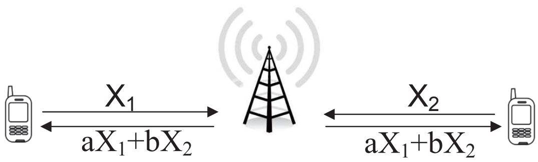

(e) Compute and forward relaying. Here a, b denotes integer coefficients

Figure 1.10: Different Relaying Protocols in a MWRN.

obtained assuming error free successive interference cancellation and diversity multiplexing tradeoff has been derived using high SNR outage probability approximation. For AF MWRNs with multi-antenna relay, space time analog network coding and repetition coding protocols have been investigated in [64]. In [64], it has also been shown that space time analog network coding protocol can outperform zero forcing detection and transceiver beamforming schemes in terms of the average sum rate.

Decode and Forward: DF MWRNs have been investigated in terms of the optimal pairing order that maximizes the achievable sum rate [50]. It has been shown in [50] that pairing the ℓ^{th} user with the $(L-\ell+1)^{th}$ user, where $\ell \in [1, L]$ and L is the total number of users in the MWRN, is the optimal pairing scheme for a DF MWRN. Besides this, some research works on DF MWRNs consider complex field network coding which utilizes a precoding vector to separate out users' symbols so that they can be distinguished at the relay [65]. In [66], an algorithm is designed in such a way that the superimposed signal of users (who transmit with different quadrature amplitude modulation (QAM) constellations) has a QAM constellation when received at the relay and the SER for this algorithm is evaluated for additive white Gaussian noise (AWGN) channels. On the other hand, in [65], the SER for complex field network coding has been investigated for Rayleigh fading channels.

Compress and Forward: CF MWRNs have been investigated in terms of outer bounds on the achievable rates and exchange rate, which is the symmetric rate point in the capacity region in a symmetric Gaussian channel [36]. In [36], AF, DF and CF protocols have also been compared in terms of the achievable rates and it has been shown that CF and AF protocols can achieve the exchange rate upper bound within $\frac{L}{2(L-1)}$ and $\frac{L(1+\log L)}{2(L-1)}$ bits. However, for DF protocol, the exchange rate is smaller than CF protocol at high SNR and vice versa.

Functional Decode and Forward: It was shown in [28] that pairwise FDF with binary linear codes is theoretically the optimal strategy for binary MWRNs, since it achieves the common rate. Also it was shown in [59] that for a MWRN with lattice codes in an

AWGN channel, the pairwise FDF achieves the common rate, which is the minimum of the maximum achievable information rates at all the users. In [27], correlated sources for a three user FDF MWRN have been considered and the minimum source-channel rate has been obtained for this channel. Different user pairing schemes for asymmetric MWRNs, where users have certain channel conditions, are studied in [50,67]. It has been shown in [50, 67] that the achievable common rate for a pairwise FDF MWRN is maximized when the ℓ^{th} user forms a pair with the $(\ell+1)^{th}$ user under the circumstances that the ℓ^{th} user's channel gain is larger than that of the $(\ell-1)^{th}$ user but smaller than that of the $(\ell+1)^{th}$ user.

Compute and Forward: The outage probability of compute and forward MWRN has been investigated in [61] and it has been shown that compute and forward outperforms non-network coding strategies for relatively small number of users. The computation rate in the presence of multiple relays has been obtained in [62].

For the rest of this thesis, we consider only AF and FDF protocols, since the first one is the simplest relaying protocol among the above protocols and the second one, which is relatively more complex, achieves the common rate for binary MWRNs.

In the following subsections, we discuss some important prior works regarding practical issues that influence MWRN performance.

1.1.5.1 Error Propagation

To the best of our knowledge, an analytical characterization of the error propagation problem in a MWRN has not been fully addressed in the literature to date. The probability for the special case of having at least one error event in AF MWRN is derived in [57]. Here, an error event is characterized by the number of users whose messages are incorrectly decoded. Apart from the one error event case, there has been no attempt to analyze the error performance of MWRNs with pairwise data exchange. However, the probabilities of discrete error events offer only a partial view of the overall error performance. From the perspective of the overall system performance, the average BER is a more useful metric since it takes all the error events into account. Thus, characterizing error propagation and obtaining the average BER of a MWRN is an open problem.

1.1.5.2 Lattice Codes

In this part, we discuss lattice codes, which form an integral part of FDF MWRNs because lattice codes can achieve the common rate for FDF MWRNs in AWGN channel. A lattice is a discrete subgroup of the Euclidean space with ordinary vector addition and reflection operation [68, 69]. It indicates that the sum of two lattice points will belong to the same lattice construction. That is, lattice codes enable transmission of codewords that are linear combination of other codewords. In [68], it has been shown that lattice codes can achieve the capacity of point-to-point AWGN channels. Moreover, lattice codes have been incorporated to multi-terminal AWGN networks in [70].

Lattice codes have been developed for multiple access networks in [71] and for TWRNs in [72]. In [73], the achievable rate of a lattice coded TWRN has been obtained within half a bit of the capacity for asymmetric power constraints. Further extensions on lattice codes include rate analysis for AWGN multiple access networks [74].

To implement lattice codes in a MWRN, the messages are first drawn from a finite field, then mapped into lattice points and finally, transmitted to the relay [28, 62, 75]. The relay then decodes a linear combination of the lattice points, which is broadcast to the users. The users perform self interference cancelation, extract the lattice points and then map the point back to a finite field message.

Lattice code based pairwise MWRNs have been investigated in [59] for AWGN channel in terms of the capacity and the achievable rates. However, lattice code based pairwise MWRNs have not been investigated for fading channels. Moreover, lattice code based pairwise MWRNs also need to be investigated in terms of error propagation and error performance. Though in [57], a binary phase shift keying (BPSK) modulated pairwise MWRN has been analyzed for error performance, the more general error performance of pairwise MWRNs with lattice codes in fading channels has not been

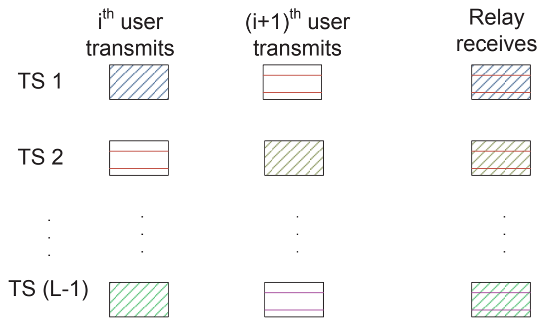

(a) Pairing scheme by Ong et al.

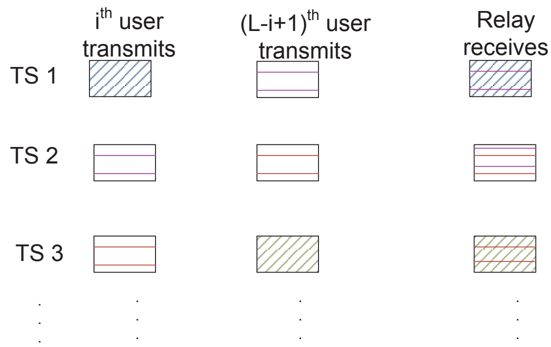

(b) Pairing scheme by Noori et al.

Figure 1.11: Comparison of different pairing schemes in a MWRN.

considered in the literature to date.

1.1.5.3 Pairing Scheme

As mentioned previously, user pair formation is a critical issue in a pairwise transmission based MWRN. In this regard, two different pairing schemes have been proposed in the literature for MWRNs. In the pairing schemes in [28] (for FDF relaying) and in [57] (for AF relaying), the ℓ^{th} and the $(\ell+1)^{th}$ users form a pair at the ℓ^{th} time slot, where $\ell \in [1, L-1]$. In the pairing scheme in [50] (for FDF relaying), instead of consecutive users as in the pairing scheme in [28], the ℓ^{th} and the $(L-\ell+1)^{th}$ user form a pair at the ℓ^{th} time slot when $1 \leq \ell \leq \lfloor L/2 \rfloor$ and the $(\ell+1)^{th}$ and $(L-\ell+1)^{th}$ user form a pair at the ℓ^{th} time slot when $\lfloor L/2 \rfloor < \ell \leq L-1$, where $\lfloor \cdot \rfloor$ denotes the integer floor operation. The achievable rates for these two existing pairing schemes were analyzed in [28, 49, 50, 59].

A major drawback of the above two pairing schemes is that they arbitrarily select users for pair formation and do not take the users' channel information into account when pairing the users. This is crucial since in a MWRN, the decision about each user depends on the decisions about all other users transmitting before it, as explained previously. Thus, in the above pairing schemes, if any user experiences poor channel conditions, it can lead to incorrect detection of another user's message, which can adversely impact the system performance due to error propagation. We also note that a recent paper on opportunistic pairing [76] also suffers from the error propagation problem similar to [28].

1.1.5.4 Channel Estimation

The impact of imperfect channel estimation on MWRNs has not been addressed in the aforementioned literature on MWRNs. However, in case of TWRNs, recent studies have quantified the impact of imperfect channel estimation. So, in this part, we discuss some established results on the channel estimation of TWRNs, as these results will be used later in this thesis for modelling and characterizing a MWRN with imperfect CSI.

A number of the research works on channel estimation for TWRNs, consider training based channel estimation. In [77], maximum likelihood (ML) channel estimation is employed at the relay and the mean square error of the channel estimation has been minimized by allocating optimum power to the training signals. On the other hand, maximum a posteriori (MAP) channel estimation has been proposed in [78], which takes into account the prior information on wireless channels to improve the channel estimation accuracy and hence, outperforms the ML based channel estimation algorithms in terms of mean squared error. Reference [79] considers training based channel estimation, where at first, the sources transmit training signals simultaneously and then the relay amplifies and forwards the received signal. It has been shown in [79] that the orthogonal training signal is optimal for the estimator performance.

On the other hand, some works consider the impact of imperfect channel estimation on the performance of training based TWRNs [80, 81]. In [80], the achievable information rates for full duplex AF TWRNs with channel estimation errors have been upper bounded. A lower bound on the sum rate of information transmission in both directions of the half-duplex multiple input multiple output (MIMO) TWRN with AF relaying has been obtained in [81] using the notion of the worst case noise at the receiver. Apart from these, some research works have considered the impact of channel estimation error on the outage probability [82] and the error performance [83] of an AF TWRN. Similarly, the achievable rates of DF TWRNs with imperfect CSI have been studied in [84].

To avoid the transmission of pilot signals and reduce transmission overhead, self interference components from users' own signal are proposed to be used for channel estimation in [85]. Though this scheme allows low complexity and low overhead benefits, its accuracy is highly dependent on correctly decoding the signal at the relay [81]. In [86], single carrier cyclic prefix modulation has been proposed for channel estimation in an AF TWRN.

Another approach to avoid the pilot transmission overhead is blind channel estimation, which has been studied in [87]. The blind channel estimation algorithm in [87] employs constant modulus signaling through deterministic maximum likelihood and can approach the true channel for higher order modulations. The semi-blind channel estimation algorithm, which is a combination of pilot based and blind channel estimation algorithms has been analyzed in [88] and it has been shown that this approach results into significant improvement in estimation performance compared to pilot based approaches.

In this thesis, we are going to use the pilot based channel estimation algorithm for MWRNs where the channel coefficients are estimated through linear minimum mean square error estimation, as this approach is widely investigated in the literature and is a very practical scheme in real-world wireless systems.

1.1.5.5 Power Allocation

Optimum power allocation is an important problem for relay networks as it assures superior performance of the system in terms of the received SNR, achievable rate, mean square error of the channel estimation and average SER. Recently, optimum power allocation between the relay and users and between the data and pilot symbols has been investigated for TWRNs. Moreover, power allocation has been studied to maximize the sum rate of all the users in a multi-user TWRN [53, 89], which is a special class of MWRNs, where each user exchanges message only with its pre-defined partner. However, in these studies, full instantaneous CSI is assumed to be available to all the users and the relay. Power allocation strategies in a more practical scenario, where only long term statistical CSI (i.e., channel variance) is available to each user and the relay, has not yet been investigated. In the following part of this subsection, we discuss some recent results on power allocation for TWRNs, as they are going to be used for studying power allocation problems in MWRNs in the later chapters, which has not been investigated yet.

For TWRNs with imperfect CSI, optimal power allocation between the training and the data signals and also among the three nodes (i.e., two users and the relay) have been performed with an objective to minimize the outage probability [82], maximize the achievable rate [80], maximize the sum rate [90], maximize the average SNR of data detection or minimize the mean square error of channel estimation [77]. In [82, 90] it has been shown that the optimal solutions for power allocation are closely related to relay location. When the relay is closer to one of the sources, the power optimization affects the system performance more than the case of equal distances between the sources and the relay, as shown in [80, 90].

In [91], the outage probability and the average BER have been optimized through power allocation in the presence of both the relay selection and imperfect CSI. It has been shown that when all the relays participate, optimum power allocation gives a 1 dB gain compared to equal power allocation, whereas, when only the best relay is chosen, the performance gain is 3 dB.

1.2 Overview and Contribution of Thesis

From the literature review presented in the previous section, it is clear that the investigation of practical issues, such as error propagation phenomenon, imperfect CSI and power allocation, and most importantly, an efficient pairing scheme design to lessen the error propagation problem can be considered as challenging open problems from the perspective of MWRNs.

1.2.1 Questions to be Answered

The following open questions are answered in this thesis:

Q1. How can we characterize the average BER for a user in FDF and AF MWRNs?

Q2. How to design a pairing scheme to improve the achievable rate and error performance of lattice coded FDF MWRNs?

Q3. How can the impact of channel estimation error and optimum power allocation coefficients on the error performance and achievable rate of lattice code based FDF and AF MWRNs be characterized in the presence of error propagation?

1.2.2 Thesis Contribution and Organization

Fig. 1.12 illustrates the flowchart of this thesis. The general system model for MWRN is presented in Chapter 2, which will be common to most chapters. In Chapter 3, the error performance of FDF and AF MWRNs with BPSK modulation will be investigated and compared for AWGN channel and fading channels. In Chapter 4, a novel pairing scheme is proposed to improve the error performance and achievable rates of FDF MWRNs with lattice codes and the common rate, sum rate and average SER are derived for the proposed pairing scheme under different channel conditions. Then the

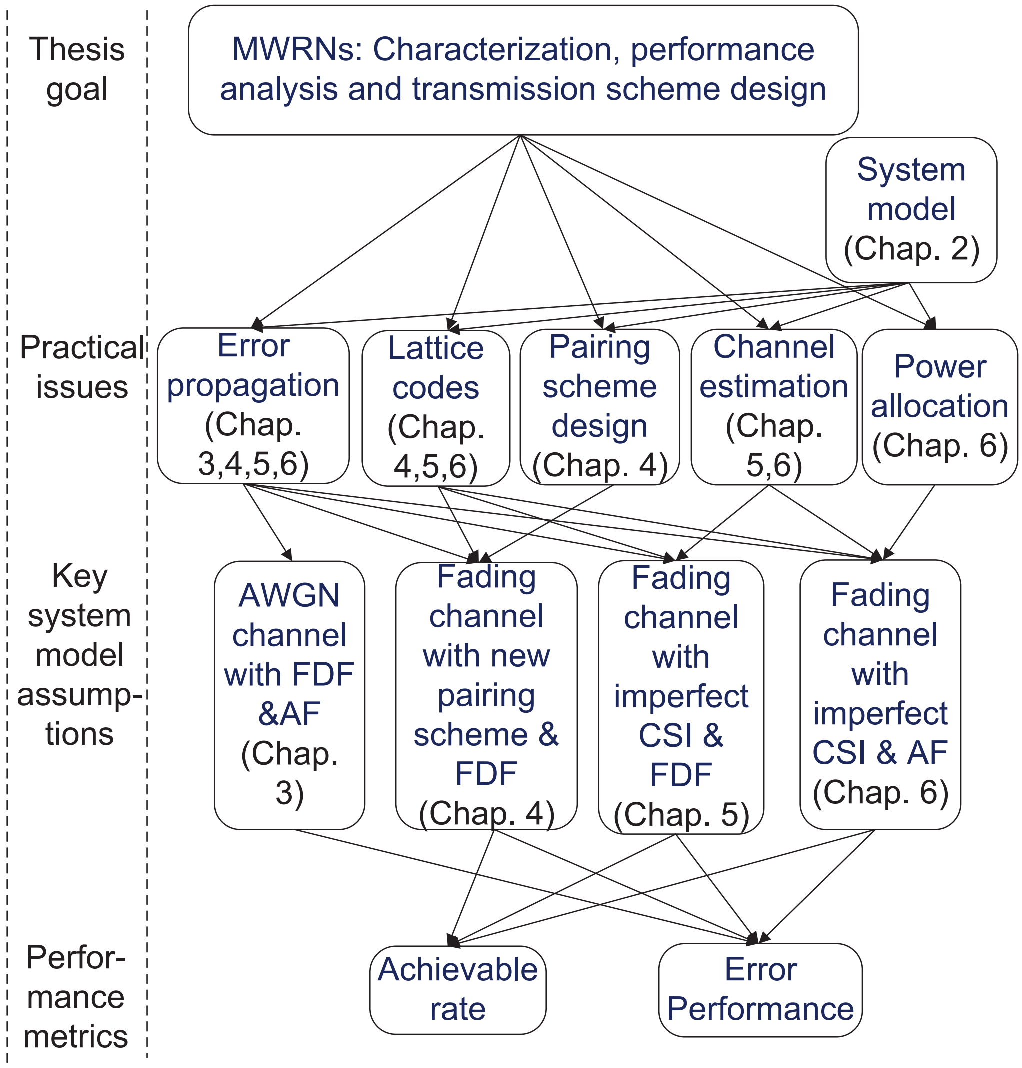

Figure 1.12: Thesis flow chart.

impact of channel estimation error on the achievable rate and error performance of FDF MWRN with lattice codes is analyzed in Chapter 5. Lattice coded AF MWRNs with imperfect CSI and tunable power allocation are studied in Chapter 6. The summary of the contributions in each chapter is as follows:

Chapter 3-Error Performance Analysis of FDF and AF Multi-way Relay Networks

Chapter 3 considers the error performance of FDF and AF MWRNs. Here, we consider a MWRN with pairwise data exchange protocol using BPSK modulation in both AWGN and Rayleigh fading channels with equal channel gain. A significant practical issue in MWRNs with pairwise data exchange is error propagation. For example, in

FDF MWRNs, if a user wrongly decodes another user's message, then this error propagates through the subsequent decoding operations unless another error is made. To address this issue, in this chapter, we provide the analytical characterization of the error propagation problem. The main contributions in this chapter are:

1. We derive accurate asymptotic bounds on the error probability for the general case of $k(k \leq L-1)$ error events in an L-user FDF or AF MWRN. These bounds are based on the insights gained from the analysis of the exact probability that a user incorrectly decodes the messages of $k=1$ and $k=2$ users.

2. Our analysis of the error probability for the general case of k error events shows that at high SNR (a) the dominant factor in the error propagation in FDF MWRN is the probability of consecutive erroneous messages resulting from a single erroneous network coded message, (b) the dominant factor in the error propagation in AF MWRN is the probability of consecutive errors involving the middle or end users in the transmission protocol and (c) the higher order error events ($k \geq 3$) are less probable in AF MWRN, but all error events are equally probable in a FDF MWRN. This affects their BER sensitivity to the number of users in the system.

3. We use the asymptotic bounds on the probability of k error events to derive closed-form expressions for the average BER of a user in FDF or AF MWRN under high SNR conditions.

4. We show that for a given number of users in an AWGN channel, AF MWRN is slightly better than FDF MWRN at low SNR, while FDF MWRN is better than AF MWRN at medium to high SNRs. For fading channels, AF MWRN begins to outperform FDF MWRN for the number of users as low as $L \approx 10$. We attribute this to the lower probability of high-order error events in AF MWRN, which makes it more robust to the increase in the number of users in terms of average BER.

The results in this chapter have been presented in the following publications and are listed again for ease of reference:

J1. **S. N. Islam**, P. Sadeghi, and S. Durrani, ”Error Performance Analysis of Decode-and-Forward and Amplify-and-Forward Multi-way Relay Networks with Binary Phase Shift Keying Modulation,” *IET Commun.*, vol. 7, no. 15, pp. 1605-1616, Oct. 2013.

C1. **S. N. Islam**, and P. Sadeghi, ”Error Propagation in a Multi-way Relay channel,” *in Proc. IEEE ICSPCS*, pp. 1-8, Dec. 2011.

Chapter 4-A Novel User Pairing Scheme for Lattice coded FDF Multi-way Relay Networks

In Chapter 4, we consider a lattice coded FDF MWRN. Lattice codes can achieve the capacity of AWGN channels and are used in digital communications as high-rate signal constellations, which motivates the potential implementation of lattice codes in a MWRN. In this chapter, we propose a novel pairing scheme, where a common user facilitates each user in the network to obtain messages from all other users. The pairing scheme is based on the principle of selecting a common user with the best average channel gain. This allows the user with the best channel conditions to contribute to the overall system performance. In this chapter, we compare the proposed pairing scheme for FDF MWRNs with existing pairing schemes in terms of the achievable common rate, sum rate and average SER. The main contributions in this chapter are:

1. Considering L-user FDF MWRNs employing sufficiently large dimension lattice codes, we derive upper bounds for the common rate and sum rate with the proposed pairing schemes.

2. Considering L-user FDF MWRNs with M-ary QAM based transmission, which is a special case of lattice code based transmission, we derive the asymptotic average SER with the proposed pairing schemes.

3. We compare the performance of the proposed pairing schemes with the existing pairing schemes and show that:

    - When the average channel gains in the user-relay channels are equal, the average common rate and the average sum rate are the same for the proposed and existing pairing schemes, but the average SER improves with the proposed pairing scheme.

- When the average channel gains are unequal but do not change with time, the average common rate, the average sum rate and the average SER all improve for the proposed pairing scheme.
- When the average channel gains are unequal and change every time frame, the average common rate for the proposed pairing scheme is almost the same as the existing schemes for FDF MWRNs. However, the average sum rate and the average SER improve for the proposed pairing scheme.

Parts of the results in this chapter have been presented in the following publication and is listed again for ease of reference:
J2. **S. N. Islam**, S. Durrani, and P. Sadeghi, "A Novel User Pairing Scheme for Functional Decode-and-Forward Multi-way Relay Network," submitted to *Physical Communications*, Sep. 2014, http://arxiv.org/abs/1402.6422v3.

Chapter 5-Lattice Coded FDF MWRNs: Achievable Rate and SER with Imperfect CSI

Chapter 5 considers lattice code based FDF MWRNs with imperfect CSI. For a MWRN, in order to perfectly recover the message of the other users by self-interference cancelation, the channels need to be perfectly estimated at both the users and the relay, which is generally not possible in practice. In the presence of imperfect channel estimation, the estimation error adds to the performance degradation resulting from error propagation and the error performance gets worse. Thus, in this chapter, we address the joint impact of lattice codes and imperfect CSI on the achievable rate and error performance of MWRNs. The main contributions in this chapter are:

1. Considering an L-user MWRN employing sufficiently large dimension lattice codes, we derive the bounds on the achievable rate expressions for FDF MWRNs with imperfect channel estimation and unequal average channel gains for the users. Moreover, considering M-ary QAM, which is a special case of lattice code based

transmission, we derive the expressions for the average SER for FDF MWRNs. The derived expressions can more accurately predict the system behavior at high SNR.

2. We show that the average SER of FDF MWRN is an increasing function of both the estimation error and the number of users. This behavior is a result of the fact that all the error events are equally probable for FDF MWRN and the number of such events increases with the increasing number of users.

3. We show that when the users' overall channel conditions improve, the achievable rates improve by the same amount for imperfect and perfect CSI. However, in terms of the average SER, when most of the users experience good channel conditions, FDF MWRNs with imperfect CSI performs closer to the one with perfect CSI due to less error propagation.

Part of the results in this chapter have been presented in the following publication and is listed again for ease of reference:

J3. **S. N. Islam**, S. Durrani, and P. Sadeghi, "Lattice Code Based Multi-way Relay Networks: SER Analysis and the Impact of Imperfect Channel Estimation," submitted to *Journal of Communications and Networks*, May 2015.

Chapter 6-Lattice Coded AF MWRNs with Imperfect CSI

Chapter 6 considers lattice coded AF MWRNs with channel estimation error. Similar to Chapter 5, in this chapter, we address the joint impact of lattice codes and imperfect CSI on the achievable rate and error performance of AF MWRNs. Moreover, we obtain the optimum power allocation coefficients for the pilot and the data of the users' and the relay's signal to maximize the sum rate. The main contributions in this chapter are:

1. Considering an L-user MWRN employing sufficiently large dimension lattice codes, we derive the bounds on the achievable rate expressions for AF MWRNs with imperfect CSI. Moreover, considering BPSK modulation, which is a special case of lattice code based transmission, we derive the expressions for the average SER and optimum power allocation coefficients for AF MWRNs.

2. We show that the achievable rates of AF MWRNs are decreasing functions of the estimation error. We also show that the the average BER of AF MWRN does not depend on the number of users, because the larger number of error events are less probable for AF.

3. We observe that to achieve the same sum rate in AF MWRN, optimum power allocation requires $7-9$ dB less power compared to equal power allocation depending upon users' channel conditions.

Part of the results in this chapter have been presented in the following publication and is listed again for ease of reference:

C2. **S. N. Islam**, S. Durrani, and P. Sadeghi, "Optimum Power Allocation for Sum Rate Improvement in AF Multi-way Relay Networks," accepted in *IEEE ICSPCS*, Dec. 2014.

Finally, Chapter 7 gives a summary of the thesis and provides suggestions for future research.

Chapter 2

System Model

In the previous chapter, we discuss the background on relay networks, existing literature on MWRNs and motivation of this thesis. In this chapter, we discuss the general system model and channel assumptions for a MWRN. Specific system model assumptions for each chapter will be discussed at the beginning of that chapter.

This chapter is organized as follows. The system model under consideration is described and the channel assumptions are presented in Section 2.1. The signal transmission protocols at the users and the relay are discussed in Section 2.2. Existing results on different performance metrics of a MWRN are presented in Section 2.3. Finally, a brief summary of the chapter is provided in Section 2.4.

2.1 System Model Description

We consider an L-user MWRN, where all the users exchange their information with each other through a single relay.

In this setup, a pair of users communicate with each other at a time, while the remaining users are silent. We assume that the users transmit in a half-duplex manner and they do not have any direct link between them. The information exchange takes place in two phases−multiple access and broadcast phase−each comprising $L-1$ time slots for an L-user MWRN [28]. In the *multiple access phase*, the users transmit their data in a pairwise manner. In the *broadcast phase*, the relay broadcasts the functionally decoded or amplified network coded message to all users depending on the relaying protocol.

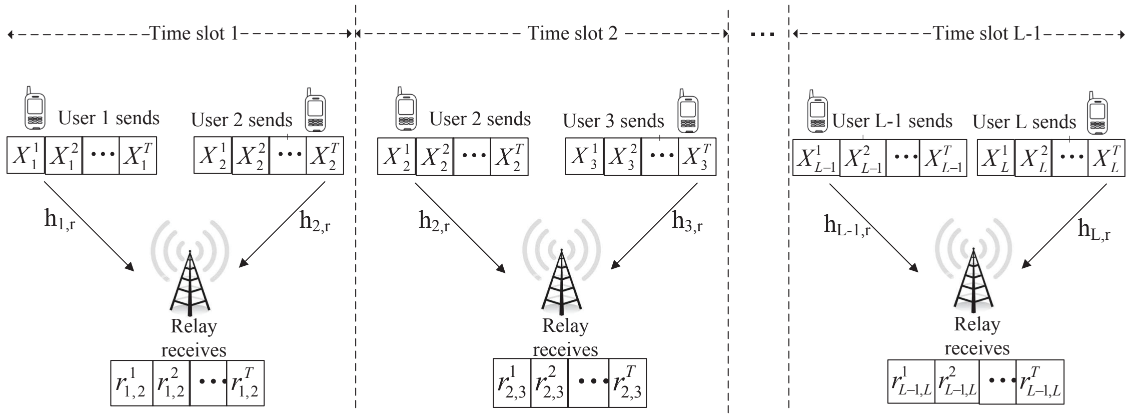

Figure 2.1: Multiple access phase for an L-user MWRN.

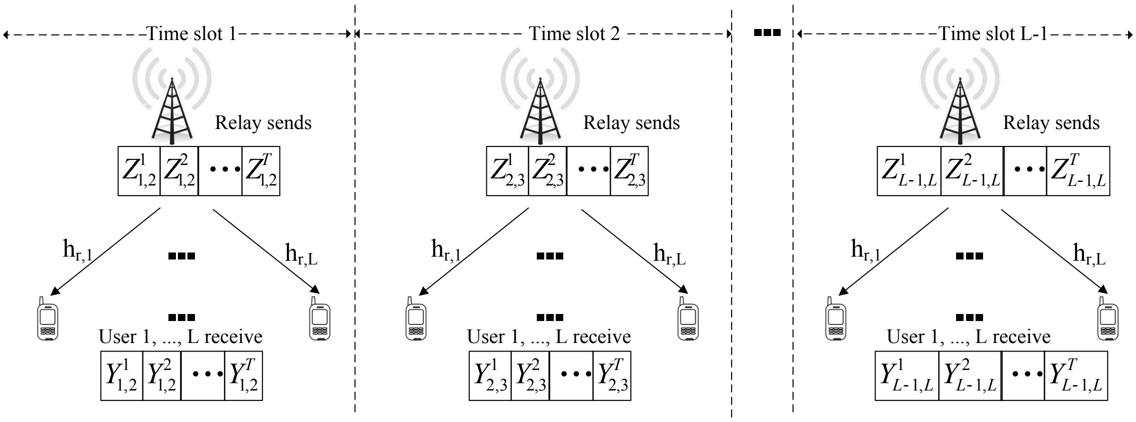

Figure 2.2: Broadcast phase for an L-user MWRN.

The above system model has been illustrated in Fig. 2.1 and Fig. 2.2. In this system, after $2(L-1)$ time slots, all users have the network coded messages corresponding to each user pair and then they utilize self information to extract the messages of all the other users.

We refer to these $2(L-1)$ time slots in the two phases as one *time frame*. That is, in each time frame, each user transmits a message packet of length T and the relay transmits $(L-1)$ message packets, each of length T. Thus, a total of $(2L-1)$ message packets are communicated in an entire time frame. We choose the index for time slot and time frame as t_s and t_f, respectively, and the message index as t where, $t_s \in [1, L-1]$, $t_f \in [1, F]$ and $t \in [1, T]$, where, F is the total number of time frames. The transmission power of each user is P, whereas, the transmission power of the relay is P_r. At the t_f^{th}

Table 2.1: Illustration of channel coefficients in multiple access and broadcast phases for an L-user MWRN.

	Time slot	Message packets	Multiple access phase	Broadcast phase
Time Frame 1	1	$\mathbf{W}_1^{1,1}, \mathbf{W}_2^{1,1}$	$h_{1,r}^{1,1}, h_{2,r}^{1,1}$	$h_{r,1}^{1,1}, ..., h_{r,L}^{1,1}$
	2	$\mathbf{W}_2^{2,1}, \mathbf{W}_3^{2,1}$	$h_{2,r}^{2,1}, h_{3,r}^{2,1}$	$h_{r,1}^{2,1}, ..., h_{r,L}^{2,1}$
	$\cdots$	$\cdots$	$\cdots$	$\cdots$
	$L-1$	$\mathbf{W}_{L-1}^{L-1,1}, \mathbf{W}_L^{L-1,1}$	$h_{L-1,r}^{L-1,1}, h_{L,r}^{L-1,1}$	$h_{r,1}^{L-1,1}, ..., h_{r,L}^{L-1,1}$
Time Frame 2	1	$\mathbf{W}_1^{1,2}, \mathbf{W}_2^{1,2}$	$h_{1,r}^{1,2}, h_{2,r}^{1,2}$	$h_{r,1}^{1,2}, ..., h_{r,L}^{1,2}$
	2	$\mathbf{W}_2^{2,2}, \mathbf{W}_3^{2,2}$	$h_{2,r}^{2,2}, h_{3,r}^{2,2}$	$h_{r,1}^{2,2}, ..., h_{r,L}^{2,2}$
	$\cdots$	$\cdots$	$\cdots$	$\cdots$
	$L-1$	$\mathbf{W}_{L-1}^{L-1,2}, \mathbf{W}_L^{L-1,2}$	$h_{L-1,r}^{L-1,2}, h_{L,r}^{L-1,2}$	$h_{r,1}^{L-1,2}, ..., h_{r,L}^{L-1,2}$
$\cdots$	$\cdots$	$\cdots$	$\cdots$	$\cdots$

time frame and the t_s^{th} time slot, the channel from the j^{th} user to the relay is denoted by $h_{j,r}^{t_s,t_f}$ and the channel from the relay to the j^{th} user by $h_{r,j}^{t_s,t_f}$, where $j \in [1, L]$. These channel coefficients in different phases and frames are shown in Table 2.1.

We make the following assumptions regarding the channels:

- The channels are assumed to be block Rayleigh fading channels, which remain constant during one message packet transmission in a certain time slot in a certain multiple access or broadcast phase. Also, the channels from users to the relay (e.g., $h_{j,r}^{t_s,t_f}$) and the channels from the relay to users (e.g., $h_{r,j}^{t_s,t_f}$) are reciprocal.

- The fading channel coefficients are zero mean complex-valued Gaussian random variables with variances $\sigma^2_{h_{j,r}} = \sigma^2_{h_{r,j}}$.

- The perfect instantaneous CSI of all users is available to the relay unless otherwise stated. If the relay implements FDF protocol, the users are required to have access to the self CSI only, which has been assumed in many research works [22, 44, 92]. However, if AF relaying protocol is chosen, the users need to have access to the global CSI to enable cancellation of interference components from other users' signal.

- Perfect channel phase synchronization is assumed because physical layer network coding requires that the signals arrive at the relay with the same phase and this allows benchmark performance to be determined [15,45].

We consider the following three different channel scenarios in a general MWRN:

1. *Equal average channel gain scenario:* All the channels from the relay to the users and the users to the relay have equal average channel gain, which remain fixed for all time frames. That is, $E[| h_{1,r}^{t_s,t_f} |^2]= E[| h_{2,r}^{t_s,t_f} |^2] = ... = E[| h_{L,r}^{t_s,t_f} |^2]$.

2. *Unequal average channel gain scenario:* All the channels from the relay to the users and the users to the relay have unequal average channel gains which remain fixed for all the time frames. That is, $E[| h_{1,r}^{t_s,t_f} |^2] \neq E[| h_{2,r}^{t_s,t_f} |^2] \neq ... \neq E[| h_{L,r}^{t_s,t_f} |^2]$ and $E[| h_{j,r}^{t_s,1} |^2] = E[| h_{j,r}^{t_s,2} |^2] = ... = E[| h_{j,r}^{t_s,F} |^2]$.

3. *Variable average channel gain scenario:* All the channels from the relay to the users and the users to the relay have unequal average channel gains and the channel conditions change after a block of T'_f ($T'_f < F$) time frames. That is, $E[| h_{1,r}^{t_s,t_f} |^2] \neq E[| h_{2,r}^{t_s,t_f} |^2] \neq ... \neq E[| h_{L,r}^{t_s,t_f} |^2]$ and $E[| h_{j,r}^{t_s,aT'_f+1} |^2] = E[| h_{j,r}^{t_s,aT'_f+2} |^2] = ... = E[| h_{j,r}^{t_s,(a+1)T'_f} |^2]$ for $j \in [1, L]$ and $0 \leq a \leq \frac{F}{T'_f} - 1$, where T'_f is the number of time frames after which the unequal average channel gains change.

The above scenarios can model a wide variety of practical channel scenarios. For example, the equal average channel gain scenario is applicable to satellite communications, where the users are equidistant from the relay. The unequal average channel gain scenario is applicable to fixed users (e.g., located at home or workplace) in a network, where the users' distances from the relay are unequal but remain fixed. The variable average channel gain scenario is applicable to mobile users in a network, where the users' distances from the relay are unequal and vary due to user mobility.

2.2 Signal Transmission Protocols

In this section, we discuss the signal transmission protocols based on lattice codes for a general MWRN. We denote each user by i, where $i \in [1, L]$. For the rest of this section, we consider message exchange within a certain time frame and a certain time slot and choose to omit the superscript t_f and t_s from the symbols for simplifying the notations.

2.2.1 Preliminaries on Lattice Codes

As our proposed system model is based on lattice codes, we first present the definitions of some primary operations on lattice codes, which we have used in the later subsections. Our notations for lattice codes follow those of [59,75]. Further details on lattice codes are available in [62,68,74,93,94].

An N-dimensional lattice is a discrete subgroup of the N-dimensional complex field $\mathbb{C}^N$ under the normal vector addition and reflection operations and can be expressed as [75,93,94]:

$$\Lambda = \{\lambda = \mathbf{G}_\Lambda c : c \in \mathbb{Z}^N\}, \tag{2.1}$$

where $\mathbf{G}_\Lambda \in \mathbb{C}^{N\times N}$ is the generator matrix corresponding to the lattice Λ and $\mathbb{Z}$ is the set of integers. This implies that if $\lambda_1, \lambda_2 \in \Lambda$, then $\lambda_1 + \lambda_2 \in \Lambda$ and if $\lambda \in \Lambda$, then $-\lambda \in \Lambda$. Note that a lattice is full-rank if its generator matrix $\mathbf{G}_\Lambda$ is full-rank.

- The nearest neighbour lattice quantizer maps a point $\mathbf{x} \in \mathbb{C}^N$ to a nearest lattice point $\lambda \in \Lambda$ in Euclidean distance [75]. That is,

$$Q_\Lambda(\mathbf{x}) = \arg\min_{\lambda} \|\mathbf{x} - \lambda\|^2. \tag{2.2}$$

- The modulo-Λ operation is defined by $\mathbf{x} \mod \Lambda = \mathbf{x} - Q_\Lambda(\mathbf{x})$ [59,68,74,93]. This can be interpreted as the error in quantizing $\mathbf{x}$ to the closest point in the lattice Λ.

- The fundamental Voronoi region $\mathcal{V}(\Lambda)$ denotes the set of all points in the N-dimensional complex field $\mathbb{C}^N$, which are closest to the zero vector [75], i.e.,

$$\mathcal{V}(\Lambda) = \{\mathbf{x} \in \mathbb{C}^N : Q_\Lambda(\mathbf{x}) = \mathbf{0}\}. \tag{2.3}$$

- $\psi(\cdot)$ denotes the mapping of messages from a finite dimensional field to lattice points, i.e., $\psi(\mathbf{w}) \in \Lambda$, where $\mathbf{w}$ is a message from a finite dimensional field.

- A coarse lattice Λ is nested in a fine lattice Λ_f, i.e., $\Lambda \subseteq \Lambda_f$, so that the messages mapped into fine lattice points remain in the Voronoi region of the coarse lattice. In this case, the coarse lattice Λ is said to be a sublattice of the fine lattice Λ_f.

- The dither vectors $\mathbf{d}$ are generated independently from a uniform distribution over the fundamental Voronoi region $\mathcal{V}(\Lambda)$. Dithering is a well known randomization technique which is necessary for achieving statistical independence between the input vector and the error vector [68].

2.2.2 Multiple Access Phase

In this phase, the users transmit in a pairwise manner using lattice codes and the relay receives the sum of the signals, i.e., in the i^{th} time slot, users i and $i+1$ transmit simultaneously.

2.2.2.1 Communication Protocol at the Users

In a certain time frame and the i^{th} time slot, the message packet of the i^{th} user is denoted by $\mathbf{W}_i = \{W_i^1, W_i^2, ..., W_i^T\}$, where the elements W_i^t are generated independently and uniformly over a finite field. Similarly, the message packet of the $(i+1)^{th}$ user at the i^{th} time slot is given by $\mathbf{W}_{i+1} = \{W_{i+1}^1, W_{i+1}^2, ..., W_{i+1}^T\}$.

During a certain time frame, at the $t_s = i^{th}$ time slot, the i^{th} and the $(i+1)^{th}$ user transmit their messages using lattice codes $\mathbf{X}_i = \{X_i^1, X_i^2, ..., X_i^T\}$ and $\mathbf{X}_{i+1} = \{X_{i+1}^1, X_{i+1}^2, ..., X_{i+1}^T\}$, respectively, which can be given by [36, 59]:

$$X_i^t = (\psi(W_i^t) + d_i) \mod \Lambda, \tag{2.4a}$$

$$X_{i+1}^t = (\psi(W_{i+1}^t) + d_{i+1}) \mod \Lambda, \tag{2.4b}$$

where d_i and d_{i+1} are the dither vectors for the i^{th} and the $(i+1)^{th}$ user, respectively. The dither vectors are generated at the users and transmitted to the relay prior to message transmission in the multiple access phase [75].

2.2.2.2 Communication Protocol at the Relay

The relay receives the signal $\mathbf{R}_{i,i+1} = \{r^1_{i,i+1}, r^2_{i,i+1}, ..., r^T_{i,i+1}\}$, where

$$r^t_{i,i+1} = \sqrt{P}h_{i,r}X^t_i + \sqrt{P}h_{i+1,r}X^t_{i+1} + n_1, \tag{2.5}$$

where n_1 is the zero mean complex AWGN at the relay with noise variance $\sigma^2_{n_1} = \frac{N_0}{2}$ per dimension.

2.2.3 Broadcast Phase

In this phase, the relay broadcasts the decoded or amplified network coded message depending on the relaying protocol and each user receives it.

2.2.3.1 Communication Protocol at the Relay

Functional Decode and Forward:

In this case, the relay scales the received signal with a scalar coefficient α and removes the dithers d_i, d_{i+1} scaled by $\sqrt{P}h_{i,r}$ and $\sqrt{P}h_{i+1,r}$, respectively [62]. The resulting signal is given by

$$\begin{aligned} X^t_r &= [\alpha r^t_{i,i+1} - \sqrt{P}h_{i,r}d_i - \sqrt{P}h_{i+1,r}d_{i+1}] \mod \Lambda \\ &= [\sqrt{P}h_{i,r}X^t_i + \sqrt{P}h_{i+1,r}X^t_{i+1} + (\alpha-1)\sqrt{P}(h_{i,r}X^t_i + h_{i+1,r}X^t_{i+1}) + \alpha n_1 - \sqrt{P}h_{i,r}d_i \\ &- \sqrt{P}h_{i+1,r}d_{i+1}] \mod \Lambda \\ &= [\sqrt{P}h_{i,r}\psi(W^t_i) + \sqrt{P}h_{i+1,r}\psi(W^t_{i+1}) + n] \mod \Lambda, \end{aligned} \tag{2.6}$$

where $n = (\alpha-1)\sqrt{P}(h_{i,r}X^t_i + h_{i+1,r}X^t_{i+1}) + \alpha n_1$ and α is chosen to minimize the noise variance [68,74].

The relay decodes the signal in (2.6) with a lattice quantizer [62, 68] to obtain an estimate $\hat{\mathbf{V}}_{i,i+1} = \{\hat{V}^1_{i,i+1}, \hat{V}^2_{i,i+1}, ..., \hat{V}^T_{i,i+1}\}$ which is a function of the messages $\mathbf{W}_i$ and

$\mathbf{W}_{i+1}$. Since, for sufficiently large N, $\Pr(n \notin \mathcal{V})$ approaches zero [62], $\hat{\mathbf{V}}_{i,i+1}$ converges to $(\psi(\mathbf{W}_i) + \psi(\mathbf{W}_{i+1})) \mod \Lambda$ with high probability. The relay then adds a dither d_r to the network coded message which is generated at the relay and broadcast to the users prior to message transmission in the broadcast phase [75]. Then it broadcasts the resulting message using lattice codes, which is given as $\mathbf{Z}_{i,i+1} = \{Z^1_{i,i+1}, Z^2_{i,i+1}, ..., Z^T_{i,i+1}\}$, where $Z^t_{i,i+1} = (\hat{V}^t_{i,i+1} + d_r) \mod \Lambda$.

Amplify and Forward:

In this case, similar to FDF relaying, the relay amplifies the received signal with scalar coefficient α [95] and removes the dithers d_i, d_{i+1} scaled by $\sqrt{P}h_{i,r}$ and $\sqrt{P}h_{i+1,r}$, respectively to obtain X^t_r as in (2.6). Then, instead of decoding, the relay simply adds a dither d_r to $\mathbf{X}_r$ and broadcasts the resulting signal $\mathbf{Z}_{i,i+1} = (\mathbf{X}_r + d_r) \mod \Lambda$ to all the users. Note that, in this case, the relay does not need to use the lattice quantizer like FDF relaying, and hence, this allows lower signal processing complexity at the relay.

2.2.3.2 Communication Protocol at the Users

The j^{th} user receives $\mathbf{Y}_{i,i+1} = \{Y^1_{i,i+1}, Y^2_{i,i+1}, ..., Y^T_{i,i+1}\}$, where

$$Y^t_{i,i+1} = \sqrt{P_r}h_{r,j}Z^t_{i,i+1} + n_2, \tag{2.7}$$

and n_2 is the zero mean complex AWGN at the user with noise variance $\sigma^2_{n_2} = \frac{N_0}{2}$ per dimension.

At the end of the broadcast phase, each user performs the following operations on the received signal based on the relaying protocol:

Functional Decode and Forward:

The j^{th} user scales the received signal with a scalar coefficient β_j and removes the dithers d_r multiplied by $\sqrt{P_r}h_{r,j}$. The resulting signal is

$$\begin{aligned}[\beta_j Y^t_{i,i+1} - \sqrt{P_r}h_{r,j}d_r] \mod \Lambda =& [\sqrt{P_r}h_{r,j}\hat{V}^t_{i,i+1} + (\beta_j - 1)\sqrt{P_r}h_{r,j}\hat{V}^t_{i,i+1} + \beta_j n_2] \mod \Lambda \\ =& [\sqrt{P_r}h_{r,j}\hat{V}^t_{i,i+1} + n'] \mod \Lambda, \end{aligned} \tag{2.8}$$

where $n' = \sqrt{P_r}h_{r,j}(\beta_j - 1)\hat{V}^t_{i,i+1} + \beta_j n_2$ and β_j is chosen to minimize the noise variance [75].

<u>*Amplify and Forward*</u>:

The j^{th} user scales the received signal with a scalar coefficient β_j and removes the dithers d_r multiplied by $\sqrt{P_r}h_{r,j}$. The resulting signal is

$$\begin{aligned}[\beta_j Y^t_{i,i+1} - \sqrt{P_r}h_{r,j}d_r] \mod \Lambda =& [\sqrt{P_r}h_{r,j}X^t_r + (\beta_j - 1)\sqrt{P_r}h_{r,j}X^t_r + \beta_j n_2] \mod \Lambda \\ =& [\sqrt{P_r}h_{r,j}\sqrt{P}h_{i,r}\psi(W^t_i) + \sqrt{P_r}h_{r,j}\sqrt{P}h_{i+1,r}\psi(W^t_{i+1}) + n'] \\ & \mod \Lambda, \end{aligned} \tag{2.9}$$

where $n' = \sqrt{P_r}h_{r,j}n + \sqrt{P_r}h_{r,j}(\beta_j - 1)X^t_r + \beta_j n_2$ and β_j is chosen to minimize the noise variance [75].

Finally, for both the relaying protocols, the users then detect the received signal with a lattice quantizer [75] and obtain the estimate $\hat{\hat{\mathbf{V}}}_{i,i+1}$ that approaches $(\psi(\mathbf{W}_i) + \psi(\mathbf{W}_{i+1})) \mod \Lambda$, assuming that the lattice dimension is large enough such that $\Pr(n' \notin \mathcal{V})$ approaches zero. After decoding all the network coded messages, each user performs message extraction of every other user by canceling self information.

2.2.3.3 Message Extraction

At first, the i^{th} user subtracts the scaled lattice point corresponding to its own message, i.e., $\psi(\mathbf{W}_i)$ from the network coded message received in the $(i+1)^{th}$ time slot (i.e., $\hat{\hat{\mathbf{V}}}_{i,i+1}$) and extracts the message of the $(i+1)^{th}$ user as $\psi(\hat{\mathbf{W}}_{i+1})$. After that, it utilizes the extracted message of the $(i+1)^{th}$ user to obtain the messages of the $(i+2)^{th}$ user to the L^{th} user in the downward extraction process in a similar manner. The downward message extraction process can be shown as

$$
\begin{aligned}
\psi(\hat{\mathbf{W}}_{i+1}) =& (\hat{\hat{\mathbf{V}}}_{i,i+1} - \psi(\mathbf{W}_i)) \mod \Lambda, \\
\psi(\hat{\mathbf{W}}_{i+2}) =& (\hat{\hat{\mathbf{V}}}_{i+1,i+2} - \psi(\hat{\mathbf{W}}_{i+1})) \mod \Lambda, \\
& \vdots \\
\psi(\hat{\mathbf{W}}_{L}) =& (\hat{\hat{\mathbf{V}}}_{L-1,L} - \psi(\hat{\mathbf{W}}_{L-1})) \mod \Lambda.
\end{aligned} \tag{2.10}
$$

Similarly the upward message extraction process can be performed to obtain the messages of the $(i-1)^{th}$ user to the 1^{st} user in the following manner:

$$
\begin{aligned}
\psi(\hat{\mathbf{W}}_{i-1}) =& (\hat{\hat{\mathbf{V}}}_{i-1,i} - \psi(\mathbf{W}_i)) \mod \Lambda, \\
\psi(\hat{\mathbf{W}}_{i-2}) =& (\hat{\hat{\mathbf{V}}}_{i-2,i-1} - \psi(\hat{\mathbf{W}}_{i-1})) \mod \Lambda, \\
& \vdots \\
\psi(\hat{\mathbf{W}}_{1}) =& (\hat{\hat{\mathbf{V}}}_{1,2} - \psi(\hat{\mathbf{W}}_{2})) \mod \Lambda.
\end{aligned} \tag{2.11}
$$

Once $\psi(\cdot)$ has been obtained, the user performs $\psi^{-1}(\cdot)$ operation to actually obtain the messages. So, wherever we write equations similar to above, this extra demapping step is understood.

2.3 Prior Results on MWRN Performance

In this section, we discuss the results on different performance metrics of a MWRN, that have already been reported in the literature of MWRNs. This allows us to present benchmark results on MWRNs with which we can compare the performance of our designed schemes in the later chapters. Previous works on MWRNs have measured the system performance in terms of common rate [50, 59], sum rate [49, 67, 76] and error performance [57, 76]. Though recently, research has been done regarding the degrees of freedom performance of MWRNs [43, 96], in our thesis, we consider only common rate, sum rate and error performance metrics to characterize MWRNs.

2.3.1 Common Rate

Common rate indicates the maximum possible information rate of the system that can be exchanged with negligible error. It can be a useful metric for systems where all users have the same amount of information to exchange or when the users are allocated with the same uplink bandwidth [59]. For a MWRN with symmetric traffic, the common rate $R = R_i$ for $i \in [1, L]$ is achievable, if and only if the rate tuple $(R, R, ..., R)$ is achievable. It has been shown in [59], that using the cut-set theorem [97], the common rate in an AWGN MWRN with FDF relaying can be upper bounded as follows:

$$R \leq \min_{\ell \in [1, L-1]} \left\{ \frac{1}{2\ell} \log \left(1 + \ell^2 \frac{P}{N_0} \right), \frac{1}{2(L-1)} \log \left(1 + \frac{P_r}{N_0} \right) \right\}, \tag{2.12}$$

where the first term on the right hand side is obtained from the cut separating the sets U and $U^c \cup R$. The second term is from the cut separating $U \cup R$ and U^c and $U \subset \{1, 2, ..., L\}$, $U^c = \{1, 2, ..., L\} \setminus U$ and R denotes the relay.

For an AWGN MWRN with AF relaying, the common rate can be upper bounded by [36]:

$$R \leq \frac{1}{2(L-1)} \log \left(1 + \frac{\frac{P}{N_0}}{1 + 2\frac{P}{P_r} + \frac{N_0}{P_r}} \right). \tag{2.13}$$

For a FDF MWRN with Rayleigh fading, the upper bound on the common rate has been obtained in [50] as:

$$R \leq \frac{1}{2(L-1)} \min_{\ell \in [1, L-1]} \left\{ \log \left(1 + \sum_{\ell=1}^{L-1} \frac{P|h_{\ell,r}|^2}{N_0} \right), \quad \log \left(1 + \frac{P_r|h_{\ell,r}|^2}{N_0} \right) \right\}. \tag{2.14}$$

In an AF MWRN with Rayleigh fading, an upper bound on the achievable common rate has been obtained in [49] as:

$$R \leq \min_{j, \ell \in [1, L], \ell \neq j} \frac{1}{2(L-1)} \log(1 + \gamma_{j,\ell}), \tag{2.15}$$

where $\gamma_{j,\ell}$ is the SNR of the ℓ^{th} user, received at the j^{th} user.

Very recently, lattice codes have been incorporated with MWRNs for their higher data rates and some rate results have been obtained only for FDF MWRNs.

In an AWGN MWRN with FDF relaying, the following common rate can be achieved using lattice codes [59]:

$$R \leq \frac{1}{2(L-1)} \min \left\{ \log\left(\frac{1}{2} + \frac{P}{N_0}\right), \quad \log\left(1 + \frac{P_r}{N_0}\right) \right\}. \tag{2.16}$$

For a FDF MWRN with Rayleigh fading, the achievable common rates using lattice codes has been derived in [50] as:

$$R \leq \frac{1}{2(L-1)} \min \left(\min_{\ell \in [1, L-1]} \left(\log\left(\frac{1}{1 + \frac{|h_{\ell,r}|^2}{|h_{\ell+1,r}|^2}} + \frac{P|h_{\ell+1,r}|^2}{N_0} \right), \log\left(\frac{1}{1 + \frac{|h_{\ell+1,r}|^2}{|h_{\ell,r}|^2}} + \frac{P|h_{\ell,r}|^2}{N_0} \right) \right), \right.$$
$$\left. \min_{\ell \in [1, L]} \log\left(1 + \frac{P_r |h_{\ell,r}|^2}{N_0}\right) \right). \tag{2.17}$$

2.3.2 Sum Rate

The sum rate indicates the maximum throughput of the system. For a MWRN, the sum rate can be defined as the sum of the achievable rates of all users for a complete round of information exchange.

An upper bound on the achievable sum rate of an AWGN MWRN with FDF relaying has been derived in [59] as:

$$R_s \leq \min_{\ell \in [1, L-1]} \left\{ \frac{1}{2} \log\left(1 + \ell^2 \frac{P}{N_0}\right), \frac{1}{2} \log\left(1 + \frac{P_r}{N_0}\right) \right\}. \tag{2.18}$$

In an AWGN MWRN with AF relaying, an upper bound on the achievable sum rate has been obtained in [36] as:

$$R_s \leq \frac{1}{2} \log\left(1 + \frac{\frac{P}{N_0}}{1 + 2\frac{P}{P_r} + \frac{N_0}{P_r}}\right). \tag{2.19}$$

In a FDF MWRN with AWGN channel, the sum rate using lattice codes has been upper bounded in [59] as:

$$R_s \leq \frac{1}{2} \min \left\{ \log\left(\frac{1}{2} + \frac{P}{N_0}\right), \log\left(1 + \frac{P_r}{N_0}\right) \right\}. \tag{2.20}$$

In an AF MWRN with Rayleigh fading, an upper bound on the sum rate has been obtained in [49] as:

$$R_s \leq \sum_{\ell=1}^{L-1} \sum_{j=1}^{L} \min_{j,\ell \in [1,L], \ell \neq j} \frac{1}{2(L-1)} \log(1 + \gamma_{j,\ell}). \tag{2.21}$$

For FDF and AF MWRNs with lattice codes and Rayleigh fading, the achievable rates have not been investigated yet in the literature.

2.3.3 Error Performance

For an error-free communication in a MWRN, each user must correctly decode the information from *all* other users. Depending on the number of users whose information is incorrectly decoded by a certain user, different error events can occur. Previous works have focused on characterizing the special cases of error events such as $k \geq 1$ [57] for AF MWRNs, which can be given by:

$$P(k \geq 1) = 1 - \sum_{j=1, j \neq i}^{L} (1 - P(i,j)), \tag{2.22}$$

where, $P(i,j)$ denotes the probability that the i^{th} user incorrectly decodes the j^{th} user's message. However, the error probability for the general case of k error events in an L-user MWRN has not been addressed yet in the literature. In addition, the discrete error events offer only a partial view of the overall error performance. For a complete characterization of the error performance, we need a metric that takes into account all the error events, as well as their relative impacts. Hence, we are going to consider the average BER as the error performance metric for a MWRN for the rest of this thesis.

2.4 Summary

In this chapter, we have discussed the general system model assumptions adopted for MWRN performance analysis. Specifically, we discussed the preliminaries on lattice codes in Section 2.2.1 and the transmission protocols in Sections 2.2.2 and 2.2.3. Also, we discussed some existing results on MWRN performance in Section 2.3.

Chapter 3

Error Performance Analysis of FDF and AF Multi-way Relay Networks

In the previous chapter, we discussed the general system model assumptions and existing performance results for FDF and AF MWRNs. In this chapter, we characterize error propagation and obtain the error performance results for FDF and AF MWRNs in AWGN channel, as well as Rayleigh fading channels for BPSK modulation which is the simplest case of lattice codes.

The chapter is organized in the following manner. The system model is presented in Section 3.1. The challenges associated with the characterization of the error performance in MWRNs are discussed in Section 3.2. The asymptotic bounds on the error probability for the general case of k error events and the average BER for a user in FDF and AF MWRNs are derived in Section 3.3 and Section 3.4, respectively. The analysis is extended to include Rayleigh fading in Section 3.6. Section 3.7 provides the simulation results for verification of the analytical solutions. Finally, a summary of the contributions in this chapter is provided in Section 3.8.

3.1 System Model

Throughout this chapter, we concentrate on a MWRN in which all user transmissions are based on BPSK modulation, the simplest form of lattice codes. This analysis can be extended to incorporate higher order modulation schemes, as well. Moreover, in this

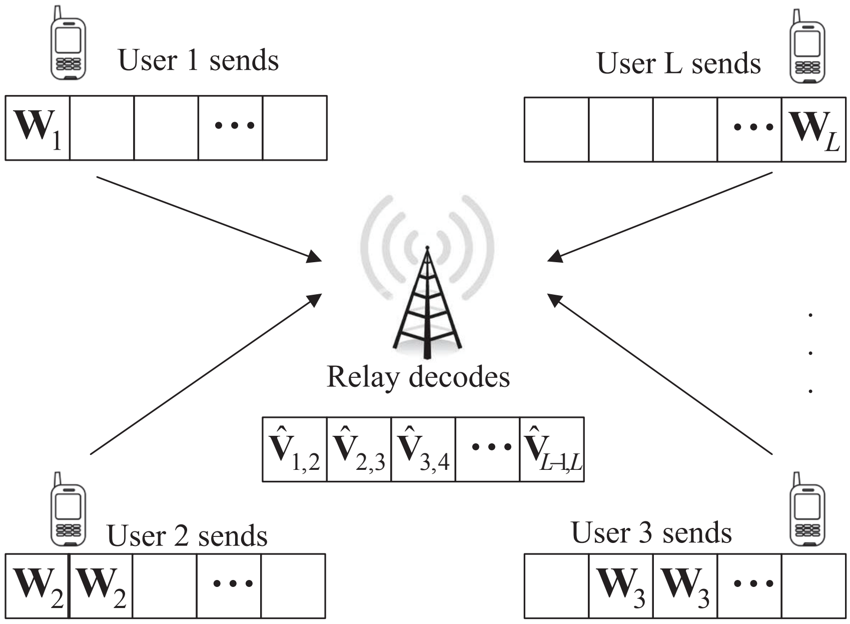

(a) MAC phase

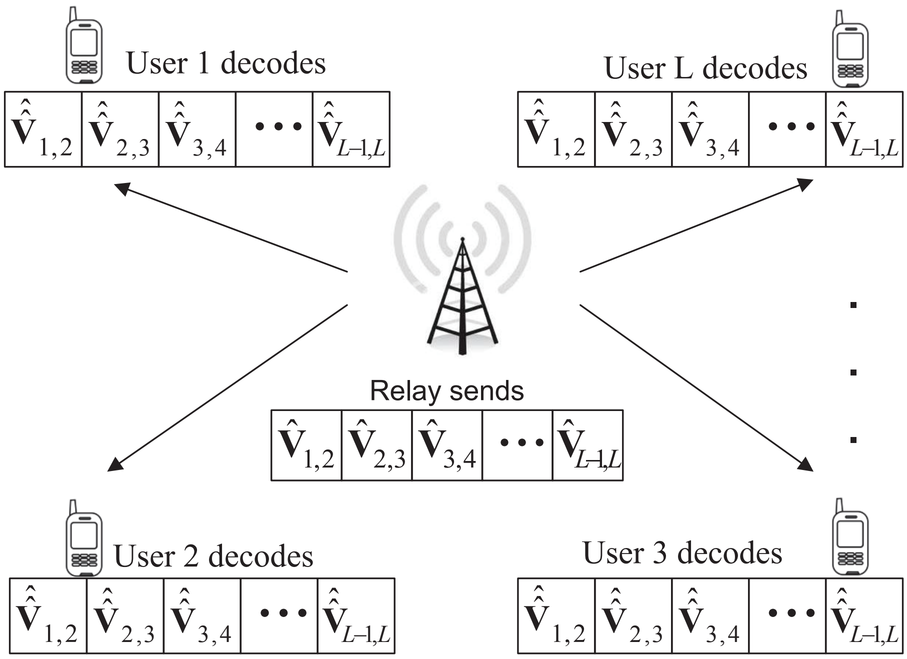

(b) BC phase

Figure 3.1: System model for an L-user functional decode and forward (FDF) multi-way relay network (MWRN), where the users exchange information with each other via the relay R. The mathematical symbols are explained in Sections 3.1.2 and 3.1.3.

section, we assume that all the channels are corrupted by AWGN only. Later in Section 3.6, we extend the model to Rayleigh fading channels.

Now we specialize the signal transmission protocols for BPSK modulation in an AWGN MWRN with FDF and AF relaying.

3.1.1 Transmission Protocol at the Users (for both FDF and AF)

Let the i^{th} and the $(i+1)^{\text{th}}$ user transmit binary message packets, $\mathbf{W}_i = \{W_i^1, W_i^2, ..., W_i^T\}$ and $\mathbf{W}_{i+1} = \{W_{i+1}^1, W_{i+1}^2, ..., W_{i+1}^T\}$, which are BPSK modulated to $\mathbf{X}_i = \{X_i^1, X_i^2, ..., X_i^T\}$ and $\mathbf{X}_{i+1} = \{X_{i+1}^1, X_{i+1}^2, ..., X_{i+1}^T\}$ respectively, where $W_i^t \in \{0, 1\}$ and $X_i^t \in \{\pm 1\}$. The relay receives the signal $\mathbf{R}_{i,i+1} = \{r_{i,i+1}^1, r_{i,i+1}^2, ..., r_{i,i+1}^T\}$, where

$$r_{i,i+1}^t = X_i^t + X_{i+1}^t + n_1, \tag{3.1}$$

where n_1 is the zero mean AWGN in the user-relay link with noise variance $\sigma_{n_1}^2 = \frac{N_0}{2}$. The distribution of the received signal is shown on Fig. 3.2.

Depending on the relay protocol (i.e., FDF or AF), the relay makes use of the received signal $\mathbf{R}_{i,i+1}$ in different ways, which is discussed in the next two subsections.

3.1.2 Transmission Protocol at the Relay for FDF Relaying

The relay first decodes the superimposed received signal $\mathbf{R}_{i,i+1}$, using the maximum a posteriori (MAP) criterion, to obtain $\hat{\mathbf{V}}_{i,i+1} = \{\hat{V}_{i,i+1}^1, \hat{V}_{i,i+1}^2, ..., \hat{V}_{i,i+1}^T\}$ (as illustrated in Fig. 3.1(a)), which is an estimate of the true network coded symbol, $\mathbf{V}_{i,i+1} = \mathbf{W}_i \oplus \mathbf{W}_{i+1}$, transmitted by the users, where $\oplus$ denotes XOR operation. The optimum threshold, γ_r, as denoted in Fig. 3.2, for MAP detection at the relay is derived in [15] and is defined later in Section 3.3 after (3.10). The relay then performs BPSK modulation on the recovered network coded symbol and retransmits to all the users, which receive a noisy version of the signal as $\mathbf{Y}_{i,i+1} = \{Y_{i,i+1}^1, Y_{i,i+1}^2, ..., Y_{i,i+1}^T\}$, where

$$Y_{i,i+1}^t = Z_{i,i+1}^t + n_2, \tag{3.2}$$

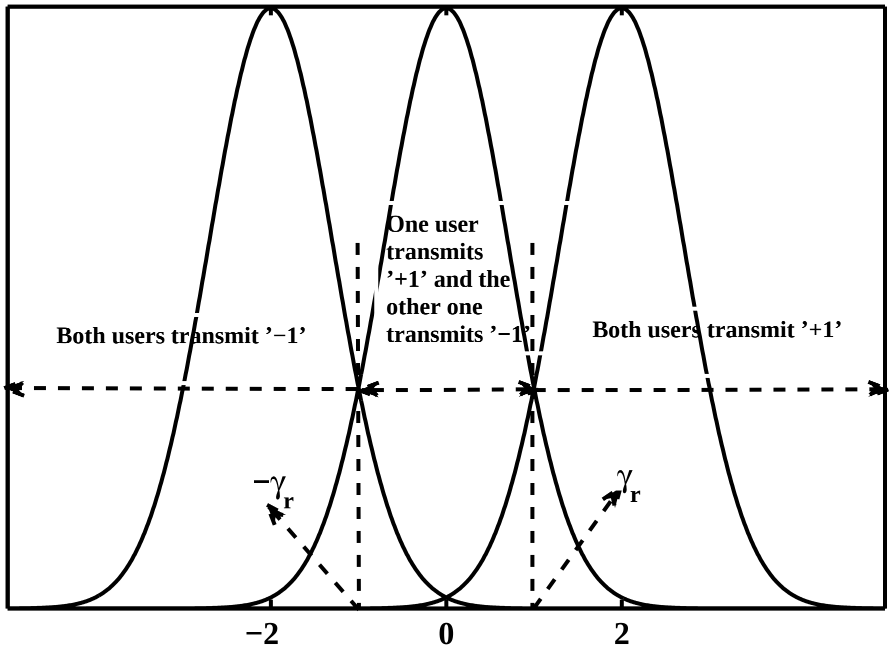

Figure 3.2: Distribution of the received signal with optimum threshold.

where $Z^t_{i,i+1} \in \{\pm 1\}$ is the relay's transmitted signal and n_2 is the zero mean AWGN in the relay-user link with noise variance $\sigma_2^2 = \frac{N_0}{2}$.

3.1.3 Message Extraction for FDF relaying

Each user receives and decodes the signal $\mathbf{Y}_{i,i+1}$ using MAP criterion to obtain the network coded symbol $\hat{\hat{\mathbf{V}}}_{i,i+1}$ (illustrated in Fig. 3.1(b)). The optimum threshold, γ, for MAP detection at the users is defined later in Section 3.3 after (3.10). After decoding the network coded information of all the user pairs, the i^{th} user performs XOR operation between its own information symbols $\mathbf{W}_i$ and the decoded symbols $\hat{\hat{\mathbf{V}}}_{i,i+1}$ to extract the information of the $(i+1)^{\text{th}}$ user as

$$\hat{\mathbf{W}}_{i+1} = \hat{\hat{\mathbf{V}}}_{i,i+1} \oplus \mathbf{W}_i. \tag{3.3}$$

This process is continued upward and downward until all the users' transmitted information is recovered. The sequential downward information extraction process can be expressed as

$$\hat{\mathbf{W}}_{i+2} = \hat{\hat{\mathbf{V}}}_{i+1,i+2} \oplus \hat{\mathbf{W}}_{i+1}, \tag{3.4a}$$

$$\ldots, \tag{3.4b}$$

$$\hat{\mathbf{W}}_{L} = \hat{\hat{\mathbf{V}}}_{L-1,L} \oplus \hat{\mathbf{W}}_{L-1}. \tag{3.4c}$$

Note that for all users other than the first user, the sequential upward information extraction process is also performed, i.e., $\hat{\mathbf{W}}_{i-1} = \hat{\hat{\mathbf{V}}}_{i-1,i} \oplus \mathbf{W}_i$, $\hat{\mathbf{W}}_{i-2} = \hat{\hat{\mathbf{V}}}_{i-2,i-1} \oplus \hat{\mathbf{W}}_{i-1}, \ldots,$ $\hat{\mathbf{W}}_1 = \hat{\hat{\mathbf{V}}}_{1,2} \oplus \hat{\mathbf{W}}_2$.

3.1.4 Transmission Protocol at the Relay for AF Relaying

The relay amplifies the superimposed received signal $\mathbf{R}_{i,i+1}$ with an amplification factor α and then retransmits to all the users, which receive a noisy version of this retransmitted signal as $\mathbf{Y}_{i,i+1} = Y^1_{i,i+1}, Y^2_{i,i+1}, ..., Y^T_{i,i+1}$, where $Y^t_{i,i+1}$ can be given as:

$$Y^t_{i,i+1} = \alpha(X^t_i + X^t_{i+1} + n_1) + n_2, \tag{3.5}$$

where with no loss of generality we assume that $P = P_r = 1$ and $\alpha = \sqrt{\frac{1}{2+\frac{N_0}{2}}}$ is chosen to maintain unity power at the relay.

3.1.5 Message Extraction for AF relaying

The i^{th} user subtracts its own signal multiplied by α from the received signal $\mathbf{Y}_{i,i+1}$ and then performs maximum likelihood (ML) detection on the resulting signal to estimate the message of the $(i+1)^{\text{th}}$ user as

$$\hat{\mathbf{W}}_{i+1} = \arg \min_{X^t_i \in \{\pm 1\}} \mid \mathbf{Y}_{i,i+1} - \alpha \mathbf{X}_i \mid^2 . \tag{3.6}$$

Then, the i^{th} user utilizes the BPSK modulated version of this extracted message, i.e.,

$\hat{\mathbf{X}}_{i+1}$ to obtain the message of the $(i+2)^{\text{th}}$ user in the same manner. This process is continued until all the users' transmitted messages are recovered. The sequential downward message extraction process can be expressed as

$$\hat{\mathbf{W}}_{i+2} = \arg \min_{\hat{X}^t_{i+1} \in \{\pm 1\}} \mid \mathbf{Y}_{i+1,i+2} - \alpha \hat{\mathbf{X}}_{i+1} \mid^2, \tag{3.7a}$$

$$\ldots, \tag{3.7b}$$

$$\hat{\mathbf{W}}_{L} = \arg \min_{\hat{X}^t_{L-1} \in \{\pm 1\}} \mid \mathbf{Y}_{L-1,L} - \alpha \hat{\mathbf{X}}_{L-1} \mid^2 . \tag{3.7c}$$

Note that for all users other than the first user, the sequential upward message extraction process can similarly be performed.

3.2 Characterizing the Error Performance in a MWRN

As discussed in Chapter 2, for a complete characterization of the error performance, we need a metric that takes into account all the error events, as well as their relative impacts. Hence, we choose the average BER as the error performance metric for a MWRN.

The average BER for the i^{th} user in a MWRN can be defined as the expected probability of all the error events, that is,

$$P_{i,avg} = \frac{1}{L-1} \sum_{k=1}^{L-1} k P_i(k), \tag{3.8}$$

where $P_i(k)$, for $k \in [1, L-1]$, represents the probability of exactly k errors at the i^{th} user, the factor k represents number of errors in the k^{th} error event and $L-1$ denotes the number of possible error events. Note that the average BER in (3.8) is the average across the message packets of all the users decoded by a user.

The average BER depends on the probability of exactly k error events, which is given by

$$P_i(k) = \frac{\text{Number of events where the } i^{\text{th}} \text{ user incorrectly decodes } k \text{ users' messages}}{\text{Packet length, } T}. \tag{3.9}$$

It is not straightforward to characterize the error probability $P_i(k)$ for the general case of k error events and consequently the average BER for a user in a MWRN due to following two main reasons. Firstly, in a FDF or AF MWRN, the decision about each user depends on the decision about previously decoded users. For example, according to (3.3) and (3.4a) in a FDF MWRN, if an error occurs in the message extraction process, the error propagates through to the following messages, until another error is made. Also according to (3.6) and (3.7a) in an AF MWRN, the mean of the next signal is shifted from its true value by the previous error. These dependencies will be explained in detail in Sections 3.3 and 3.4, respectively. Secondly, while a TWRN has only one possible error event, i.e, only one user's message can be incorrectly decoded, an L-user MWRN consists of $(L-1)$ user pairs and so $(L-1)$ error events are possible. The set of events can be quite large, depending on the number of users.

In the next two sections, we address these challenges and characterize the error probability $P_i(k)$ for the general case of k error events and the average BER for a user in FDF and AF MWRN.

3.3 Probability of k Error Events and Average BER for a User in FDF MWRN

In this section, we first derive exact closed-form expressions for the probability of $k = 1$ and $k = 2$ error events in an L-user FDF MWRN. Based on the insights provided by this analysis, we then obtain an approximate expression for the probability of $k \geq 3$ error events $P_i(k)$ at high SNR, which we use to obtain the average BER for a user.

First, we obtain the probability of incorrectly decoding a network coded message at any user.

Lemma 3.1. *The probability that the network coded message of any one user pair is incorrectly decoded, is given by*

$$\begin{aligned} P_{FDF} =& \frac{1}{8}\left[erfc\left(\frac{-\gamma-1}{\sqrt{N_0}}\right)\left\{ erf\left(\frac{\gamma_r+2}{\sqrt{N_0}}\right) + erf\left(\frac{\gamma_r-2}{\sqrt{N_0}}\right) + 2erfc\left(\frac{\gamma_r}{\sqrt{N_0}}\right) \times \right.\right. \\ & erfc\left.\left(\frac{\gamma-1}{\sqrt{N_0}}\right)\right\} + erfc\left(\frac{1-\gamma}{\sqrt{N_0}}\right)\left\{ erfc\left(\frac{\gamma_r+2}{\sqrt{N_0}}\right) + erfc\left(\frac{\gamma_r-2}{\sqrt{N_0}}\right) + \right. \\ & \left.\left. 2erf\left(\frac{\gamma_r}{\sqrt{N_0}}\right) erfc\left(\frac{\gamma+1}{\sqrt{N_0}}\right)\right\}\right], \end{aligned} \tag{3.10}$$

where $\gamma_r = 1 + \frac{N_0}{4}\ln\left(1+\sqrt{1-e^{-8/N_0}}\right)$ *[15] and*

$$\gamma = \frac{N_0}{4}\ln\left(4\left(erfc\left(\frac{\gamma_r+2}{\sqrt{N_0}}\right) + erfc\left(\frac{\gamma_r-2}{\sqrt{N_0}}\right) + 2erfc\left(\frac{\gamma_r}{\sqrt{N_0}}\right)\right)^{-1} - 1\right), \tag{3.11}$$

are the optimum thresholds for MAP detection at the relay and user, respectively and $erf(x) = \frac{2}{\sqrt{\pi}}\int_0^x e^{-t^2}dt$ *and* $erfc(x) = \frac{2}{\sqrt{\pi}}\int_x^\infty e^{-t^2}dt$ *are the error function and complementary error function, respectively.*

Proof. A network coded message can be incorrectly decoded (i.e., $\hat{\hat{\mathbf{V}}}_{i,i+1} \neq \mathbf{V}_{i,i+1}$) in two cases. Either the relay makes an error to estimate the network coded message and the destination correctly decodes the message from the relay ($\hat{\mathbf{V}}_{i,i+1} \neq \mathbf{V}_{i,i+1}$ and $\hat{\hat{\mathbf{V}}}_{i,i+1} = \hat{\mathbf{V}}_{i,i+1}$) or the relay has correctly decoded the network coded message but the destination wrongly detects the message from the relay ($\hat{\mathbf{V}}_{i,i+1} = \mathbf{V}_{i,i+1}$ and $\hat{\hat{\mathbf{V}}}_{i,i+1} \neq \hat{\mathbf{V}}_{i,i+1}$). The probability that the relay has made an error is given by [15]:

$$\Pr(\hat{\mathbf{V}}_{i,i+1} \neq \mathbf{V}_{i,i+1}) = \frac{1}{2}\text{erfc}\left(\frac{\gamma_r}{\sqrt{N_0}}\right) + \frac{1}{4}\text{erf}\left(\frac{\gamma_r+2}{\sqrt{N_0}}\right) + \frac{1}{4}\text{erf}\left(\frac{\gamma_r-2}{\sqrt{N_0}}\right), \tag{3.12}$$

where, the first term in (3.12) indicates the case when the users transmit dissimilar signals and the network coded message is detected as '1' instead of '0'. The last two terms indicate the case when the users transmit similar signals and the network coded message is detected as '0' instead of '1'.

The probability of incorrectly decoding the network coded message from the relay at the users, would be similar to that of incorrectly decoding a BPSK signal. Then using the fact that $\Pr(\hat{\hat{\mathbf{V}}}_{i,i+1} \neq \mathbf{V}_{i,i+1}) = (1 - \Pr(\hat{\mathbf{V}}_{i,i+1} \neq \mathbf{V}_{i,i+1}))\Pr(\hat{\hat{\mathbf{V}}}_{i,i+1} \neq \hat{\mathbf{V}}_{i,i+1}) + (1 - \Pr(\hat{\hat{\mathbf{V}}}_{i,i+1} \neq \hat{\mathbf{V}}_{i,i+1}))\Pr(\hat{\mathbf{V}}_{i,i+1} \neq \mathbf{V}_{i,i+1})$, (3.10) can be obtained with some simple algebraic manipulations. □

The expression in (3.10) will be used to obtain the probabilities of different error events through the following analysis.

3.3.1 Probability of $k = 1$ Error Event

Lemma 3.2. *The exact probability of one error event in a FDF MWRN can be expressed as*

$$P_{i,FDF}(1) = \begin{cases} (L-3)P_{A_1} + 2P_{B_1}, & i \neq 1 \text{ and } i \neq L \\ (L-2)P_{A_1} + P_{B_1}, & i = 1 \text{ or } i = L \end{cases} \tag{3.13}$$

where A_1 and B_1 are the following error cases for $k = 1$ error event:

- *error case A_1: two consecutive erroneous network coded messages or,*
- *error case B_1: an error in the network coded messages involving one of the end users.*

The probabilities of the above error cases are given as:

$$P_{A_1} = (1 - P_{FDF})^{L-3} P_{FDF}^2, \tag{3.14a}$$

$$P_{B_1} = (1 - P_{FDF})^{L-2} P_{FDF}, \tag{3.14b}$$

where P_{FDF} is defined as in (3.10).

Before providing the formal proof, consider the following simple example.

Example 3.1. *As illustrated in Table 3.1, error case A_1 can occur when user 1 wrongly decodes the message of user 2 by making consecutive errors in the detection of $\hat{\hat{\boldsymbol{V}}}_{1,2}$ and $\hat{\hat{\boldsymbol{V}}}_{2,3}$. Similarly, error case B_1 can occur if there is an error in the decoding of $\hat{\hat{V}}_{1,2}$ at any user $i \neq 1$ (or $\hat{\hat{\boldsymbol{V}}}_{L-1,L}$*

Table 3.1: Illustration of the error cases for one and two error events in a 10-user FDF MWRN. Here, ✓and × represent correct and incorrect detection, respectively.

Error case	Decoding user i	$\hat{\mathbf{V}}_{1,2}$	$\hat{\mathbf{V}}_{2,3}$	$\hat{\mathbf{V}}_{3,4}$	$\hat{\mathbf{V}}_{4,5}$	$\hat{\mathbf{V}}_{5,6}$	$\hat{\mathbf{V}}_{6,7}$	$\hat{\mathbf{V}}_{7,8}$	$\hat{\mathbf{V}}_{8,9}$	$\hat{\mathbf{V}}_{9,10}$	Error event
		Network coded message									
A_1	$i \in \{1, L\}$	×	×	✓	✓	✓	✓	✓	✓	✓	1
B_1	$i \neq 1$	×	✓	✓	✓	✓	✓	✓	✓	✓	1
B_1	$i \neq L$	✓	✓	✓	✓	✓	✓	✓	✓	×	1
C_1	$i \in \{1, L\}$	×	✓	×	✓	✓	✓	✓	✓	✓	2
D_1	$i \neq 1, 2$	✓	×	✓	✓	✓	✓	✓	✓	✓	2
D_1	$i \neq L-1, L$	✓	✓	✓	✓	✓	✓	✓	×	✓	2
E_1	$i \in \{1, L\}$	✓	×	×	✓	×	×	✓	✓	✓	2
F_1	$i \neq 1$	×	✓	✓	✓	×	×	✓	✓	✓	2
F_1	$i \neq L$	✓	✓	✓	✓	×	×	✓	✓	×	2
G_1	$i \neq 1, L$	×	✓	✓	✓	✓	✓	✓	✓	×	2

at any user $i \neq L$). Note that the error examples shown in Table 3.1 are not unique and other combinations of errors are also possible.

Proof. see Appendix A.1. □

3.3.2 Probability of $k = 2$ Error Events

Lemma 3.3. *The exact probability of two error events in a FDF MWRN can be expressed as*

$$P_{i,FDF}(2) = \begin{cases} (L-3)P_{C_1} + P_{D_1} + \sum_{m=2}^{L-3}(L-2-m)P_{E_1} + \\ (L-3)P_{F_1}, & i = 1 \text{ or } i = L \\ (L-4)P_{C_1} + P_{D_1} + \sum_{m=2}^{L-4}(L-3-m)P_{E_1} + \\ 2(L-4)P_{F_1} + P_{C_1}, & i = 2 \text{ or } i = L-1 \\ (L-5)P_{C_1} + 2P_{D_1} + \sum_{m=2}^{L-4}(L-3-m)P_{E_1} + \\ 2(L-4)P_{F_1} + P_{C_1}, & i = 3 \text{ or } i = L-2 \\ (L-5)P_{C_1} + 2P_{D_1} + \sum_{m=2}^{i-2}(L-4-m)P_{E_1} + \\ \sum_{m=i-1}^{L-i-1}(L-3-m)P_{E_1} + \sum_{m=L-i}^{L-3}(L-2-m)P_{E_1} + \\ 2(L-4)P_{F_1} + P_{C_1}, & i \notin \{1,2,3,L-2,L-1,L\} \end{cases} \quad (3.15)$$

where m is the decoding order difference between the two users that are incorrectly decoded,

$(L-2-m)$ *indicates the number of such user pairs and* C_1*,* D_1*,* E_1*,* F_1 *and* G_1 *are the error cases for* $k=2$ *error event, defined as:*

- *error case* C_1*: if two wrong network coded messages are separated by one correct network coded message or,*
- *error case* D_1*: if the network coded message involving one end user is correct but the following (or preceding) message is incorrect or,*
- *error case* E_1*: if there are two pairs of consecutive erroneous network coded messages or,*
- *error case* F_1*: if the network coded message involving one end user, as well as two other consecutive network coded messages, are incorrect or,*
- *error case* G_1*: if the network coded messages involving both the end users are incorrect.*

The probabilities of the above error cases are given by:

$$P_{C_1} = (1-P_{FDF})^{L-3}P_{FDF}^2, \tag{3.16a}$$

$$P_{D_1} = (1-P_{FDF})^{L-2}P_{FDF}, \tag{3.16b}$$

$$P_{E_1} = (1-P_{FDF})^{L-5}P_{FDF}^4, \tag{3.16c}$$

$$P_{F_1} = (1-P_{FDF})^{L-4}P_{FDF}^3, \tag{3.16d}$$

$$P_{G_1} = (1-P_{FDF})^{L-3}P_{FDF}^2 = P_{C_1}. \tag{3.16e}$$

Example 3.2. *Referring to Table 3.1, error case* C_1 *can occur if user 1 incorrectly decodes user 2 and 3's messages by making errors in detecting* $\hat{\hat{\boldsymbol{V}}}_{1,2}$ *and* $\hat{\hat{\boldsymbol{V}}}_{3,4}$*. Other error cases can similarly be explained.*

Proof. see Appendix A.2. □

3.3.3 Probability of k Error Events

The preceding subsections help to illustrate the point that finding an exact general expression for the probability of k error events, where $k \geq 3$, is difficult due to the many different ways k error events can occur. Hence, in this subsection, we focus on finding an approximate expression for the probability of k error events using high SNR assumption. This will be useful in deriving the average BER in the next subsection. Note that the use of the high SNR assumption to facilitate closed-form results is commonly used in two-way [24,44,91] and other types of relay networks [11,13].

Lemma 3.4. *The probability of k error events can be asymptotically approximated as*

$$P_{i,FDF}(k) \approx P_{FDF}, \tag{3.17}$$

where P_{FDF} is given in (3.10)*.*

Proof. Comparing (3.14) and (3.16), we can see that $P_{C_1} = P_{A_1}$ and $P_{D_1} = P_{B_1}$. At high SNR, the higher order terms involving P_{FDF}^2 and higher powers can be neglected and only the terms P_{B_1} and P_{D_1} effectively contribute to the probability of one and two error events in (3.13) and (3.15), respectively. Recall that P_{B_1} is the probability of one error about the network coded message involving an end user and P_{D_1} is the probability of an erroneous network coded message involving users just following (or preceding) the end user. Extending this analogy to the case of k error events, the dominating factor at high SNR would represent the scenario when the network coded message involving the k^{th} and the $(k+1)^{\text{th}}$ (or the $(L-k+1)^{\text{th}}$ and the $(L-k)^{\text{th}}$) users is incorrectly decoded, resulting in error about k users' messages. Thus, the probability of k error events can be asymptotically approximated as

$$P_{i,FDF}(k) \approx (1 - P_{FDF})^{L-2} P_{FDF} \approx P_{FDF}, \tag{3.18}$$

where in the last step we have used the fact that at high SNR $P_{FDF} \ll 1$ and hence the approximation $(1 - P_{FDF})^{L-2} \approx 1$ is valid when L is not too large. □

Remark 3.1. *Equation (3.18) shows that at high SNR in an L-user FDF MWRN, all the error events are equally probable and their probability can be asymptotically approximated as P_{FDF},* *given in* (3.10).

3.3.4 Average BER

Substituting (3.18) in (3.8) and simplifying, the average BER for a user in FDF MWRN is

$$\begin{aligned} P_{i,avg,FDF} &= \left(\sum_{k=1}^{L-1} k\right) \frac{P_{FDF}}{L-1} = \frac{L(L-1)}{2} \frac{P_{FDF}}{L-1} \\ &= \frac{L}{2} P_{FDF}. \end{aligned} \tag{3.19}$$

3.4 Probability of k Error Events and Average BER for a User in AF MWRN

In this section, we characterize the average BER for a user in an L-user AF MWRN. The general approach in our analysis is similar to the case of FDF MWRN, with some important differences which are highlighted in the following subsections.

First, we obtain the probability of incorrectly decoding a user's message, given that the previous user's message is correctly decoded, in an AF MWRN. The probability, that the message of any user in an AF MWRN is incorrectly decoded, is given by [98]

$$P_{AF} = \frac{1}{2}\text{erfc}\left(\frac{\alpha}{\sqrt{(\alpha^2+1)(N_0)}}\right), \tag{3.20}$$

where α is the amplification factor defined below (3.5).

Now, we obtain the probability of incorrectly decoding a user's message, given that the previous user's message is incorrectly decoded.

Lemma 3.5. *The probability of wrongly detecting the message of a user given that the previous user's message is also incorrect, is given by:*

$$P'_{AF} = \frac{1}{4}\left[erfc\left(\frac{3\alpha}{\sqrt{(\alpha^2+1)(N_0)}}\right) + erfc\left(\frac{-\alpha}{\sqrt{(\alpha^2+1)(N_0)}}\right)\right]. \tag{3.21}$$

Proof. To find P'_{AF}, we need to find the probability $P(\hat{\mathbf{W}}_{i+2} \neq \mathbf{W}_{i+2} | \hat{\mathbf{W}}_{i+1} \neq \mathbf{W}_{i+1})$. If $\hat{\mathbf{X}}_{i+1} \neq \mathbf{X}_{i+1}$, then $\hat{\mathbf{X}}_{i+2} = \alpha \mathbf{X}_{i+1} + \alpha \mathbf{X}_{i+2} + \alpha n_1 + n_2 - \alpha \hat{\mathbf{X}}_{i+1} = \alpha \mathbf{X}_{i+2} + \alpha n_1 + n_2 + 2\alpha \mathbf{X}_{i+1}$. Thus, the mean of the received signal is shifted by either 2α or -2α. Using this fact and (3.20), (3.21) can be readily proved. □

Remark 3.2. *Assume that $X^t_{i+2} = 1$. While the shift of the mean of the signal by 2α (when $X^t_{i+1} = 1$) is helpful in reducing the probability of error in detecting $X^t_{i+2} = 1$, the shift in the mean by -2α (when $X^t_{i+1} = -1$) would be seriously detrimental for its detection. We will use this fact later in our high SNR BER analysis by setting $P'_{AF} \approx \frac{1}{2}$.*

3.4.1 Probability of $k = 1$ Error Event

Lemma 3.6. *The exact probability of one error event in an AF MWRN can be expressed as*

$$P_{i,AF}(1) = \begin{cases} (L-3)P_{A_2} + 2P_{B_2}, & i \neq 1 \text{ and } i \neq L \\ (L-2)P_{A_2} + P_{B_2}, & i = 1 \text{ or } i = L \end{cases} \tag{3.22}$$

where A_2 and B_2 are the following error cases from which $k = 1$ error event can occur:

- *error case A_2: a middle user's message is wrongly estimated with correct decision about the following user or,*
- *error case B_2: an error in the estimated signal of one of the end users.*

The probabilities of these error cases are given as:

$$P_{A_2} = (1 - P_{AF})^{L-3} P_{AF} (1 - P'_{AF}), \tag{3.23a}$$

$$P_{B_2} = (1 - P_{AF})^{L-2} P_{AF}. \tag{3.23b}$$

and P_{AF} and P'_{AF} are defined as in (3.20) and (3.21), respectively.

Proof. see Appendix A.3. □

Table 3.2: Illustration of the error cases for one and two error events in a 10-user AF MWRN. Here, ✓and × represent correct and incorrect detection, respectively.

Error case	Decoding user i	$\hat{X}_1$	$\hat{X}_2$	$\hat{X}_3$	$\hat{X}_4$	$\hat{X}_5$	$\hat{X}_6$	$\hat{X}_7$	$\hat{X}_8$	$\hat{X}_9$	$\hat{X}_{10}$	Error event
A_2	$i \in \{1, L\}$	✓	×	✓	✓	✓	✓	✓	✓	✓	✓	1
B_2	$i \neq 1$	×	✓	✓	✓	✓	✓	✓	✓	✓	✓	1
B_2	$i \neq L$	✓	✓	✓	✓	✓	✓	✓	✓	✓	×	1
C_2	$i \in \{1, L\}$	✓	✓	×	×	✓	✓	✓	✓	✓	✓	2
D_2	$i \neq 1, 2$	×	×	✓	✓	✓	✓	✓	✓	✓	✓	2
D_2	$i \neq L-1, L$	✓	✓	✓	✓	✓	✓	✓	✓	×	×	2
E_2	$i \in \{1, L\}$	✓	×	✓	✓	×	✓	✓	✓	✓	✓	2
F_2	$i \neq 1$	×	✓	✓	✓	×	✓	✓	✓	✓	✓	2
F_2	$i \neq L$	✓	✓	✓	✓	×	✓	✓	✓	✓	×	2
G_2	$i \neq 1, L$	×	✓	✓	✓	✓	✓	✓	✓	✓	×	2

Example 3.3. *As illustrated in Table 3.2, error case A_2 can occur when user 1 wrongly decodes the message of user 2 and user 3. Similarly, error case B_2 can occur if there is an error in the decoding of user 10.*

3.4.2 Probability of $k = 2$ Error Events

Lemma 3.7. *The exact probability of two error events in an AF MWRN can be expressed as*

$$P_{i,AF}(2) = \begin{cases} (L-3)P_{C_2} + P_{D_2} + \sum_{m=2}^{L-3}(L-2-m)P_{E_2} + \\ (L-3)P_{F_2}, & i = 1 \text{ or } i = L \\ (L-4)P_{C_2} + P_{D_2} + \sum_{m=2}^{L-4}(L-3-m)P_{E_2} + \\ 2(L-4)P_{F_2} + P_{G_2}, & i = 2 \text{ or } i = L-1 \\ (L-5)P_{C_2} + 2P_{D_2} + \sum_{m=2}^{L-4}(L-3-m)P_{E_2} + \\ 2(L-4)P_{F_2} + P_{G_2}, & i = 3 \text{ or } i = L-2 \\ (L-5)P_{C_2} + 2P_{D_2} + \sum_{m=2}^{i-2}(L-4-m)P_{E_2} + \\ \sum_{m=i-1}^{L-i-1}(L-3-m)P_{E_2} + \sum_{m=L-i}^{L-3}(L-2-m)P_{E_2} + \\ 2(L-4)P_{F_2} + P_{G_2}, & i \notin \{1, 2, 3, L-2, L-1, L\} \end{cases} \quad (3.24)$$

where m is the decoding order difference between the two users that are incorrectly decoded, C_2, D_2, E_2, F_2 and G_2 are the possible error cases for $k = 2$ error event, given as follows:

- *error case C_2: if messages of two consecutive middle users are incorrectly decoded but the message of the user next to them is correct or,*
- *error case D_2: if the estimated messages of the end user and that of the following (or preceding) user are incorrect or,*
- *error case E_2: if two middle users' messages are incorrectly estimated provided that the message of the users adjacent to each of them are correct or,*
- *error case F_2: if there is error about the message of one end user and any other user, provided that the messages of the users in between them are correctly estimated or,*
- *error case G_2: if both the end users' messages are incorrectly estimated.*

The probabilities of the above error cases are:

$$P_{C_2} = (1 - P_{AF})^{L-4} P_{AF} (1 - P'_{AF}) P'_{AF}, \tag{3.25a}$$

$$P_{D_2} = (1 - P_{AF})^{L-3} P_{AF} P'_{AF}, \tag{3.25b}$$

$$P_{E_2} = (1 - P_{AF})^{L-5} P^2_{AF} (1 - P'_{AF})^2, \tag{3.25c}$$

$$P_{F_2} = (1 - P_{AF})^{L-4} P^2_{AF} (1 - P'_{AF}), \tag{3.25d}$$

$$P_{G_2} = (1 - P_{AF})^{L-3} P^2_{AF} \neq P_{C_2}. \tag{3.25e}$$

Proof. see Appendix A.4. □

3.4.3 Probability of k Error Events

As for the case of FDF MWRN, it is very hard to find an exact general expression for the probability of k error events in AF MWRN. Hence, in this subsection, we focus on finding an approximate expression for the probability of k error events using high SNR assumption.

Lemma 3.8. *At high SNR, the probability of k error events in an AF MWRN can be asymptot-*

ically approximated as

$$P_{i,AF}(k) \approx \frac{L-k+1}{2^k} P_{AF}. \tag{3.26}$$

Proof. At high SNR, we can neglect P_{E_2}, P_{F_2} and P_{G_2} in (3.25) since they involve higher order product terms of probabilities. Comparing (3.23) and (3.25), we can see that the relationship between the dominating terms in the probability of one and two error events at high SNR is $C_2 = \frac{P'_{AF}}{1-P_{AF}} A_2$, $D_2 = \frac{P'_{AF}}{1-P_{AF}} B_2$. Recall that C_2 and D_2 correspond to the cases of two consecutive errors involving middle users and two consecutive errors involving one of the end users, respectively. Extending this analogy to the case of k error events, the dominating terms at high SNR would represent the cases of k consecutive errors in the middle users and k consecutive errors involving one end user and $k-1$ following (or preceding) users. Thus, the probability of k error events can be asymptotically approximated as

$$P_{i,AF}(k) \approx \left(\frac{P'_{AF}}{1-P_{AF}}\right)^{k-1} \left\{(L-k-1)(1-P_{AF})^{L-3} P_{AF}(1-P'_{AF}) + (1-P_{AF})^{L-2} P_{AF}\right\} \tag{3.27}$$

$$\approx \frac{L-k+1}{2^k} P_{AF}, \tag{3.28}$$

where in the last step we have used the fact that at high SNR $P'_{AF} \approx \frac{1}{2}$ and $1 - P_{AF} \approx 1$. □

3.4.4 Average BER

Substituting (3.28) in (3.8) and simplifying, the average BER for a user in AF MWRN is derived as

$$\begin{aligned} P_{i,avg,AF} &= P_{AF} \sum_{k=1}^{L-1} \frac{L-k+1}{2^k} \\ &= \left(\frac{L+1}{L-1}\left(2 - \frac{L}{2^{L-2}}\right) - \frac{3}{L-1}\left(2 - \frac{L^2-3}{2^{L-2}}\right)\right) P_{AF}. \end{aligned} \tag{3.29}$$

3.5 Comparison of MWRN Error Performances with FDF and AF relaying

From the above discussion in Section 3.3 and Section 3.4, we present the comparison between FDF and AF relaying in terms of error performance in the following remarks:

Remark 3.3. *Comparing (3.28) and (3.18) we can see that, at high SNR, the higher order error events are less probable in an L-user AF MWRN, but all error events are equally probable in an L-user FDF MWRN.*

Remark 3.4. *Comparing* (3.19) *and* (3.29), *we can see that the larger number of error events have a smaller contribution in the average BER for a user in AF MWRN, whereas they have the same contribution as the small number of error events in a FDF MWRN.*

The reason behind such traits is that in a FDF MWRN, a single error about a network coded message, leads to incorrect decision about all the remaining users (see (3.4a)). On the other hand, in an AF MWRN, a user has to incorrectly decode exactly k network coded messages for incorrectly decoding k users (see Section 3.4.3). These insights will be verified through numerical simulation in Section 3.7.

3.6 Average BER for a user in MWRN with Rayleigh Fading

In this section, we demonstrate that the preceding analysis is also applicable for the case of FDF or AF MWRN with Rayleigh fading channels. Recall that according to the channel assumptions in Chapter 2, we assume that the channel coefficients are modeled as independent zero-mean and unit-variance complex-valued Gaussian random variables, that are correctly estimated or available at the users requiring them. Taking Rayleigh fading into account, the received signal at the relay can be given by (2.5).

3.6.1 FDF MWRN with Rayleigh Fading

The relay decodes the received signal using ML criterion [22] and obtains an estimate of the corresponding network coded message. The relay then broadcasts the estimated signal and the users detect the received signal as in (2.7) through ML criterion [22].

With the modified signal model, the error propagation in FDF MWRN is almost similar to the AWGN case. Thus, it can be shown that the probability of large number of errors is asymptotically the same as that of small number of errors, even in the presence of fading. Hence, we can use (3.19) to find the average BER for a user. In order to do this, we need an expression for the probability of incorrectly decoding a network coded message in a FDF MWRN with Rayleigh fading, P_{FDF}. No exact expression is available in the literature for computing this probability in the presence of Rayleigh fading. However, upper and lower bounds have been derived in [22]. In this section, we use the upper bound for P_{FDF}, which is given by [22]

$$P_{FDF} = 2\Phi_1(\bar{\gamma}) + \frac{1}{2}\Xi(\bar{\gamma}), \tag{3.30}$$

where $\bar{\gamma} = \frac{1}{N_0}$, $\Phi_1(\bar{\gamma}) = \frac{1-\sqrt{\frac{\bar{\gamma}}{1+\bar{\gamma}}}}{2}$, $\Xi(\bar{\gamma}) = 2\Phi_1(\bar{\gamma}) - 4\{\Phi_1(\bar{\gamma})\}^2 - 2\Phi_2(\bar{\gamma}) - 2\sqrt{\frac{\bar{\gamma}}{1+\bar{\gamma}}}\Phi_3(\bar{\gamma})$, $\Phi_2(\bar{\gamma}) = \frac{1}{2\pi}[\frac{\pi}{2} - 2\sqrt{\frac{\bar{\gamma}}{1+\bar{\gamma}}}(\frac{\pi}{2} - \tan^{-1}\sqrt{\frac{\bar{\gamma}}{1+\bar{\gamma}}})]$, $\Phi_3(\bar{\gamma}) = \frac{1}{2\pi}[\frac{\pi}{2} - \delta_1(\frac{\pi}{2} + \tan^{-1}\zeta_1) - \delta_2(\frac{\pi}{2} + \tan^{-1}\zeta_2)]$, $\delta_1 = \sqrt{\frac{1+\bar{\gamma}}{3+\bar{\gamma}}}$, $\delta_2 = \sqrt{\frac{\bar{\gamma}}{2+\bar{\gamma}}}$ and $\zeta_j = -\delta_j \cot(\sqrt{\frac{\bar{\gamma}}{1+\bar{\gamma}}})$ for $j = 1, 2$.

3.6.2 AF MWRN with Rayleigh Fading

For AF MWRN, the amplified and retransmitted signal in (3.5) modifies to

$$Y^t_{i,i+1} = h_{i,r}\alpha(h_{i,r}X^t_i + h_{i+1,r}X^t_{i+1} + n_1) + n_2. \tag{3.31}$$

After subtracting self information, user i performs ML detection to estimate the other user's message. The sequential downward and upward message extraction process is the same as before.

With the modified signal model, the error propagation in AF MWRN is different from the AWGN case. This is because the primary cause of error propagation in AF MWRN is the shifting of the mean of the received signal when the previous message has been incorrectly detected. For example, if $\hat{X}_{i+1}^t \neq X_{i+1}^t$, then $\hat{X}_{i+2}^t = \alpha h_{i,r} h_{i+2,r} X_{i+2}^t + \alpha h_{i,r} n_1 + n_2 + 2\alpha h_{i,r} h_{i+1,r} X_{i+1}^t$. Thus we can see that the mean of the received signal is affected by the channel coefficients. That is why, we cannot simply ignore P'_{AF} and obtain (3.28) from (3.27). So, instead of (3.28), we will directly use (3.27) to provide the analytical expression of average BER for a user, where the exact probability of incorrectly decoding a user's message in AF MWRN is given by [25, 45]

$$P_{AF} = Q\left(\sqrt{\frac{|h_{i,r}|^2 |h_{i+1,r}|^2}{2|h_{i,r}|^2 N_0 + |h_{i+1,r}|^2 N_0 + (N_0)^2}}\right), \tag{3.32}$$

and the expression for P'_{AF} is similarly derived as

$$P'_{AF} = Q\left(\sqrt{\frac{|h_{i,r}|^2 |h_{i+2,r}|^2}{4|h_{i,r}|^2 |h_{i+1,r}|^2 + 2|h_{i,r}|^2 N_0 + |h_{i+2,r}|^2 N_0 + (N_0)^2}}\right), \tag{3.33}$$

where $Q(x) = \frac{1}{\sqrt{2\pi}} \int_x^\infty e^{-\frac{t^2}{2}} dt$ is the Gaussian Q-function.

3.7 Numerical Results

In this section, we compare the BER expressions obtained by our analysis with the BER results obtained by Monte Carlo simulations. We consider two cases $L = 10$ and $L = 20$ and each user transmits a packet of $T = 10000$ bits. The SNR is assumed to be SNR per message per user and user 1 is assumed to be decoding the messages of all other users. The simulation results are averaged over 1000 Monte Carlo trials per SNR point.

3.7.1 Probability of different error events in an AWGN FDF MWRN

Fig. 3.3 plots the probability of k error events $P_{i,FDF}(k)$ in an $L = 10$ user FDF MWRN in the case of AWGN. The simulation results are plotted for $k = 1, 2, 3, 5, 7$ and compared with the asymptotic bound in (3.18). For $k = 1, 2$ the exact probabilities are also plotted

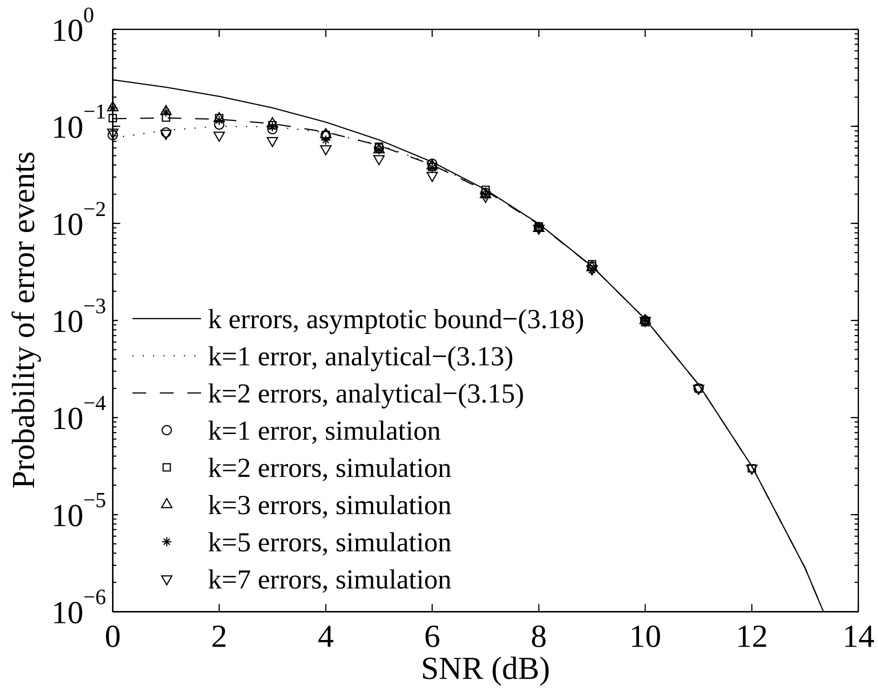

Figure 3.3: Probability of $k = 1, 2, 3, 5, 7$ error events in an $L = 10$ user FDF MWRN with AWGN.

using (3.13) and (3.15), respectively. As highlighted in Remark 3.1, in an L-user FDF MWRN, all the error events are equally probable and their probability can be asymptotically approximated as (3.18). This is confirmed by the results in Fig. 3.3. We can see that for medium to high SNRs (SNR > 5 dB), the asymptotic expression in (3.18) is very accurate in predicting the probability of k error events, for all the considered values of k. This verifies the accuracy of (3.18).

3.7.2 Probability of different error events in an AWGN AF MWRN

Fig. 3.4(a) and Fig. 3.4(b) plot the probability of k error events $P_{i,AF}(k)$ in an $L = 10$ user AF MWRN corrupted by AWGN for $k = 1, 2$ error events and $k = 3, 5, 7$ error events, respectively. The simulation results are plotted for $k = 1, 2, 3, 5, 7$ and compared with the asymptotic bound in (3.28). For $k = 1, 2$ the exact probabilities are also plotted using (3.22) and (3.24), respectively. As highlighted in Remark 3.3, in an L-user AF MWRN, the probability of error events depends on the value of k, with the higher order

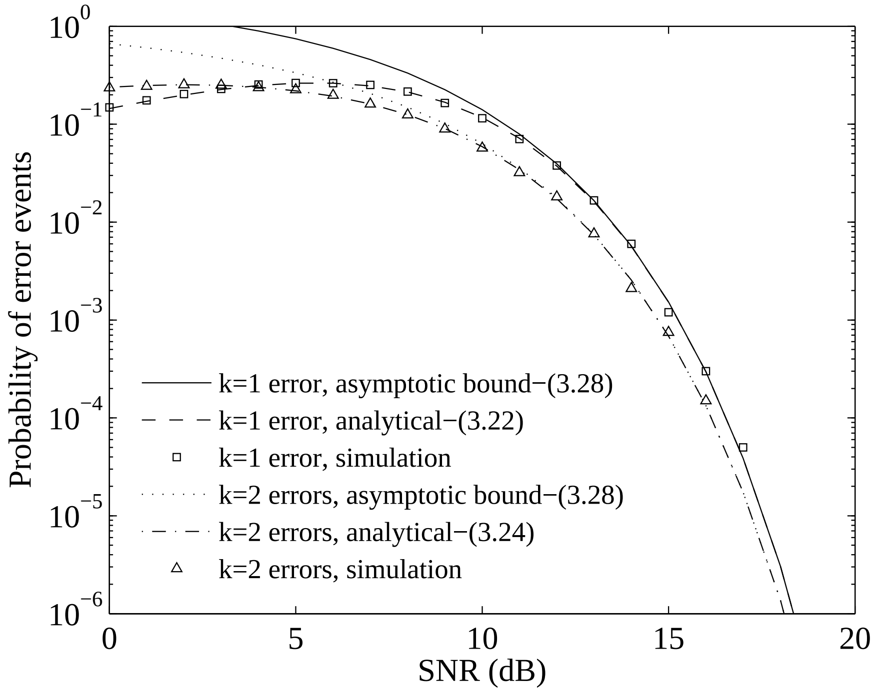

(a) $k = 1, 2$

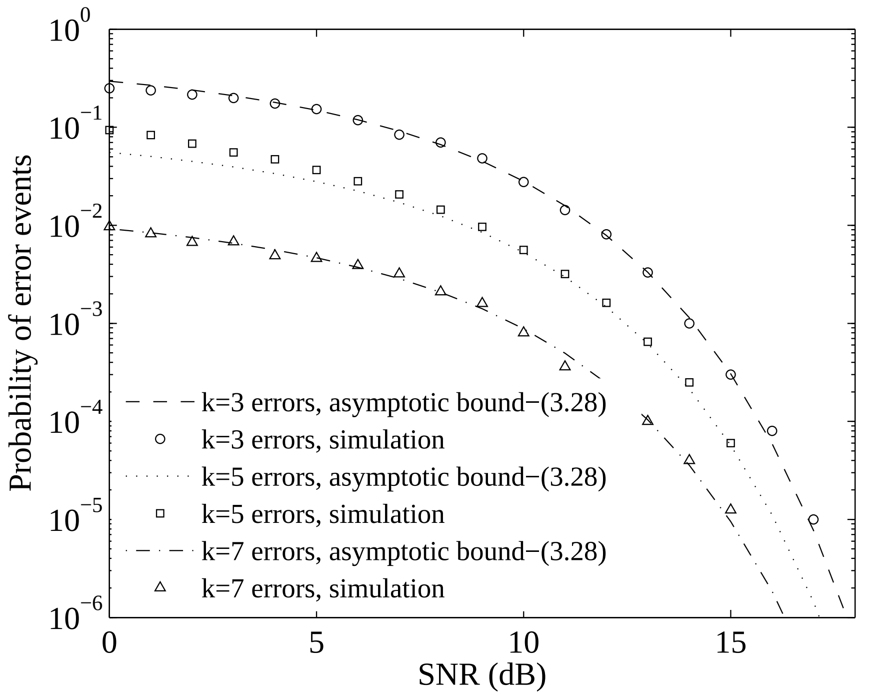

(b) $k = 3, 5, 7$

Figure 3.4: Probability of k error events in an $L = 10$ user AF MWRN with AWGN.

error events being less probable. This is confirmed by the results in Fig. 3.4(a) and Fig. 3.4(b). We can see that for medium to high SNR (SNR $>$ 10 dB), the asymptotic expression in (3.28) for k error events matches very well with the simulation results. This verifies the accuracy of (3.28).

3.7.3 Average BER for a user in AWGN FDF or AF MWRN

Fig. 3.5(a) and Fig. 3.5(b) plot the average BER for a user in an AWGN FDF or AF MWRN with $L = 10$ and $L = 20$ users, respectively. The average BER of FDF and AF MWRN is plotted using (3.19) and (3.29), respectively. From the figures, we can see that as the number of users increases ($L = 10, 20$), the average BER increases for both FDF or AF MWRN, which is intuitive. For FDF MWRN, (3.19) can predict the average BER for a user accurately in medium to high SNR (approximately SNR $>$ 7 dB for $L = 10$ users and SNR $>$ 10 dB for $L = 20$ users). Also for AF MWRN, (3.29) can accurately predict the average BER for a user in medium to high SNR (approximately SNR $>$ 10 dB).

Comparing FDF and AF MWRNs, we can see that for low SNR, AF MWRN is slightly better than FDF MWRN. However, at medium to high SNRs, FDF MWRN is better than AF MWRN. In MWRN, the high SNR penalty for using AF, compared to FDF, decreases as the number of users increases, e.g., from Fig. 3.5(a) and Fig. 3.5(b), it is about 4 dB for $L = 10$ users and about 2.5 dB for 20 users at an average BER of 10^{-4}. This can be explained using our analysis as follows. From (3.19) we can see that for FDF MWRN the effective number of error terms in the average BER equation increases in proportion to the number of users. However, for AF MWRN, (3.29) shows that the probability of larger number of error events is very small, hence, the increase in the effective number of error terms for larger number of users is smaller. This results in a smaller SNR penalty for AF MWRN when larger number of users are involved, which agrees with the observations from (3.19) and (3.29).

Fig. 3.6 compares the average BER for FDF and AF MWRN with the increasing number of users. In this figure, we maintain the same average power per user for

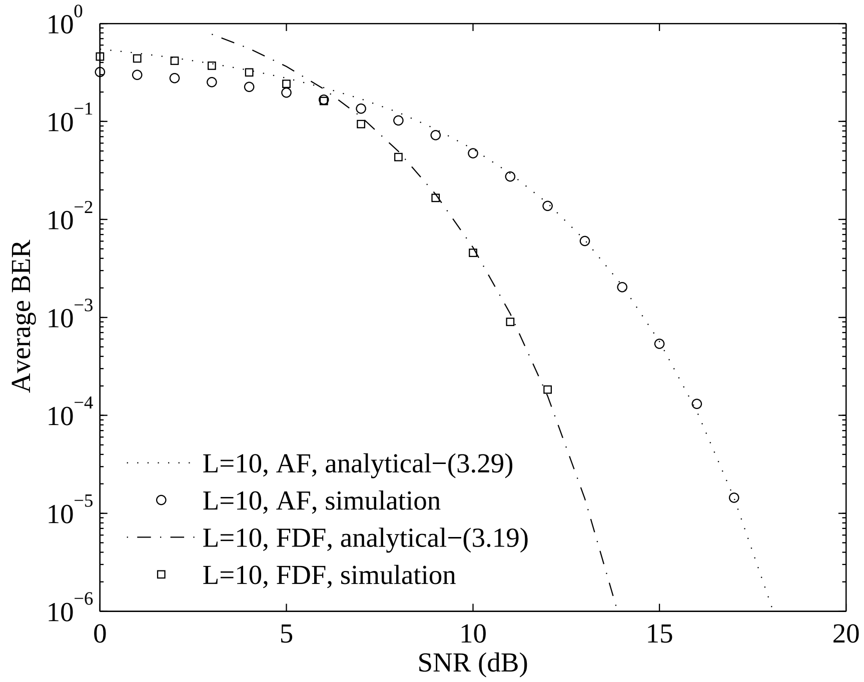

(a) $L = 10$

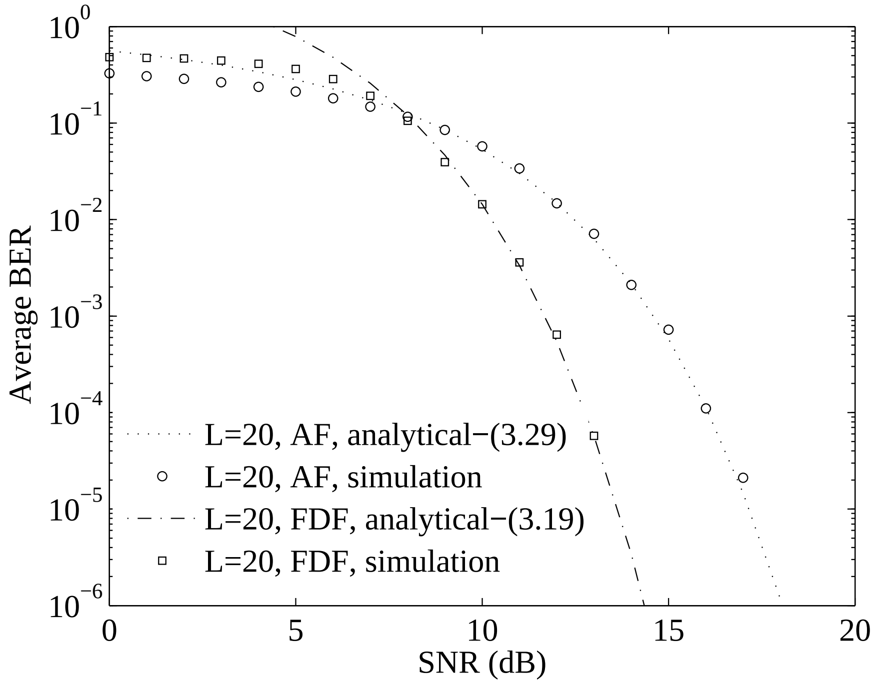

(b) $L = 20$

Figure 3.5: Average BER for a user in $L = 10$ and $L = 20$ user FDF and AF MWRN with AWGN.

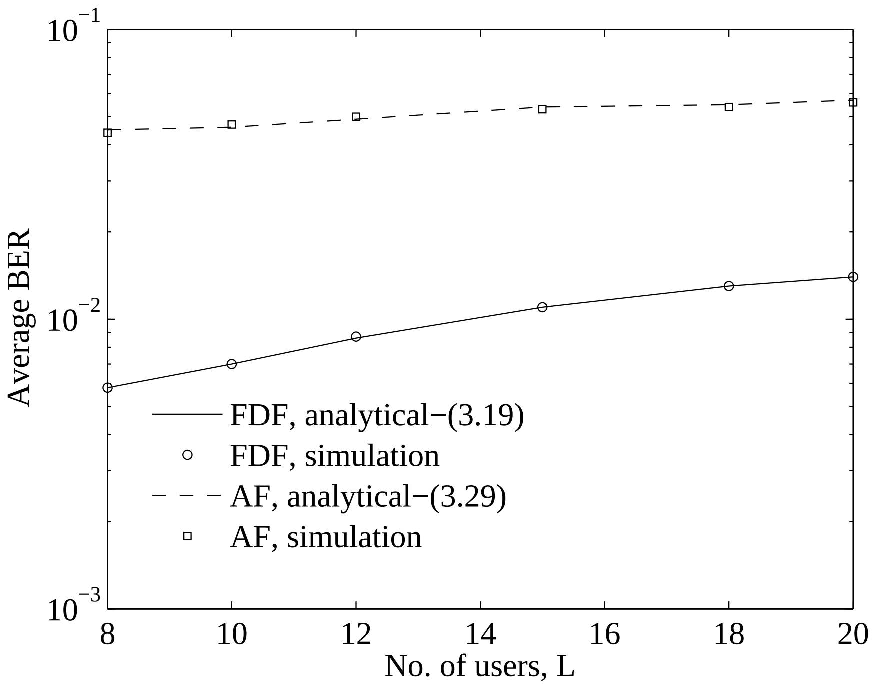

Figure 3.6: Average BER for different number of users in FDF or AF MWRN with AWGN where the SNR is defined as in (3.34).

different number of users in a MWRN and set $\sigma_{n_1}^2 = \frac{2L-2}{L}\frac{N_0}{2}$ (since, in an L-user MWRN, $(2L-2)$ time slots are needed for complete information exchange). Thus, in this figure, the SNR per bit per user can be defined as

$$\rho = \frac{1}{\left(\frac{2L-2}{L}\right) N_0}. \tag{3.34}$$

Here, we can see that though AF MWRN has larger average BER compared to FDF MWRN, the error performance does not degrade significantly with the increasing number of users, which is expected from the discussion under remark 3.1 and remark 3.3. However, in FDF MWRN, the average BER increases with the number of users. This is due to the fact that the average BER in FDF MWRN is an increasing function of the number of users (see (3.19)). This indicates that AF MWRN exhibits more robustness against increasing number of users, whereas, FDF MWRN's error performance degrades for large number of users.

3.7.4 Rayleigh Fading

Figures 3.7(a) and 3.7(b) plot the average BER for a user in FDF or AF MWRN in Rayleigh fading channels and $L = 10$ and $L = 20$ users, respectively. The analytical result for FDF MWRN is plotted using (3.19) and (3.30) and the analytical result for AF MWRN is plotted using (3.8), (3.27), (3.32) and (3.33). We can see that for both FDF and AF MWRN, the analytical results are within 1 dB of the simulation results for high SNR. Comparing the curves for $L = 10$ and $L = 20$ users, we can see that the average BER for a user in FDF MWRN degrades significantly as the number of users increases. However, the average BER for a user in AF MWRN is more robust to the increase in the number of users. This observation is consistent with the discussion after (3.31). As explained before, this is due to the fact that the probability of larger number of error events in AF is much smaller compared to FDF MWRN.

3.8 Summary

In this chapter, we analyzed the error performance of FDF and AF MWRNs. We considered a MWRN with pair-wise data exchange protocol using BPSK modulation in both AWGN and Rayleigh fading channels. The analysis can be extended to higher order modulation schemes, as well, which we are going to address in the following chapters. In this chapter, specifically, we made the following contributions:

- In Sections 3.3 and 3.4, we quantified the possible error events in an L-user FDF or AF MWRN and derived accurate asymptotic bounds on the probability for the general case that a user incorrectly decodes the messages of exactly k ($k \in [1, L-1]$) users.

- In Sections 3.3.3 and 3.4.3, we showed that at high SNR, the higher order error events ($k \geq 3$) are less probable in AF MWRN, but all error events are equally probable in a FDF MWRN.

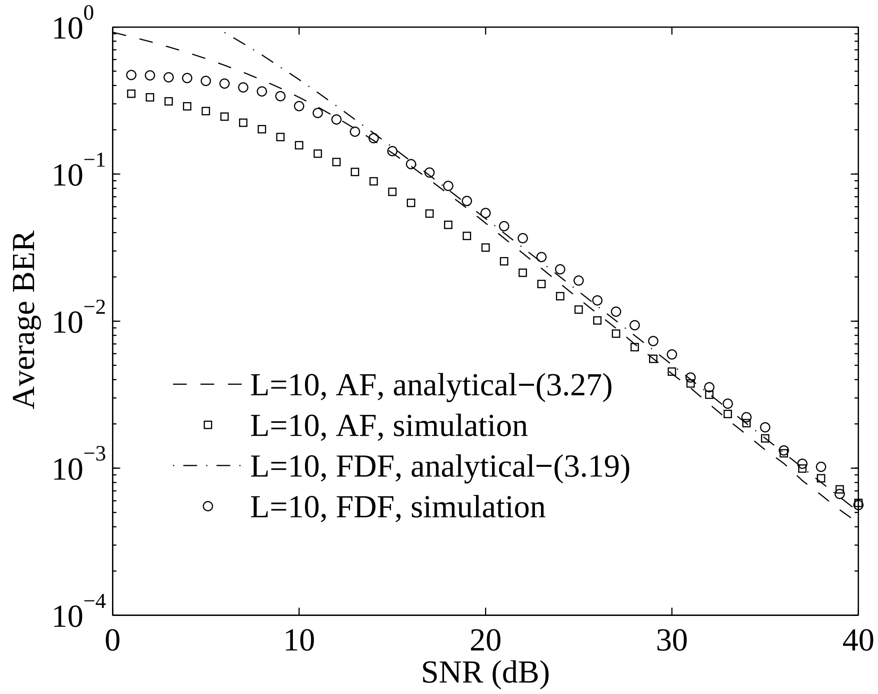

(a) $L = 10$

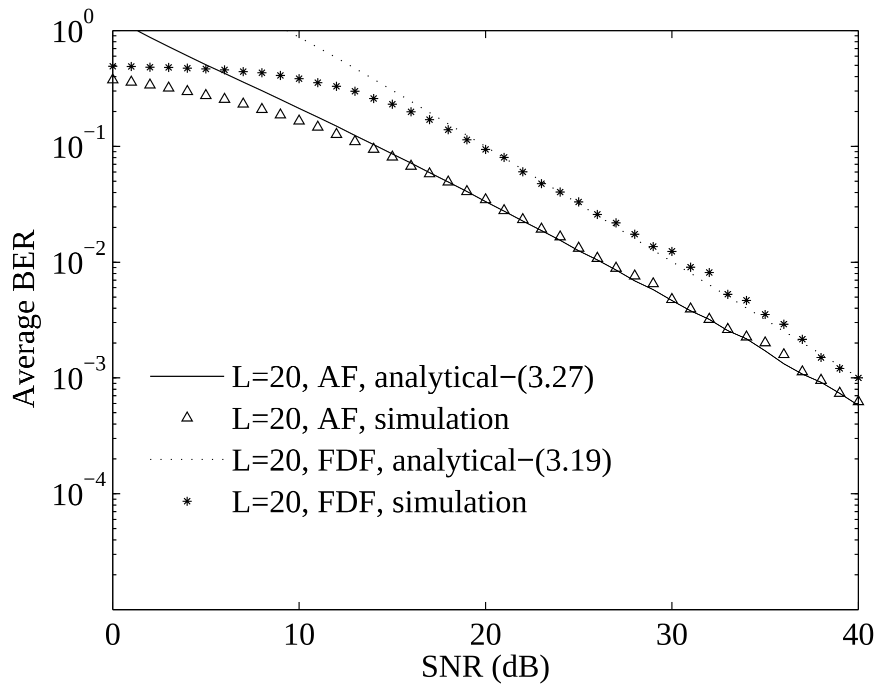

(b) $L = 20$

Figure 3.7: Average BER for a user in FDF or AF MWRN with Rayleigh fading and $L = 10, 20$ users.

- In Sections 3.3.4 and 3.4.4, we derived the average BER of a user in a FDF or AF MWRN in AWGN channels under high SNR conditions. In Section 3.6, average BER results were derived for Rayleigh fading channels.

- In Section 3.7, our numerical results showed that at medium to high SNR, FDF MWRN provides better error performance than AF MWRN in AWGN channels even with a large number of users (for example, $L = 20$). Whereas, AF MWRN outperforms FDF MWRN in Rayleigh fading channels even for much smaller number of users (for example, $L > 10$).

Chapter 4

A Novel User Pairing Scheme for Lattice Coded FDF Multi-way Relay Networks

In Chapter 3, we considered the error performance for AWGN and fading MWRNs with BPSK modulation. In this chapter, we consider more generalized lattice coded FDF MWRNs and propose a new pairing scheme that can negate the adverse effects of error propagation in FDF MWRNs. As identified in Chapter 1, pairing scheme design is an important problem for a pairwise transmission based MWRNs. In Chapter 3, we have shown that the existing pairing scheme in [28] suffers severe error propagation which limits the error performance of a MWRN.

In this chapter, our goal is to design a new pairing scheme to solve the error propagation problem in a generalized lattice code based MWRN. To obtain the solution, we pair each user with a common user which has the best average channel gain in the system. Choosing the common user as the best channel gain user enables the network coded messages to be decoded correctly with higher probability. In this way, error propagation for a MWRN can be reduced and the proposed pairing scheme is expected to improve the performance of a MWRN. In this chapter, we compare the achievable rate and error performance of the proposed pairing scheme with the existing pairing schemes in [28] and [50] and show that our scheme outperforms the existing schemes.

The chapter is organized as follows. The proposed pairing scheme for FDF MWRNs

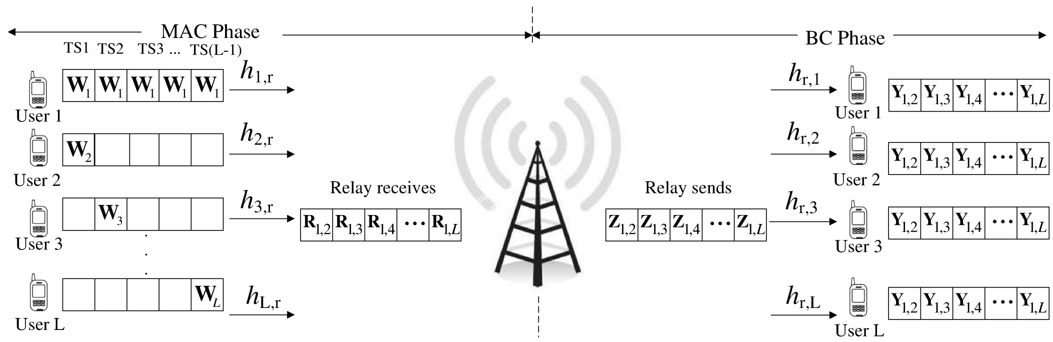

Figure 4.1: System model for an L-user multi-way relay network (MWRN), where the users exchange information with each other via the relay R. Here, 'TS' means time slot and user 1 is considered to be the common user (for illustration purposes).

is discussed in Section 4.1 and the general lattice code based transmissions with the proposed pairing scheme are presented in Section 4.2. The common rate and the sum rate for a FDF MWRN with the proposed pairing scheme is derived in Section 4.3. The average SER for FDF MWRNs with the proposed pairing scheme is derived in Section 4.4. The numerical and simulation results for verification of the analytical solutions are provided in Section 4.5. Finally, a summary of the contributions in this chapter is provided in Section 4.6.

4.1 Proposed Pairing Scheme for FDF MWRN

In this section, we propose a new pairing scheme for user pair formation in the multiple access phase (illustrated in Fig. 4.1) which is defined by the following set of principles:

P1 The common user is selected by the relay to be the user that has the best average channel gain in the system. The reason for this choice will be explained in Section 4.1.1.

P2 The common user's index is broadcast by the relay prior to each multiple access phase. This common user transmits in all the time slots in the multiple access phase and the other users take turns to form a pair with this common user.

P3 The common user is kept fixed for all the time slots within a certain time frame.

After some time frames, the common user might change depending upon the changing channel conditions.

4.1.1 Rationale Behind Choosing the Best Channel Gain User

In the proposed pairing scheme, choosing the best channel gain user allows its channel gain benefits to contribute towards the error-free detection of the network coded messages. This would not be possible if the common user is chosen without considering the channel conditions, as in [28, 50]. Note that taking channel state information into account is a well established design principle in wireless communication systems [99].

In this scheme, the common user transmits more than other users and as a result, the sum rate (when compared to the sum rate for the existing pairing scheme as in (4.1)) would have more terms corresponding to the best channel gain user than it would have for existing pairing schemes. Thus, it can be expected that pairing each user with the best channel gain user would improve the sum rate performance.

$$R_s = \frac{1}{2(L-1)} \sum_{\ell=1}^{L-1} \left(\log \left(\frac{| h_{\ell,r} |^2}{| h_{\ell,r} |^2 + | h_{\ell+1,r} |^2} + \frac{P | h_{\ell,r} |^2}{N_0} \right) + \log \left(\frac{| h_{\ell+1,r} |^2}{| h_{\ell,r} |^2 + | h_{\ell+1,r} |^2} + \frac{P | h_{\ell+1,r} |^2}{N_0} \right) \right). \tag{4.1}$$

Moreover, when most of the users undergo worse channel conditions, the existing schemes' performances degrade. This is because all the users' channel gains get equal emphasis on the sum rate expression in (4.1). However, for the proposed scheme, the common user's channel gain is present in more terms and the sum rate degrades less. On the other hand, when most of the users' channel conditions improve, the error propagation problem still persists for the existing pairing schemes. However, for the proposed pairing scheme, the error performance improves significantly because all the network coded messages along with the common user's message are decoded correctly with higher probability.

Another important advantage of this scheme is that each user has to correctly decode only the common user's message to avoid error propagation. However, existing pairing schemes suffer error propagation whenever any of the users' messages are incorrectly decoded. Thus, error propagation is less for the proposed pairing scheme, which improves the SER.

These reasonings will be supported with analytical proofs throughout this chapter.

4.1.2 Transmission Fairness Issues

In the proposed scheme, since the common user is involved in all the transmissions in the multiple access phase, an issue of transmission fairness arises. In the context of the proposed scheme, on average, each user should transmit the same number of times (equivalently consume the same amount of energy overall). We propose to achieve transmission fairness for the three channel scenarios, considered in this work, in the following manner

1. *Equal average channel gain scenario:* In this scenario, to maintain transmission fairness among the users, we randomly select a different common user in each time frame so that, on average, every user gets the opportunity to become the common user.

2. *Unequal average channel gain scenario:* In this scenario, the common user's transmission power must be scaled down by a factor of $(L-1)$, since it transmits $(L-1)$ times, whereas, other users transmit only once.

3. *Variable average channel gain scenario:* In this scenario, during each time frame, the user with the best average channel gain is chosen as the common user and this process is repeated for every time frame so that, on average, every user with changing channel conditions, gets the opportunity to become the common user. Therefore, we do not impose any external fairness measures.

4.2 Signal Transmissions With the Proposed Pairing Scheme

In this section, we discuss the general lattice code based transmissions with the proposed pairing scheme in a FDF MWRN. The notations for lattice codes have been defined in Chapter 2. Further details on lattice codes are available in [62, 68, 74, 93]. We denote the i^{th} user as the common user and the ℓ^{th} user as the other user, where, $i, \ell \in [1, L]$ and $\ell \neq i$. Here, we consider message exchange within a certain time frame in the multiple access and the broadcast phases.

4.2.1 Multiple Access Phase

In this phase, the common user and one other user transmit simultaneously using FDF based on lattice codes and the relay receives the sum of the signals, i.e., at the $(\ell-1)^{th}$ time slot, users i and ℓ transmit simultaneously.

4.2.1.1 Communication Protocol at the Users

In the $(\ell-1)^{th}$ time slot, the message packet of the ℓ^{th} user is denoted by

$$\mathbf{W}_\ell = \{W_\ell^1, W_\ell^2, ..., W_\ell^T\}, \tag{4.2}$$

where the elements W_ℓ^t are generated independently and uniformly over a finite field. At other time slots, $\mathbf{W}_\ell = 0$. Similarly, the message packet of the i^{th} user at all the $L-1$ time slots is given by $\mathbf{W}_i = \{W_i^1, W_i^2, ..., W_i^T\}$.

During a certain time frame, in the $t_s = (\ell-1)^{th}$ time slot, the i^{th} user and the ℓ^{th} user transmit their messages using lattice codes $\mathbf{X}_i = \{X_i^1, X_i^2, ..., X_i^T\}$ and $\mathbf{X}_\ell = \{X_\ell^1, X_\ell^2, ..., X_\ell^T\}$, respectively, which can be given by [36, 59]:

$$X_i^t = (\psi(W_i^t) + d_i) \mod \Lambda, \tag{4.3a}$$

$$X_\ell^t = (\psi(W_\ell^t) + d_\ell) \mod \Lambda, \tag{4.3b}$$

where d_i and d_ℓ are the dither vectors for the i^{th} and the ℓ^{th} user. The dither vectors are generated at the users and transmitted to the relay prior to message transmission in the multiple access phase [75].

4.2.1.2 Communication Protocol at the Relay

The relay receives the signal $\mathbf{R}_{i,\ell} = \{r^1_{i,\ell}, r^2_{i,\ell}, ..., r^T_{i,\ell}\}$, where

$$r^t_{i,\ell} = \sqrt{P} h_{i,r} X^t_i + \sqrt{P} h_{\ell,r} X^t_\ell + n_1, \tag{4.4}$$

where n_1 is the zero mean complex AWGN at the relay with noise variance $\sigma^2_{n_1} = \frac{N_0}{2}$ per dimension.

4.2.2 Broadcast Phase

In this phase, the relay broadcasts the decoded network coded message and each user receives it.

4.2.2.1 Communication Protocol at the Relay

The relay scales the received signal with a scalar coefficient α [62] and removes the dithers d_i, d_ℓ scaled by $\sqrt{P}h_{i,r}$ and $\sqrt{P}h_{\ell,r}$, respectively. The resulting signal is given by

$$\begin{aligned} X^t_r &= [\alpha r^t_{i,\ell} - \sqrt{P} h_{i,r} d_i - \sqrt{P} h_{\ell,r} d_\ell] \mod \Lambda \\ &= [\sqrt{P} h_{i,r} X^t_i + \sqrt{P} h_{\ell,r} X^t_\ell + (\alpha - 1)\sqrt{P}(h_{i,r} X^t_i + h_{\ell,r} X^t_\ell) + \alpha n_1 - \sqrt{P} h_{i,r} d_i - \sqrt{P} h_{\ell,r} d_\ell] \mod \Lambda \\ &= [\sqrt{P} h_{i,r} \psi(W^t_i) + \sqrt{P} h_{\ell,r} \psi(W^t_\ell) + n] \mod \Lambda, \end{aligned} \tag{4.5}$$

where $n = (\alpha - 1)\sqrt{P}(h_{i,r} X^t_i + h_{\ell,r} X^t_\ell) + \alpha n_1$ and α is chosen to minimize the noise variance [68,74].

The relay decodes the signal in (4.5) with a lattice quantizer [62,68] to obtain an estimate $\hat{\mathbf{V}}_{i,\ell} = \{\hat{V}^1_{i,\ell}, \hat{V}^2_{i,\ell}, ..., \hat{V}^T_{i,\ell}\}$ which is a function of the messages $\mathbf{W}_i$ and $\mathbf{W}_\ell$. Since, for sufficiently large N, $\Pr(n \notin \mathcal{V})$ approaches zero [62], $\hat{\mathbf{V}}_{i,\ell} = (\psi(\mathbf{W}_i) + \psi(\mathbf{W}_\ell)) \mod \Lambda$. The relay then adds a dither d_r with the network coded message which is generated at the relay and broadcast to the users prior to message transmission in the broadcast phase [75]. Then it broadcasts the resulting message using lattice codes, which is given as $\mathbf{Z}_{i,\ell} = \{Z^1_{i,\ell}, Z^2_{i,\ell}, ..., Z^T_{i,\ell}\}$, where $Z^t_{i,\ell} = (\hat{V}^t_{i,\ell} + d_r) \mod \Lambda$.

4.2.2.2 Communication Protocol at the Users

The j^{th} user receives $\mathbf{Y}_{i,\ell} = \{Y^1_{i,\ell}, Y^2_{i,\ell}, ..., Y^T_{i,\ell}\}$ as in (2.7). At the end of the broadcast phase, the j^{th} user scales the received signal with a scalar coefficient β_j and removes the dithers d_r multiplied by $\sqrt{P_r} h_{r,j}$. The resulting signal is

$$\begin{aligned}[\beta_j Y^t_{i,\ell} - \sqrt{P_r} h_{r,j} d_r] \mod \Lambda =& [\sqrt{P_r} h_{r,j} \hat{V}^t_{i,\ell} + (\beta_j - 1)\sqrt{P_r} h_{r,j} \hat{V}^t_{i,\ell} + \beta_j n_2] \mod \Lambda \\ =& [\sqrt{P_r} h_{r,j} \hat{V}^t_{i,\ell} + n'] \mod \Lambda, \end{aligned} \tag{4.6}$$

where $n' = \sqrt{P_r} h_{r,j} (\beta_j - 1) \hat{V}^t_{i,\ell} + \beta_j n_2$ and β_j is chosen to minimize the noise variance [75]. The users then detect the received signal with a lattice quantizer [75] and obtain the estimate $\hat{\hat{\mathbf{V}}}_{i,\ell} = (\psi(\mathbf{W}_i) + \psi(\mathbf{W}_\ell)) \mod \Lambda$, assuming that the lattice dimension is large enough such that $\Pr(n' \notin \mathcal{V})$ approaches zero. After decoding all the network coded messages, each user performs message extraction of every other user by canceling self information.

4.2.3 Message Extraction at the Common User

For the common user (i^{th} user), this message extraction involves simply subtracting the lattice point corresponding to its own message from the lattice network coded messages $\hat{\hat{\mathbf{V}}}_{i,\ell}$. The process can be shown as

$$\psi(\hat{\mathbf{W}}_\ell) = (\hat{\hat{\mathbf{V}}}_{i,\ell} - \psi(\mathbf{W}_i)) \mod \Lambda, \quad \ell \in [1, L], \ell \neq i. \tag{4.7}$$

Note that, the message extracted by the common user depends only on the network coded message received from the relay as the common user perfectly knows its own message. Thus, the common user does not suffer from any error propagation.

4.2.4 Message Extraction at Other Users

For other users, the process is different from the common user. At first, the ℓ^{th} user subtracts the scaled lattice point corresponding to its own message, i.e., $\psi(\mathbf{W}_\ell)$ from the network coded message received at the $(\ell-1)^{th}$ time slot (i.e., $\hat{\hat{\mathbf{V}}}_{i,\ell}$) and extracts the message of the i^{th} user as $\psi(\hat{\mathbf{W}}_i)$[1]. After that, it utilizes the extracted message of the i^{th} user to obtain the messages of other users in a similar manner. The message extraction process in this case can be shown as

$$\begin{aligned}\psi(\hat{\mathbf{W}}_i) &= (\hat{\hat{\mathbf{V}}}_{i,\ell} - \psi(\mathbf{W}_\ell)) \mod \Lambda,\\ \psi(\hat{\mathbf{W}}_m) &= (\hat{\hat{\mathbf{V}}}_{i,m} - \psi(\hat{\mathbf{W}}_i)) \mod \Lambda, \quad m \in [1, L], m \neq i, \ell.\end{aligned} \tag{4.8}$$

4.3 Common Rate and Sum Rate Analysis

In this section, we investigate common rate and sum rate of the MWRN with the proposed pairing scheme. We first analyze the SNR of each user pair in a MWRN and use these results to obtain expressions for the achievable rates.

4.3.1 SNR analysis

In this subsection, we consider the SNR at the users and the SNR at the relay for a FDF MWRN with the proposed pairing scheme.

4.3.1.1 SNR at the Users

The SNR at the users have the same expressions for all the three pairing schemes (i.e., the proposed scheme, pairing scheme in [28] and in [50]). The signal transmission from

[1] Once $\psi(\cdot)$ has been obtained, the users perform $\psi^{-1}(\cdot)$ operation to actually obtain the messages.

the relay to any user $j \in [1, L]$ is the same as that in a point-to-point fading channel. Thus, the SNR of the $m^{th}(m \in [1, L])$ user's signal received at the j^{th} user is given by:

$$\gamma_j = \frac{P_r \mid h_{r,j} \mid^2}{\mid \beta_j \mid^2 N_0 + P_r \mid \beta_j - 1 \mid^2 \mid h_{r,j} \mid^2}, \tag{4.9}$$

where the numerator represents the power of the signal part in (4.6) and the denominator represents the power of the noise term n' in (4.6).

4.3.1.2 SNR at the Relay

In a FDF MWRN based on lattice coding with the proposed pairing scheme, the SNR of the received signal at the relay can be obtained from (4.5) as

$$\gamma_r(i, \ell) = \frac{P \min(\mid h_{i,r} \mid^2, \mid h_{\ell,r} \mid^2)}{\mid \alpha \mid^2 N_0 + P \mid \alpha - 1 \mid^2 (\mid h_{i,r} \mid^2 + \mid h_{\ell,r} \mid^2)}, \tag{4.10}$$

where the numerator represents the power of the signal part (i.e., $\sqrt{P} h_{i,r} \psi(W_i^t) + \sqrt{P} h_{\ell,r} \psi(W_\ell^t)$ in (4.5)) and the denominator represents the power of the noise terms n in (4.5).

To provide comparison, for the pairing scheme in [28], the SNR received at the relay can be expressed as

$$\gamma_r(i) = \frac{P \min(\mid h_{\ell,r} \mid^2, \mid h_{\ell+1,r} \mid^2)}{\mid \alpha \mid^2 N_0 + P \mid \alpha - 1 \mid^2 (\mid h_{\ell,r} \mid^2 + \mid h_{\ell+1,r} \mid^2)}. \tag{4.11}$$

Similarly, for the pairing scheme in [50], the SNR at the relay is given by

$$\gamma_r(i) = \frac{P \min(\mid h_{\ell,r} \mid^2, \mid h_{L-\ell+2,r} \mid^2)}{\mid \alpha \mid^2 N_0 + P \mid \alpha - 1 \mid^2 (\mid h_{\ell,r} \mid^2 + \mid h_{L-\ell+2,r} \mid^2)}. \tag{4.12}$$

Note that (4.10), (4.11) and (4.12) have the same form and differ in the indices of the channel coefficients, which is determined by the pairing scheme.

4.3.2 Common Rate

Assuming lattice codes with sufficiently large dimensions are employed, the common rate for an L-user FDF MWRN is given by [28, 50]

$$R_c = \frac{1}{L-1} \min_{\ell-1 \in [1, L-1]} \{R_{c,\ell-1}\}, \tag{4.13}$$

where the factor $\frac{1}{L-1}$ is due to the fact that the complete message exchange requires $L-1$ time slots and $R_{c,\ell-1}$ is the achievable rate at the $(\ell-1)^{th}$ time slot, given by

$$R_{c,\ell-1} = \min\{R_{M,\ell-1}, R_{B,\ell-1}\}, \tag{4.14}$$

where, $R_{M,\ell-1}$ and $R_{B,\ell-1}$ are the maximum achievable rates at the $(\ell-1)^{th}$ time slot during the multiple access phase and the broadcast phase, respectively. Next, we derive the upper bounds on the maximum achievable rates in the multiple access and broadcast phases.

Theorem 4.1. *For the proposed pairing scheme in a FDF MWRN, the maximum achievable rate during the $(\ell-1)^{th}$ time slot in the multiple access phase is upper bounded by*

$$R_{M,\ell-1} \leq \frac{1}{2} \log \left(\min \left(\frac{|\, h_{i,r} \,|^2}{|\, h_{i,r} \,|^2 + |\, h_{\ell,r} \,|^2} + \frac{P \,|\, h_{i,r} \,|^2}{N_0}, \frac{|\, h_{\ell,r} \,|^2}{|\, h_{i,r} \,|^2 + |\, h_{\ell,r} \,|^2} + \frac{P \,|\, h_{\ell,r} \,|^2}{N_0} \right) \right), \tag{4.15}$$

Proof. The proof can be obtained as follows. Since, the lattice dimension N is large enough to ensure $Pr(n \notin \mathcal{V}) \to 0$, the volume to noise ratio of the lattice, $\mu > 2\pi e$ is satisfied. To ensure a very small probability of error, the volume of the voronoi region must satisfy: $\mu = \frac{(\mathrm{Vol}(\mathcal{V}_{\Lambda_f}))^{2/N}}{N'}$, where N' is the variance of the noise terms in n (see (4.5)). The rate of a nested lattice code is given by: $R = \frac{1}{N} \log \frac{\mathrm{Vol}(\mathcal{V}_\Lambda)}{\mathrm{Vol}(\mathcal{V}_{\Lambda_f})}$, where $\mathcal{V}_\Lambda$ denotes the voronoi region of the coarse lattice in which the fine lattice Λ_f is nested. The volume of the voronoi region of the coarse lattice can be given by: $\mathrm{Vol}(\mathcal{V}_\Lambda) = (\frac{P \min(|h_{i,r}|^2, |h_{\ell,r}|^2)}{G})^{N/2}$, where G denotes the second moment of the coarse lattice. Thus, the achievable rates satisfy: $R \leq \frac{1}{2} \log \left(\frac{P \min(|h_{i,r}|^2, |h_{\ell,r}|^2)}{G 2\pi e N'} \right)$. For $\delta > 0$ and large enough dimension of the lattice, it can be shown that $G2\pi e < (1+\delta)$. Thus, the achievable rate can be given as:

$$R \leq \frac{1}{2}\log\left(\frac{P\min(|h_{i,r}|^2, |h_{\ell,r}|^2)}{N'}\right) - \log(1+\delta). \tag{4.16}$$

Now, the optimum value of α in (4.10) is obtained by setting $\frac{dn}{d\alpha} = 0$, where n is given in (4.5). For δ small enough and substituting $\alpha = \frac{P|h_{i,r}|^2 + P|h_{\ell,r}|^2}{P|h_{i,r}|^2 + P|h_{\ell,r}|^2 + N_0}$, the achievable rates can approach the upper bound in (4.15). □

And

Theorem 4.2. *The maximum achievable rate during the $(\ell-1)^{th}$ time slot in the broadcast phase is upper bounded by*

$$R_{B,\ell-1} \leq \frac{1}{2}\log\left(1 + \frac{\min\limits_{j\in[1,L]} \mid h_{j,r}\mid^2 P_r}{N_0}\right). \tag{4.17}$$

Proof. Next, the upper bound in (4.17) can be obtained using the similar steps as in the proof of Theorem 4.1. First, we obtain the optimum value of β_j in (4.9), obtained by setting $\frac{dn'}{d\beta_j} = 0$, where n' is given in (4.6). Then, we consider that the volume of the voronoi region must satisfy $\mu = \frac{(\mathrm{Vol}(\mathcal{V}_{\Lambda_f}))^{2/N}}{N''}$, where N'' is the variance of the noise terms n' in (4.6) and set $\mathrm{Vol}(\mathcal{V}_\Lambda) = (\frac{P_r|h_{r,j}|^2}{G})^{N/2}$ and finally, substitute $\beta_j = \frac{P_r|h_{j,r}|^2}{P_r|h_{j,r}|^2 + N_0}$. □

Note that the common rate for the pairing scheme in [28] and in [50] can be obtained by replacing the subscript i with $\ell-1$ and $L-\ell+2$, respectively in (4.15) and using (4.17), (4.14) and (4.13).

Using Theorem 4.1 and Theorem 4.2 and substituting in (4.14) and (4.13), the average common rate for the proposed pairing scheme can be given as in (4.18d) at the next page, where the inequality in (4.18b) holds from Jensen's inequality and the inequality (4.18c) comes from the fact that $E[\min(A_1, A_2)] \leq E[A_1], E[A_2]$, where A_1, A_2 are independent random variables.

Similarly, the average common rate for the pairing scheme in [28] can be expressed

$$E[R_c] \leq \frac{1}{2(L-1)} E\left[\log\left(\min\left(\frac{1}{1+\frac{|h_{\ell,r}|^2}{|h_{i,r}|^2}} + \frac{P \mid h_{i,r} \mid^2}{N_0}, \frac{1}{1+\frac{|h_{i,r}|^2}{|h_{\ell,r}|^2}} + \frac{P \mid h_{\ell,r} \mid^2}{N_0}\right)\right)\right] \tag{4.18a}$$

$$\leq \frac{1}{2(L-1)} \log\left(E\left[\min\left(\frac{1}{1+\frac{|h_{\ell,r}|^2}{|h_{i,r}|^2}} + \frac{P \mid h_{i,r} \mid^2}{N_0}, \frac{1}{1+\frac{|h_{i,r}|^2}{|h_{\ell,r}|^2}} + \frac{P \mid h_{\ell,r} \mid^2}{N_0}\right)\right]\right) \tag{4.18b}$$

$$\leq \frac{1}{2(L-1)} \log\left(\min\left(E\left[\frac{1}{1+\frac{|h_{\ell,r}|^2}{|h_{i,r}|^2}} + \frac{P \mid h_{i,r} \mid^2}{N_0}\right], E\left[\frac{1}{1+\frac{|h_{i,r}|^2}{|h_{\ell,r}|^2}} + \frac{P \mid h_{\ell,r} \mid^2}{N_0}\right]\right)\right) \tag{4.18c}$$

$$= \frac{1}{2(L-1)} \log\left(\min\left(\frac{1}{1+\frac{\sigma^2_{h_{\ell,r}}}{\sigma^2_{h_{i,r}}}} + \frac{P\sigma^2_{h_{i,r}}}{N_0}, \frac{1}{1+\frac{\sigma^2_{h_{i,r}}}{\sigma^2_{h_{\ell,r}}}} + \frac{P\sigma^2_{h_{\ell,r}}}{N_0}\right)\right), \tag{4.18d}$$

as

$$E[R_c] \leq \frac{1}{2(L-1)} \log\left(\min\left(\frac{1}{1+\frac{\sigma^2_{h_{\ell,r}}}{\sigma^2_{h_{\ell-1,r}}}} + \frac{P\sigma^2_{h_{\ell-1,r}}}{N_0}, \frac{1}{1+\frac{\sigma^2_{h_{\ell-1,r}}}{\sigma^2_{h_{\ell,r}}}} + \frac{P\sigma^2_{h_{\ell,r}}}{N_0}\right)\right), \tag{4.19}$$

and the average common rate for the pairing scheme in [50] can be given as

$$E[R_c] \leq \frac{1}{2(L-1)} \log\left(\min\left(\frac{1}{1+\frac{\sigma^2_{h_{\ell-1,r}}}{\sigma^2_{h_{L-\ell+2,r}}}} + \frac{P\sigma^2_{h_{L-\ell+2,r}}}{N_0}, \frac{1}{1+\frac{\sigma^2_{h_{L-\ell+2,r}}}{\sigma^2_{h_{\ell-1,r}}}} + \frac{P\sigma^2_{h_{\ell-1,r}}}{N_0}, \right.\right.$$
$$\left.\left. \frac{1}{1+\frac{\sigma^2_{h_{\ell,r}}}{\sigma^2_{h_{L-\ell+2,r}}}} + \frac{P\sigma^2_{h_{L-\ell+2,r}}}{N_0}, \frac{1}{1+\frac{\sigma^2_{h_{L-\ell+2,r}}}{\sigma^2_{h_{\ell,r}}}} + \frac{P\sigma^2_{h_{\ell,r}}}{N_0}\right)\right). \tag{4.20}$$

Note that, though the common rate for AWGN MWRNs has been obtained for the existing pairing schemes (see Section 2.3), the expressions in (4.19) and (4.20) have not been derived in the literature.

While (4.18d)−(4.20) do not provide tight upper bounds on the average common rate, they allow an analytical comparison of the proposed and existing pairing schemes. The main results from the analytical comparison are summarized in the Propositions 4.1−4.3. Note that in the numerical results section (Section 4.5), the actual expressions of the instantaneous rates are averaged over a large number of channel realizations to corroborate the insights presented in Propositions 4.1−4.3.

Proposition 4.1. *The average common rate for the proposed pairing scheme and the pairing schemes in [28] and [50] are the same for the equal average channel gain scenario.*

Proof. See Appendix B.1. □

Proposition 4.2. *The average common rate for the proposed pairing scheme is larger than that of the pairing schemes in [28] and [50] for the unequal average channel gain scenario.*

Proof. See Appendix B.1. □

Proposition 4.3. *The average common rate for the proposed pairing scheme is practically the same as that of the pairing schemes in [28] and [50], for the variable average channel gain scenario.*

Proof. See Appendix B.1. □

Remark 4.1. *For unequal channel gain scenario, the common user's power is scaled to maintain fairness. This decreases the ratio of the maximum (i.e., the* i^{th} *user's) and minimum average channel gains in* (4.18d)*. As a result, the common rate improves for the proposed pairing scheme.*

Remark 4.2. *For variable channel gain scenario, the minimum channel gain user actually controls the common rate and it is the same for both the proposed and the existing pairing schemes. As a result, the common rates are practically the same.*

4.3.3 Sum Rate

From Chapter 2, the sum rate can be defined as the sum of the achievable rates of all users for a complete round of information exchange.

$$E[R_s] \leq \frac{1}{2(L-1)} \sum_{\ell=1,\ell\neq i}^{L} \left(\log \left(\frac{1}{1+\frac{\sigma^2_{h_{\ell,r}}}{\sigma^2_{h_{i,r}}}} + \frac{P\sigma^2_{h_{i,r}}}{N_0} \right) + \log \left(\frac{1}{1+\frac{\sigma^2_{h_{i,r}}}{\sigma^2_{h_{\ell,r}}}} + \frac{P\sigma^2_{h_{\ell,r}}}{N_0} \right) \right). \quad (4.22)$$

Theorem 4.3. *For the proposed pairing scheme in a FDF MWRN, the sum rate is given by:*

$$R_s \leq \frac{1}{2(L-1)} \sum_{\ell=1,\ell\neq i}^{L} \left(\log \left(\frac{|\ h_{i,r}\ |^2}{|\ h_{i,r}\ |^2 + |\ h_{\ell,r}\ |^2} + \frac{P\ |\ h_{i,r}\ |^2}{N_0} \right) + \log \left(\frac{|\ h_{\ell,r}\ |^2}{|\ h_{i,r}\ |^2 + |\ h_{\ell,r}\ |^2} + \frac{P\ |\ h_{\ell,r}\ |^2}{N_0} \right) \right). \quad (4.21)$$

Proof. The achievable rate at the $(\ell-1)^{th}$ time slot can be obtained from (4.15). Since, $\frac{|h_{i,r}|^2}{|h_{i,r}|^2+|h_{\ell,r}|^2} < 1$, the achievable rate at the i^{th} time slot will be determined by the achievable rate at the corresponding time slot in the multiple access phase. Then, obtaining the achievable rate in all the time slots and adding them results into (4.21). The detailed steps are omitted here for the sake of brevity. □

Note that the sum rate for the pairing scheme in [28] and the pairing scheme in [50] can be obtained by replacing the subscript i with $\ell-1$ and $L-\ell+2$, respectively in (4.21).

Using Theorem 4.3, the average sum rate (averaged over all channel realizations) for the proposed pairing scheme can be upper bounded as in (4.22), using similar steps as in (4.18a), (4.18b) and (4.18d).

Similarly, the average sum rate for the pairing scheme in [28] can be written as

$$E[R_s] \leq \frac{1}{2(L-1)} \sum_{\ell=2}^{L} \left(\log \left(\frac{1}{1+\frac{\sigma^2_{h_{\ell,r}}}{\sigma^2_{h_{\ell-1,r}}}} + \frac{P\sigma^2_{h_{\ell-1,r}}}{N_0} \right) + \log \left(\frac{1}{1+\frac{\sigma^2_{h_{\ell-1,r}}}{\sigma^2_{h_{\ell,r}}}} + \frac{P\sigma^2_{h_{\ell,r}}}{N_0} \right) \right), \quad (4.23)$$

and the average sum rate for the pairing scheme in [50] can be written as

$$E[R_s] \leq \frac{1}{2(L-1)} \sum_{\ell=2}^{\lfloor L/2 \rfloor+1} \left(\log\left(\frac{1}{1+\frac{\sigma^2_{h_{\ell-1,r}}}{\sigma^2_{h_{L-\ell+2,r}}}} + \frac{P\sigma^2_{h_{L-\ell+2,r}}}{N_0} \right) + \log\left(\frac{1}{1+\frac{\sigma^2_{h_{L-\ell+2,r}}}{\sigma^2_{h_{\ell-1,r}}}} + \frac{P\sigma^2_{h_{\ell-1,r}}}{N_0} \right) \right)$$
$$+ \sum_{\ell=\lfloor L/2 \rfloor+2}^{L} \left(\log\left(\frac{1}{1+\frac{\sigma^2_{h_{\ell,r}}}{\sigma^2_{h_{L-\ell+2,r}}}} + \frac{P\sigma^2_{h_{L-\ell+2,r}}}{N_0} \right) + \log\left(\frac{1}{1+\frac{\sigma^2_{h_{L-\ell+2,r}}}{\sigma^2_{h_{\ell,r}}}} + \frac{P\sigma^2_{h_{\ell,r}}}{N_0} \right) \right). \tag{4.24}$$

Note that, though the sum rate for AWGN MWRNs has been obtained for the existing pairing schemes (see Section 2.3), the expressions in (4.23) and (4.24) have not been derived in the literature.

Equations (4.22)−(4.24) provide upper bounds on the actual average sum rate and they allow an analytical comparison of the proposed and existing pairing schemes. The main results are summarized in Propositions 4.4−4.6. Note that similar to the case of common rate, in the numerical results section (Section 4.5), the actual expression for the instantaneous sum rate in (4.21) is averaged over a large number of channel realizations to validate the insights presented in the Propositions 4.4−4.6.

Proposition 4.4. *The average sum rate of the proposed pairing scheme and the pairing schemes in [28] and [50] are the same for the equal average channel gain scenario.*

Proof. See Appendix B.2. □

Proposition 4.5. *The average sum rate of the proposed pairing scheme is larger than that of the pairing schemes in [28] and [50] for the unequal average channel gain scenario.*

Proof. See Appendix B.2. □

Proposition 4.6. *The average sum rate of the proposed pairing scheme is larger than that of the pairing schemes in [28] and [50] for the variable average channel gain scenario.*

Proof. See Appendix B.2. □

Remark 4.3. *Since, the common user's channel gain is present in more terms in* (4.22)*, compared to* (4.23) *and* (4.24)*, the sum rate is better for unequal and variable average channel gains. For equal channel gains, since, all the channel gains are equal, the expressions in* (4.22)*,* (4.23) *and* (4.24) *become the same and hence, the sum rates are the same for the existing and the proposed pairing schemes.*

4.4 Error Performance Analysis

In this section, we characterize the error performance of a FDF MWRN with the new pairing scheme. First, we obtain the SER results for the proposed pairing scheme and then show that the error performance is better than that of the existing pairing schemes under different channel scenarios. We provide the analytical derivations for M-QAM modulation, which is a 2 dimensional lattice code and is widely used in practical wireless communication systems.

4.4.1 System Model

In the square M-QAM modulated FDF MWRN system, during a certain time frame, in the $t_s = (\ell - 1)^{th}$ time slot, the i^{th} user and the ℓ^{th} user transmit their messages $\mathbf{W}_i$ and $\mathbf{W}_\ell$ which are M-QAM modulated to $\mathbf{X}_i = \{X_i^1, X_i^2, ..., X_i^T\}$ and $\mathbf{X}_\ell = \{X_\ell^1, X_\ell^2, ..., X_\ell^T\}$, respectively, where $X_i^t, X_\ell^t = a + jb$ and $a, b \in \{\pm 1, \pm 3, ..., \pm(\sqrt{M} - 1)\}$. The relay receives the signal $\mathbf{R}_{i,\ell}$ (see (4.4)) and decodes it using ML criterion [22] and obtains an estimate $\hat{\mathbf{V}}_{i,\ell}$ of the network coded symbol $\mathbf{V}_{i,\ell} = (\mathbf{W}_i + \mathbf{W}_\ell) \mod M$ as in [15,23]. The relay then broadcasts the estimated network coded signal after M-QAM modulation, which is given as $\mathbf{Z}_{i,\ell}$. The j^{th} ($j \in [1, L]$) user receives $\mathbf{Y}_{i,\ell}$ (see (2.7)) and detects the received signal through ML criterion [22] to obtain the estimate $\hat{\hat{\mathbf{V}}}_{i,\ell}$. After decoding all the network coded messages, each user performs message extraction. For the common user (i^{th} user), this message extraction involves subtracting its own message $\mathbf{W}_i$ from the network coded messages $\hat{\hat{\mathbf{V}}}_{i,\ell}$ and then performing the modulo-M operation. The process can be shown as

$$\hat{\mathbf{W}}_\ell = (\hat{\hat{\mathbf{V}}}_{i,\ell} - \mathbf{W}_i + M) \mod M, \tag{4.25a}$$

$$\hat{\mathbf{W}}_{\ell+1} = (\hat{\hat{\mathbf{V}}}_{i,\ell+1} - \mathbf{W}_i + M) \mod M, \tag{4.25b}$$

$$..., \tag{4.25c}$$

$$\hat{\mathbf{W}}_L = (\hat{\hat{\mathbf{V}}}_{i,L} - \mathbf{W}_i + M) \mod M. \tag{4.25d}$$

For other users, the message extraction process can be shown as

$$\hat{\mathbf{W}}_i = (\hat{\hat{\mathbf{V}}}_{i,\ell} - \mathbf{W}_\ell + M) \mod M, \tag{4.26a}$$

$$\hat{\mathbf{W}}_{\ell+1} = (\hat{\hat{\mathbf{V}}}_{i,\ell+1} - \hat{\mathbf{W}}_i + M) \mod M, \tag{4.26b}$$

$$..., \tag{4.26c}$$

$$\hat{\mathbf{W}}_L = (\hat{\hat{\mathbf{V}}}_{i,L} - \hat{\mathbf{W}}_i + M) \mod M. \tag{4.26d}$$

4.4.2 SER Analysis for the Proposed Pairing Scheme

In this subsection, we investigate the error performance of a FDF MWRN with the proposed pairing scheme. Unlike the pairing schemes in [28] and [50], the error performance of all the users is not the same for the proposed pairing scheme. Hence, we need to obtain separate expressions for the error probabilities at the common user (i^{th} user) and other users (ℓ^{th} user).

First, we obtain the probability of incorrectly decoding a network coded message at the common user and the other users. Since, any M-QAM signal with square constellation (i.e., $\sqrt{M} \in \mathbb{Z}$) can be decomposed to two $\sqrt{M}$-PAM signals [99], the network coded signal from a linear combination of two M-QAM signals can be decomposed to a network coded signal from two $\sqrt{M}$-PAM signals. Thus, we can obtain the probability of incorrectly decoding a network coded message as in the following lemma.

Lemma 4.1. *The probability that the i^{th} (common) user incorrectly decodes the network coded message involving its own message and the m^{th} user's message is given by*

$$P_{FDF}(i,m) = 1 - \left(1 - P_{\sqrt{M}-PAM,NC}(i,m)\right)^2, \tag{4.27}$$

where $P_{\sqrt{M}-PAM,NC}(i,m)$ *is the probability of incorrectly decoding a network coded message resulting from the sum of two* $\sqrt{M}$*-PAM signals from the* i^{th} *and the* m^{th} *user and is given by*

$$P_{\sqrt{M}-PAM,NC}(i,m) = \frac{1}{\sqrt{M}}\left(\sum_{p,q=0}^{\sqrt{M}-1} c_{p,q} \sum_{p',q'=0,p'\neq p,q'\neq q}^{\sqrt{M}-1} d_{p',q'}\right), \tag{4.28}$$

where $c_{p,q}$ *can be expressed as*

$$c_{p,q} = \begin{cases} \sum_{u=1,u=odd}^{2(2\sqrt{M}-2)-1} a_{p,q,u} Q(u\sqrt{\gamma_r(i,m)}), & p \neq q \\ 1 + \sum_{u=1,u=odd}^{2(2\sqrt{M}-2)-1} a_{p,q,u} Q(u\sqrt{\gamma_r(i,m)}), & p = q \end{cases} \tag{4.29}$$

and $\gamma_r(i,m)$ *represents the SNR of the* i^{th} *and the* m^{th} *users' signal at the relay for* $\sqrt{M}$*-PAM modulation and can be obtained as*

$$\gamma_r(i,m) = \frac{P\min(\mid h_{i,r}\mid^2, \mid h_{m,r}\mid^2)}{E_{av}N_0}. \tag{4.30}$$

where E_{av} *is the average energy of symbols for* $\sqrt{M}$*-PAM modulation (e.g.,* $E_{av} = 5$ *for* $M = 16$*) and* $d_{p',q'}$ *can be expressed as*

$$d_{p',q'} = \begin{cases} \sum_{v=1,v=odd}^{2(\sqrt{M}-1)-1} b_{p',q',v} Q(v\sqrt{\gamma_i}), & p' \neq q' \\ 1 + \sum_{v=1,v=odd}^{2(\sqrt{M}-1)-1} b_{p',q',v} Q(v\sqrt{\gamma_i}), & p' = q' \end{cases} \tag{4.31}$$

where $\gamma_i = \frac{P_r|h_{r,i}|^2}{E_{av}N_0}$ *represents the SNR at the* i^{th} *user.*

Proof. See Appendix B.3. The coefficients $a_{p,q,u}$ and $b_{p',q',v}$ for $M = 16$ (or $\sqrt{M} = 4$),

Table 4.1: Illustration of the coefficients $a_{p,q,u}$ and $b_{p',q',v}$ for $M = 16$ corresponding to (4.29) and (4.31), respectively.

		$a_{p,q,u}$					$b_{p',q',v}$			
p, p'	u \ q	$q = 0$	$q = 1$	$q = 2$	$q = 3$	v \ q'	$q' = 0$	$q' = 1$	$q' = 2$	$q' = 3$
$p = 0$	$u = 1$	$-7/4$	1	0	$3/4$	$v = 1$	$1/4$	$1/4$	0	0
	$u = 3$	0	-1	$7/4$	$-3/4$					
	$u = 5$	0	$3/4$	-1	$1/4$	$v = 3$	0	$-1/4$	$1/4$	0
	$u = 7$	1	$-3/4$	0	$-1/4$					
	$u = 9$	$-1/4$	$1/4$	0	0	$v = 5$	0	0	$-1/4$	$1/4$
	$u = 11$	0	$-1/4$	$1/4$	0					
$p = 1$	$u = 1$	1	1	0	0	$v = 1$	$1/4$	$-1/4$	$1/4$	0
	$u = 3$	-1/2	0	$-1/2$	1					
	$u = 5$	$1/2$	0	$1/2$	-1	$v = 3$	$-1/4$	$1/4$	$-1/4$	$1/4$
	$u = 7$	$-1/2$	1	$-1/2$	0					
	$u = 9$	$1/2$	-1	$1/2$	0	$v = 5$	0	$1/4$	0	$-1/4$
	$u = 11$	0	0	0	0					
$p = 2$	$u = 1$	1	1	$-7/4$	$3/4$	$v = 1$	0	$1/4$	$-1/4$	$1/4$
	$u = 3$	$7/4$	-1	0	$-3/4$					
	$u = 5$	-1	$3/4$	0	$1/4$	$v = 3$	$1/4$	$-1/4$	$1/4$	$1/4$
	$u = 7$	0	$-3/4$	1	$-1/4$					
	$u = 9$	0	$1/4$	$-1/4$	0	$v = 5$	$-1/4$	0	$1/4$	0
	$u = 11$	$1/4$	$-1/4$	0	0					
$p = 3$	$u = 1$	1	0	1	-2	$v = 1$	0	0	$1/4$	$-1/4$
	$u = 3$	-1	2	-1	0					
	$u = 5$	1	-2	1	0	$v = 3$	$1/4$	$1/4$	$-1/4$	0
	$u = 7$	0	0	0	0					
	$u = 9$	0	0	0	0	$v = 5$	0	$-1/4$	0	0
	$u = 11$	0	0	0	0					

have been tabulated in Table 4.1.

$\square$

Similarly, the probability that the ℓ^{th} (other) user incorrectly decodes the network coded message involving the i^{th} user's message and its own message or other user's messages is given as:

$$P_{FDF}(\ell, m) = \begin{cases} 1 - \left(1 - P_{\sqrt{M}-PAM,NC}(\ell, m)\right)^2, & m = i \\ 1 - \left(1 - P_{\sqrt{M}-PAM,NC}(i, m)\right)^2, & m \in [1, L], m \neq i, \ell. \end{cases} \tag{4.32}$$

where $P_{\sqrt{M}-PAM,NC}(\ell, m)$ is the probability of incorrectly decoding a network coded message, i.e., the sum of two $\sqrt{M}$-PAM signals of the ℓ^{th} and the m^{th} user and can be obtained from Appendix B.3 and using tables similar to table 4.1.

Using (4.27) and (4.32), the average SER at the common user and the other users can be derived using the technique proposed in Chapter 3. The result is summarized in the following Theorem.

Theorem 4.4. *For the proposed pairing scheme in a FDF MWRN, the average SER at the i^{th} (common) user is given by:*

$$P_{i,avg} = \frac{1}{L-1} \sum_{m=1, m\neq i}^{L} P_{FDF}(i, m), \tag{4.33}$$

and the average SER at the ℓ^{th} (other) users is given by:

$$P_{\ell,avg} = \frac{1}{L-1} \left(\sum_{m=1, m\neq i,\ell}^{L} P_{FDF}(\ell, m) + (L-1) P_{FDF}(\ell, i) \right). \tag{4.34}$$

Proof. See Appendix B.4. □

Remark 4.4. *From Theorem 4.4, it can be identified that the average SER at the other (ℓ^{th}) users is at least twice compared to the average SER at the common (i^{th}) user. This can be intuitively explained from the fact that the i^{th} user needs to correctly decode only one network coded message ($V_{i,m}$) to correctly decode the m^{th} user's message. In other words, there is no error propagation for the common user. However, the ℓ^{th} user needs to correctly decode two network coded messages ($V_{i,m}$ and $V_{i,\ell}$) to correctly decode the m^{th} user's message. Thus, the average SER at the other users would at least be twice compared to that at the common user.*

Using Theorem 4.4 and the average SER result for the pairing scheme in [28], we can compare the performance of the proposed and the existing pairing schemes. Note that the error performance of the pairing scheme in [50] would be the same as the pairing scheme in [28], as the basic pairing process is the same for both these schemes and only the pairing orders are different. The main results are summarized in Propositions

4.7−4.9.

Proposition 4.7. *The average SER of an L-user FDF MWRN with the proposed pairing scheme is lower than the pairing scheme in [28] by a factor of* $\frac{L}{2}$ *for the common user and a factor of approximately* $\frac{L}{4}$ *for other users under the equal average channel gain scenario.*

Proof. See Appendix B.5. □

Proposition 4.8. *The average SER of an L-user FDF MWRN with the proposed pairing scheme is always lower than the pairing scheme in [28] for all users under the unequal average channel gain scenario.*

Proof. See Appendix B.5. □

Proposition 4.9. *The average SER of an L-user FDF MWRN with the proposed pairing scheme is always lower than the pairing scheme in [28] for all users under the variable average channel gain scenario.*

Proof. See Appendix B.5. □

From Propositions 4.7-4.9, it is clear that choosing the user with the best average channel gain as the common user reduces the average SER of the FDF MWRN.

4.5 Numerical Results

In this section, we provide numerical results to verify the insights provided in Propositions 4.1−4.6. We also provide simulation results to verify Propositions 4.7−4.9. The power at the users, P and the power at the relay, P_r are assumed to be equal and normalized to unity. The transmit SNR per bit per user is defined as $\frac{1}{N_0}$. Following [49], the average channel gain for the j^{th} user is modeled by $\sigma^2_{h_{j,r}} = (1/(d_j/d_0))^{\nu}$, where d_0 is the reference distance, d_j is the distance between the j^{th} user and the relay which is assumed to be uniformly randomly distributed between 0 and d_0, and ν is the path loss exponent, which is assumed to be 3. Such a distance based channel model takes into account large scale path loss and has been widely considered in the literature [15, 44, 53, 80, 100, 101]. All distances, once chosen, remain constant for unequal channel gain scenario and are randomly chosen every time frame (i.e., worst case, $T'_f = 1$) for variable channel gain scenario. Note that all the distances are the same for the equal average channel gain scenario.

4.5.1 Common Rate

Fig. 4.2 shows the common rate for the proposed and the existing pairing schemes in an $L = 10$ user FDF MWRN. All the numerical results are obtained by averaging the instantaneous common rates for the pairing schemes over a large number of channel realizations. Fig. 4.2(a) shows that all the pairing schemes have the same average common rate in equal average channel gain scenario, which verifies Proposition 4.1. The common rate of the proposed pairing scheme is larger than the existing pairing schemes for the unequal average channel gain scenario in Fig. 4.2(b). This is because, scaling the common user's power to ensure transmission fairness decreases the ratio of the maximum and the minimum average channel gains in (4.18d), as identified in Remark 4.1. For variable average channel gain scenario, we can see that the common rate for the proposed scheme is practically the same as that of the existing pairing schemes, which is explained in 4.2. This verifies Propositions 4.2 and 4.3, respectively.

4.5.2 Sum Rate

Fig. 4.3 shows the sum rate for the proposed and the existing pairing schemes in an $L = 10$ user FDF MWRN for the three channel scenarios. All the numerical results are obtained by averaging the instantaneous sum rates for the pairing schemes over a large number of channel realizations. Fig. 4.3(a) shows that all the pairing schemes have the same average sum rate for equal average channel gain scenario, which verifies Proposition 4.4. Similarly, Fig. 4.3(b) and Fig. 4.3(c) show that the average sum rate for the proposed pairing scheme is larger than the existing pairing schemes, which is

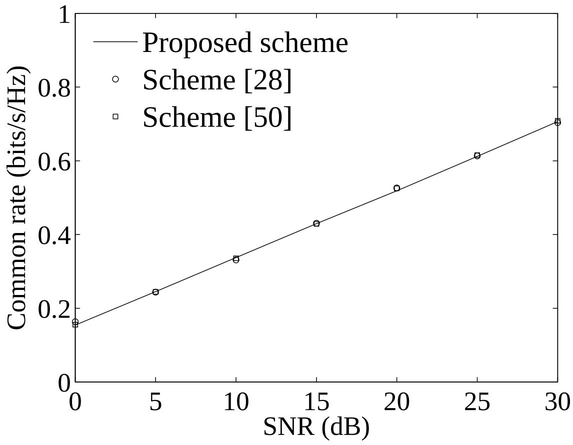

(a) Equal channel gain scenario

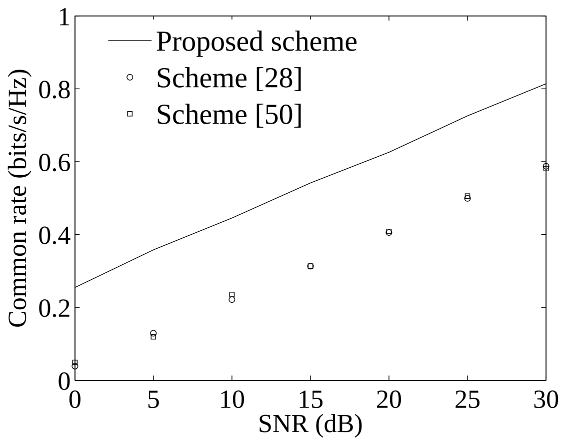

(b) Unequal channel gain scenario

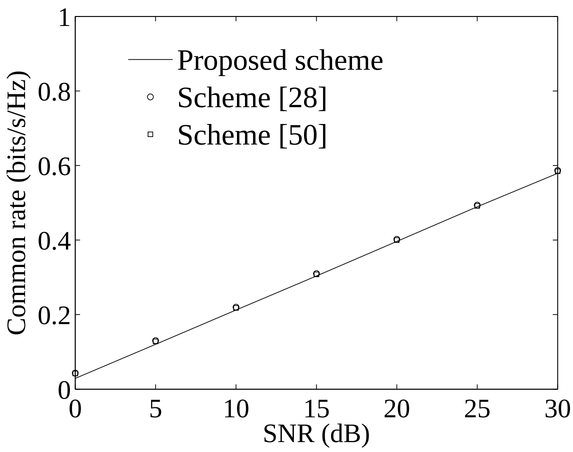

(c) Variable channel gain scenario

Figure 4.2: Common rate for a $L = 10$ user FDF MWRN with different pairing schemes and different channel scenarios.

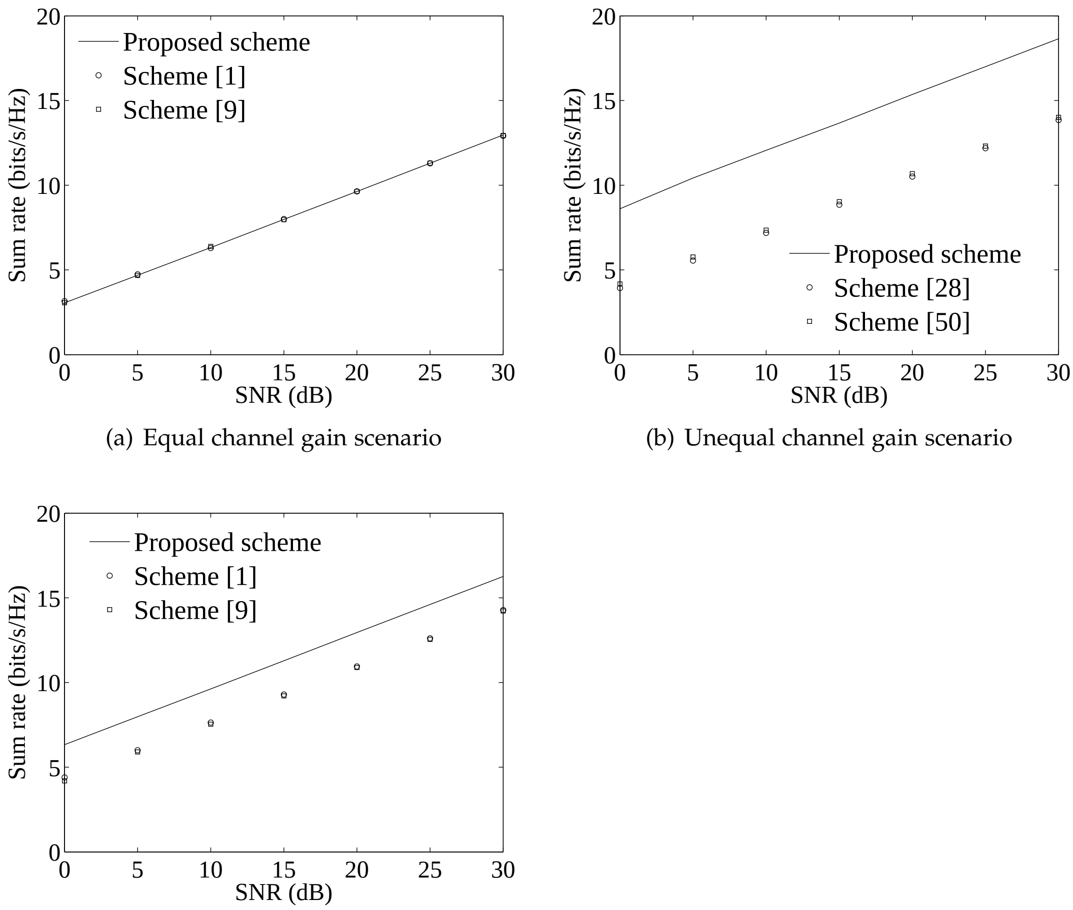

(a) Equal channel gain scenario

(b) Unequal channel gain scenario

(c) Variable channel gain scenario

Figure 4.3: Sum rate for a $L = 10$ user FDF MWRN with different pairing schemes and different channel scenarios.

in line with the Propositions 4.5 and 4.6. Intuitively, this can be explained as follows. In the proposed pairing scheme, the common user with the maximum average channel gain transmits more times than the other users. Unless all the average channel gains are equal, this results in a larger sum rate compared to the existing pairing schemes.

4.5.3 Robustness of the Proposed Pairing Scheme

To illustrate robustness of the proposed pairing scheme, we consider two special cases of the variable average channel gain scenario, where (i) 10% of the users have distances below $0.1d_0$ (i.e., only a small proportion of the users are close to the relay and so, they have good channel conditions) and (ii) 90% of the users have distances below $0.1d_0$ (i.e., a large proportion of users have good channel conditions). Fig. 4.4(a) plots the average common rate and Fig. 4.4(b) plots the average sum rate for the proposed and existing pairing schemes. We can see from Fig. 4.4(a) that the common rate does not change much when either 10% or 90% of users have good channel conditions as it depends upon the minimum average channel gain in the system. However, we can see from Fig. 4.4(b) that when the number of users with good channel conditions falls from 90% to 10%, the sum rate of the proposed scheme degrades to a much lesser extent, compared to the existing pairing schemes. This is because the average sum rate of the proposed pairing scheme depends to a greater extent on the common user's average channel gain compared to the other users' average channel gain (as evident from (4.22)). However, for the existing pairing schemes, the sum rate depends on all the channel gains equally (as evident from (4.23) and (4.24)) and degrades to a greater extent. This illustrates the robustness of the proposed pairing scheme to varying channel conditions.

4.5.4 Average SER

Figures 4.5(a), 4.5(b) and 4.6(a) plot the average SER of the proposed and the existing pairing schemes in an $L = 10$ user FDF MWRN for equal channel gain scenario (Fig. 4.5(a)), unequal channel gain scenario (Fig. 4.5(b)) and variable channel gain scenario (Fig. 4.6(a)). We can see from all the figures that the simulation results match perfectly with the analytical results at mid to high SNRs. This verifies the accuracy of Theorem 4.4. Note that the existing pairing schemes in [28] and [50] have the same average SER. Figures 4.5(a), 4.5(b) and 4.6(a) show that the proposed pairing scheme outperforms the existing pairing schemes, in terms of average SER, which verifies Propositions 4.7-4.9. In addition, Fig. 4.5(a) shows that the average SER at the common user and other users are 5 times and nearly 2.5 times less than that of the existing pairing schemes. This verifies the insight presented by Remark 4.4 and Proposition 4.7.

Fig. 4.6(b) plots the average SER of the proposed and the existing pairing schemes

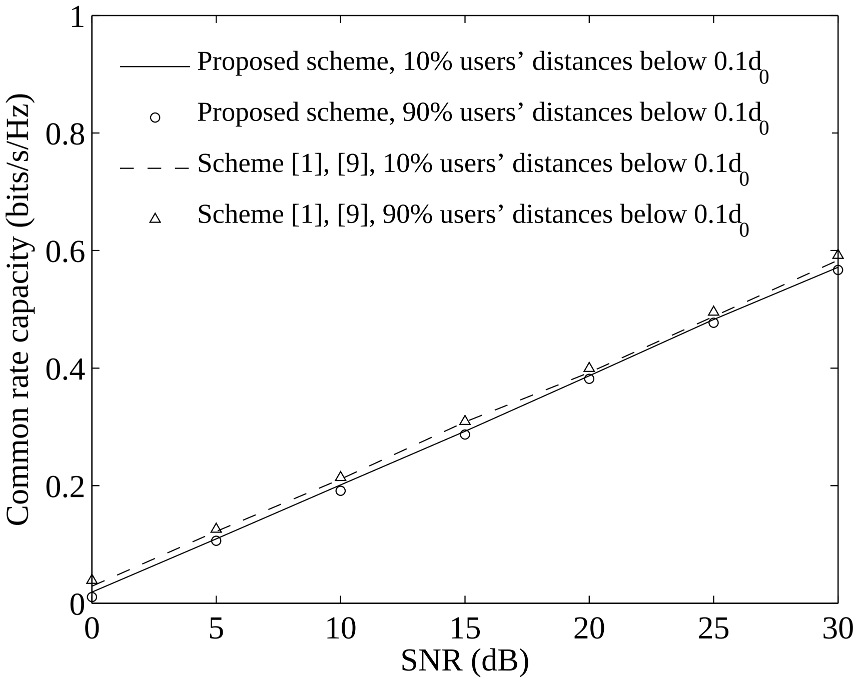

(a) Common rate

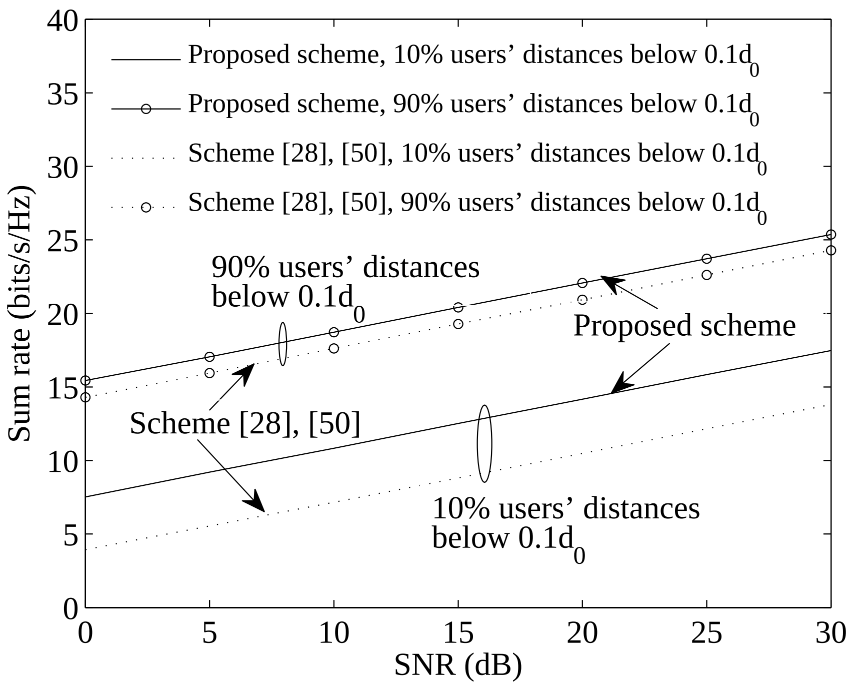

(b) Sum rate

Figure 4.4: Common rate and sum rate of an $L = 10$ user FDF MWRN when 10% and 90% users have distances below $0.1d_0$.

for the special cases of the variable average channel gain scenario when (i) 10% of the users have distances below $0.1d_0$ and (ii) 90% of the users have distances below $0.1d_0$. The figure shows that the average SER for the existing pairing schemes worsens by a larger extent compared to that of the proposed scheme with the degradation in the users' channel conditions. For the proposed pairing scheme, when the number of users with good channel conditions increases from 10% to 90%, the average SER at other users improve significantly and approaches the average SER at the common user. This is because the average SER at the ℓ^{th} user depends not only on its own channel conditions, but also the channel conditions of the common (i^{th}) user and the m^{th} user (see (4.34)). This improvement in the overall channel conditions results in improvement in the average SER, which illustrates the superiority of the proposed pairing scheme.

4.6 Summary

In this chapter, we proposed a novel pairing scheme to reduce error propagation in FDF MWRNs. We compared the proposed pairing scheme with the existing pairing schemes in terms of the common rate, sum rate and error performance and showed that the proposed scheme outperforms the existing pairing schemes. Specifically, we made the following contributions in this chapter:

- In Section 4.1, we showed that pairing each user with the best channel gain user is beneficial for FDF MWRN performance improvement. Specifically, we showed that the proposed pairing scheme can eliminate error propagation problem for the common user and significantly reduce the chances of error propagation for other users. This results in better average common rate, sum rate and error performance.
- In Section 4.3, we derived upper bounds on the common rate and sum rate of a lattice coded FDF MWRN with the proposed pairing scheme.
- In Section 4.4, we derived average SER for a FDF MWRN with the proposed scheme and square M-QAM modulation, as a special case of lattice codes.

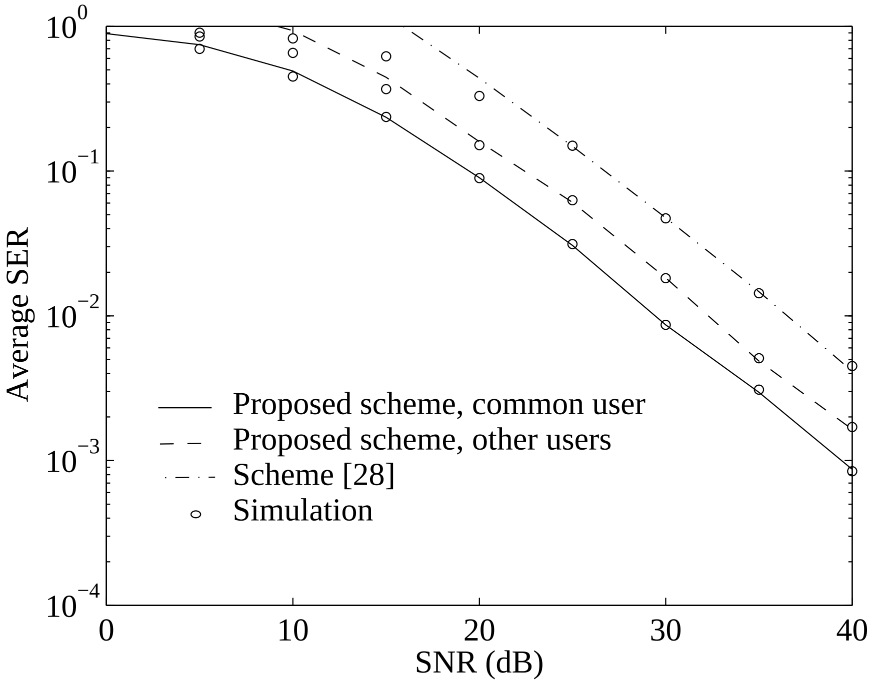

(a) Equal channel gain scenario

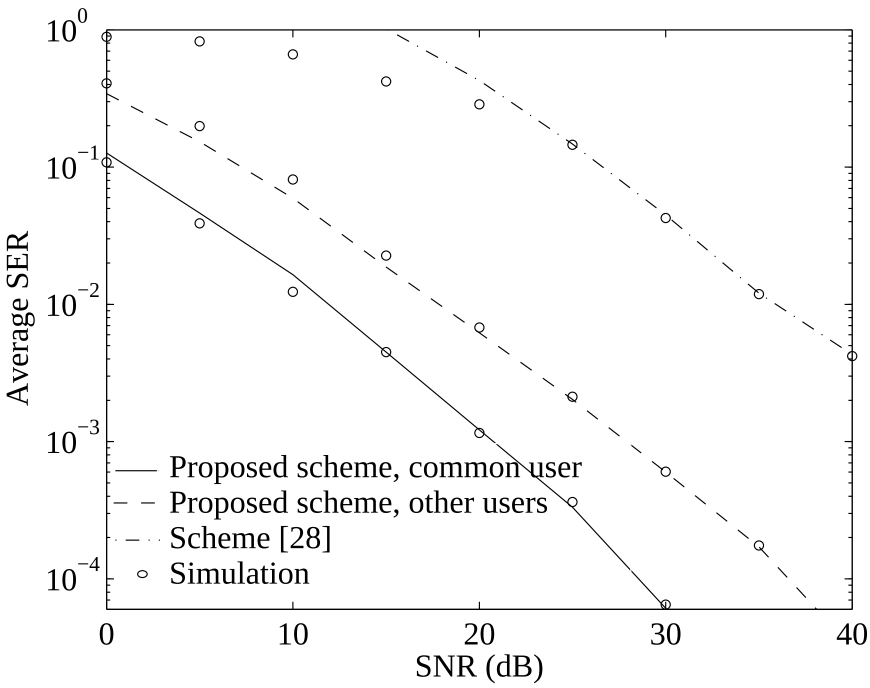

(b) Unequal channel gain scenario

Figure 4.5: Average SER for equal and unequal average channel gains in an $L = 10$ user FDF MWRN with different pairing schemes.

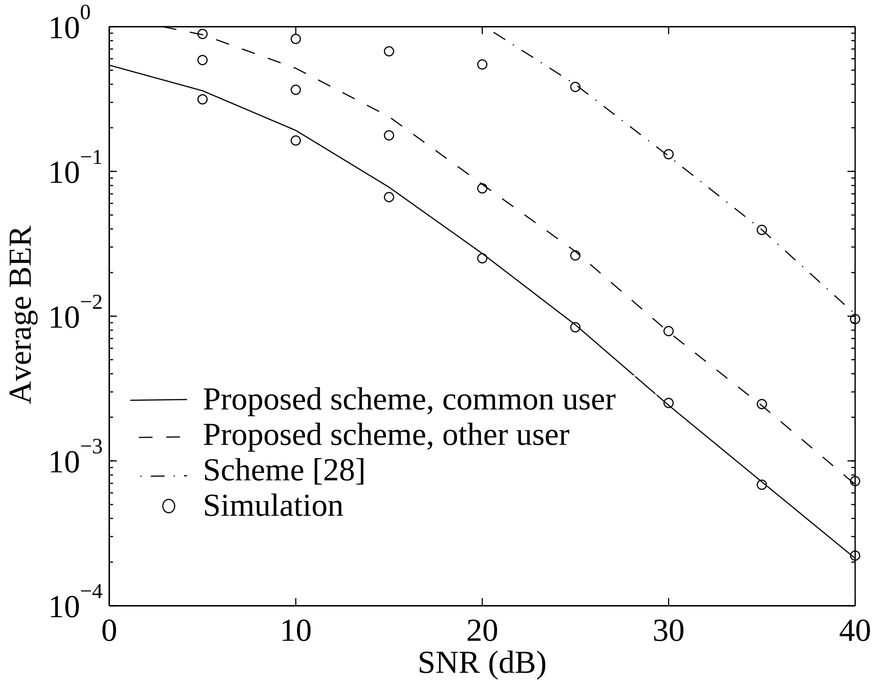

(a) Variable channel gain scenario

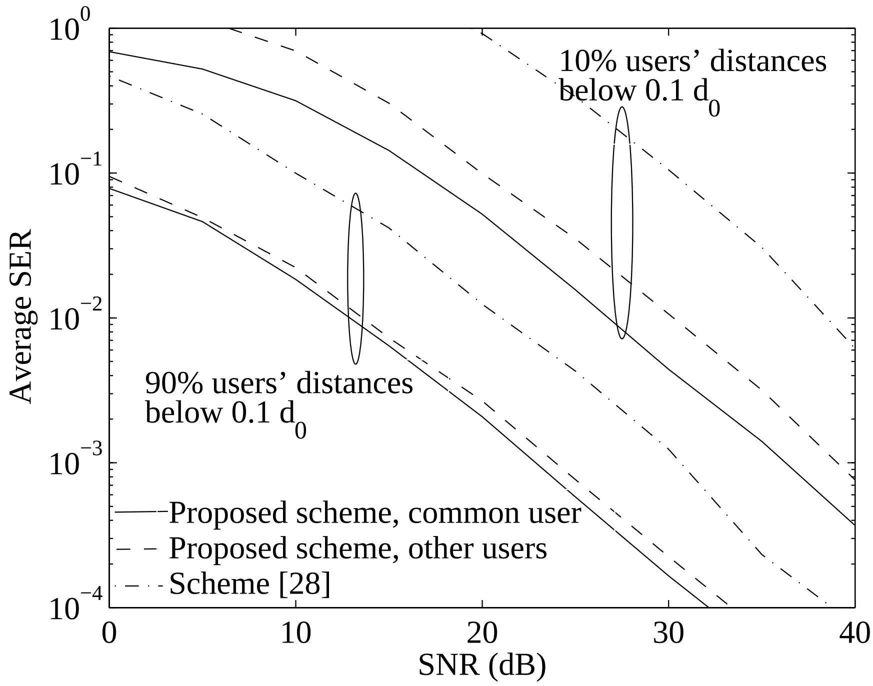

(b) Variable channel gain scenario where 10% and 90% users, respectively, have distances below $0.1d_0$.

Figure 4.6: Average SER for variable average channel gains in an $L = 10$ user FDF MWRN with different pairing schemes.

- In Propositions 4.1, 4.4 and 4.7, we showed that when the average channel gains are equal, the average common rate and the average sum rate in a FDF MWRN are the same for the proposed and existing pairing schemes, but the average SER improves with the proposed pairing scheme.
- In Propositions 4.2, 4.5 and 4.8, we showed that for the unequal average channel gain scenario, the average common rate, the average sum rate and the average SER in a FDF MWRN all improve for the proposed pairing scheme.
- In Propositions 4.3, 4.6 and 4.9, we showed that for the variable average channel gain scenario, the average common rate in a FDF MWRN with the proposed pairing scheme is practically the same as the existing schemes, whereas, the average sum rate and the average SER improve for the proposed pairing scheme.

Pairing scheme design for an AF MWRN with BPSK modulation has been investigated in our work [37]. We do not include here the detailed analysis from the paper so that the readability and flow of this chapter is not hampered. However, we would like to mention the main contributions of the paper for its relevance with this chapter:

- We proposed a novel pairing scheme for an AF MWRN, where the relay chooses a user based on its average channel gain, which is then paired with every other user in the network. That is, the chosen user serves as a common user for all the user pairs.
- We showed that choosing the user with the *minimum* average channel gain as the common user reduces error propagation at other users by lessening the influence of interference components from the common user's signal in the extracted signals of other users.
- We investigated the average BER at different users for the proposed pairing scheme and compared with existing pairing schemes. The proposed scheme is found to achieve better error performance than the existing pairing schemes.

Chapter 5

Lattice Coded FDF MWRNs: Achievable Rate and SER with Imperfect CSI

In Chapter 4, we considered a novel pairing scheme for lattice coded FDF MWRNs. In this chapter, we consider the joint impact of channel estimation error and error propagation for FDF relaying protocol in terms of the achievable rate and the error performance. The impact of imperfect CSI on AF MWRNs will be addressed in the next chapter. For this chapter and the next chapter, we consider the existing pairing scheme in [28]. The impact of imperfect CSI can be similarly addressed for the pairing scheme proposed in the last chapter and has not been included in this chapter.

The chapter is organized in the following manner. The proposed signal model for a lattice code based FDF MWRN with channel estimation is presented in Section 5.1. The SNR analysis is provided in Section 5.2. The achievable common rate and sum rate analysis are discussed in Section 5.3. The average SER for a user in FDF MWRN is derived in Section 5.4. The simulation results for verification of the analytical solutions are provided in Section 5.5. Finally, a summary of the contributions in this chapter is provided in Section 5.6.

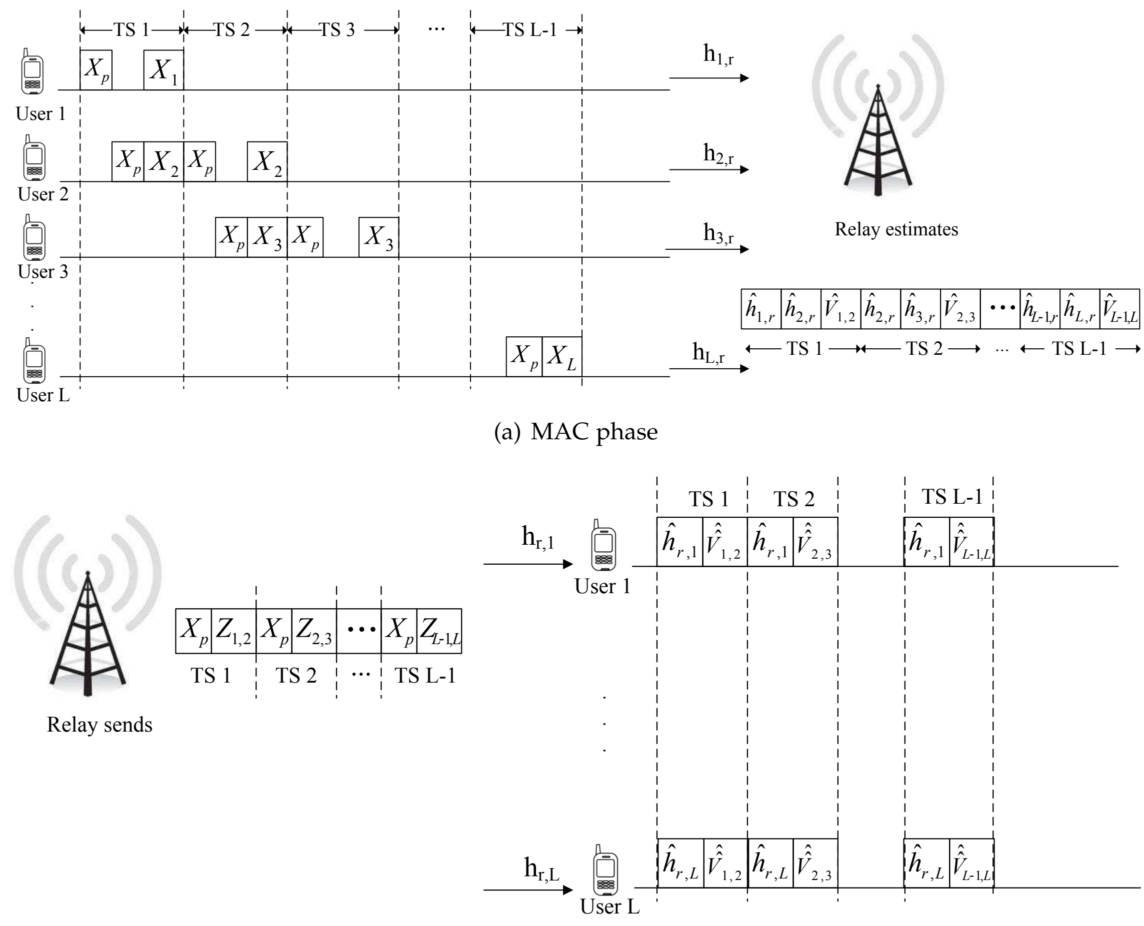

(a) MAC phase

(b) BC phase

Figure 5.1: Pilot and data transmission for an L-user functional decode and forward (FDF) multi-way relay network (MWRN) with imperfect channel estimation. The mathematical symbols are explained in Section 5.1.

5.1 Proposed Lattice Code Based Signal Model with Channel Estimation

In the proposed system model, we assume that the channel coefficients are not known a priori at any of the users or the relay but the statistical parameters of the corresponding channels, for example, channel variances are known beforehand, which is a common assumption and can be practically obtained [80, 101, 102] at the users and the relay. In this setup, each phase (i.e., multiple access and broadcast) is composed of a pilot transmission and a data transmission step, as illustrated in Fig. 5.1(a) and Fig. 5.1(b). The pilot transmission step is required for minimum mean square error (MMSE) based channel estimation and the data transmission step is based on lattice codes. Thus, we can model the channel $h_{i,r}$ as

$$h_{i,r} = \hat{h}_{i,r} + \tilde{h}_{i,r}, \tag{5.1}$$

where $\hat{h}_{i,r}$ is the estimated channel and $\tilde{h}_{i,r}$ represents the estimation error [80, 102]. We denote the power of the pilot signal at the users and at the relay as P_s^{p} and P_r^{p}, respectively, where the superscript $(\cdot)^{\text{p}}$ denotes the pilot. Similarly, we denote the power of the data signal at the users and the relay by P and P_r, respectively.

Now, we discuss the pilot and the data transmission protocols in the multiple access and the broadcast phases in the subsections 5.1.1 and 5.1.2. For the following part of this chapter (in particular, Section 5.1 and subsection 5.4.1), we consider pilot and data transmission in a certain time slot.

5.1.1 Pilot Transmission

5.1.1.1 Multiple Access Phase

In this phase, the users in a pair transmit their pilot symbols individually in different time slots and the relay estimates the corresponding channels through MMSE estimation. Such pilot symbol based MMSE is a frequently used estimator for cellular channels [80,102,103]. Since the channel is constant during one message packet transmission, only one pilot bit per message packet is required. Note that when the data and the pilot powers are optimized, one pilot symbol transmission is optimal to achieve the highest information rate [80, 104]. However, assuming equal power for data and pilot symbols enables a simpler interpretation of the problem.

At the i^{th} time slot, first the i^{th} user transmits pilot symbol X_p and the relay receives the signal

$$Y_p = \sqrt{P_s^{\text{p}}} h_{i,r} X_p + n_p. \tag{5.2}$$

We assume that $X_p = 1$ and n_p is a zero mean complex valued AWGN with variance $\sigma_n^2 = \frac{N_0}{2}$ per dimension. The relay then obtains the estimate [100]

$$\hat{h}_{i,r} = \frac{\sqrt{P_s^{\mathrm{p}}}\sigma_{h_{i,r}}^2}{P_s^{\mathrm{p}}\sigma_{h_{i,r}}^2 + \sigma_n^2} Y_p, \tag{5.3}$$

and the estimation error variance at the relay is [100]

$$\sigma_{\tilde{h}_{i,r}}^2 = \frac{\sigma_{h_{i,r}}^2 \sigma_n^2}{P_s^{\mathrm{p}}\sigma_{h_{i,r}}^2 + \sigma_n^2}. \tag{5.4}$$

Note that, the estimation error is independent of the channel estimate $\hat{h}_{i,r}$ because $\hat{h}_{i,r}$ is the MMSE estimate of Gaussian distributed $h_{i,r}$ [91]. Similarly, the relay can estimate the channel coefficient of the $(i+1)^{th}$ user.

5.1.1.2 Broadcast Phase

The relay broadcasts its own pilot, as well as the estimated channel coefficients in the multiple access phase. Then the m^{th} ($m \in [1, L]$) user performs MMSE estimation similar to (5.3), to obtain the estimate $\hat{h}_{r,m}$. The channel estimation error in this case is $\tilde{h}_{r,m} = h_{r,m} - \hat{h}_{r,m}$, with variance

$$\sigma_{\tilde{h}_{r,m}}^2 = \frac{\sigma_{h_{r,m}}^2 \sigma_n^2}{P_r^{\mathrm{p}}\sigma_{h_{r,m}}^2 + \sigma_n^2}. \tag{5.5}$$

5.1.2 Data Transmission

Here, we discuss the general lattice code based data transmissions in a MWRN with pairwise transmission.

5.1.2.1 Multiple Access Phase

The expressions for the received signal at the relay are the same as that given in Section 2.2.2.

5.1.2.2 Broadcast Phase

In this phase, the relay broadcasts the decoded network coded message to all the users. When all the users have the network coded messages corresponding to each user pair, they utilize self information to extract the messages of the other users.

First, the relay decodes the received signal with the estimated channel coefficients $\hat{h}_{i,r}$ and $\hat{h}_{i+1,r}$ and obtains an estimate of the corresponding network coded message (which is a function of the transmitting users' messages). The relay then broadcasts the estimated network coded signal after pilot transmission.

That is, the relay scales the received signal with a scalar coefficient α [62] and removes the dithers d_i, d_{i+1} scaled by $\sqrt{P}\hat{h}_{i,r}$ and $\sqrt{P}\hat{h}_{i+1,r}$, respectively. The resulting signal is given by

$$\begin{aligned}
X_r^t &= [\alpha r_{i,i+1}^t - \sqrt{P}\hat{h}_{i,r}d_i - \sqrt{P}\hat{h}_{i+1,r}d_{i+1}] \mod \Lambda \\
&= [\sqrt{P}\hat{h}_{i,r}X_i^t + \sqrt{P}\hat{h}_{i+1,r}X_{i+1}^t + (\alpha-1)\sqrt{P}(\hat{h}_{i,r}X_i^t + \hat{h}_{i+1,r}X_{i+1}^t) + \alpha n_1 \\
&+ \alpha\sqrt{P}(\tilde{h}_{i,r}X_i^t + \tilde{h}_{i+1,r}X_{i+1}^t) - \sqrt{P}\hat{h}_{i,r}d_i - \sqrt{P}\hat{h}_{i+1,r}d_{i+1}] \mod \Lambda \\
&= [\sqrt{P}\hat{h}_{i,r}\psi(W_i^t) + \sqrt{P}\hat{h}_{i+1,r}\psi(W_{i+1}^t) + n] \mod \Lambda,
\end{aligned} \tag{5.6}$$

where $n = (\alpha-1)\sqrt{P}(\hat{h}_{i,r}X_i^t + \hat{h}_{i+1,r}X_{i+1}^t) + \alpha n_1 + \alpha\sqrt{P}(\tilde{h}_{i,r}X_i^t + \tilde{h}_{i+1,r}X_{i+1}^t)$ and α is chosen to minimize the noise variance and computed using the estimated channel coefficients [105].

The relay decodes the signal in (5.6) with a lattice quantizer to obtain an estimate $\hat{\mathbf{V}}_{i,i+1}$ that approaches $(\psi(\mathbf{W}_i) + \psi(\mathbf{W}_{i+1})) \mod \Lambda$ for sufficiently large dimension of the lattice such that $\Pr(n \notin \mathcal{V})$ approaches zero, where $\mathcal{V}$ is the fundamental voronoi region. The relay then adds a dither d_r with the network coded message which is generated at the relay and broadcast to the users prior to message transmission in the broadcast phase. Then it broadcasts the resulting message using lattice codes, which is given as $\mathbf{Z}_{i,i+1} = (\hat{\mathbf{V}}_{i,i+1} + d_r) \mod \Lambda$.

Then the m^{th} user receives

$$\mathbf{Y}_{i,i+1} = \sqrt{P_r} h_{r,m} \mathbf{Z}_{i,i+1} + n_2, \tag{5.7}$$

where n_2 is the zero mean complex AWGN at the user with noise variance $\sigma_{n_2}^2 = \frac{N_0}{2}$ per dimension.

At the end of the broadcast phase, the m^{th} user scales the received signal with a scalar coefficient β_m and removes the dithers d_r multiplied by $\sqrt{P_r}\hat{h}_{r,m}$. The resulting signal is

$$\begin{aligned}
&[\beta_m Y_{i,i+1}^t - \sqrt{P_r}\hat{h}_{r,m} d_r] \mod \Lambda \\
&= [\sqrt{P_r}\hat{h}_{r,m}\hat{V}_{i,i+1}^t + (\beta_m - 1)\sqrt{P_r}\hat{h}_{r,m}\hat{V}_{i,i+1}^t + \beta_m n_2 + \beta_m \sqrt{P_r}\tilde{h}_{r,m}\hat{V}_{i,i+1}^t] \mod \Lambda \\
&= [\sqrt{P_r}\hat{h}_{r,m}\hat{V}_{i,i+1}^t + n'] \mod \Lambda,
\end{aligned} \tag{5.8}$$

where, $n' = (\beta_m - 1)\sqrt{P_r}\hat{h}_{r,m}\hat{V}_{i,i+1}^t + \beta_m n_2 + \beta_m \sqrt{P_r}\tilde{h}_{r,m}\hat{V}_{i,i+1}^t$ and β_m is chosen to minimize the noise variance.

The users then detect the received signal with a lattice quantizer and obtain the estimate $\hat{\hat{\mathbf{V}}}_{i,i+1}$ that approaches $(\psi(\mathbf{W}_i) + \psi(\mathbf{W}_{i+1})) \mod \Lambda$ for the lattice dimension large enough such that $\Pr(n' \notin \mathcal{V})$ approaches zero. After decoding all the network coded messages, each user performs message extraction of every other user by canceling self information.

5.1.2.3 Message Extraction

The message extraction process is similar to that provided for perfect CSI case in Section 2.2.3.3.

Remark 5.1. (5.6) *and* (5.8) *show that the error performance of a MWRN depends on the channel estimation error. The expressions of the channel estimates (see* (5.3)*) and estimation error (see* (5.4) *and* (5.5)*) show that these are functions of the noise variance and the channel variance. Thus, we can expect the channel variance and the noise variance to play a key role in* *determining the error performance of MWRNs.*

5.2 SNR Analysis

In this section, we investigate the received SNR of FDF MWRNs with lattice codes and imperfect CSI. The SNR results obtained in this section, will be utilized in the achievable rate and error performance analysis in the following sections. In a FDF MWRN, the decoding operation is performed after both the multiple access phase and the broadcast phase. Thus, we need to consider the SNR at the relay and the SNR at the users, separately.

5.2.1 SNR at the Relay

The SNR of the received signal with imperfect channel estimation at the relay can be obtained from (5.6) as

$$\gamma_r(i) = \frac{P\min(\mid \hat{h}_{i,r} \mid^2, \mid \hat{h}_{i+1,r} \mid^2)}{\mid \alpha \mid^2 N_0 + P \mid \alpha - 1 \mid^2 (\mid \hat{h}_{i,r} \mid^2 + \mid \hat{h}_{i+1,r} \mid^2) + P \mid \alpha \mid^2 (\sigma^2_{\tilde{h}_{i,r}} + \sigma^2_{\tilde{h}_{i+1,r}})}, \tag{5.9}$$

where, the numerator represents the power of the signal part (i.e., $\sqrt{P}\hat{h}_{i,r}\psi(W_i^t) + \sqrt{P}\hat{h}_{i+1,r}\psi(W_{i+1}^t)$ in (5.6)) and the denominator represents the power of the noise terms n in (5.6). The optimum value of α can be obtained by setting $\frac{dn}{d\alpha} = 0$ in (5.6) and is given by

$$\alpha = \frac{P \mid \hat{h}_{i,r} \mid^2 + P \mid \hat{h}_{i+1,r} \mid^2}{P\sigma^2_{\tilde{h}_{i,r}} + P\sigma^2_{\tilde{h}_{i+1,r}} + N_0} \tag{5.10}$$

Now, substituting α from (5.10) in (5.9) and after some algebraic manipulations, the SNR at the relay can be expressed as:

$$\gamma_r(i) = \frac{\min(|\hat{h}_{i,r}|^2, |\hat{h}_{i+1,r}|^2)}{|\hat{h}_{i,r}|^2 + |\hat{h}_{i+1,r}|^2} + \frac{P\min(\mid \hat{h}_{i,r} \mid^2, \mid \hat{h}_{i+1,r} \mid^2)}{P\sigma^2_{\tilde{h}_{i,r}} + P\sigma^2_{\tilde{h}_{i+1,r}} + N_0}. \tag{5.11}$$

Thus, in general, for the user pair formed by the m^{th} and the $(m \pm 1)^{th}$ user, the SNR at the relay can be given as:

$$\gamma_r(m) = \frac{\min(|\hat{h}_{m,r}|^2, |\hat{h}_{m\pm1,r}|^2)}{|\hat{h}_{m,r}|^2 + |\hat{h}_{m\pm1,r}|^2} + \frac{P \min(|\ \hat{h}_{m,r}\ |^2, |\ \hat{h}_{m\pm1,r}\ |^2)}{P\sigma^2_{\tilde{h}_{m,r}} + P\sigma^2_{\tilde{h}_{m\pm1,r}} + N_0}. \tag{5.12}$$

5.2.2 SNR at the Users

The signal transmission from the relay to the $m^{th}(m \in [1, L])$ user is the same as that in a point-to-point fading channel. Thus, the SNR of the relay's signal received at the m^{th} user is given by:

$$\gamma_m = \frac{P_r\ |\ \hat{h}_{r,m}\ |^2}{|\ \beta_m\ |^2\ N_0 + P_r\ |\ \beta_m - 1\ |^2 |\ \hat{h}_{r,m}\ |^2 + |\beta_m|^2 P_r \sigma^2_{\tilde{h}_{r,m}}}, \tag{5.13}$$

where the numerator represents power of the signal part in (5.8) and the denominator represents the power of the noise term n' in (5.8). The optimum value of β_m can be obtained by setting $\frac{dn'}{d\beta_m} = 0$ in (5.8) and is given by:

$$\beta_m = \frac{P_r|\hat{h}_{r,m}|^2}{P_r\sigma^2_{\tilde{h}_{r,m}} + N_0}. \tag{5.14}$$

Then substituting β_m from (5.14) in (5.13) and after some algebraic manipulations, the SNR at the m^{th} user can be obtained as:

$$\gamma_m = \frac{P_r\ |\ \hat{h}_{r,m}\ |^2}{P_r\sigma^2_{\tilde{h}_{r,m}} + N_0}. \tag{5.15}$$

5.2.3 Special Case: Perfect Channel Estimation

When the channel estimation is perfect (i.e., $\sigma^2_{\tilde{h}_{i,r}} = \sigma^2_{\tilde{h}_{i+1,r}} = \sigma^2_{\tilde{h}_{r,m}} = 0$), the SNR at the relay is given as:

$$\gamma_r^{pe}(i) = \frac{\min(|h_{i,r}|^2, |h_{i+1,r}|^2)}{|h_{i,r}|^2 + |h_{i+1,r}|^2} + \frac{P_d \min(|\ h_{i,r}\ |^2, |\ h_{i+1,r}\ |^2)}{N_0}. \tag{5.16}$$

Also, the SNR at the m^{th} user is given by:

$$\gamma_m^{pe} = \frac{P_r \mid h_{r,m} \mid^2}{N_0}. \tag{5.17}$$

The expressions (5.16) and (5.17) coincide with the results in [50]. Thus, the results in [50] can be considered as a special case of the formulation in (5.13) and (5.15).

5.3 Achievable Rate Analysis

In this section, we study the achievable common rate and sum rate based on the SNR results in the previous section.

5.3.1 Common Rate

Common rate denotes the maximum possible information rate of the system that can be exchanged with negligible error. In the following part of this subsection, we investigate the achievable common rate of FDF MWRNs with lattice codes and imperfect CSI.

Assuming lattice codes with sufficiently large dimensions are employed, the common rate of an L-user FDF MWRN is given by [28, 50]

$$R_c = \frac{1}{L-1} \min_{\ell \in [1, L-1]} \{R_{c,\ell}\}, \tag{5.18}$$

where the factor $\frac{1}{L-1}$ is due to the fact that the complete message exchange requires $L-1$ time slots and $R_{c,\ell}$ is the achievable rate at the ℓ^{th} time slot, given by

$$R_{c,\ell} = \min\{R_m, R_b\}, \tag{5.19}$$

where R_m and R_b are the maximum achievable rates at the ℓ^{th} time slot during the multiple access phase and the broadcast phase, respectively. Next, we derive the upper bounds on the maximum achievable rates in the multiple access and broadcast phases.

Theorem 5.1. *The maximum possible information rate at the relay during the i^{th} time slot in the multiple access phase is upper bounded by:*

$$R_m \leq \frac{1}{2}\log\left(\frac{\min(|\hat{h}_{i,r}|^2, |\hat{h}_{i+1,r}|^2)}{|\hat{h}_{i,r}|^2 + |\hat{h}_{i+1,r}|^2} + \frac{P\min(|\hat{h}_{i,r}|^2, |\hat{h}_{i+1,r}|^2)}{P\sigma^2_{\tilde{h}_{i,r}} + P\sigma^2_{\tilde{h}_{i+1,r}} + N_0}\right). \tag{5.20}$$

Proof. Proof is similar to the proof of Theorem 4.1 and is omitted. □

Theorem 5.2. *The maximum possible information rate at the users during the i^{th} time slot in the broadcast phase, can be upper bounded by:*

$$R_b = \frac{1}{2}\log\left(\min_{m\in[1,L]} \frac{P_r \mid \hat{h}_{r,m} \mid^2}{P_r\sigma^2_{\tilde{h}_{r,m}} + N_0}\right). \tag{5.21}$$

Proof. Proof is similar to the proof of Theorem 4.2 and is omitted. □

5.3.2 Sum Rate

The sum rate indicates the maximum throughput of the system, as defined in Chapter 2. The achievable sum rate of FDF MWRNs with imperfect CSI and lattice codes has been derived in the following theorem.

Theorem 5.3. *The achievable sum rate of lattice code based FDF MWRN with imperfect CSI is obtained as:*

$$R_s = \frac{1}{2(L-1)}\sum_{i=1}^{L-1}\log\left(\frac{\min(|\hat{h}_{i,r}|^2, |\hat{h}_{i+1,r}|^2)}{|\hat{h}_{i,r}|^2 + |\hat{h}_{i+1,r}|^2} + \frac{P\min(|\hat{h}_{i,r}|^2, |\hat{h}_{i+1,r}|^2)}{P\sigma^2_{\tilde{h}_{i,r}} + P\sigma^2_{\tilde{h}_{i+1,r}} + N_0}\right). \tag{5.22}$$

Proof. Proof is similar to the proof of Theorem 4.3 and is omitted. □

5.4 Error Performance Analysis

In this section, we characterize the error performance of FDF MWRNs through average SER analysis. In Chapter 3, the average BER analysis was performed for BPSK modulation in AWGN and fading channels with perfect estimation and equal channel variances.

However, in this chapter, we consider fading channels with imperfect CSI and unequal channel variances and provide the analytical derivations for the average SER of a FDF MWRN with square M-QAM modulation, which is a 2 dimensional lattice code.

5.4.1 Data Transmission with M-QAM Modulation

In the M-QAM modulated FDF MWRN system, during the i^{th} time slot, the i^{th} user and the $(i+1)^{th}$ user transmit their messages $\mathbf{W}_i$ and $\mathbf{W}_{i+1}$ which are M-QAM modulated to $\mathbf{X}_i$ and $\mathbf{X}_{i+1}$, respectively, where $X_i^t, X_{i+1}^t = a + jb$ and $a, b \in \{\pm 1, \pm 3, ..., \pm(\sqrt{M} - 1)\}$. The relay receives the signal $\mathbf{R}_{i,i+1}$ (see (2.5)) and decodes it to obtain an estimate $\hat{\mathbf{V}}_{i,i+1}$ of the network coded symbol $\mathbf{V}_{i,i+1} = (\mathbf{W}_i + \mathbf{W}_{i+1}) \mod M$ as in [15, 23]. The relay then broadcasts the estimated network coded signal after M-QAM modulation, which is given as $\mathbf{Z}_{i,i+1}$. The j^{th} ($j \in [1, L]$) user receives $\mathbf{Y}_{i,i+1}$ (see (2.7)) and detects the received signal to obtain the estimate $\hat{\hat{\mathbf{V}}}_{i,i+1}$. After decoding all the network coded messages, each user performs message extraction upward and downward. In the downward extraction process, the i^{th} user subtracts its own message $\mathbf{W}_i$ from the network coded message $\hat{\hat{\mathbf{V}}}_{i,i+1}$ and then performs the modulo-M operation. The process can be shown as

$$\begin{aligned}
\hat{\mathbf{W}}_{i+1} &= (\hat{\hat{\mathbf{V}}}_{i,i+1} - \mathbf{W}_i + M) \mod M, \\
\hat{\mathbf{W}}_{i+2} &= (\hat{\hat{\mathbf{V}}}_{i+1,i+2} - \hat{\mathbf{W}_{i+1}} + M) \mod M, \\
&..., \\
\hat{\mathbf{W}}_L &= (\hat{\hat{\mathbf{V}}}_{L-1,L} - \hat{\mathbf{W}}_{L-1} + M) \mod M.
\end{aligned} \tag{5.23}$$

Similarly, the upward message extraction process can be shown as

$$\begin{aligned}
\hat{\mathbf{W}}_{i-1} &= (\hat{\hat{\mathbf{V}}}_{i,i-1} - \mathbf{W}_i + M) \mod M, \\
\hat{\mathbf{W}}_{i-2} &= (\hat{\hat{\mathbf{V}}}_{i-1,i-2} - \hat{\mathbf{W}}_{i-1} + M) \mod M, \\
&..., \\
\hat{\mathbf{W}}_1 &= (\hat{\hat{\mathbf{V}}}_{1,2} - \hat{\mathbf{W}}_2 + M) \mod M.
\end{aligned} \tag{5.24}$$

5.4.2 Steps for Error Performance Analysis

In this part, we outline the general steps to be followed for obtaining the average SER of a MWRN. These steps summarize how the analysis technique in Chapter 3 can be applied to the more general problem considered in this chapter.

- *Step 1:* Obtain the probability of incorrectly decoding a $\sqrt{M}$-PAM network coded message, $P_{\sqrt{M}-PAM,NC}(i,k)$. This is important because any M-QAM signal with square constellation (i.e., $\sqrt{M} \in \mathbb{Z}$) can be decomposed to two $\sqrt{M}$-PAM signals [99]. Thus, the network coded signal resulting from M-QAM signals can be correctly decoded when both the component $\sqrt{M}$-PAM signals are correctly decoded.

- *Step 2:* Obtain the probability of incorrectly decoding a network coded message resulting from M-QAM signals, $P_{FDF}(i,k)$.

- *Step 3:* Obtain the probability of the k^{th} error event, $P_i(k)$, in terms of $P_{FDF}(i,k)$, where the k^{th} error event is denoted as the occurrence when exactly k number of users' messages are incorrectly decoded.

- *Step 4:* Since there are $L-1$ possible error events in an L-user MWRN, find the expected probability of all these error events to obtain the average SER, $P_{i,avg}$.

The next section summarizes the main results from steps 1-4 in the form of Lemmas 4.1-4.3 and Theorem 4.

5.4.3 SER Analysis

In this section, we obtain the average SER for FDF MWRN with imperfect CSI following the steps outlined in Section 5.4.2. First, we obtain the probability of incorrectly decoding a network coded message as in the following lemma.

Lemma 5.1. *The probability that the i^{th} user incorrectly decodes the M-QAM network coded message of the k^{th} and the $(k \pm 1)^{th}$ user in a FDF MWRN is given as:*

$$P_{FDF}(i,k) = 1 - \left(1 - P_{\sqrt{M}-PAM,NC}(i,k)\right)^2, \tag{5.25}$$

where $P_{\sqrt{M}-PAM,NC}(i,k)$ is the probability of incorrectly decoding a network coded message at the i^{th} user, resulting from the sum of two $\sqrt{M}$-PAM signals from the k^{th} and the $(k \pm 1)^{th}$ users and can be obtained from Appendix B.3, replacing the actual channel coefficients with the estimated ones for obtaining (4.29) *and* (4.31) *and using table 4.1.*

Proof. (5.25) follows from the fact that any M-QAM signal with square constellation can be decomposed to two $\sqrt{M}$-PAM signals [99]. Thus, the network coded signal resulting from M-QAM signals can be correctly decoded when both the component $\sqrt{M}$-PAM signals are correctly decoded. □

Using (5.25) and (4.28) and following the steps in 5.4.2, the probability of k error events with imperfect CSI for FDF relaying can be obtained as in the following lemma.

Lemma 5.2. *At high SNR, the expression for the probability of the k^{th} error event can be given by:*

$$P_i(k) = \begin{cases} P_{FDF}(i, L-k), & i = 1,2 \\ P_{FDF}(i,k), & i = L, L-1 \\ P_{FDF}(i,k) + P_{FDF}(i, L-k) & i \notin \{1,2,L-1,L\}. \end{cases} \tag{5.26}$$

Proof. See Appendix C.1. □

Using Lemmas 4.1-4.3 (corresponding to the main results from steps 1-3 in Section 5.4.2), we can obtain the main result as stated below.

Theorem 5.4. *At high SNR, the average SER of a FDF MWRN with imperfect CSI can be* *given as:*

$$P_{i,avg} = \frac{1}{L-1} \begin{cases} \sum_{k=1}^{L-1} kP_{FDF}(i, L-k), & i = 1,2 \\ \sum_{k=1}^{L-1} kP_{FDF}(i,k), & i = L, L-1 \\ \sum_{k=1}^{L-1} k\left(P_{FDF}(i, L-k) + P_{FDF}(i,k)\right) & i \notin \{1,2,L-1,L\}. \end{cases} \tag{5.27}$$

Proof. Averaging the probability of the k^{th} error event over the $L-1$ possible error events, the average SER at the i^{th} user can be obtained as:

$$P_{i,avg} = \frac{1}{L-1} \sum_{k=1}^{L-1} kP_i(k), \tag{5.28}$$

Then, substituting (5.26) into (5.28) gives the average SER of a FDF MWRN, which completes the proof. □

The accuracy of the derived expression for $P_{i,avg}$ at high SNR will be demonstrated in Section 5.5.

5.5 Results

In this section, we provide insights from the achievable rate and error performance analysis. We also verify the error performance results with Monte Carlo simulations. The users' distances are chosen similar to that in Section 4.5. Note that, in this model, the estimation error variance (see (5.4)) is a function of distances. The SNR is assumed to be SNR per message per user. We denote the decoding user as the i^{th} user, where i is assumed to be 1 and other users as the m^{th} user, where $m \in [1, L], m \neq i$. The simulation results are averaged over 1000 Monte Carlo trials per SNR point.

5.5.1 Achievable Rate

Fig. 5.2(a) and Fig. 5.2(b) show the achievable common rate and sum rate, respectively with lattice codes for $L = 6, 8$ and 10 user FDF MWRNs in the presence of imperfect channel estimation. As defined in (5.4), the estimation error varies linearly with SNR.

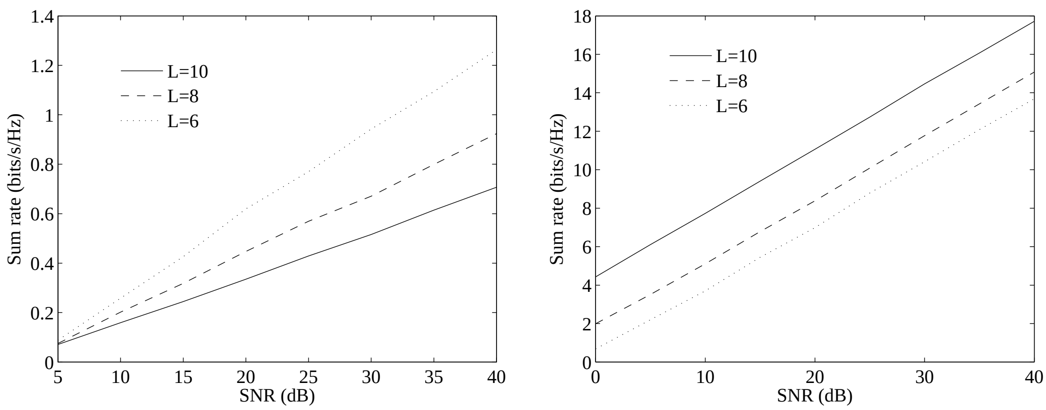

(a) Common rate

(b) Sum rate

Figure 5.2: Achievable common rate and sum rate for $L = 6, 8, 10$ user FDF MWRNs with channel estimation error, as given in (5.4).

From Fig. 5.2(a), it is clear that for larger number of users, the common rate will be lower, which can be identified from (5.18). Also, common rate increases at a smaller rate with SNR for larger number of users, as the slope of (5.18) decreases with increasing number of users. However, from Fig. 5.2(b), it can be noted that the sum rate increases with increasing number of users, because of larger number of terms are present in (5.22) for larger number of users.

5.5.1.1 Impact of Estimation Error

Fig. 5.3(a) and Fig. 5.3(b) show the impact of different levels of channel estimation errors on the achievable common rate and sum rate for $L = 6, 8$ and 10 user. In this analysis, the estimation errors are set using the following technique, which is illustrated for two estimation errors of 0.1% and 0.01% of the combined variance of the fading channel and the complex AWGN noise. These values of channel estimation errors have been introduced by setting σ_n^2 equal to 0.001 and 0.0001, respectively in (5.4) and noting that $\sigma^2_{\hat{h}_{i,r}} \approx \sigma^2_{h_{i,r}} + \sigma_n^2$ at high SNR and $\nu = 3$. Fig. 5.3(a) and Fig. 5.3(b) show that both the achievable common rate and sum rate decreases with increasing estimation error. However, the achievable common rate for larger number of users degrades at a lower

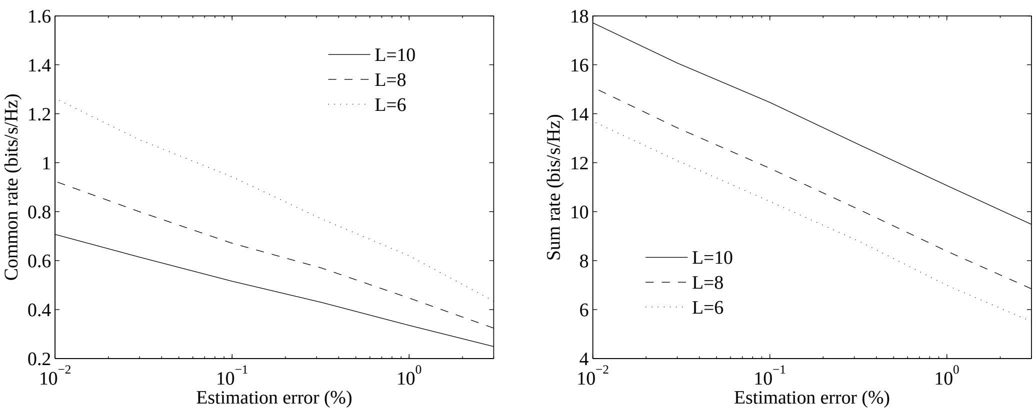

(a) Common rate (b) Sum rate

Figure 5.3: Achievable common rate and sum rate for for different levels of channel estimation error in $L = 6, 8, 10$ user FDF MWRNs.

rate compared to the case for smaller number of users, as the slope of (5.18) decreases with increasing number of users. On the other hand, the level of sum rate degradation with increasing estimation error is the same for different number of users because the slope of (5.22) does not change with the number of users.

5.5.1.2 Impact of Overall Channel Conditions

Fig. 5.4(a) and Fig. 5.4(b) show the achievable common rate and sum rate for $L = 10$ user FDF MWRN for the cases when (i) 10% of the users have distances below $0.1d_0$ (corresponds to the case when most of the users have poor channel conditions) and (ii) 90% of the users have distances below $0.1d_0$ (corresponds to the case when most of the users have good channel conditions). It can be observed that when most of the users experience good channel conditions, the achievable common rate and sum rate improve. Also, it can be noted that the degradation in the overall channel conditions leads to achievable common rate and sum rate loss in FDF MWRN by nearly the same degree for the cases when perfect CSI is available or not. This is because, the impact of users' channel gains is much greater than the impact of channel estimation errors in (5.18) and (5.22).

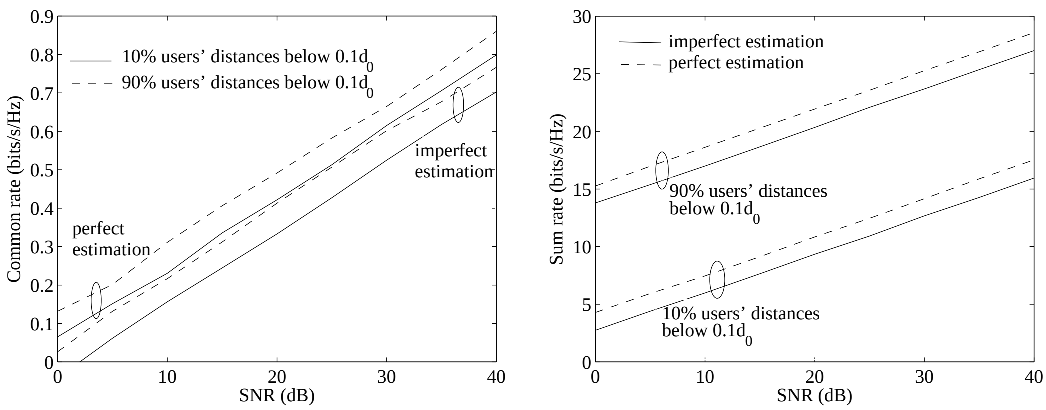

(a) Common rate (b) Sum rate

Figure 5.4: Achievable common rate and sum rate when 10% and 90% users' distances below $0.1d_0$ in $L = 10$ user FDF MWRN.

5.5.2 Average SER

Fig. 5.5 shows the average SER for FDF MWRN with $L = 6, 8, 10$ users in the presence of imperfect channel estimation. Here, the analytical results are plotted using (5.27) and compared with the simulation results. We consider that each user transmits a message packet of $T = 1000$ bits. For each of the message packets, one pilot signal is transmitted. The simulation results are averaged over 1000 Monte Carlo trials per SNR point. It can be seen from the figure that the analytical results match very well with the simulations at high SNR. It can be seen from the figure that larger number of users results into larger average SER, which is expected from (5.27).

5.5.2.1 Impact of Estimation Error

Fig. 5.6 plots average SER for $L = 6, 8, 10$ user FDF MWRNs for different levels of the estimation error and different channel conditions. It can be noted from this figure that the average SER is an increasing function of the estimation error. Also, it can be seen that for larger number of users, the average SER is higher compared to the case for smaller number of users.

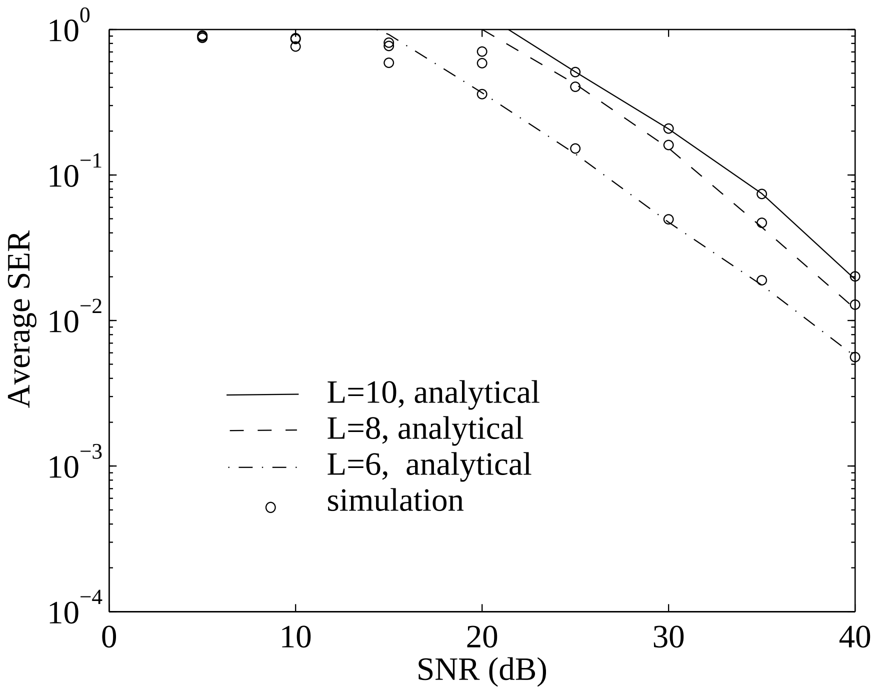

Figure 5.5: Average SER for $L = 6$, $L = 8$ and $L = 10$ users in a FDF MWRN with imperfect channel estimation.

5.5.2.2 Impact of Overall Channel Conditions

Fig. 5.7 shows average SER for $L = 10$ user FDF MWRN for the cases when (i) 10% of the users have distances below $0.1d_0$ and (ii) 90% of the users have distances below $0.1d_0$. It can be observed from the figure that for both the imperfect and perfect estimation, when most of the users experience good channel conditions, the average SER of FDF MWRN improves compared to the other case. This is because, when most of the users' channel conditions are good, the chance of error propagation in the decoding process of FDF MWRN is less. Moreover, when most of the users have good channel conditions, FDF MWRN with imperfect CSI performs 4 dB closer to the perfect CSI performance. Thus, the overall channel conditions of the users have a greater impact on the average SER when perfect CSI is not available.

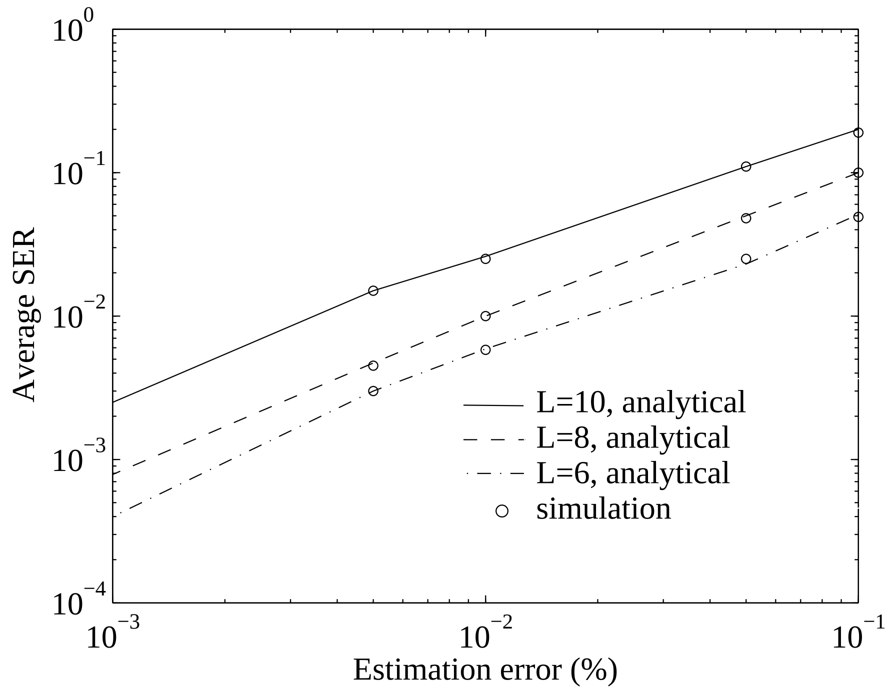

Figure 5.6: Average SER vs. estimation error in a FDF MWRN with different number of users.

5.6 Summary

In this chapter, we investigated the impact of channel estimation error on the achievable rate and error performance of FDF MWRNs. We considered a generalized lattice code based FDF MWRN with MMSE channel estimation for achievable rate analysis and then obtained the error performance results with M-QAM modulation, which is a special case of lattice codes. Specifically, we made the following contributions in this chapter:

- Considering L-user FDF MWRNs in Section 5.3 with sufficiently large dimension lattice codes, we derived the achievable rate expressions for FDF MWRNs with imperfect channel estimation and unequal average channel gains for the users.
- In Section 5.4, considering M-ary QAM based transmission, which is a special case of lattice code based transmission, we derived the expressions for the average symbol error rate (SER) for FDF MWRNs.

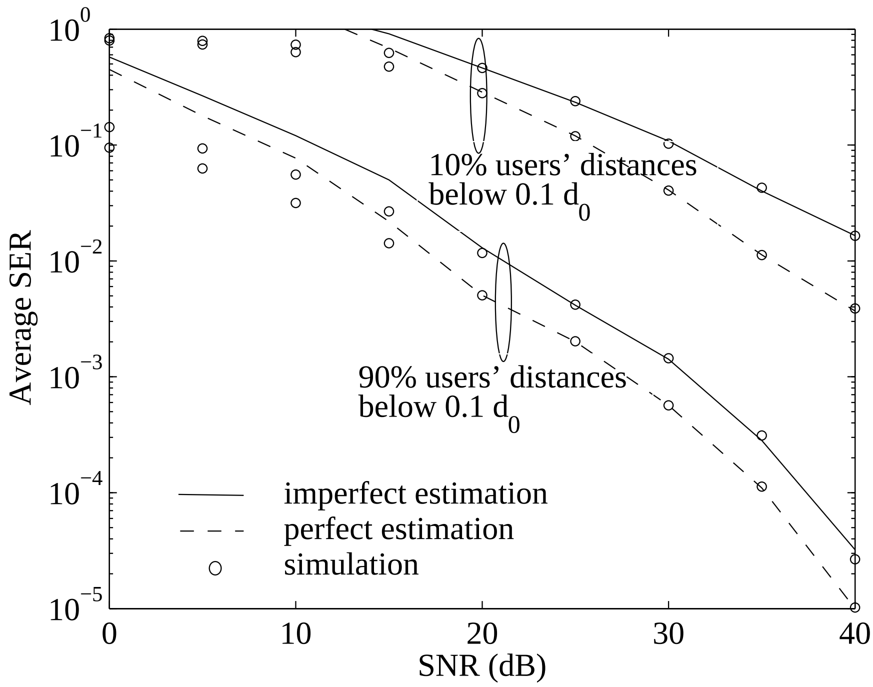

Figure 5.7: Average SER when 10% and 90% users' distances are below $0.1d_0$ in $L = 10$ users FDF MWRN.

- In Section 5.5, we showed that the achievable rates of FDF MWRNs are decreasing functions of the estimation error. Also, we showed that the average SER of FDF MWRN is an increasing function of both the estimation error and the number of users.

- In Section 5.5, we showed that when the overall channel conditions are good, the achievable rates improve by the same rate for imperfect and perfect CSI. However, the average SER gap between perfect and imperfect CSI cases, decreases by about 4 dB when most of the users experience good channel conditions.

Chapter 6

Lattice Coded AF MWRNs with Imperfect CSI

In Chapter 5, the impact of channel estimation error on lattice coded FDF MWRNs was investigated. In this chapter, the impact of imperfect CSI on MWRNs is addressed for AF relaying protocol in terms of the achievable rate for general lattice codes. Also, the error performance of an AF MWRN with channel estimation errors is investigated for BPSK modulation, which is the simplest case of lattice codes. Moreover, we obtain the optimum power allocation coefficients to optimize the sum rate of an AF MWRN with imperfect CSI and BPSK modulation.

The chapter is organized in the following manner. The proposed signal model for a lattice code based AF MWRN with imperfect channel estimation is presented in Section 6.1. The SNR analysis is provided in Section 6.2. The achievable common rate and sum rate analysis is discussed in Section 6.3. The average BER for a user in AF MWRN is derived in Section 6.4. The optimum power allocation coefficients to maximize the sum rate of an AF MWRN are derived in Section 6.5. The simulation results for verification of the analytical solutions are provided in Section 6.6. Finally, a summary of the contributions in this chapter is provided in Section 6.7.

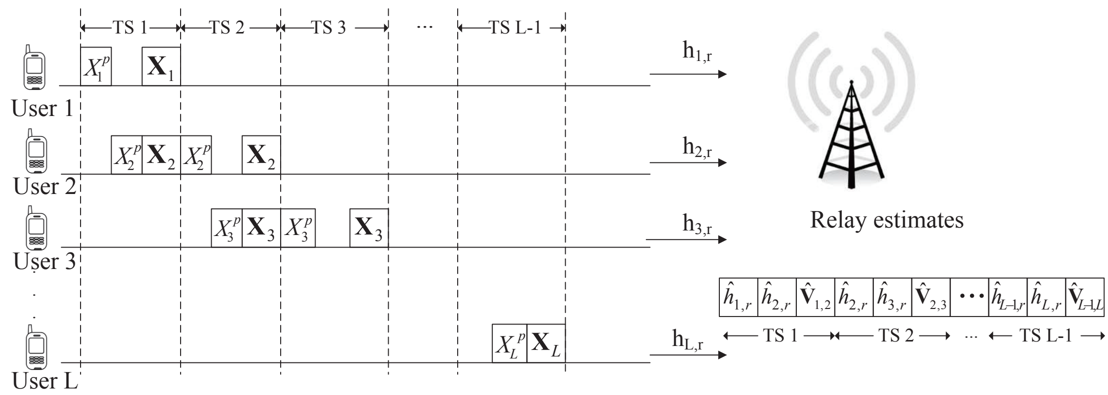

(a) MAC phase

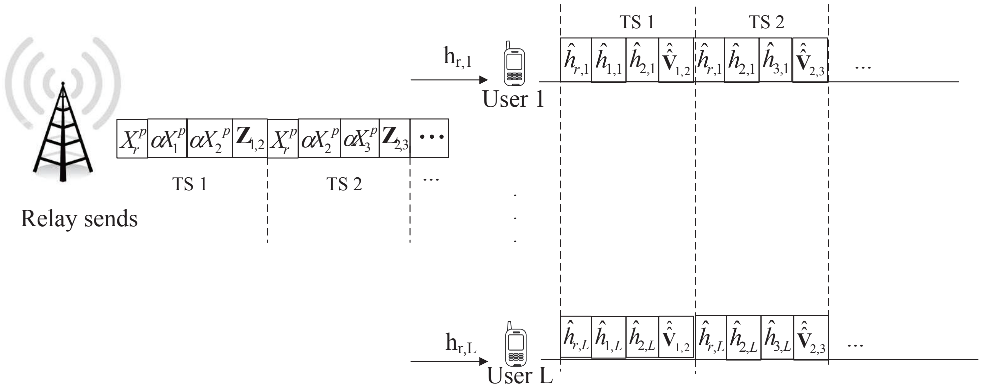

(b) BC phase

Figure 6.1: Pilot and data transmission for an L-user AF MWRN with imperfect channel estimation.

6.1 Proposed Lattice Code Based Signal Model with Channel Estimation

Similar to the previous chapter, in this system model, we assume that only the statistical parameters of the corresponding channels, i.e., channel variances are known beforehand at the users and the relay. Here, the pilot and the data transmission steps in each phase (i.e., multiple access and broadcast) are illustrated in Fig. 6.1(a) and Fig. 6.1(b).

In subsections 6.1.1 and 6.1.2, we discuss the pilot and the data transmission protocols in the multiple access and the broadcast phases. For the following part of this chapter (in particular, Section 6.1 and subsection 6.4), we consider pilot and data transmission in a certain time slot.

6.1.1 Pilot Transmission

6.1.1.1 Multiple Access Phase

The pilot transmission protocols in the multiple access phase are the same as that in 5.1.1.1.

6.1.1.2 Broadcast Phase

In this phase, the relay sends its own pilot signal to enable the users to estimate their own channel coefficients. Since each user needs the channel coefficients of other users for self-interference cancelation, the relay also sends the pilot signals received at the multiple access phase. For this, the relay amplifies the received pilot signals and forwards them to all the users. In the i^{th} time slot, the j^{th} ($j \in [1, L]$) user receives the signal

$$Y_i = \alpha_i h_{r,j}(\sqrt{P_s^{\mathrm{p}}} h_{i,r} X_i^{\mathrm{p}} + n_p) + n'_p, \tag{6.1}$$

where, $\alpha_i = \sqrt{\frac{P_r^{\mathrm{p}}}{P_s^{\mathrm{p}}\sigma^2_{h_{q,r}} + N_0}}$ is the amplification factor and n'_p is a zero mean complex valued AWGN with variance $\sigma_n^2 = \frac{N_0}{2}$ per dimension.

Finally, the j^{th} user performs linear MMSE estimation to obtain the estimate of the cascaded channel $h_{j,i} = h_{r,j}h_{i,r}$ as $\hat{h}_{j,i}$. We can model the channel $h_{j,i}$ as

$$h_{j,i} = \hat{h}_{j,i} + \tilde{h}_{j,i}, \tag{6.2}$$

where $\hat{h}_{j,i}$ is the estimated channel and $\tilde{h}_{j,i}$ represents the estimation error [100]. Thus, the user estimates:

$$\begin{aligned} \hat{h}_{j,i} &= E[h_{j,i}Y_i^*]E^{-1}[\mid Y_i \mid^2]Y_i \\ &= \frac{\alpha_i \sigma^2_{h_{i,r}} \sqrt{P_s^{\text{p}}} \sigma^2_{h_{r,j}}}{\alpha_i^2 \sigma^2_{h_{i,r}} P_s^{\text{p}} \sigma^2_{h_{r,j}} + \alpha_i^2 \sigma^2_{h_{r,j}} N_0 + N_0} Y_i, \end{aligned} \tag{6.3}$$

and the estimation error variance at the relay is:

$$\begin{aligned} \sigma^2_{\tilde{h}_{j,i}} &= E[\mid h_{j,i} \mid^2] - E[\mid \hat{h}_{j,i} \mid^2] \\ &= \frac{\sigma^2_{h_{i,r}} \sigma^2_{h_{r,j}} (\alpha_i^2 \sigma^2_{h_{r,j}} + 1) N_0}{\alpha_i^2 \sigma^2_{h_{i,r}} \sigma^2_{h_{r,j}} P_s^{\text{p}} + (\alpha_i^2 \sigma^2_{h_{r,j}} + 1)\sigma_n^2}. \end{aligned} \tag{6.4}$$

Substituting the value of α_i and omitting the higher order noise term σ_n^4, the above expression can be written as:

$$\sigma^2_{\tilde{h}_{j,i}} = \frac{1}{\frac{P_s^{\text{p}} P_r^{\text{p}}}{(P_r^{\text{p}} \sigma^2_{h_{r,j}} + P_s^{\text{p}} \sigma^2_{h_{i,r}}) N_0} + \frac{1}{\sigma^2_{h_{i,r}} \sigma^2_{h_{r,j}}}}. \tag{6.5}$$

Similarly, the relay forwards the $(i+1)^{th}$ user's pilot signal and the j^{th} user estimates $\hat{h}_{j,i+1}$.

6.1.2 Data Transmission

Here, we discuss the general lattice code based data transmissions in an AF MWRN with pairwise transmission.

6.1.2.1 Multiple Access Phase

The expressions for the received signal at the relay is the same as that given in Section 2.2.2.

6.1.2.2 Broadcast Phase

Similar to FDF relaying, the relay amplifies the received signal with an amplification factor α and removes the dithers d_i, d_{i+1} scaled by $\sqrt{P}\hat{h}_{i,r}$ and $\sqrt{P}\hat{h}_{i+1,r}$, respectively. The resulting signal was given by (5.8). The relay then adds a dither d_r with the network coded message and broadcasts the resulting message using lattice codes, which is given as $\mathbf{Z}_{i,i+1} = (\mathbf{X}_r + d_r) \mod \Lambda$.

The m^{th} user receives the signal as in (2.7). At the end of the broadcast phase, the m^{th} user scales the received signal with a scalar coefficient β_m and removes the dithers d_r multiplied by $\sqrt{P_r}\hat{h}_{r,m}$. The resulting signal is

$$\begin{aligned}
&[\beta_m Y^t_{i,i+1} - \sqrt{P_r}\hat{h}_{r,m} d_r] \mod \Lambda \\
&= [\sqrt{P_r P}\hat{h}_{m,i}\psi(W^t_i) + \sqrt{P_r P}\hat{h}_{m,i+1}\psi(W^t_{i+1}) + (\beta_m - 1)\sqrt{P_r P}(\hat{h}_{m,i}\psi(W^t_i) + \hat{h}_{m,i+1}\psi(W^t_{i+1})) \\
&+ \beta_m\sqrt{P_r}\hat{h}_{r,m} n + \beta_m n_2 + \beta_m\sqrt{P_r P}\tilde{h}_{m,i}\psi(W^t_i) + \beta_m\sqrt{P_r P}\tilde{h}_{m,i+1}\psi(W^t_{i+1})] \mod \Lambda \\
&= [\sqrt{P_r P}(\hat{h}_{m,i}\psi(W^t_i) + \hat{h}_{m,i+1}\psi(W^t_{i+1})) + n'] \mod \Lambda, \qquad (6.6)
\end{aligned}$$

where, $n' = \sqrt{PP_r}\hat{h}_{r,m} n + (\beta_m - 1)\sqrt{P_r P}\hat{h}_{m,i}\psi(W^t_i) + \sqrt{P_r P}\hat{h}_{m,i+1}\psi(W^t_{i+1}) + \beta_m\sqrt{P_r}\hat{h}_{r,m} n + \beta_m n_2 + \beta_m\sqrt{P_r P}\tilde{h}_{m,i}\psi(W^t_i) + \beta_m\sqrt{P_r P}\tilde{h}_{m,i+1}\psi(W^t_{i+1})$ and β_m is chosen to minimize the noise variance [75]. Then the users obtain the estimate $\hat{\mathbf{V}}_{i,i+1}$ of $\mathbf{V}_{i,i+1} = (\psi(\mathbf{W}_i) + \psi(\mathbf{W}_{i+1})) \mod \Lambda$.

6.1.2.3 Message Extraction

The message extraction process is the same as that in Section 2.2.3.3.

6.2 SNR Analysis

In this section, we investigate the received SNR of AF MWRNs with lattice codes and imperfect CSI.

The end-to-end SNR of the i^{th} user's signal, received at the m^{th} user with imperfect channel estimation can be obtained from (6.6) as

$$\gamma_{i,m} = \frac{P_r P \mid \hat{h}_{m,i} \mid^2}{N'}, \tag{6.7}$$

where N' denotes the variance of the noise terms n' in (6.6) and is given by:

$$\begin{aligned} N' =& \beta_m P_r |\hat{h}_{m,i}|^2 (|\alpha - 1|^2 P(|\hat{h}_{i,r}|^2 + |\hat{h}_{i+1,r}|^2) + |\alpha|^2 N_0 + |\alpha|^2 P(\sigma^2_{\tilde{h}_{i,r}} + \sigma^2_{\tilde{h}_{i+1,r}}) + \mid \beta_m \mid^2 N_0 + \\ & P_r P \mid \beta_m - 1 \mid^2 (\mid \hat{h}_{m,i} \mid^2 + \mid \hat{h}_{m,i+1} \mid^2) + |\beta_m|^2 P_r P(\sigma^2_{\tilde{h}_{m,i}} + \sigma^2_{\tilde{h}_{m,i+1}}). \end{aligned} \tag{6.8}$$

The optimum value of α can be obtained by differentiating N' with respect to α and then setting it to zero (i.e., $\frac{dN'}{d\alpha} = 0$) and can be given as:

$$\alpha = \frac{P \mid \hat{h}_{i,r} \mid^2 + P \mid \hat{h}_{i+1,r} \mid^2}{P\sigma^2_{h_{i,r}} + P\sigma^2_{h_{i+1,r}} + N_0}. \tag{6.9}$$

The optimum value of β_m can be obtained by differentiating N' with respect to β_m and then setting it to zero (i.e., $\frac{dN'}{d\beta_m} = 0$) and can be given as:

$$\beta_m = \frac{P_r P(|\hat{h}_{m,i}|^2 + |\hat{h}_{m,i+1}|^2)}{P_r \sigma^2_{h_{r,m}} N'' + P_r P(\sigma^2_{h_{i,r}} \sigma^2_{h_{r,m}} + \sigma^2_{h_{i+1,r}} \sigma^2_{h_{r,m}})}, \tag{6.10}$$

where $N'' = |\alpha - 1|^2 P(|\hat{h}_{i,r}|^2 + |\hat{h}_{i+1,r}|^2) + |\alpha|^2 N_0 + |\alpha|^2 P(\sigma^2_{\tilde{h}_{i,r}} + \sigma^2_{\tilde{h}_{i+1,r}}) + N_0$.

Substituting α from (6.9) and β_m from (6.10) into (6.7), the SNR of the i^{th} user's signal received at the m^{th} user, can be obtained as:

$$\gamma_{i,m} = \frac{|\hat{h}_{m,i}|^2 \left(P_r |\hat{h}_{r,m}|^2 \left(\frac{1}{P|\hat{h}_{i,r}|^2 + P|\hat{h}_{i+1,r}|^2} + \frac{1}{P\left(\sigma^2_{\hat{h}_{i,r}} + \sigma^2_{\hat{h}_{i+1,r}} + N_0\right)} \right) + N_0 + P_r P_s \left(|\hat{h}_{m,i}|^2 + |\hat{h}_{m,i+1}|^2 \right) \right)}{1 - 2PP_r(|\hat{h}_{m,i}|^2 + |\hat{h}_{m,i+1}|^2) + PP_r(|\hat{h}_{m,i}|^2 + |\hat{h}_{m,i+1}|^2)^2}. \tag{6.11}$$

6.2.1 Special Case: Perfect Channel Estimation

When the channel estimation is perfect, the modified SNR $\gamma^{pe}_{i,m}$ is given by:

$$\gamma^{pe}_{i,m} = \frac{|h_{i,r}|^2 |h_{r,m}|^2 \left(P_r |h_{r,m}|^2 \left(\frac{1}{P|h_{i,r}|^2 + P|h_{i+1,r}|^2} + \frac{1}{N_0} \right) + N_0 + P_r P_s \left(|h_{i,r}|^2 |h_{r,m}|^2 + |h_{i+1,r}|^2 |h_{r,m}|^2 \right) \right)}{1 - 2PP_r(|h_{i,r}|^2 |h_{r,m}|^2 + |h_{i+1,r}|^2 |h_{r,m}|^2) + PP_r(|h_{i,r}|^2 |h_{r,m}|^2 + |h_{i+1,r}|^2 h_{r,m}|^2)^2}, \tag{6.12}$$

which is also a new result on its own.

6.3 Achievable Rate Analysis

In this section, we discuss the achievable common rate and sum rate analysis based on the SNR results in the previous section.

6.3.1 Common Rate

The maximum achievable common rate of an AF MWRN can be given as [49]:

$$R_c = \frac{1}{L-1} \min_{i,m} R_{i,m}, \tag{6.13}$$

where the factor $(L-1)$ comes from the fact that there are $(L-1)$ time slots in each of the MAC and the BC phases and $R_{i,m}$ denotes the achievable information rate with which the i^{th} user's message is received at the m^{th} user, as upper bounded in the following theorem.

Theorem 6.1. *The maximum possible information rate from the i^{th} user to the m^{th} user, can be* *upper bounded by:*

$$R_{i,m} \leq \frac{1}{2} \times \log\left(\frac{|\hat{h}_{m,i}|^2 \left(P_r |\hat{h}_{r,m}|^2 \left(\frac{1}{P|\hat{h}_{i,r}|^2 + P|\hat{h}_{i+1,r}|^2} + \frac{1}{P\left(\sigma^2_{\tilde{h}_{i,r}} + \sigma^2_{\tilde{h}_{i+1,r}}\right) + N_0} \right) + N_0 + P_r P_s \left(|\hat{h}_{m,i}|^2 + |\hat{h}_{m,i+1}|^2 \right) \right)}{1 - 2PP_r(|\hat{h}_{m,i}|^2 + |\hat{h}_{m,i+1}|^2) + PP_r(|\hat{h}_{m,i}|^2 + |\hat{h}_{m,i+1}|^2)^2} \right). \tag{6.14}$$

Proof. The proof can be obtained using the similar steps in the proof of Theorem 4.1. Here, we consider that the volume of the voronoi region must satisfy $\mu = \frac{(\mathrm{Vol}(\mathcal{V}))^{2/N}}{N'}$ and set $\mathrm{Vol}(\mathcal{V}_\Lambda) = (\frac{PP_r|\hat{h}_{m,i}|^2}{G})^{N/2}$ and then substitute β_m from (6.10). □

6.3.2 Sum Rate

Theorem 6.2. *For AF MWRNs with imperfect CSI and lattice codes, the achievable sum rate can be upper bounded as:*

$$R_s \leq \frac{1}{2(L-1)} \sum_{i=1}^{L-1} \log\left(\frac{|\hat{h}_{m,i}|^2 \left(P_r |\hat{h}_{r,m}|^2 \left(\frac{1}{P|\hat{h}_{i,r}|^2 + P|\hat{h}_{i+1,r}|^2} + \frac{1}{P\left(\sigma^2_{\tilde{h}_{i,r}} + \sigma^2_{\tilde{h}_{i+1,r}} + N_0\right)} \right) + N_0 + P_r P_s \left(|\hat{h}_{m,i}|^2 + |\hat{h}_{m,i+1}|^2 \right) \right)}{1 - 2PP_r(|\hat{h}_{m,i}|^2 + |\hat{h}_{m,i+1}|^2) + PP_r(|\hat{h}_{m,i}|^2 + |\hat{h}_{m,i+1}|^2)^2} \right). \tag{6.15}$$

Proof. The achievable rate at the i^{th} time slot can be obtained from (6.14). Then, obtaining the achievable rate at all the time slots and adding them results into (6.15). The detailed steps are omitted here for the sake of brevity. □

6.4 Error Performance Analysis

In this section, we characterize the error performance of AF MWRNs through average BER analysis for BPSK modulation, which is the simplest lattice code.

6.4.1 Data Transmission with BPSK Modulation

In the BPSK modulated AF MWRN , during the i^{th} time slot, the i^{th} and the $(i+1)^{th}$ user transmit their messages $\mathbf{W}_i$ and $\mathbf{W}_{i+1}$ which are BPSK modulated to $\mathbf{X}_i$ and $\mathbf{X}_{i+1}$, respectively, where $X_i^t, X_{i+1}^t \in \{-1, 1\}$. The relay receives the signal $\mathbf{R}_{i,i+1}$ (see (2.5)) and amplifies and broadcasts the network coded signal, which is given as $\mathbf{Z}_{i,i+1}$. The i^{th} user receives $\mathbf{Y}_{i,i+1}$ (see (2.7)) and subtracts its own signal $\mathbf{X}_i$ multiplied by $\alpha\sqrt{PP_r}\hat{h}_{i,i}$ to detect the $(i+1)^{th}$ user's signal as $\hat{\mathbf{X}}_{i+1}$. Then the user detects the signal of the $(i+2)^{th}$ user to the L^{th} user in the downward message extraction. The process can be shown as

$$\begin{aligned}
\hat{\mathbf{X}}_{i+1} =& \mathbf{Y}_{i,i+1} - \alpha\hat{h}_{i,i}\sqrt{PP_r}\mathbf{X}_i, \\
\hat{\mathbf{X}}_{i+2} =& \mathbf{Y}_{i+1,i+2} - \alpha\hat{h}_{i,i+1}\sqrt{PP_r}\hat{\mathbf{X}}_{i+1}, \\
& ..., \\
\hat{\mathbf{X}}_{L} =& \mathbf{Y}_{L-1,L} - \alpha\hat{h}_{i,L-1}\sqrt{PP_r}\hat{\mathbf{X}}_{L-1}.
\end{aligned} \tag{6.16}$$

Similarly, the upward message extraction process for extracting the messages of the $(i-1)^{th}$ user to the 1^{st} user can be shown as

$$\begin{aligned}
\hat{\mathbf{X}}_{i-1} =& \mathbf{Y}_{i,i-1} - \alpha\hat{h}_{i,i}\sqrt{PP_r}\mathbf{X}_i, \\
\hat{\mathbf{X}}_{i-2} =& \mathbf{Y}_{i-1,i-2} - \alpha\hat{h}_{i,i-1}\sqrt{PP_r}\hat{\mathbf{X}}_{i-1}, \\
& ..., \\
\hat{\mathbf{X}}_{1} =& \mathbf{Y}_{1,2} - \alpha\hat{h}_{i,2}\sqrt{PP_r}\hat{\mathbf{X}}_{2}.
\end{aligned} \tag{6.17}$$

To obtain the error performance of AF MWRN with channel estimation error, we need to follow the general steps 2-4 in Section 5.4.2. First, we obtain the probability of incorrectly decoding a user's message given that the previous user's message is correct and the probability of incorrectly decoding a user's message given that the previous user's message is also incorrect in an AF MWRN.

Lemma 6.1. *The probability that the i^{th} user incorrectly decodes the $k^{th}(k \neq i)$ user's message, given that the $(k \pm 1)^{th}$ user's message is correctly decoded, can be obtained as:*

$$P_{AF}(i,k) = Q\left(\sqrt{2\gamma_{i,k}}\right), \tag{6.18}$$

where $\gamma_{i,k}$ is the SNR of the k^{th} user's signal received at the i^{th} user and can be given as:

$$\gamma_{i,k} = \frac{PP_r\sigma^2_{h_{r,i}}\sigma^2_{h_{i\pm1,r}}}{N_k}. \tag{6.19}$$

where N_k denotes the variance of the noise terms in the k^{th} user's signal, received at the i^{th} user and can be given by:

$$N_k = \begin{cases} P_rP\sigma^2_{\tilde{h}_{i,i}} + P_rP\sigma^2_{\tilde{h}_{i,i\pm1}} + (P+P_r)\sigma^2_{h_{r,i}}N_0 + P\sigma^2_{h_{i\pm1,r}}N_0, & k = i \pm 1 \\ P_rP\sigma^2_{\tilde{h}_{i,k}} + P_rP\sigma^2_{\tilde{h}_{i,k\pm1}} + P_r\sigma^2_{h_{r,i}}N_0 + P\sigma^2_{h_{k,r}}N_0 + P\sigma^2_{h_{k\pm1,r}}N_0. & k \neq i, i \pm 1 \end{cases}$$

Proof. See Appendix D.1. □

Lemma 6.2. *The probability that the i^{th} user incorrectly decodes the $k^{th}(k \neq i, i \pm 1)$ user's message, given that the $(k \pm 1)^{th}$ user's message is incorrectly decoded, can be obtained from* (6.21) *as:*

$$P_{AF}(i,k) = Q\left(\sqrt{2\gamma^e_{i,k}}\right), \tag{6.20}$$

where $\gamma^e_{i,k}$ represents the SNR of the k^{th} user's signal at the i^{th} user when $\hat{X}_{k\pm1} = X_{k\pm1}$ and can be given by:

$$\gamma^e_{i,k} = \frac{P_rP\sigma^2_{h_{r,i}}\sigma^2_{h_{k,r}}}{4P_rP \mid \hat{h}_{r,i} \mid^2 \mid \hat{h}_{k\pm1,r} \mid^2 + N_k}. \tag{6.21}$$

Proof. When $\hat{X}_{k\pm1} \neq X_{k\pm1}$, the noise terms in the k^{th} user's signal can be written as:

$$\begin{aligned} n_k^e =& 2\alpha\hat{h}_{i,k\pm1}\hat{h}_{k\pm1,r} + \alpha\sqrt{P}\hat{h}_{i,k\pm1}(X_{k\pm1}^t - \hat{X}_{k\pm1})\alpha\sqrt{P}\tilde{h}_{i,k\pm1}X_{k\pm1}^t + \alpha\sqrt{P}\tilde{h}_{i,k}X_k^t + \alpha\hat{h}_{r,i}n_1 + \\ & \alpha\tilde{h}_{r,i}n_1 + n_2. \end{aligned} \tag{6.22}$$

Thus, the SNR of the k^{th} user' s signal can be obtained using similar process as the proof of Lemma 6.1 and can be given as in (6.21). □

Using (6.18) and (6.20) and following the steps in Section 5.4.2, the probability of k error events with imperfect CSI for AF relaying can be obtained as in the following lemma.

Lemma 6.3. *The probability of exactly k error events can be asymptotically approximated as:*

$$P_i(k) = \begin{cases} \sum_{p=2}^{L-k+1} P_C(p) + P_{D'}, & i = 1,2,3 \\ \sum_{p=k}^{L-1} P_{C'}(p) + P_D, & i = L, L-1, L-2 \\ \sum_{p=i+1}^{L-k+1} P_C(p) + P_D + \sum_{p=k}^{i-1} P_{C'}(p) + P_{D'} & i \notin \{1,2,3,L-2,L-1,L\}. \end{cases} \tag{6.23}$$

Proof. see Appendix D.2. □

Using Lemmas 5.1-5.3, we can obtain the average BER for AF relaying, which is stated below.

Theorem 6.3. *At high SNR, the average BER for an AF MWRN can be given as:*

$$P_{i,avg,AF} = \frac{1}{L-1}\begin{cases} \sum_{k=1}^{L-1} k \Big(\sum_{p=2}^{L-k+1} \prod_{t=1}^{k-1} P'_{AF}(i,p+t) P_{AF}(i,p) \\ + \prod_{t=1}^{k-2} P'_{AF}(i,L) P'_{AF}(i,L-t) P_{AF}(i,L-k+1) \Big), \quad i = 1,2,3 \\ \\ \sum_{k=1}^{L-1} k \Big(\sum_{p=k}^{L-1} \prod_{t=1}^{k-1} P'_{AF}(i,p-t) P_{AF}(i,p) \\ + \prod_{t=1}^{k-2} P'_{AF}(i,1) P'_{AF}(i,1+t) P_{AF}(i,k) \Big), \qquad i = L, L-1, L-2 \\ \\ \sum_{k=1}^{L-1} k \Big(\sum_{p=i+1}^{L-k+1} \prod_{t=1}^{k-1} P'_{AF}(i,p+t) P_{AF}(i,p) \\ + \prod_{t=1}^{k-2} P'_{AF}(i,1) P'_{AF}(i,1+t) P_{AF}(i,k) \\ + \sum_{p=k}^{i-1} \prod_{t=1}^{k-1} P'_{AF}(i,p-t) P_{AF}(i,p) \\ + \prod_{t=1}^{k-2} P'_{AF}(i,L) P'_{AF}(i,L-t) P_{AF}(i,L-k+1) \Big) \quad i \notin \{1,2,3,L-2,L-1,L\}. \end{cases} \tag{6.24}$$

Proof. Similar to the proof of Theorem 5.4 with $P_i(k)$ substituted from (6.23). □

6.5 Power Allocation

In this section, we obtain the power allocation coefficients in terms of users' long-term statistical CSI (i.e., channel variances) for the pilot and the data signal powers of users and the relay to optimize the achievable sum rate of AF MWRN with BPSK modulation.

In an AF MWRN with BPSK modulation, the maximum achievable rate at the $(k-1)^{th}$ time slot is upper bounded by [49]:

$$R \leq \frac{1}{2}\log(1+\gamma_{i,k}), \tag{6.25}$$

where, $\gamma_{i,k}$ denotes the SNR of the $k^{th}(k \neq i)$ user received at the i^{th} user, given by (6.19).

Then substituting (6.19) in (6.25), adding the maximum achievable rates at all the time slots and after some algebraic manipulations, we can obtain the sum rate for symmetric traffic as:

$$R_s = \frac{1}{2(L-1)} \sum_{k=1,k\neq i}^{L} \log\left(1 + \frac{P_r P \sigma^2_{h_{r,i}} \sigma^2_{h_{k,r}}}{N_k}\right), \tag{6.26}$$

where, $N_k = P_r P \sigma^2_{\tilde{h}_{i,k}} + P_r P \sigma^2_{\tilde{h}_{i,k\pm1}} + P_r \sigma^2_{h_{r,i}} N_0 + P \sigma^2_{h_{k,r}} N_0 + P \sigma^2_{h_{k\pm1,r}} N_0$ denotes the variance of the noise terms in Lemma 6.1. Here, we assume that at high SNR, $\hat{X}_{k\pm1} = X_{k\pm1}$, i.e., the individual error probabilities are zero and thus, no error propagation occurs.

Now, we assume that the average power per signal is P_t and thus, the total power for one pair of message exchange between a user pair is $(2T+4)P_t$ (T data signals from the two users and T data signals from the relay, 1 pilot signal from each user and 2 pilot signals from the relay), as shown in Fig. 6.2. Since, the total energy is conserved, we can write

$$2P_s^{\mathrm{p}} + 2PT + 2P_r^{\mathrm{p}} + P_r T = (2T+4)P_t. \tag{6.27}$$

From (6.26), we can see that the sum rate is maximized when the achievable rate at each time slot is maximized. Since, both the users in a user pair are allocated with the same transmission power at each time slot, optimizing the achievable rate at each time slot, ensures optimum performance for both the users. Further, from (6.25), it can be identified that the achievable rate at each time slot is maximized when the denominator of $\gamma_{i,k}$ is minimized. Thus, the optimum power allocation problem for a MWRN can be posed as allocating the average power to users' and the relay's pilot and data signals, such that the denominator in (6.26) is minimized, that is:

$$\begin{aligned} &\min_{P_s^{\mathrm{p}}, P_r^{\mathrm{p}}, P, P_r} f_k \\ &s.t. \quad 2P_s^{\mathrm{p}} + 2P_r^{\mathrm{p}} + 2PT + P_r T = (2T+4)P_t, \end{aligned} \tag{6.28}$$

where, f_k denotes the objective function at the k^{th} time slot ($k \in [1, L-1]$). f_k can be

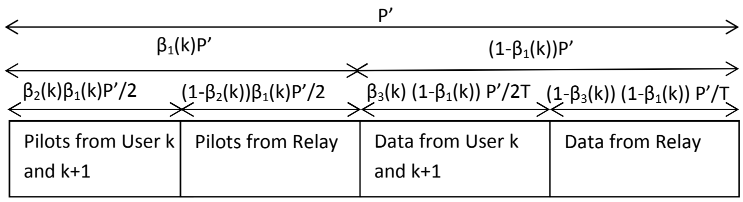

Figure 6.2: Transmission structure for the pilot and data signals from the users and the relay at the $k^{th}(k \in [1, L-1])$ time slot. Here, $P' = \frac{(2T+4)}{2}P_t$, P_t denotes the total power during one pair of message exchange and T represents the number of transmission blocks in the data signal. The optimum power allocation coefficients are shown at the top of the transmission blocks.

expressed as a function of the k^{th} and the $(k+1)^{th}$ users' statistical CSI and given by

$$f_k = \begin{cases} \sigma^2_{\tilde{h}_{i,k}} + \sigma^2_{\tilde{h}_{i,k\pm1}} + \frac{\sigma^2_{\tilde{h}_{r,i}} N_0}{P} + \frac{\sigma^2_{\tilde{h}_{k,r}} N_0}{P_r} + \frac{\sigma^2_{\tilde{h}_{k\pm1,r}} N_0}{P_r}, & k \neq i \pm 1 \\ \sigma^2_{\tilde{h}_{i,i}} + \sigma^2_{\tilde{h}_{i,k}} + \frac{\sigma^2_{\tilde{h}_{r,i}} N_0}{P} + \frac{\sigma^2_{\tilde{h}_{r,i}} N_0}{P_r} + \frac{\sigma^2_{\tilde{h}_{k,r}} N_0}{P_r}. & k = i \pm 1 \end{cases} \tag{6.29}$$

We assume that at the k^{th} time slot, a fraction $\beta_1(k)$ of the total power is allocated to the pilot signals. We also assume that at the same time slot, $\beta_2(k)$ fraction of the pilot signal power and $\beta_3(k)$ fraction of the data signal power are allocated to the users. These power allocation coefficients are illustrated in Fig. 6.2 and can be represented as:

$$P_s^{\mathrm{p}} = \beta_2(k)\beta_1(k)\frac{(2T+4)P_t}{2}, \tag{6.30a}$$

$$P_r^{\mathrm{p}} = (1-\beta_2(k))\beta_1(k)\frac{(2T+4)P_t}{2}, \tag{6.30b}$$

$$P = \beta_3(k)(1-\beta_1(k))\frac{(2T+4)P_t}{2T}, \tag{6.30c}$$

$$P_r = (1-\beta_3(k))(1-\beta_1(k))\frac{(2T+4)P_t}{T}. \tag{6.30d}$$

Now, substituting (6.30) in (6.29), the optimization problem in (6.28) is solved to obtain the optimum power allocation coefficients $\beta_1(k), \beta_2(k)$ and $\beta_3(k)$ as in the following theorems.

Theorem 6.4. *The optimum fraction of pilot signal power and data signal power, allocated to users, can be given by:*

$$\beta_2(k) = \beta_3(k) = \begin{cases} \frac{\sigma_{h_{i,r}}}{\sigma_{h_{i,r}} + \sqrt{\frac{\sigma^2_{h_{k,r}} + \sigma^2_{h_{k\pm1,r}}}{2}}}, & k \neq i \pm 1 \\ \frac{\sigma_{h_{i,r}}}{\sigma_{h_{i,r}} + \sqrt{\frac{\sigma^2_{h_{i,r}} + \sigma^2_{h_{i\pm1,r}}}{2}}}. & k = i \pm 1 \end{cases} \tag{6.31}$$

Proof. See Appendix D.3. □

Theorem 6.5. *The optimum fraction of the total power allocated to the pilot signals, can be given by:*

$$\beta_1(k) = \frac{C_2 - \sqrt{C_2^2 - 4C_1C_2}}{2C_1}, \tag{6.32}$$

where, the coefficients are given by: $C_1 = A_1\beta^2(k)(1-\beta^2(k))P'^2(2-T)$, $C_2 = 2A_1\beta(k)(1-\beta(k))P'(2\beta(k)(1-\beta(k))P' + A_1A_2T)$, $C_3 = 2A_1\beta^2(k)(1-\beta^2(k))P'^2 - A_1^3TA_2^2$, $\beta(k) = \beta_2(k) = \beta_3(k)$, $A_1 = ((1-\beta(k))\sigma^2_{h_{r,i}} + \beta(k)\sigma^2_{h_{avg}})N_0$, $A_2 = \frac{1}{\sigma^2_{h_{r,i}}\sigma^2_{h_{avg}}}$ *and* $\sigma^2_{h_{avg}} = \frac{\sigma^2_{h_{k,r}} + \sigma^2_{h_{k\pm1,r}}}{2}$.

Proof. see Appendix D.4. □

Remark 6.1. *From* (6.31)*, it can be noted that when the* i^{th} *(receiving) user has large average channel gain, less power is allocated to the relay and more to the* k^{th} *and the* $(k\pm1)^{th}$ *(transmitting) users and vice versa.*

6.6 Results

In this section, we verify the analytical results with Monte Carlo simulations and provide insights from the achievable rate and error performance analysis. We consider that each user transmits a message packet of $T = 1000$ bits. For each of the message packets, one pilot signal is transmitted. Similar to Chapters 4 and 5, the average channel gain for the j^{th} user is modeled by $\sigma^2_{h_{j,r}} = (1/(d_j/d_0))^{\nu}$. The SNR is assumed to be SNR per message per user. We denote the decoding user as the i^{th} user, where i is assumed to

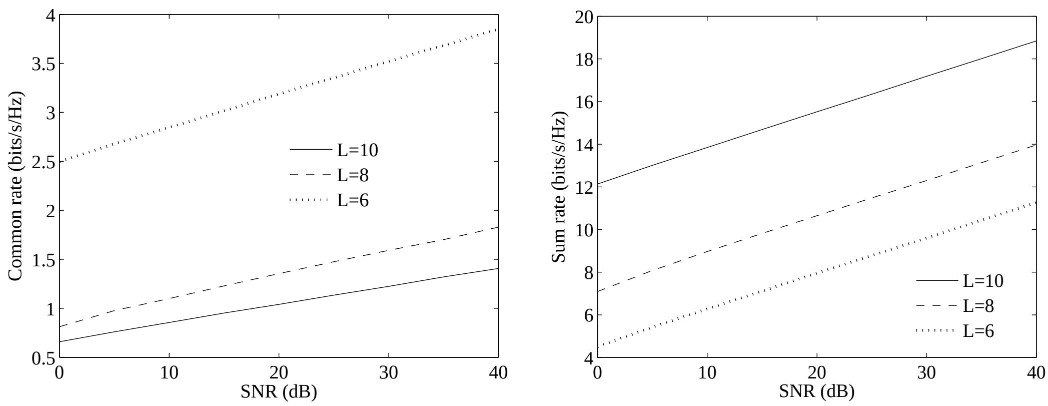

(a) Common rate (b) Sum rate

Figure 6.3: Achievable common rate and sum rate for $L = 6, 8, 10$ user AF MWRNs with channel estimation error, as given in (5.5).

be 1 and other users as the m^{th} user, where $m \in [1, L], m \neq i$. The simulation results are averaged over 1000 Monte Carlo trials per SNR point.

6.6.1 Achievable Rate

Fig. 6.3(a) and Fig. 6.3(b) show the achievable common rate and sum rate, respectively for $L = 6, 8$ and 10 user AF MWRNs in the presence of imperfect channel estimation. Similar to FDF relaying in the last chapter, the common rate of AF MWRN decreases for larger number of users, as evident from Fig. 6.3(a). Also, common rate increases at a smaller rate with SNR for larger number of users, which is evident from (6.13). However, from Fig. 6.3(b), it can be noted that the sum rate increases with increasing number of users, as expected from (6.15).

6.6.1.1 Impact of the Estimation Error

Fig. 6.4(a) and Fig. 6.4(b) show the impact of different levels of channel estimation errors on the achievable common rate and sum rate for $L = 6, 8$ and 10 user. Similar to FDF relaying in the last chapter, Fig. 6.4(a) and Fig. 6.4(b) show that both the achievable common rate and sum rate is a linearly decreasing function of the estimation error. The achievable common rate degrades at a smaller rate for larger number of users, since the slope of (6.13) decreases with the increasing number of users. However, the sum rate

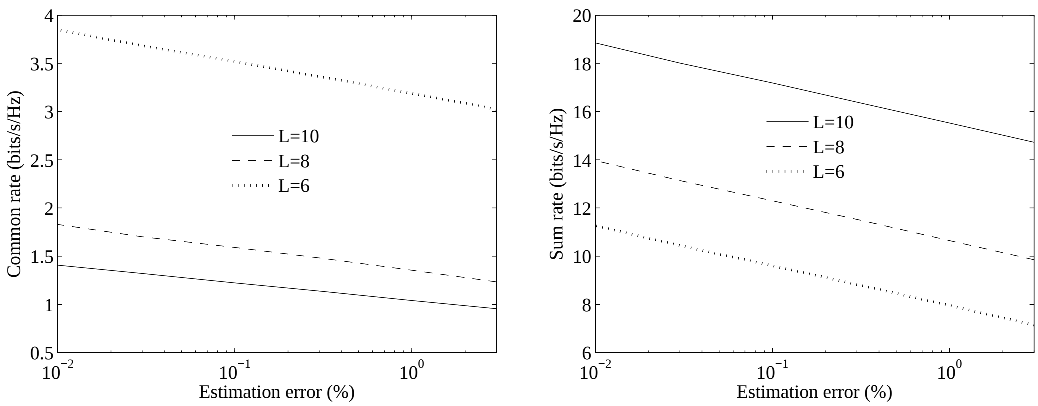

(a) Common rate (b) Sum rate

Figure 6.4: Achievable common rate and sum rate for $L = 6, 8, 10$ user AF MWRNs with different levels of channel estimation error.

degrades nearly at the same rate for large and small number of users, as the slope of (6.15) does not depend on the number of users.

6.6.1.2 Impact of the Overall Channel Conditions

Fig. 6.5(a) and Fig. 6.5(b) show the achievable common rate for $L = 10$ user AF MWRN for the cases when (i) 10% of the users have distances below $0.1d_0$ and (ii) 90% of the users have distances below $0.1d_0$. It can be observed that when most of the users experience good channel conditions, the achievable common rate and sum rate improve. Also, it can be noted that when the overall channel conditions are poor, the common rate and sum rate performance in AF MWRN degrade by nearly the same degree for perfect and imperfect CSI cases.

6.6.2 Optimum Power Allocation

Fig. 6.6 shows the optimum power allocation coefficients at the k^{th} time slot for two sets of channel conditions of the users: (i) $d_i = 0.1d_0, d_{k\pm1} = 0.9d_0$ (the i^{th} user has good channel conditions) and (ii) $d_i = 0.9d_0, d_{k\pm1} = 0.1d_0$ (the i^{th} user has poor channel conditions). For all the above cases, we have considered the distance of the k^{th} user as

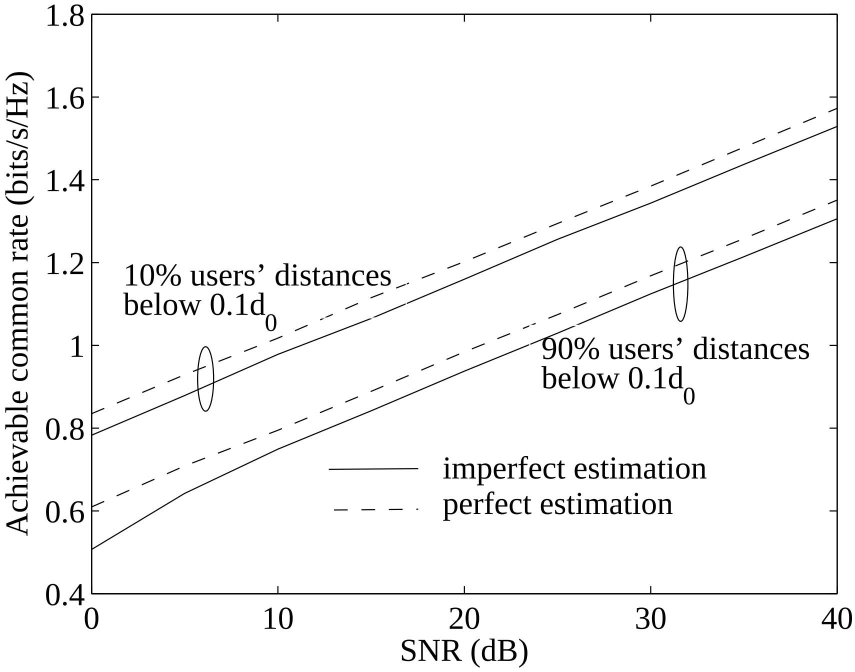

(a) Common rate

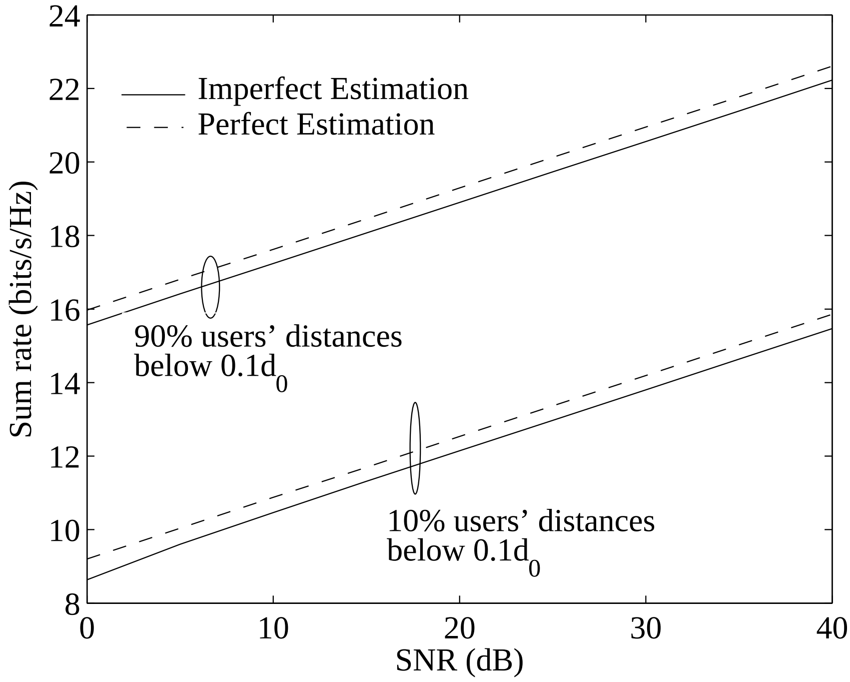

(b) Sum rate

Figure 6.5: Achievable common rate and sum rate when 10% and 90% users' distances are below $0.1d_0$ in $L = 10$ user AF MWRN.

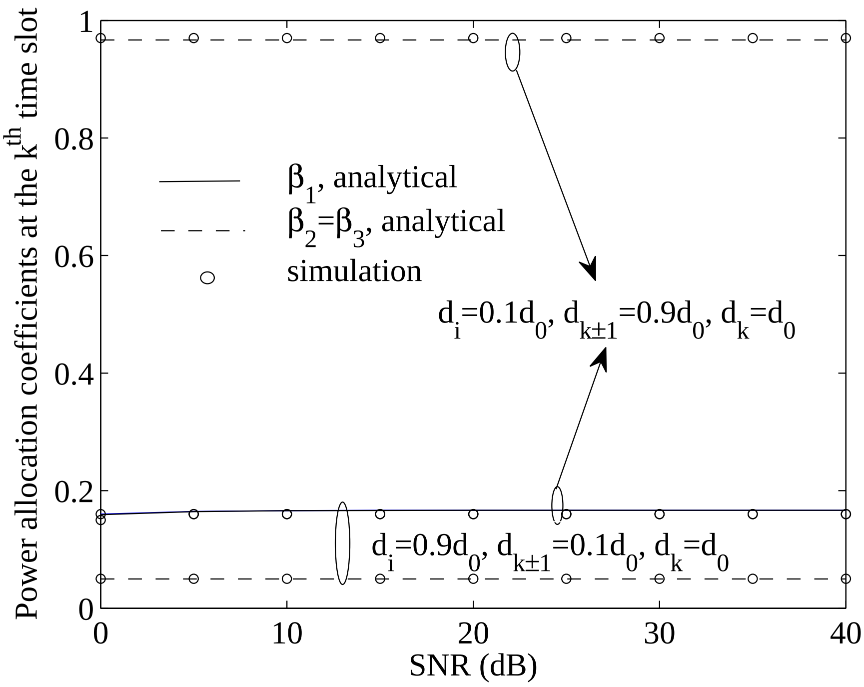

Figure 6.6: Optimum power allocation coefficients at the $k^{th}(k \in [1, L-1])$ time slot in an $L = 10$-user AF MWRN for different channel conditions.

d_0 which corresponds to the worst possible channel conditions. The distances of other users (except the i^{th}, k^{th} and the $(k \pm 1)^{th}$ users) are randomly distributed between $[0, d_0]$. In this figure, the analytical results for the optimum coefficient $\beta_1(k)$ (see (6.32)) and $\beta_2(k) = \beta_3(k)$ (see (6.31)) are verified through numerical search. Here, for the channel conditions in (i), we can see that a larger fraction of the pilot power and the data power are allocated to the transmitting users ($(k \pm 1)^{th}$ and k^{th}), compared to the relay (i.e., larger $\beta_2(k)$ and $\beta_3(k)$), as explained in Remark 6.1. However, the power allocated to the pilot signals (i.e., $\beta_1(k)$) remains the same for both the channel conditions. This is due to the fact that the parameter A_1 (see after Theorem 6.5) is nearly the same for both the channel conditions, because for both the cases, $d_i = d_0 - d_{k\pm1}$. As a result, the coefficient $\beta_1(k)$ remains unchanged for the set of distances $\{d_i, d_{k\pm1}\}$ that satisfy $d_i = d_0 - d_{k\pm1}$.

Fig. 6.7 shows that optimum power allocation gives higher sum rate for the cases

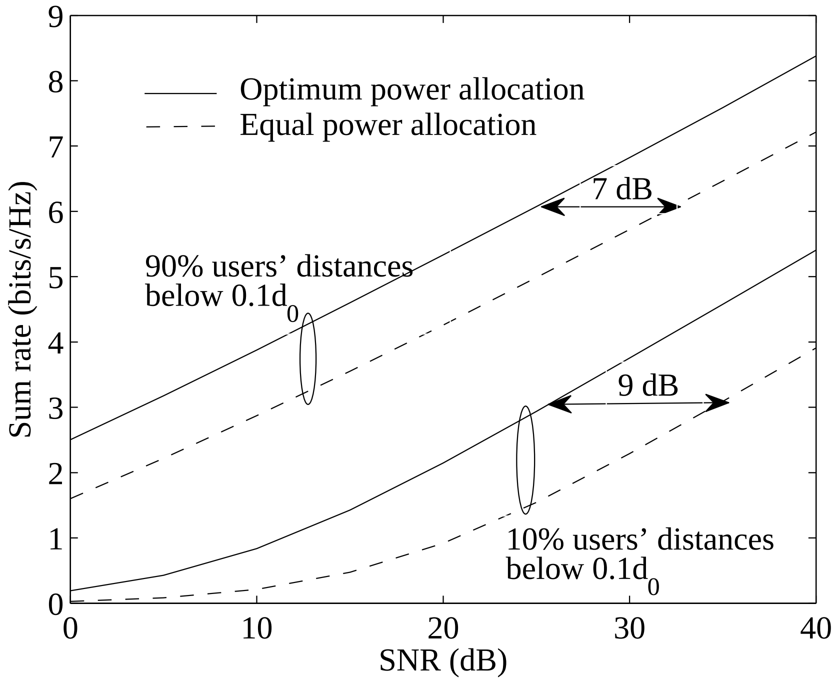

Figure 6.7: Sum rate when 10% and 90% users' distances are below $0.1d_0$ in an $L = 10$-user AF MWRN.

when (i) 10% users have distances below $0.1d_0$ (most of the users have bad channel conditions) and (ii) 90% users have distances below $0.1d_0$ (most of the users have good channel conditions). It can be seen from the figure that when most of the users experience poor channel conditions, the performance degradation for optimum power allocation is smaller compared to that for equal power allocation. Thus, optimum power allocation makes the network performance less vulnerable towards degradation in the overall channel conditions. It can be seen that when most of the users experience good and bad channel conditions, optimum power allocation saves the power by 7 dB and 9 dB, respectively, compared to equal power allocation, to achieve the sum rate 3 bits/s/Hz.

Fig. 6.8 shows the impact of optimum power allocation on the achievable sum rate in the presence of imperfect and perfect channel estimation. It can be seen from the figure that when there is no channel estimation error, the degree of improvement in the sum rate provided by optimum power allocation is relatively small. However, in the

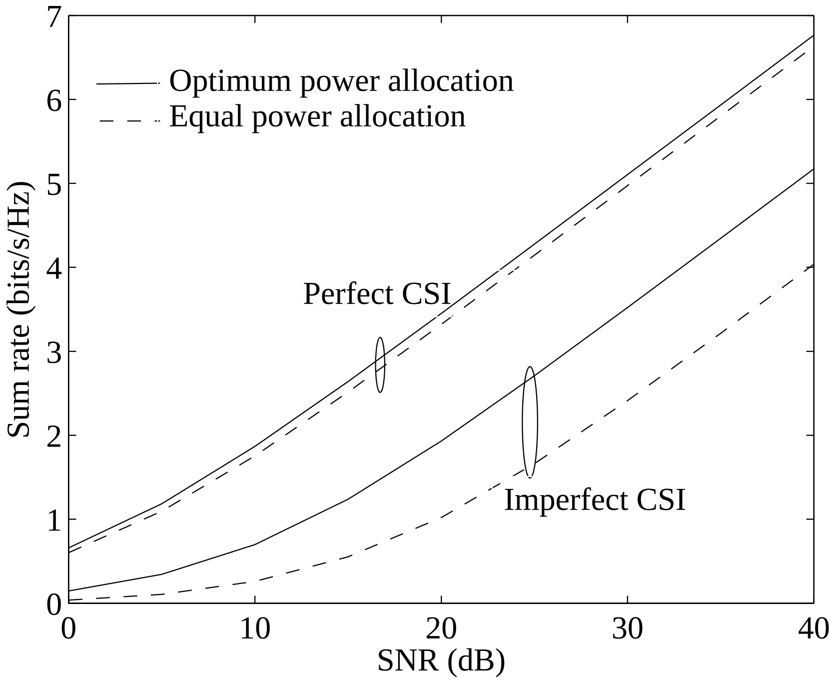

Figure 6.8: Sum rate with imperfect and perfect CSI for an $L = 10$-user AF MWRN.

presence of imperfect channel estimation, optimum power allocation provides a large improvement in the sum rate compared to equal power allocation, e.g., we can see from the figure that for equal power allocation, when perfect CSI is not available, the sum rate drops by 2.7 bits/s/Hz at 40 dB SNR. On the other hand, for optimum power allocation, the drop is about 1.2 bits/s/Hz at 40 dB SNR. Thus, optimum power allocation helps to make the system performance more robust to imperfect CSI.

6.6.3 Average BER

Fig. 6.9 shows the average BER for AF MWRN with $L = 6$, $L = 8$ and $L = 10$ users in the presence of imperfect channel estimation. Here, the analytical results are plotted using (6.24) and compared with the simulation results. It can be seen from the figure that the analytical results match with the simulations at medium to high SNR. It can be seen from the figure that the average BER remains almost the same with the increasing number of users. This is because larger number of error events in AF MWRN are less

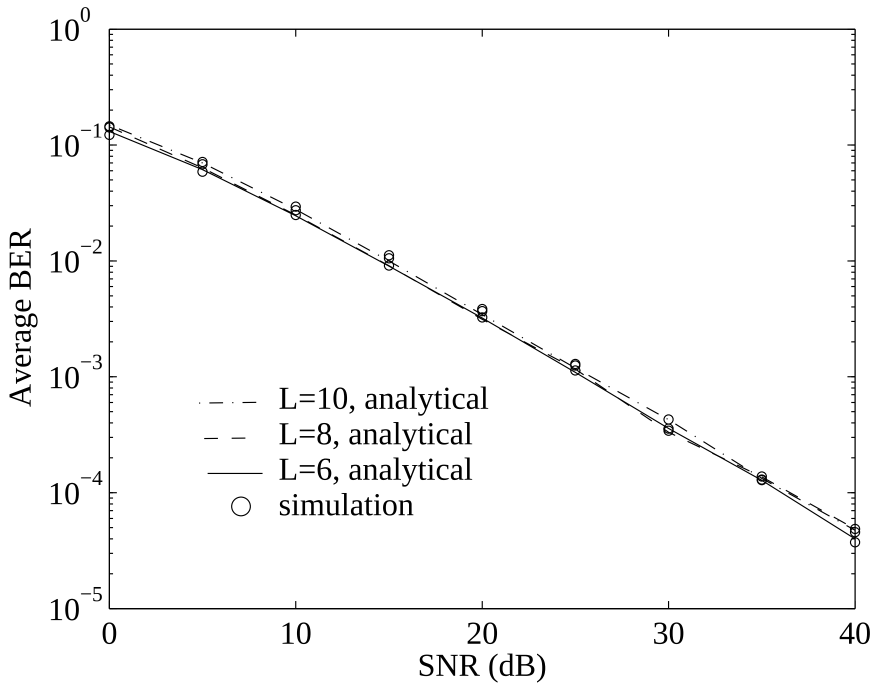

Figure 6.9: Average BER for different channel conditions in $L = 6$, $L = 8$ and $L = 10$ user AF MWRNs.

probable, as explained in Lemma 6.3. For this reason, the average BER does not increase with increasing number of users, as expected from (6.24).

6.6.3.1 Impact of the Estimation Error

Fig. 6.10 plots average BER for $L = 6$, $L = 8$ and $L = 10$ users AF MWRN for different levels of the estimation error and different channel conditions. It can be noted from this figure that the average BER has a linear correlation with the estimation error. With increasing estimation error, the average BER increases at the same rate for different number of users. The reason is that the larger number of error events are less probable than the smaller number of error events in AF MWRN (see (6.23) and Appendix D.2).

6.6.3.2 Impact of the Overall Channel Conditions

Fig. 6.11 shows average BER for $L = 10$ users AF MWRN for the cases when (i) 10% of the users have distances below $0.1d_0$ and (ii) 90% of the users have distances below

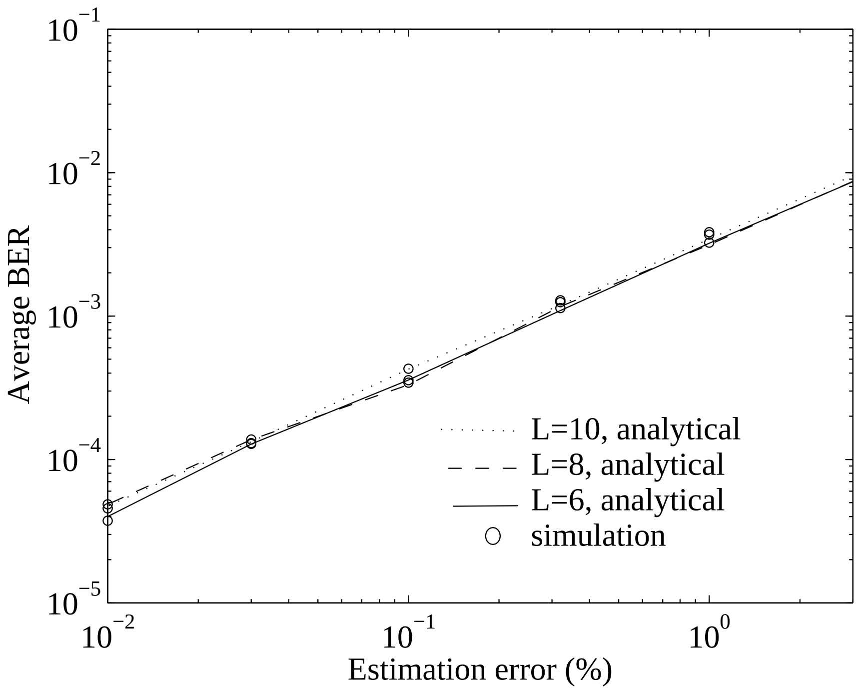

Figure 6.10: Average BER for different levels of estimation error in $L = 6$, $L = 8$ and $L = 10$ user AF MWRNs.

$0.1d_0$. It can be observed from the figure that when most of the users experience good channel conditions, the average BER of AF MWRN decreases by the same level for both imperfect and perfect estimation. Thus, it can be identified that reducing the channel estimation error (by improved channel estimation technique) cannot improve the system performance unless most of the users experience good channel conditions.

6.7 Summary

In this chapter, we investigated the impact of channel estimation error on the achievable rate and error performance of AF MWRNs. We considered a generalized lattice code based AF MWRN with linear MMSE channel estimation for achievable rate analysis and then obtained the BER results with BPSK modulation, which is the simplest lattice code. We also obtained the optimum power allocation coefficients to maximize the achievable sum rate. Specifically, we made the following contributions in this chapter:

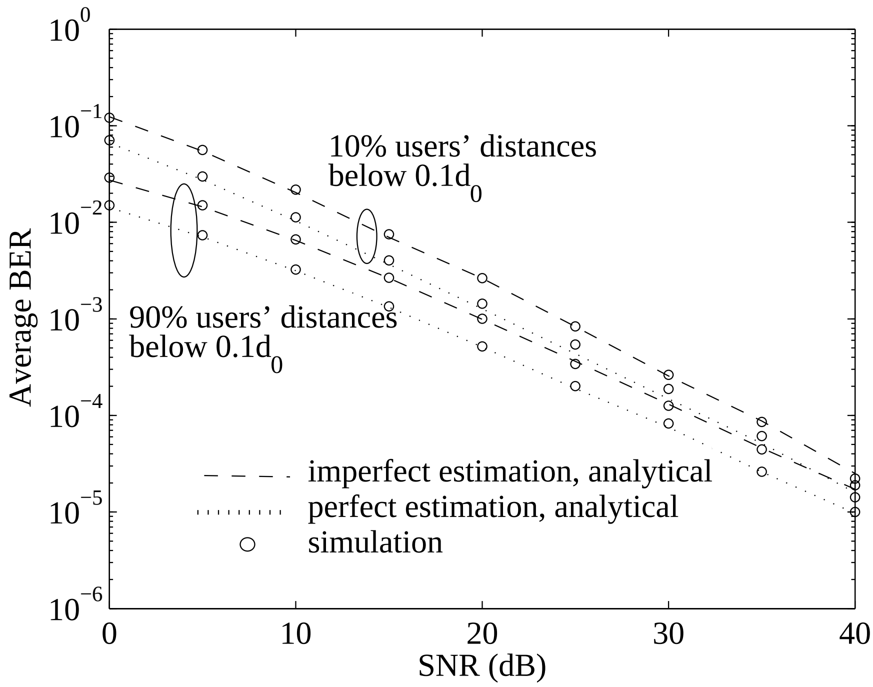

Figure 6.11: Average BER when 10% and 90% users' distances are below $0.1d_0$ in $L = 10$ users AF MWRN.

- Considering L-user AF MWRNs in Section 6.3 with sufficiently large dimension lattice codes, we derived the achievable rate expressions with imperfect channel estimation and unequal average channel gains for the users.

- In Section 6.4 and Section 6.5, we derived the expressions for the average BER and the optimum power allocation coefficients to maximize the achievable sum rate, respectively for AF MWRNs with BPSK modulation.

- In Section 6.6, we showed that the achievable rates of AF MWRNs are decreasing functions of the estimation error, as expected. Also, we showed that the average BER of AF MWRN does not depend on the number of users, because the larger number of error events are less probable for AF.

- In Section 6.6, we showed that to achieve the same sum rate in AF MWRN, optimum power allocation requires $7 - 9$ dB less power compared to equal power allocation depending upon users' channel conditions.

Chapter 7

Conclusions and Future Research Directions

In Chapters 3-6, we investigated several performance aspects of MWRNs. In this chapter, we discuss the general conclusions drawn from this thesis. More detailed technical contributions can be found at the end of each chapter and are not repeated here. We also outline some future research directions emerging from this work.

7.1 Conclusions

The primary focus of this thesis was to identify key performance factors of a MWRN and investigate the impact of practical issues that critically influence these performance factors. Specifically, we first characterized error propagation phenomenon in a pairwise transmission based MWRN, then proposed a novel pairing scheme that can outperform existing pairing schemes in terms of the achievable rates and error performance and finally, considered imperfect CSI and optimum power allocation for more practical channel models.

For both FDF and AF MWRNs, we presented a method for analyzing the probability of k error events and the average BER. The method was based on insights provided by the exact analysis of $k = 1$ and $k = 2$ error events, which led to an accurate asymptotic expression for k error events in such systems. For both FDF and AF MWRN in AWGN and Rayleigh fading channels, the derived expression can accurately predict the BER of a user in medium to high SNR. Using our analysis, we showed that FDF MWRN outperforms AF MWRN in AWGN channels even with a larger number of users, while AF MWRN outperforms DF MWRN in Rayleigh fading channels even for a much smaller number of users.

We investigated generalized lattice code based FDF MWRNs in terms of the achievable rate and error performance. To improve the performance of a pairwise transmission based lattice coded FDF MWRN, we have proposed a novel user pairing scheme. We showed that pairing each user with the user which has the best channel gain is beneficial for FDF MWRN performance improvement. We derived the upper bound on the average common rate and the average sum rate and the asymptotic average SER for the proposed pairing scheme in a lattice coded FDF MWRN. We compared the performance of the proposed scheme with existing pairing schemes in terms of the average common rate, sum rate and error performance under different channel scenarios. Our analysis has shown that the proposed pairing scheme improves the aforementioned performance metrics compared to that of the existing pairing schemes.

We incorporated the channel imperfections like imperfect CSI in the common rate, sum rate and error performance analysis for lattice coded FDF MWRNs. We have shown that the average SER of a FDF MWRN is an increasing function of both the estimation error from MMSE channel estimation and the number of users. On the other hand, we found that the common rate and sum rate are decreasing functions of the channel estimation error. The common rate decreases with the number of users, whereas, the sum rate increases with increasing users. Moreover, we observed that when most of the users experience good channel conditions, the error performance gap between imperfect and perfect CSI decreases because of reduced error propagation.

Similarly, we considered the impact of channel estimation error on the average common rate, sum rate and error performance of lattice coded AF MWRNs. Also, we obtained optimum power allocation coefficients to maximize the sum rate of this system. We showed that the average BER increases linearly and the achievable common rate and the sum rate decreases linearly with the estimation error. Moreover, we found that AF MWRN is robust against the increase in the number of users in terms of average BER. Also, we showed that to achieve the same sum rate in AF MWRN, optimum power allocation requires $7-9$ dB less power compared to equal power allocation depending upon users' channel conditions.

7.2 Future Research Directions

The following open problems can be addressed in future research.

Imperfect Synchronization and Channel Coding: In this thesis, we assumed perfect phase synchronization at the users and the relay. However, in practice, it is difficult to maintain accurate synchronization [106]. Since, synchronization needs to be strictly maintained for PNC protocols, MWRNs based on PNC are expected to have a performance loss in the absence of imperfect synchronization. Moreover, channel coding needs to be considered to nullify the impact of asynchronous transmissions. Though asynchronous TWRNs and channel coding issues have been investigated in [107], the aforementioned factors have not yet been considered from the perspective of MWRNs and can be an interesting open problem.

MWRN with Direct Links: In this thesis, we have assumed that the users do not have any direct links between them. In the presence of direct links, more sophisticated relay processing needs to be employed. Some initial work in this respect has been done in [43] where beamforming at the relay is considered to cancel interference components. However, relaying protocols like FDF, AF or compute and forward have not been investigated for MWRNs with direct links and are regarded as open problems.

MWRN with Non-pairwise Transmission: In this thesis, we have focussed towards MWRNs with pairwise transmission. However, non-pairwise transmission strategies in a MWRN allows higher multiplexing gain [49]. AF MWRNs with non-pairwise transmission have been investigated for outage probability and sum rate in [49]. However, other relaying protocols, as well as error performance of non-pairwise MWRNs can be considered as interesting open problems.

MIMO MWRN: In this thesis, we considered MWRNs with single antenna relay. However, for improving the transmission efficiency of a MWRN in terms of the time slots, non-pairwise transmission strategies are more suitable. To enable signal processing for such non-pairwise transmission, the relay needs to incorporate multiple antennas. Though general MIMO systems have been investigated in the literature along with the impact of imperfect CSI and optimum power allocation [108], MIMO MWRNs have been considered only for AF relaying in [49]. In this regard, more complex relaying protocols, like FDF and compute and forward for MIMO MWRNs are yet to be considered in the literature.

Satellite Communications through MWRNS: In this thesis, we have stated that MWRNs have potential applications in Satellite Communications where the satellite acts as a relay node. Satellite communication through two-way relaying has been investigated in the previous literature [109]. However, practical satellite communications need to take into account the timing and synchronization aspects to effectively harness the benefits of network coding. Thus, satellite communications based on practical MWRNs incorporated with the challenges of imperfect timing, imperfect synchronization and imperfect CSI can be an interesting open problem.

Appendix A

This appendix contains the proof of the lemmas presented in Chapter 3. The appendix is organized as follows. In Section A.1, the Lemma 3.2 on page 49 is proved. In Section A.2, the Lemma 3.3 on page 50 is proved. Section A.3 contains the proof of Lemma 3.6 on page 54. Finally, Section A.4 contains the proof of Lemma 3.3 on page 55.

A.1 Proof of Lemma 3.2

First, we obtain the probability of error case A_1. Since, P_{FDF} is the probability of incorrectly decoding a network coded message, the factor P_{FDF}^2 represents the probability of incorrectly decoding two consecutive erroneous network coded messages from two user pairs and the factor $(1 - P_{FDF})^{L-3}$ represents the probability that the network coded messages of the remaining $L - 3$ user pairs are correctly decoded. Thus, (3.14a) can be obtained by computing the product of these two factors.

Next, we obtain the probability of error case B_1. The factor P_{FDF} represents the probability of incorrectly decoding the network coded message involving an end user and the factor $(1 - P_{FDF})^{L-2}$ represents the probability that the network coded messages of the remaining $L - 2$ user pairs are correctly decoded. Thus, (3.14b) can be proved in a similar manner as (3.14a).

Now, a middle user (i.e., $i \neq 1$ and $i \neq L$) can incorrectly decode any of the two end users' messages (error case B_1) or any of the remaining $(L - 3)$ middle users' messages (error case A_1) for $k = 1$ error event. However, an end user can incorrectly decode another end user's message (error case B_1) or any of the remaining $(L-2)$ middle users' messages (error case A_1) for $k=1$. Using these facts and the expressions in (3.14), we can obtain the probability of $k=1$ error event as in (3.13).

A.2 Proof of Lemma 3.3

First, we obtain the probability of the error case C_1. The probability of incorrectly decoding two network coded messages is given by P_{FDF}^2. Similarly, the probability of correctly decoding the remaining $L-3$ users' network coded messages can be obtained as $(1-P_{FDF})^{L-3}$. Then, combining these terms gives the expression for P_{C_1} as in (3.16a).

Next, we obtain the probability of the error case D_1. The probability of incorrectly decoding the network coded message involving the users preceding the end user is P_{FDF}. The probability of correctly decoding the remaining $(L-2)$ network coded messages is $(1-P_{FDF})^{L-2}$. Combining these terms, we can obtain P_{D_1}.

Then, we obtain the probability of the error case E_1. The probability of incorrectly decoding two pairs (i.e., four) network coded messages is P_{FDF}^4. The probability of incorrectly decoding the remaining $(L-5)$ network coded messages is $(1-P_{FDF})^{L-5}$. Thus, P_{E_1} can be obtained by taking the product of these two terms.

Next, we obtain the probability of the error case F_1. The probability of incorrectly decoding the network coded message involving an end user is P_{FDF}. The probability of incorrectly decoding two consecutive network coded messages is P_{FDF}^2. The probability of incorrectly decoding the remaining $(L-4)$ network coded messages is $(1-P_{FDF})^{L-4}$. Combining these, we can obtain P_{F_1}.

Finally, we obtain the probability of the error case G_1. The probability of incorrectly decoding both of the network coded messages involving one end user is P_{FDF}^2. The probability of incorrectly decoding the remaining $(L-3)$ network coded messages is $(1-P_{FDF})^{L-3}$. Taking the product of these terms, P_{G_1} can be obtained. These error cases are illustrated in Table 3.1.

The end users ($i=1$ or $i=L$) can incorrectly decode any of the $L-3$ combinations of incorrect network coded message pairs separated by one correct network coded message (error case C_1) for $k = 2$ error event. Also, they can incorrectly decode the other end user's message and the preceding (or the following) user's message (error case D_1) or they can incorrectly decode any of the $(L - 3)$ pairs of consecutive network coded messages and the other end user's network coded message (error case F_1) for $k = 2$. Otherwise, they can incorrectly decode $L - 2 - m$ ($L - 2 - m > 0$ or $m < L - 2$) combinations of two pairs of consecutive network coded messages, which leads to incorrect detection of two users' message separated by $m - 1$ ($m > 1$) correctly decoded users' messages (error case E_1). For example, if $i = 1$, $L = 10$ and $m = 2$, then user 1 can make error about $(10 - 2 - 2) = 6$ combinations of two pairs of consecutive network coded messages. That is, user 1 can incorrectly decode the combinations ($\mathbf{V}_{1,2}$, $\mathbf{V}_{2,3}$, $\mathbf{V}_{3,4}$, $\mathbf{V}_{4,5}$), ($\mathbf{V}_{2,3}$, $\mathbf{V}_{3,4}$, $\mathbf{V}_{4,5}$, $\mathbf{V}_{5,6}$), ($\mathbf{V}_{3,4}$, $\mathbf{V}_{4,5}$, $\mathbf{V}_{5,6}$, $\mathbf{V}_{6,7}$), ($\mathbf{V}_{4,5}$, $\mathbf{V}_{5,6}$, $\mathbf{V}_{6,7}$, $\mathbf{V}_{7,8}$), ($\mathbf{V}_{5,6}$, $\mathbf{V}_{6,7}$, $\mathbf{V}_{7,8}$, $\mathbf{V}_{8,9}$) which results into erroneous detection of the messages of user pairs (2, 4), (3, 5), (4, 6), (5, 7), (6, 8) and (7,9), respectively.

Combining the different error cases for $i = 1$ or $i = L$ after multiplication with their appropriate weights (as discussed above), the first equation in (3.15) can be obtained. Similarly, other equations in (3.15) can be obtained and the expressions in (3.16) can be substituted in (3.15) to obtain the probability of $k = 2$ error events.

A.3 Proof of Lemma 3.6

First, we obtain the probability of the error case A_2. The probability of incorrectly decoding a middle user's message is given by P_{AF}. The probability that the next user's message will be correctly decoded is given by $(1 - P'_{AF})$. The probability that the remaining $(L - 3)$ users' messages will be correctly decoded is $(1 - P_{AF})^{L-3}$. Now, taking the product of these three terms gives P_{A_2} as in (3.23a).

Next, we obtain the probability of the error case B_2. The probability of incorrectly decoding an end user's message is given by P_{AF} and the probability of correctly decoding the remaining $(L - 2)$ users' messages correctly can be given by $(1 - P_{AF})^{L-2}$.

Then , taking the product of these terms lead to P_{B_2} as in (3.23b). These error cases are illustrated in Table 3.2.

The middle users ($i \neq 1$ and $i \neq L$) can incorrectly decode any of the two end users' messages (error case B_2) or any of the $(L-3)$ remaining middle users' messages (error case A_2) for $k = 1$ error event. Similarly, the end users can incorrectly decode the other end user's message (error case B_2) or any of the $(L-2)$ middle users' messages (error case A_2) for $k = 1$. Using these facts and the expression in (3.23), we can obtain the probability of $k = 1$ error event as in (3.22).

A.4 Proof of Lemma 3.7

First, we obtain the probability of the error case C_2. The probability of incorrectly decoding a middle user's message is P_{AF} and the probability that the next user's message is incorrectly decoded is P'_{AF}. The probability that the message of the user next to the aforementioned two users (whose messages are incorrectly decoded) is correctly decoded is given by $(1 - P'_{AF})$. The probability that the remaining $(L-4)$ users' messages are correctly decoded is $(1 - P_{AF})^{L-4}$. Then, taking the product of these terms gives P_{C_2} as in (3.25a).

Next, we obtain the probability of the error case D_2. The probability of incorrectly decoding the message of a user just before an end user is P_{AF} and the probability that the end user's message is incorrectly decoded is P'_{AF}. The probability that the remaining $(L-3)$ users' messages are correctly decoded, is $(1 - P_{AF})^{L-3}$. Combining these terms, P_{D_2} can be obtained as in (3.25b).

Now, we obtain the probability of the error case E_2. The probability of incorrectly decoding a middle user's message is P_{AF} and the probability that the next user's message is correctly decoded is $(1 - P'_{AF})$. Similarly, the probability of incorrectly decoding another user's message while making no error about the next user's message is obtained by $P_{AF}(1 - P'_{AF})$. The probability of correctly decoding the remaining $(L-5)$ users' messages is $(1 - P_{AF})^{L-5}$. Taking the product of these terms leads to P_{E_2} as in

(3.25c).

Then, we obtain the probability of the error case F_2. The probability of incorrectly decoding an end user's message is P_{AF}. The probability that a middle user's message is incorrectly decoded while correctly decoding the next user's message is $P_{AF}(1 - P'_{AF})$. The probability that the remaining $(L - 4)$ users' messages are incorrectly decoded, is $(1 - P_{AF})^{L-4}$. Then, taking the product gives the expression for P_{F_2} as in (3.25d).

Finally, we obtain the probability of the error case G_2. The probability of incorrectly decoding both the end users' messages is P_{AF}^2. The probability that the remaining $(L-3)$ users' messages are correctly decoded is $(1 - P_{AF})^{L-3}$. Combining these probabilities, we can obtain P_{G_2} as in (3.25e). These error cases are illustrated in Table 3.2.

Now, if we consider the first equation on the right hand side of (3.24), an end user ($i = 1$ or $i = L$) can incorrectly decode the other end user and the preceding (or the following) user's message (error case D_2) for $k = 2$ error event. Otherwise, it can incorrectly decode any of the $(L - 3)$ possible combinations of two consecutive middle users' messages (error case C_2) or the other end user's message and any one of the $(L - 3)$ middle user's message (error case F_2) for $k = 2$. Alternatively, it can incorrectly decode any of the $(L - 2 - m)$ ($L - 2 - m > 0$ or $m < L - 2$) combinations of two non-consecutive users' messages separated by $m - 1$ ($m > 1$) correctly decoded users' messages (error case E_2) for $k = 2$. For example, if $i = 1$, $L = 10$ and $m = 2$, then user 1 can make error about $(10 - 2 - 2) = 6$ combinations of two middle users separated by correct decision about one middle user. That is, user 1 can incorrectly decode the user pairs (2, 4), (3, 5), (4, 6), (5, 7), (6, 8) and (7,9), respectively.

Combining these error cases with appropriate weights, the probability of $k = 2$ error events at the end users can be obtained. Similarly, the remaining expressions in (3.24) can be proved.

Appendix B

This appendix contains the proof of the lemmas, theorems and propositions presented in Chapter 4. The appendix is organized as follows. In Section B.1, the Propositions 4.1-4.3 on page 81 are proved. In Section B.2, the Propositions 4.4-4.6 on page 83 are proved. In Section B.3, the Lemma 4.1 on page 85 is proved. Section B.4 contains the proof of Theorem 4.4 on page 88. In Section B.5, the Propositions 4.7-4.9 on page 89 are proved.

B.1 Proof of Propositions 4.1−4.3

Proof of Proposition 4.1: For the equal average channel gain scenario, $\sigma^2_{h_{i,r}} = \sigma^2_{h_{\ell,r}} = \sigma^2_{h_{\ell-1,r}} = \sigma^2_{h_{L-\ell+2,r}}$. Thus, the average common rate expressed by (4.19), (4.20) and (4.18d) becomes the same for all the three pairing schemes. This proves Proposition 4.1.

Proof of Proposition 4.2: For unequal average channel gain scenario, as explained in Section 4.1, the transmit power of the i^{th} user needs to be scaled by $(L-1)$ to ensure transmission fairness. As a result, $\mid h_{i,r} \mid^2$ can be replaced by $\frac{|h_{i,r}|^2}{L-1}$ in (4.10). In addition, for a fair comparison with the existing pairing schemes, the transmit power P in the proposed scheme, needs to be multiplied by a factor $(2L-2)$. This is because in the proposed pairing scheme, the common user transmits $(L-1)$ times with power $\frac{P}{L-1}$ and the other $(L-1)$ users transmit once with power P. Hence, the average power per user becomes P. However, for the existing pairing schemes, the average power per user is $\frac{2L-2}{L}P$. Overall, (4.18d) can be modified by scaling $\sigma^2_{h_{i,r}}$ with $L-1$ and replacing P

with $(2L-2)P$. Thus, the average common rate in (4.18d) is

$$E[R_c] \leq \frac{1}{2(L-1)} \log \left(\min \left(\frac{1}{1+\frac{(L-1)\sigma^2_{h_{\ell,r}}}{\sigma^2_{h_{i,r}}}} + \frac{(2L-2)P\sigma^2_{h_{i,r}}}{(L-1)N_0}, \frac{1}{1+\frac{\sigma^2_{h_{i,r}}}{(L-1)\sigma^2_{h_{\ell,r}}}} + \frac{(2L-2)P\sigma^2_{h_{\ell,r}}}{N_0} \right) \right). \tag{B.1}$$

We consider two cases:

- *case 1*: $\sigma^2_{h_{i,r}} > (L-1)\sigma^2_{h_{\ell,r}}$. In this case, the second quantity in the right hand side of (B.1) will be the minimum. Then, comparing (B.1) and (4.19) shows that $\frac{(2L-2)P\sigma^2_{h_{\ell,r}}}{N_0} > \frac{P\sigma^2_{h_{\ell,r}}}{N_0}$. Thus, the average common rate for scheme [28] will be smaller than that for the proposed pairing scheme, when $\sigma^2_{h_{i,r}} < (L-1)\sigma^2_{h_{\ell-1,r}}$. Similarly, it can be shown that for the pairing scheme in [50], the average common rate is smaller than that for the proposed scheme for $\sigma^2_{h_{i,r}} < (L-1)\sigma^2_{h_{L-\ell+2,r}}$.
- *case 2*: $\sigma^2_{h_{i,r}} < (L-1)\sigma^2_{h_{\ell,r}}$. In this case, the first quantity in the right hand side of (B.1) will be the minimum. Then comparing (B.1) and (4.19) shows that the common rate of scheme [28] will be smaller than that of the proposed pairing scheme, when $\sigma^2_{h_{i,r}} > (L-1)\sigma^2_{h_{\ell-1,r}}$. Similarly, it can be shown that for the pairing scheme in [50], the average common rate is smaller than that of the proposed scheme for $\sigma^2_{h_{i,r}} > (L-1)\sigma^2_{h_{L-\ell+2,r}}$.

Combining the result from the two cases, the proposed pairing scheme will have larger average common rate compared to the two other pairing schemes, which proves Proposition 4.2.

Proof of Proposition 4.3: For the variable channel gain scenario, $\sigma^2_{h_{i,r}}$ in (4.18d) is the largest average channel gain in the system. Thus, from (4.18d), it can be shown that $\frac{\sigma^2_{h_{i,r}}}{\sigma^2_{h_{\ell,r}}} > \frac{\sigma^2_{h_{\ell,r}}}{\sigma^2_{h_{i,r}}}$ and the second quantity in the right hand side of the inequality in (4.18d) is the minimum. Then comparing (4.18d) and (4.19) shows that $\frac{\sigma^2_{h_{\ell-1,r}}}{\sigma^2_{h_{\ell,r}}} \leq \frac{\sigma^2_{h_{i,r}}}{\sigma^2_{h_{\ell,r}}}$. Similarly, from (4.18d) and (4.20), it can be shown that $\frac{\sigma^2_{h_{L-\ell+2,r}}}{\sigma^2_{h_{\ell-1,r}}} \leq \frac{\sigma^2_{h_{i,r}}}{\sigma^2_{h_{\ell,r}}}$ and $\frac{\sigma^2_{h_{L-\ell+2,r}}}{\sigma^2_{h_{\ell,r}}} \leq \frac{\sigma^2_{h_{i,r}}}{\sigma^2_{h_{\ell,r}}}$. However, the impact of either of these ratios on the overall average common rate is small compared to that of the term $\frac{P\sigma^2_{h_{\ell,r}}}{N_0}$ in (4.18d), (4.19) and (4.20) at moderate to high SNRs. Thus, the common rate for the proposed scheme will be almost the same as that of the existing pairing schemes in [28] and [50], which proves Proposition 4.3.

B.2 Proof of Propositions 4.4–4.6

Proof of Proposition 4.4: For the equal average channel gain scenario, $\sigma^2_{h_{i,r}} = \sigma^2_{h_{\ell,r}} = \sigma^2_{h_{\ell-1,r}} = \sigma^2_{h_{L-\ell+2,r}}$. Thus, the sum rates expressed by (4.22), (4.23) and (4.24) become the same for all the three pairing schemes, which proves Proposition 4.4.

Proof of Proposition 4.5: For the unequal average channel gain scenario, if the common user is made to transmit at all the time slots with scaled power, the sum rate can be obtained from (4.22) with $\sigma^2_{h_{i,r}}$ scaled by $L-1$ and P replaced with $(2L-2)P$. In this case, the average sum rate in (4.22) becomes

$$E[R_s] = \frac{1}{2(L-1)} \sum_{\ell=1,\ell\neq i}^{L} \left(\log\left(\frac{1}{1+\frac{(L-1)\sigma^2_{h_{\ell,r}}}{\sigma^2_{h_{i,r}}}} + \frac{(2L-2)P\sigma^2_{h_{i,r}}}{(L-1)N_0} \right) + \log\left(\frac{1}{1+\frac{\sigma^2_{h_{i,r}}}{(L-1)\sigma^2_{h_{\ell,r}}}} + \frac{(2L-2)P\sigma^2_{h_{\ell,r}}}{N_0} \right) \right). \tag{B.2}$$

Comparing (B.2) and (4.23) shows that $2\sigma^2_{h_{i,r}} > \sigma^2_{h_{\ell-1,r}}$ and $(2L-2)\sigma^2_{h_{\ell,r}} > \sigma^2_{h_{\ell,r}}$. In a similar manner, it can be shown that the average sum rate of the proposed scheme is larger than that of the scheme in [50]. This completes the proof for Proposition 4.5.

Proof of Proposition 4.6: For the variable average channel gain scenario, we have $\sigma^2_{h_{i,r}} \geq \sigma^2_{h_{\ell-1,r}}$. Hence, it is clear that $\sum_{\ell=1,\ell\neq i}^{L} \sigma^2_{h_{i,r}} > \sum_{\ell=2}^{L} \sigma^2_{h_{\ell-1,r}}$. Similarly, it can be shown that $\sum_{\ell=1,\ell\neq i}^{L} \sigma^2_{h_{i,r}} > \sum_{\ell=2}^{L} \sigma^2_{h_{L-\ell+2,r}}$. Thus the proposed pairing scheme will have a larger average sum rate (given by (4.22)), compared to that of the pairing schemes in [28] and [50] (given by (4.23) and (4.24), respectively). This proves Proposition 4.6.

B.3 Proof of Lemma 4.1

We assume $\sqrt{M}$-PAM signals at the k^{th} and the $(k \pm 1)^{th}$ users, such that the users' signals can take values from the set $\mathcal{S} = \{\pm 1, \pm 3, ..., \pm(\sqrt{M}-1)\}$ and we denote each element of the set $\mathcal{S}$ as s. The true network coded signal resulting from the sum of the $\sqrt{M}$-PAM signals have a constellation with $(2\sqrt{M}-1)$ points, which takes values from the set $\mathcal{S}_{NC} = \{0, \pm 2, ..., \pm(2\sqrt{M}-2)\}$.

In a noiseless environment, the relay maps the network coded signal to a $\sqrt{M}$-PAM signal s in such a way that the same network coded signal is not mapped to different elements of $\mathcal{S}$ (i.e., there is no ambiguity). This can be ensured by mapping the network coded signal into modulo-$\sqrt{M}$ sum of the actual symbols at the k^{th} and the $(k \pm 1)^{th}$ user. In a noisy environment, the relay maps the network coded signal into $\hat{s}$ and broadcasts to the users, who decode the signal as $\hat{\hat{s}}$. The end-to-end probability of incorrectly detecting a network-coded signal resulting from $\sqrt{M}$-PAM signals, can be obtained from the sum of the off-diagonal elements of the product of two $\sqrt{M} \times \sqrt{M}$ matrices C and D, with elements $c_{p,q} = P(\hat{s} = q | s = p)$ and $d_{p',q'} = P(\hat{\hat{s}} = q' | \hat{s} = p')$, respectively, where $p, q, p', q' \in [0, \sqrt{M}-1]$, multiplied by the factor $\sqrt{M}$. That is,

$$P_{\sqrt{M}-PAM,NC}(k, k \pm 1) = \frac{1}{\sqrt{M}} \left(\sum_{p,q=0}^{\sqrt{M}-1} c_{p,q} \sum_{p',q'=0, p' \neq p, q' \neq q}^{\sqrt{M}-1} d_{p',q'} \right). \tag{B.3}$$

The coefficients $c_{p,q}$ can be expressed as

$$c_{p,q} = \begin{cases} \sum_{u=1, u=\text{odd}}^{2(2\sqrt{M}-2)-1} a_{p,q,u} Q(u\sqrt{\gamma_r(i,m)}), & p \neq q \\ \\ 1 + \sum_{u=1, u=\text{odd}}^{2(2\sqrt{M}-2)-1} a_{p,q,u} Q(u\sqrt{\gamma_r(i,m)}), & p = q \end{cases} \tag{B.4}$$

and the coefficients $d_{p',q'}$ can be expressed as

$$d_{p',q'} = \begin{cases} \sum_{v=1,v=\text{odd}}^{2(\sqrt{M}-1)-1} b_{p',q',v} Q(v\sqrt{\gamma_i}), & p' \neq q' \\ \\ 1 + \sum_{v=1,v=\text{odd}}^{2(\sqrt{M}-1)-1} b_{p',q',v} Q(v\sqrt{\gamma_i}), & p' = q' \end{cases} \tag{B.5}$$

where

$$\gamma_r(i,m) = \frac{P \min(\mid h_{i,r} \mid^2, \mid h_{m,r} \mid^2)}{E_{av} N_0}, \tag{B.6}$$

and $\gamma_i = \frac{P_r |h_{r,i}|^2}{E_{av} N_0}$.

The coefficients $a_{p,q,u}$ and $b_{p',q',v}$ for $M = 16$ (or $\sqrt{M} = 4$), have been tabulated in Table 4.1. For example, when $p = p' = q = q' = 0$, in case of 16-QAM modulation, using Table 4.1, the coefficients $c_{0,0}$ and $d_{0,0}$ can be expressed as follows:

$$\begin{aligned} c_{0,0} &= 1 - \frac{7}{4} Q(\sqrt{\gamma_r(i,m)}) + Q(7\sqrt{\gamma_r(i,m)}) - \frac{1}{4} Q(9\sqrt{\gamma_r(i,m)}), \\ d_{0,0} &= 1 + \frac{1}{4} Q(\sqrt{\gamma_i}). \end{aligned} \tag{B.7}$$

B.4 Proof of Theorem 4.4

The proof follows the steps outlined in Section 5.4.2, which are applicable to any user pairing scheme. However, for the proposed pairing scheme, we need to modify these steps to take into account different error probabilities at the common user and the other users. The modified steps can be summarized as follows:

1. Determine the probabilities that the i^{th} user and the ℓ^{th} user incorrectly decode a network coded message, respectively.

2. Express the probability of the k^{th} error event at the i^{th} and the ℓ^{th} user in terms of the probabilities of incorrectly decoding a network coded message.

3. Obtain the expected probability of all the error events to determine the exact av-

erage SER expression.

4. Apply the high SNR approximation to obtain approximate but accurate average SER expressions.

Now, we illustrate these steps in detail:

Step-1: The probabilities of incorrectly decoding a network coded message at the i^{th} and the ℓ^{th} user are obtained in (4.27) and (4.32), respectively.

Step-2: In the proposed pairing scheme, k error events can occur in two cases

- A_k: If the decoding user incorrectly extracts exactly k users' messages except the i^{th} user's message. That is, the decoding user (j^{th} user, where $j \in [1, L]$) incorrectly decodes k network coded messages $V_{i,m_1}, V_{i,m_2}, ..., V_{i,m_k}$ and correctly decodes the remaining $L-1-k$ network coded messages, where $m_1, m_2, ..., m_k \in [1, L], m_1 \neq m_2 \neq ... \neq m_k \neq j$.

- B_k: If the decoding user incorrectly decodes exactly k users' messages including the i^{th} user's message. This happens when the decoding user (ℓ^{th} user, where $\ell \in [1, L], \ell \neq i$) incorrectly decodes $V_{i,\ell}$ and correctly decodes $k-1$ other network coded messages, $V_{i,m_1}, V_{i,m_2}, ..., V_{i,m_{k-1}}$ and incorrectly decodes the remaining $L - 1 - k$ messages, where $m_1, m_2, ..., m_{k-1} \in [1, L], m_1 \neq m_2 \neq ... \neq m_{k-1} \neq i, \ell$.

Note that, the error case A_k is applicable both for the common user and the other users. However, case B_k is applicable only for users except the common user.

The probabilities of the aforementioned error cases for the i^{th} and the ℓ^{th} users are

$$P_{i,A_k} = \sum_{m_a=1, m_a \neq i}^{L} \prod_{a=1}^{k} P_{FDF}(i, m_a) \prod_{m_b=1, m_b \neq m_a, i}^{L} \{1 - P_{FDF}(i, m_b)\}. \tag{B.8}$$

$$P_{\ell,A_k} = \sum_{m_a=1, m_a \neq i, \ell}^{L} \prod_{a=1}^{k} P_{FDF}(\ell, m_a) \prod_{m_b=1, m_b \neq \ell, m_a}^{L} \{1 - P_{FDF}(\ell, m_b)\}. \tag{B.9}$$

$$P_{\ell,B_k} = \begin{cases} P_{FDF}(\ell,i)\sum_{m_a=1,m_a\neq i,\ell}^{L}\prod_{a=1}^{k-1}\{1-P_{FDF}(\ell,m_a)\}\prod_{m_b=1,m_b\neq i,\ell,m_a}^{L} \\ \times P_{FDF}(\ell,m_b) & 1<k<L-1 \\ P_{FDF}(\ell,i)\prod_{m_b=1,m_b\neq i,\ell}^{L}\{1-P_{FDF}(\ell,m_b)\} & k=1 \\ P_{FDF}(\ell,i)\sum_{m_a=1,m_a\neq i,\ell}^{L}\prod_{a=1}^{L-1}\{1-P_{FDF}(\ell,m_a)\} & k=L-1. \end{cases} \tag{B.10}$$

The probability of k error events for the i^{th} and the ℓ^{th} user can be expressed as

$$P(i,k) = P_{i,A_k}, P(\ell,k) = P_{\ell,A_k} + P_{\ell,B_k}. \tag{B.11}$$

<u>*Step-3*</u>: Since, each user decodes $L-1$ other users' messages in an L-user MWRN, there are $L-1$ possible error events. Thus, averaging over all the possible error events, the average SER at the i^{th} and the ℓ^{th} user can be obtained as:

$$P_{i,avg} = \frac{1}{L-1}\sum_{k=1}^{L-1} kP_{i,A_k}, P_{j,avg} = \frac{1}{L-1}\sum_{k=1}^{L-1} k(P_{\ell,A_k} + P_{\ell,B_k}) \tag{B.12}$$

<u>*Step-4*</u>: At high SNR, the higher order error terms in (B.11) can be neglected. Thus, $P_{i,A_k} \approx 0$ and $P_{\ell,A_k} \approx 0$ for $k > 1$ (see (B.8) and (B.9)). Similarly, $P_{\ell,B_k} \approx 0$ for $k < L-1$ (see (B.10)). Thus, at high SNR, (B.12) can be approximated as

$$\begin{aligned} P_{i,avg} &= \frac{1}{L-1} P_{i,A_1}, \\ P_{\ell,avg} &= \frac{1}{L-1}\left(P_{\ell,A_1} + (L-1)P_{\ell,B_{L-1}}\right). \end{aligned} \tag{B.13}$$

In addition, at high SNR, we can approximate the terms $\{1 - P_{FDF}(i,m_b)\}$, $\{1 - P_{FDF}(\ell,m_b)\}$ and $\{1 - P_{FDF}(\ell,m_a)\}$ in (B.8), (B.9) and (B.10) to be 1. Thus, substituting (B.8), (B.9) and (B.10) in (B.13), the average SER at the i^{th} and the ℓ^{th} user at high SNR can be expressed as

$$P_{i,avg} = \frac{1}{L-1} \sum_{m_1=1, m_1 \neq i}^{L} P_{FDF}(i, m_1),$$
$$P_{\ell,avg} = \frac{1}{L-1} \left(\sum_{m_1=1, m_1 \neq i,\ell}^{L} P_{FDF}(\ell, m_1) + (L-1) P_{FDF}(\ell, i) \right). \quad \text{(B.14)}$$

Finally, replacing m_1 with m in the above equation completes the proof.

B.5 Proof of Propositions 4.7–4.9

Proof of Proposition 4.7: For the equal average channel gain scenario, the error probabilities $P_{FDF}(j,1) = P_{FDF}(j,2) = ... = P_{FDF}(j, L-1) = P_{FDF}$ for all $j \in [1, L]$. Thus, the average SER expressions in (4.33) and (4.34) for the proposed pairing scheme can be simplified as:

$$P_{i,avg} = P_{FDF},$$
$$P_{\ell,avg} = \left(\frac{2L-3}{L-1} \right) P_{FDF}. \quad \text{(B.15)}$$

The average SER for the scheme in [28] can be given from Chapter 3 as:

$$P_{avg} = \frac{L}{2} P_{FDF}. \quad \text{(B.16)}$$

Comparing (B.15) and (B.16), we arrive at Proposition 4.7.

Proof of Proposition 4.8: For the unequal average channel gain scenario, the average SER expressions for the proposed pairing scheme is given by (4.33) and (4.34), with $\gamma_r(i,m) = \frac{(2L-2)P \min\left(\frac{|h_{i,r}|^2}{L-1}, |h_{m,r}|^2\right)}{E_{av} N_0}$ and $\gamma_i = \frac{(2L-2)P_r |h_{i,r}|^2}{E_{av} N_0}$ where E_{av} is the average energy of symbols for $\sqrt{M}$-PAM modulation (e.g., $E_{av} = 5$ for $M = 16$). For the scheme in [28], the average SER at the $j^{th}(j \in [1, L])$ user can be written as

$$P_{j,avg} = \frac{1}{L-1} \sum_{m=1}^{L-1} m P_{FDF}(j, m), \quad \text{(B.17)}$$

where

$$P_{FDF}(j,m) = 1 - (1 - P_{\sqrt{M}-PAM,NC}(j,m))^2, \tag{B.18}$$

with $\gamma_r(m) = \frac{P\min(|h_{m,r}|^2,|h_{m+1,r}|^2)}{E_{av}N_0}$ and $\gamma_j = \frac{P_r|h_{j,r}|^2}{E_{av}N_0}$ in (4.29) and (4.31), respectively. Now we consider two cases:

- *case 1*: $E[\frac{|h_{i,r}|^2}{L-1}] > E[\mid h_{m,r} \mid^2]$. In this case,

$$\begin{aligned}
&E\left[\min\left(\frac{(2L-2)P \mid h_{i,r} \mid^2}{E_{av}(L-1)N_0}, \frac{(2L-2)P \mid h_{m,r} \mid^2}{E_{av}N_0}\right)\right] \\
&\le \min\left(E\left[\frac{(2L-2)P \mid h_{i,r} \mid^2}{E_{av}(L-1)N_0}\right], E\left[\frac{(2L-2)P \mid h_{m,r} \mid^2}{E_{av}N_0}\right]\right) \\
&= E\left[\frac{(2L-2)P \mid h_{m,r} \mid^2}{E_{av}N_0}\right] \\
&\ge \min\left(E\left[\frac{P \mid h_{m,r} \mid^2}{E_{av}N_0}\right], E\left[\frac{P \mid h_{m+1,r} \mid^2}{E_{av}N_0}\right]\right) \\
&\ge E\left[\min\left(\frac{P \mid h_{m,r} \mid^2}{E_{av}N_0}, \frac{P \mid h_{m+1,r} \mid^2}{E_{av}N_0}\right)\right].
\end{aligned} \tag{B.19}$$

  Thus, $E[\gamma_r(i,m)] \ge E[\gamma_r(m)]$.

- *case 2*: $E[\frac{|h_{i,r}|^2}{L-1}] < E[\mid h_{m,r} \mid^2]$. In this case, $E\left[\min\left(\frac{(2L-2)P|h_{i,r}|^2}{E_{av}(L-1)N_0}, \frac{(2L-2)P|h_{m,r}|^2}{E_{av}N_0}\right)\right] \le E[\frac{(2L-2)P|h_{i,r}|^2}{E_{av}(L-1)N_0}]$ and since, $\mid h_{i,r} \mid^2 > \mid h_{m,r} \mid^2, \mid h_{m+1,r} \mid^2$, $E\left[\min\left(\frac{|h_{m,r}|^2}{E_{av}N_0}, \frac{|h_{m+1,r}|^2}{E_{av}N_0}\right)\right] \le E\left[\frac{(2L-2)P|h_{i,r}|^2}{E_{av}(L-1)N_0}\right]$. Thus, $E[\gamma_r(i,m)] \ge E[\gamma_r(m)]$.

From the above cases, the probability $P_{FDF}(i,m)$ and $P_{FDF}(\ell,m)$ for the proposed scheme would be larger than $P_{FDF}(j,m)$ for scheme [28]. Thus, comparing (4.33), (4.34) and (B.17) shows that the average SER for the proposed scheme would be smaller than that for scheme [28]. This proves Proposition 4.8.

Proof of Proposition 4.9: For the variable average channel gain scenario, the average SER expression for the proposed pairing scheme is given by (4.33) and (4.34). The average SER for the pairing scheme in [28] is the same as in (B.17). Now, comparing $P_{FDF}(i,m)$ (from (4.27)), $P_{FDF}(\ell,m)$ (from (4.32)) and $P_{FDF}(j,m)$ (from (B.18)) shows that the only terms which are different in all these probabilities are $\gamma_r(i,m)$ and $\gamma_r(m)$. Note that, if $E[| h_{i,r} |^2] > E[| h_{m+1,r} |^2]$, then $E[\min(| h_{i,r} |^2, | h_{m,r} |^2)] \geq E[\min(| h_{m+1,r} |^2, | h_{m,r} |^2)]$. Thus, $E[\gamma_r(i,m)] \geq E[\gamma_r(m)]$ and in effect, from (4.27), (4.32) and (B.18), the error probability for the new pairing scheme would be less than that for scheme [28]. As a result, the average SER for the proposed scheme is less than that of scheme [28] (in (B.17)) for both $j = i$ and $j = \ell$, which proves Proposition 4.9.

Appendix C

This appendix contains the proof of the lemmas presented in Chapter 5. The appendix is organized as follows. In Section C.1, the Lemma 5.2 on page 111 is proved.

C.1 Proof of Lemma 5.2

First, we need to investigate different error cases for the k^{th} error event in a FDF MWRN as in Chapter 3. For $k = 1$, the possible error cases are

- when two consecutive erroneous network coded messages occur or,
- when an error in the network coded messages involving one of the end users occurs.

For larger values of k, there will be many more error cases and considering all the possible error cases would make the analysis complicated. For a tractable analysis, we consider only the dominating error cases that influence the k^{th} error event at high SNR. That is, we consider the higher order error terms (e.g., P_{FDF}^2) and the corresponding error cases negligible.

At high SNR, the dominating case for the k^{th} error event occurs when the network coded message involving the k^{th} and the $(k+1)^{\text{th}}$ (or $(L-k+1)^{\text{th}}$ and $(L-k)^{\text{th}}$) users is incorrectly decoded, resulting in error about k users' messages. For example, if $k = 2$, 2 error events result from an error in the network coded message $V_{2,3}$ or $V_{L-2,L-1}$. Thus, the dominating error cases for the k^{th} error event can be expressed as:

$$P_D = P_{FDF}(i,k) \prod_{m=1, m\neq k}^{L-1} (1 - P_{FDF}(i,m)), \tag{C.1a}$$

$$P_{D'} = P_{FDF}(i, L-k) \prod_{m=1, m\neq L-k}^{L-1} (1 - P_{FDF}(i,m)). \tag{C.1b}$$

Here, the subscripts D and D' indicate the case of k consecutive errors involving the first user and the $k-1$ following users and the case of k consecutive errors involving the last user and the $k-1$ preceding users, respectively. At high SNR, the terms $\prod_{m=1,m\neq k}^{L-1}(1 - P_{FDF}(i,m))$ in (C.1a) and $\prod_{m=1,m\neq L-k}^{L-1}(1 - P_{FDF}(i,m))$ in (C.1b) can be approximated to 1. Thus, (C.1) can be rewritten as:

$$P_D = P_{FDF}(i,k), \tag{C.2a}$$

$$P_{D'} = P_{FDF}(i, L-k). \tag{C.2b}$$

Now for $i = 1, 2, L-1, L$, there is only one possible user combination in which the messages of the first user and the $k-1$ following users (or the last user and the $k-1$ preceding users) can be incorrectly decoded. Thus the expression for the probability of the k^{th} error event can be given by:

$$P_i(k) = \begin{cases} P_{D'} & i = 1, 2 \\ P_D & i = L, L-1 \\ P_D + P_{D'} & i \notin \{1, 2, L-1, L\}. \end{cases} \tag{C.3}$$

Then substituting (C.2) in (5.26) completes the proof.

Appendix D

This appendix contains the proof of the lemmas and theorems needed in Chapter 6. The appendix is organized as follows. In Section D.1, the Lemma 6.1 on page 128 is proved. In Section D.2, the Lemma 6.3 on page 129 is proved. Section D.3 contains the proof of Theorem 6.4 on page 132. Finally, Section D.4 contains the proof of Theorem 6.5 on page 133.

D.1 Proof of Lemma 6.1

First, we obtain the SNR expression in (6.19) for the k^{th} user's signal at the i^{th} user. For $k = i \pm 1$, where $i \pm 1$ indicates the user whose message is decoded in the downward and in the upward extraction processes, respectively, the received signal can be written from (5.23) and (5.24) as:

$$\hat{X}^t_{i\pm1} = Y^t_{i,i\pm1} - \alpha\sqrt{P}\hat{h}_{i,i}X^t_i = \alpha\hat{h}_{r,i}\hat{h}_{i\pm1,r}\sqrt{P}X^t_{i\pm1} + n_{i\pm1}, \tag{D.1}$$

where $n_{i\pm1}$ denotes the noise terms, given as:

$$n_{i\pm1} = \alpha\sqrt{P}\tilde{h}_{i,i}X^t_i + \alpha\sqrt{P}\tilde{h}_{i,i\pm1}\tilde{h}_{i,r}X^t_{i\pm1} + \alpha\sqrt{P}\hat{h}_{r,i}n_1 + \alpha\sqrt{P}\tilde{h}_{r,i}n_1 + n_2. \tag{D.2}$$

Remark D.1. *Note that the first term indicates self-interference that cannot be completely cancelled out due to imperfect channel estimation, the second term is a component of the desired signal that is lost due to channel estimation error and the last three terms indicate complex*

AWGN noises.

From (D.1), the SNR of the $(i \pm 1)^{th}$ user's signal, when received at the i^{th} user, is given by:

$$\gamma_{i\pm1} = \frac{\alpha_d^2 P \sigma_{\hat{h}_{r,i}}^2 \sigma_{\hat{h}_{i\pm1,r}}^2}{N_{i\pm1}}. \tag{D.3}$$

Here, $N_{i\pm1}$ represents the variance of the noise terms present in $n_{i\pm1}$ (see (D.2)) and is expressed as:

$$N_{i\pm1} = \alpha^2 P \sigma_{\tilde{h}_{i,i}}^2 + \alpha^2 P \sigma_{\tilde{h}_{i,i\pm1}}^2 + \alpha^2 P \sigma_{\hat{h}_{r,i}}^2 \sigma_n^2 + \alpha^2 P \sigma_{\tilde{h}_{r,i}}^2 N_0 + N_0, \tag{D.4}$$

where, $\mid \hat{h}_{a,b} \mid^2$ represents the variance of the channel estimate $\hat{h}_{a,b}$ and $\sigma_{\tilde{h}_{a,b}}^2$ represents the variance of the estimation error $\tilde{h}_{a,b}$, $a, b \in \{r, i, i \pm 1\}$.

After substituting the value of $\alpha = \sqrt{\frac{P_r}{P\sigma_{\hat{h}_{i,r}}^2 + P\sigma_{\hat{h}_{i\pm1,r}}^2 + N_0}}$ from (5.10), the expression of the SNR in (D.3) can be given as

$$\gamma_{i\pm1} = \frac{P_r P_d \sigma_{\hat{h}_{r,i}}^2 \sigma_{\hat{h}_{i\pm1,r}}^2}{N'_{i\pm1}}, \tag{D.5}$$

where,

$$N'_{i\pm1} = P_r P \sigma_{\tilde{h}_{i,i}}^2 + P_r P \sigma_{\tilde{h}_{i,i\pm1}}^2 + (P + P_r)\sigma_{\hat{h}_{r,i}}^2 N_0 + P\sigma_{\hat{h}_{i\pm1,r}}^2 N_0. \tag{D.6}$$

For $k \neq i, i \pm 1$, from (5.23) and from (5.24), the signal of the k^{th} user can be written as:

$$\hat{X}_k^t = Y_{k\pm1,k}^t - \alpha\sqrt{P}\hat{h}_{i,k\pm1}\hat{X}_{k\pm1}^t = \alpha\sqrt{P}\hat{h}_{i,k}X_k^t + n_k, \tag{D.7}$$

where, $k \pm 1$ denotes the user whose signal is detected before (or after) the k^{th} user in the downward (or upward) extraction process and n_k denotes the noise terms present at the extracted signal of the k^{th} user's signal and is given as:

$$n_k = \alpha\sqrt{P}\tilde{h}_{i,k\pm1}X_{k\pm1}^t + \alpha\sqrt{P}\tilde{h}_{i,k}X_k^t + \alpha\hat{h}_{r,i}n_1 + \alpha\tilde{h}_{r,i}n_1 + n_2. \tag{D.8}$$

If $\hat{\mathbf{X}}_{k\pm1} = \mathbf{X}_{k\pm1}$ (i.e., no error propagation), the SNR of the k^{th} user's signal can be obtained from (D.7) as:

$$\gamma_{i,k} = \frac{P_r P \sigma^2_{h_{r,i}} \sigma^2_{h_{k,r}}}{N_k}, \tag{D.9}$$

where, $N_k = P_r P \sigma^2_{\tilde{h}_{i,k}} + P_r P \sigma^2_{\tilde{h}_{i,k\pm1}} + P_r \sigma^2_{h_{r,i}} N_0 + P \sigma^2_{h_{k,r}} N_0 + P \sigma^2_{h_{k\pm1,r}} N_0$.

The exact probability density function (pdf) of the noise $n_{i\pm1}$ in (D.2) and n_k in (D.8) is not Gaussian due to the presence of product terms of two Gaussian variables (i.e., the first two terms in (D.2) and the first two terms in (D.8)). However, the pdf of the noise can be numerically shown to match closely to that of a Gaussian distribution at high transmit SNR [34]. Thus, the probability of incorrectly decoding the k^{th} user's message, given that the $(k \pm 1)^{th}$ user's message is correctly decoded, can be obtained from (6.18) under Gaussian noise approximation.

D.2 Proof of Lemma 6.3

First, we need to investigate different error cases for the k^{th} error event in an AF MWRN. For $k = 1$, the possible error cases are illustrated in Chapter 3 as

- when a middle user's message is wrongly estimated with correct decision about the following user
- when an error occurs in the estimated signal of one of the end users.

For larger values of k, there will be many more error cases and considering all the possible error cases would make the analysis complicated. For a tractable analysis, we consider only the dominating error cases that influence the k^{th} error event at high SNR. That is, we consider the higher order error terms (e.g., P'^2_{AF} and P^2_{AF}) and the corresponding error cases negligible.

At high SNR, the dominating cases for the k^{th} error event are either k consecutive errors in the middle users or k consecutive errors involving one end user and $k-1$ following (or preceding) users. For example, if $k = 2, i = 5, L = 10$, the error cases would be either 2 consecutive errors in the middle users (i.e., the 5^{th} user incorrectly decodes any one of the message pairs (W_2, W_3), (W_3, W_4), (W_6, W_7), (W_7, W_8), (W_8, W_9)) or 2 consecutive errors involving the end user and the following (preceding) user (i.e., either (W_1, W_2) or (W_9, W_{10})). The probability of the above error cases is expressed as in:

$$P_C(p) = \prod_{t=1}^{k-1} P'_{AF}(i, p+t) P_{AF}(i, p) \prod_{m=1, m\neq i, p, p+t, p+k}^{L-1} (1 - P'_{AF}(i, p+k))(1 - P_{AF}(i, m)), \tag{D.10a}$$

$$P_{C'}(p) = \prod_{t=1}^{k-1} P'_{AF}(i, p-t) P_{AF}(i, p) \prod_{m=1, m\neq i, p, p-t, p-k}^{L-1} (1 - P'_{AF}(i, p-k))(1 - P_{AF}(i, m)), \tag{D.10b}$$

$$P_D = \prod_{t=1}^{k-2} P'_{AF}(i, 1) P'_{AF}(i, 1+t) P_{AF}(i, k) \prod_{m=1, m\neq i, t+1, k}^{L-1} (1 - P_{AF}(i, m)), \tag{D.10c}$$

$$P_{D'} = \prod_{t=1}^{k-2} P'_{AF}(i, L) P'_{AF}(i, L-t) P_{AF}(i, L-k+1) \prod_{m=1, m\neq i, L-t, L-k+1}^{L-1} (1 - P_{AF}(i, m)), \tag{D.10d}$$

where, the term C (C') represents k errors involving the middle users for the downward (upward) extraction process and D (D') represents k errors involving the end user for $i \neq 1, 2$ ($i \neq L, L-1$). At high SNR, the terms $\prod_{m=1, m\neq i, p, p+t, p+k}^{L-1} (1 - P'_{AF}(i, p+k))(1 - P_{AF}(i, m))$, $\prod_{m=1, m\neq i, p, p-t, p-k}^{L-1} (1 - P'_{AF}(i, p-k))(1 - P_{AF}(i, m))$, $\prod_{m=1, m\neq i, t+1, k}^{L-1} (1 - P_{AF}(i, m))$ and $\prod_{m=1, m\neq i, L-t, L-k+1}^{L-1} (1 - P_{AF}(i, m))$ in (D.10a), (D.10b), (D.10c) and (D.10d), respectively, can be considered as 1.

Thus, the exact expressions can be simplified to

$$P_C(p) = \prod_{t=1}^{k-1} P'_{AF}(i, p+t) P_{AF}(i, p), \tag{D.11a}$$

$$P_{C'}(p) = \prod_{t=1}^{k-1} P'_{AF}(i, p-t) P_{AF}(i, p), \tag{D.11b}$$

$$P_D = \prod_{t=1}^{k-2} P'_{AF}(i, 1) P'_{AF}(i, 1+t) P_{AF}(i, k), \tag{D.11c}$$

$$P_{D'} = \prod_{t=1}^{k-2} P'_{AF}(i, L) P'_{AF}(i, L-t) P_{AF}(i, L-k+1). \tag{D.11d}$$

Now, there are $L-k-1$ number of user combinations, where exactly k number of middle users' messages are incorrectly decoded and one combination, where k errors occur involving the end user. Then, adding the expressions (D.11a) and (D.11d) or (D.11b) and (D.11c) for the possible user combinations would give the probability of exactly k error events.

D.3 Proof of Theorem 6.4

First, we consider the $k \neq (i \pm 1)^{th}$ time slot. The objective function then becomes, $f_k = f_{p,k} + f_{d,k}$, where, $f_{p,k} = \sigma^2_{\tilde{h}_{i,k}} + \sigma^2_{\tilde{h}_{i,k\pm1}}$ and $f_{d,k} = \frac{\sigma^2_{h_{r,i}} N_0}{P} + \frac{\sigma^2_{h_{k,r}} N_0}{P_r} + \frac{\sigma^2_{h_{k\pm1,r}} N_0}{P_r}$ represent the functions involving the pilot signal power and the data signal power, respectively. Using (6.30), we can write $f_{p,k}$ and $f_{d,k}$ in terms of the power allocation coefficients, as:

$$\begin{aligned} f_{p,k} = & \frac{1}{\frac{(2T+4)P_t\beta_2(k)\beta_1(k)(1-\beta_2(k))}{2((1-\beta_2(k))\sigma^2_{h_{r,i}}+\beta_2(k)\sigma^2_{h_{k,r}})N_0} + \frac{1}{\sigma^2_{h_{k,r}}\sigma^2_{h_{r,i}}}} \\ & + \frac{1}{\frac{(2T+4)P_t\beta_2(k)\beta_1(k)(1-\beta_2(k))}{2((1-\beta_2(k))\sigma^2_{h_{r,i}}+\beta_2(k)\sigma^2_{h_{k\pm1,r}})N_0} + \frac{1}{\sigma^2_{h_{k\pm1,r}}\sigma^2_{h_{r,i}}}}, \end{aligned} \tag{D.12}$$

and

$$f_{d,k} = \left(\frac{2\sigma^2_{h_{r,i}}}{\beta_3(k)} + \frac{\sigma^2_{h_{k,r}} + \sigma^2_{h_{k\pm1,r}}}{(1-\beta_3(k))} \right) \frac{TN_0}{(1-\beta_1(k))(2T+4)P_t}. \tag{D.13}$$

Now, setting $\frac{df_{d,k}}{d\beta_3(k)} = 0$ yields

$$\beta_3^2(k)(\sigma^2_{h_{r,i}} - \frac{\sigma^2_{h_{k,r}} + \sigma^2_{h_{k\pm1,r}}}{2}) - 2\beta_3(k)\sigma^2_{h_{r,i}} + \sigma^2_{h_{r,i}} = 0.$$

Solving the above equation leads to the optimum value of $\beta_3(k)$ as in (6.31). Similarly, setting $\frac{df_k}{d\beta_2(k)} = 0$, gives $\beta_2(k) = \beta_3(k)$, which completes the proof. For $k = (i \pm 1)^{th}$ time slot, the proof can be completed with $\sigma^2_{h_{k,r}}$ replaced by $\sigma^2_{h_{i,r}}$ in the above equations.

D.4 Proof of Theorem 6.5

If we set $\beta_2(k) = \beta_3(k) = \beta(k)$ and $\frac{(2T+4)}{2}P_t = P'$, $P_s^{\mathrm{p}}, P_r^{\mathrm{p}}, P$ and P_r can be substituted by $\beta_1(k)\beta(k)P'$, $(1-\beta(k))\beta_1(k)P'$, $\beta(k)(1-\beta_1(k))P'/T$ and $2(1-\beta(k))(1-\beta_1(k))P'/T$, respectively. Then (6.29) can be written as:

$$\begin{aligned} f = & \frac{1}{\frac{\beta(k)\beta_1(k)(1-\beta(k))P'}{((1-\beta(k))\sigma^2_{h_{r,i}}+\beta(k)\sigma^2_{h_{k,r}})N_0} + \frac{1}{\sigma^2_{h_{r,i}}\sigma^2_{h_{k,r}}}} + \\ & \frac{1}{\frac{\beta(k)\beta_1(k)(1-\beta(k))P'}{((1-\beta(k))\sigma^2_{h_{r,i}}+\beta(k)\sigma^2_{h_{k\pm1,r}})N_0} + \frac{1}{\sigma^2_{h_{r,i}}\sigma^2_{h_{k\pm1,r}}}} + \\ & \left(\frac{\sigma^2_{h_{r,i}}}{\beta(k)} + \frac{\sigma^2_{h_{k,r}} + \sigma^2_{h_{k\pm1,r}}}{2(1-\beta(k))}\right)\frac{N_0 T}{(1-\beta_1(k))P'}. \end{aligned} \tag{D.14}$$

Now, setting $\frac{df_{d,k}}{d\beta_1(k)} = 0$ leads to the optimum $\beta_1(k)$. However, the exact solution of this equation would be very complicated. To simplify the analysis, we set $\sigma^2_{h_{k,r}} = \sigma^2_{h_{k\pm1,r}} = \frac{\sigma^2_{h_{k,r}}+\sigma^2_{h_{k\pm1,r}}}{2} = \sigma^2_{h_{avg}}$, which can quantify the average impact of the transmitting users' channel conditions on the optimum solution of $\beta_1(k)$. Thus, (D.14) can be simplified to

$$f = \frac{2}{\frac{\beta_1(k)\beta(k)(1-\beta(k))P'}{A_1} + A_2} + \frac{A_1 T}{(1-\beta_1(k))\beta(k)(1-\beta(k))P'}, \tag{D.15}$$

where $A_1 = ((1-\beta(k))\sigma^2_{h_{r,i}} + \beta(k)\sigma^2_{h_{avg}})N_0$ and $A_2 = \frac{1}{\sigma^2_{h_{r,i}}\sigma^2_{h_{avg}}}$. Now, using (D.15) and setting $\frac{df}{d\beta_1(k)} = 0$ leads to a quadratic equation, the root of which gives the optimal $\beta_1(k)$ in (6.32), such that $\beta_1(k) < 1$. Thus, the proof is completed.

References

1. M. Dohler and Y. Li, *Cooperative Communications: Hardware, Channel & PHY*. Wiley, 2010.

2. Y.-W. Hong, W.-J. Huang, F.-H. Chiu, and C.-C. Kuo, "Cooperative communications in resource-constrained wireless networks," *IEEE Signal Process. Mag.*, vol. 24, no. 3, pp. 47–57, May 2007.

3. J. N. Laneman, D. N. C. Tse, and G. W. Wornell, "Cooperative diversity in wireless networks: Efficient protocols and outage behavior," *IEEE Trans. Inf. Theory*, vol. 50, no. 12, pp. 3062–3080, Dec. 2004.

4. R. Pabst, B. H. Walke, D. Schultz, P. Herhold, H. Yanikomeroglu, S. Mukherjee, H. Viswanathan, M. Lott, W. Zirwas, M. Dohler, H. Aghvami, D. Falconer, and G. Fettweis, "Relay-based deployment concepts for wireless and mobile broadband radio," *IEEE Commun. Mag.*, vol. 42, no. 9, pp. 80–89, Sep. 2004.

5. H.-C. Lu, W. Liao, and F.-S. Lin, "Relay station placement strategy in IEEE 802.16j wimax networks," *IEEE Trans. Commun.*, vol. 59, no. 1, pp. 151–158, Jan. 2011.

6. E. C. V. D. Meulen, "Three-terminal communication channels," *Advances in Applied Probability*, vol. 3, no. 1, pp. 120–154, 1971.

7. M. Hasna and M.-S. Alouini, "End-to-end performance of transmission systems with relays over Rayleigh-fading channels," *IEEE Trans. Wireless Commun.*, vol. 2, no. 6, pp. 1126–1131, Nov 2003.

8. M. Hasna and M.-S. Alouini, "Optimal power allocation for relayed transmissions over Rayleigh-fading channels," *IEEE Trans. Wireless Commun.*, vol. 3, no. 6, pp. 1999–2004, Nov. 2004.

9. J. Boyer, D. Falconer, and H. Yanikomeroglu, "Multihop diversity in wireless relaying channels," *IEEE Trans. Commun.*, vol. 52, no. 10, pp. 1820–1830, Oct. 2004.

10. O. Oyman, J. Laneman, and S. Sandhu, "Multihop relaying for broadband wireless mesh networks: From theory to practice," *IEEE Commun. Mag.*, vol. 45, no. 11, pp. 116–122, Nov. 2007.

11. Y. Zhao, R. Adve, and T. J. Lim, "Symbol error rate of selection amplify-and-forward relay systems," *IEEE Commun. Lett.*, vol. 10, no. 11, pp. 757–759, Nov. 2006.

12. J. Laneman and G. Wornell, "Energy-efficient antenna sharing and relaying for wireless networks," in *Proc. IEEE WCNC*, vol. 1, Oct. 2000, pp. 7–12.

13. W. Su, A. Sadek, and K. Ray Liu, "Cooperative communication protocols in wireless networks: Performance analysis and optimum power allocation," *Wireless Personal Communications*, vol. 44, pp. 181–217, Aug. 2008.

14. A. Nosratinia, T. Hunter, and A. Hedayat, "Cooperative communication in wireless networks," *IEEE Commun. Mag.*, vol. 42, no. 10, pp. 74–80, Oct. 2004.

15. S. Zhang, S. C. Liew, and P. P. Lam, "Hot topic: physical-layer network coding," in *Proc. ACM MOBICOM*, Sep. 2006, pp. 358–365.

16. S. Katti, S. Gollakota, and D. Katabi, "Embracing wireless interference: Analog network coding," in *Proc. ACM SIGCOMM*, Aug. 2007, pp. 397–408.

17. B. Rankov and A. Wittneben, "Spectral efficient signaling for half-duplex relay channels," in *Proc. Asilomar Conference on Signals, Systems and Computers*, Nov. 2005, pp. 1066–1071.

18. P. Larsson, N. Johansson, and K.-E. Sunell, "Coded bi-directional relaying," in *Proc. IEEE VTC(Spring)*, vol. 2, May 2006, pp. 851–855.

19. Z. Chen, T. J. Lim, and M. Motani, "Digital network coding aided two-way relaying: Energy minimization and queue analysis," *IEEE Trans. Wireless Commun.*, vol. 12, no. 4, pp. 1947–1957, Apr. 2013.

20. S. L. H. Nguyen, A. Ghrayeb, G. Al-Habian, and M. Hasna, "Mitigating error propagation in two-way relay channels with network coding," *IEEE Trans. Wireless Commun.*, vol. 9, no. 11, pp. 3380–3390, Nov. 2010.

21. X. Zhang, A. Ghrayeb, and M. Hasna, "On hierarchical network coding versus opportunistic user selection for two-way relay channels with asymmetric data rates," *IEEE Trans. Commun.*, vol. 61, no. 7, pp. 2900–2910, Jul. 2013.

22. M. Ju and I.-M. Kim, "Error performance analysis of BPSK modulation in physical layer network coded bidirectional relay networks," *IEEE Trans. Commun.*, vol. 58, no. 10, pp. 2770–2775, Oct. 2010.

23. R. Chang, S.-J. Lin, and W.-H. Chung, "Symbol and bit mapping optimization for physical-layer network coding with pulse amplitude modulation," *IEEE Trans. Wireless Commun.*, vol. 12, no. 8, pp. 3956–3967, Aug. 2013.

24. L. Song, "Relay selection for two-way relaying with amplify-and-forward protocols," *IEEE Trans. Veh. Technol.*, vol. 60, no. 4, pp. 1954–1959, May 2011.

25. K.-S. Hwang, Y.-C. Ko, and M.-S. Alouini, "Performance analysis of two-way amplify and forward relaying with adaptive modulation over multiple relay network," *IEEE Trans. Commun.*, vol. 59, no. 2, pp. 402–406, Feb. 2011.

26. D. Gündüz, A. Yener, A. Goldsmith, and H. Poor, "The multi-way relay channel," in *Proc. IEEE ISIT*, Jul. 2009, pp. 339–343.

27. L. Ong, G. Lechner, S. Johnson, and C. Kellett, "The three-user finite-field multi-way relay channel with correlated sources," *IEEE Trans. Commun.*, vol. 61, no. 8, pp. 3125–3135, Aug. 2013.

28. L. Ong, S. J. Johnson, and C. M. Kellett, "An optimal coding strategy for the binary multi-way relay channel," *IEEE Commun. Lett.*, vol. 14, no. 4, pp. 330–332, Apr. 2010.

29. R. Timo, G. Lechner, L. Ong, and S. Johnson, "Multi-way relay networks: Orthogonal uplink, source-channel separation and code design," *IEEE Trans. Commun.*, vol. 61, no. 2, pp. 753–768, Feb. 2013.

30. S. Sharifian, B. Hashemitabar, and T. Gulliver, "Improved throughput physical-layer network coding in multi-way relay channels with binary signaling," *IEEE Wireless Commun. Lett.*, vol. 2, no. 1, pp. 30–33, Feb. 2013.

31. S. N. Islam, P. Sadeghi, and S. Durrani, "Error performance analysis of decode-and-forward and amplify-and-forward multi-way relay networks with binary phase shift keying modulation," *IET Commun.*, vol. 7, no. 15, pp. 1605–1616, Oct. 2013.

32. S. N. Islam and P. Sadeghi, "Error propagation in a multi-way relay channel," in *Proc. IEEE ICSPCS*, Dec. 2011, pp. 1–8.

33. S. N. Islam, S. Durrani, and P. Sadeghi, "A novel user pairing scheme for functional decode-and-forward multi-way relay network," *Physical Communication*, Sep. 2014, submitted. [Online]. Available: http://arxiv.org/abs/1402.6422v3

34. S. N. Islam, S. Durrani, and P. Sadeghi, "Lattice code based multi-way relay networks: Ser analysis and the impact of imperfect channel estimation," *Journal of Communications and Networks*, May. 2015, submitted.

35. S. Islam and P. Sadeghi, "Joint decoding: Extracting the correlation among user pairs in a multi-way relay channel," in *Proc. IEEE PIMRC*, Sep. 2012, pp. 54–59.

36. D. Gündüz, A. Yener, A. Goldsmith, and H. V. Poor, "The multi-way relay channel," *IEEE Trans. Inf. Theory*, vol. 59, no. 1, pp. 51–63, Jan. 2013.

37. S. N. Islam, P. Sadeghi, and S. Durrani, "A novel pairing scheme to reduce error propagation in an amplify and forward multi-way relay network," in *Proc. IEEE SSP*, Jun. 2014, pp. 544–547.

38. S. Islam and P. Sadeghi, "Joint user decoding: A technique to enhance the benefits of coding in a multi-way relay channel," in *Proc. IEEE ICSPCS*, Dec. 2012, pp. 1–7.

39. S. Islam, "Optimal user pairing to improve the sum rate of a pairwise AF multi-way relay network," *IEEE Wireless Commun. Lett.*, vol. PP, no. 99, 2015.

40. R. Ahlswede, N. Cai, S.-Y. Li, and R. Yeung, "Network information flow," *IEEE Trans. Inf. Theory*, vol. 46, no. 4, pp. 1204–1216, Jul. 2000.

41. S. Katti, H. Rahul, W. Hu, D. Katabi, M. Médard, and J. Crowcroft, "XORs in the air: Practical wireless network coding," in *Proc. ACM SIGCOMM*, 2006, pp. 243–254.

42. A. Dana, R. Gowaikar, R. Palanki, B. Hassibi, and M. Effros, "Capacity of wireless erasure networks," *IEEE Trans. Inf. Theory*, vol. 52, no. 3, pp. 789–804, Mar. 2006.

43. N. Lee and R. W. H. Jr., "Space-time physical-layer network coding," *IEEE J. Sel. Areas Commun.*, Mar. 2014, to appear. [Online]. Available: http://arxiv.org/abs/1405.0029

44. R. H. Y. Louie, Y. Li, and B. Vucetic, "Practical physical layer network coding for two-way relay channels: performance analysis and comparison," *IEEE Trans. Wireless Commun.*, vol. 9, no. 2, pp. 764–777, Feb. 2010.

45. T. Cui, T. Ho, and J. Kliewer, "Memoryless relay strategies for two-way relay channels," *IEEE Trans. Commun.*, vol. 57, no. 10, pp. 3132–3143, Oct. 2009.

46. M. Huang and J. Yuan, "Error performance of physical-layer network coding in multiple-antenna TWRC," *IEEE Trans. Veh. Technol.*, vol. 63, no. 8, pp. 3750–3761, Oct. 2014.

47. R. Wang and X. Yuan, "MIMO multiway relaying with pairwise data exchange: A degrees of freedom perspective," *IEEE Trans. Signal Process.*, vol. 62, no. 20, pp. 5294–5307, Oct. 2014.

48. L. Ong, S. J. Johnson, and C. M. Kellett, "Optimal coding functions for pairwise message sharing on finite-field multi-way relay channels," in *Proc. IEEE ICC*, Jun. 2014, pp. 1872–1877.

49. G. Amarasuriya, C. Tellambura, and M. Ardakani, "Multi-way MIMO amplify-and-forward relay networks with zero-forcing transmission," *IEEE Trans. Commun.*, vol. 61, no. 12, pp. 4847–4863, Dec. 2013.

50. M. Noori and M. Ardakani, "Optimal user pairing for asymmetric multi-way relay channels with pairwise relaying," *IEEE Commun. Lett.*, vol. 16, no. 11, pp. 1852–1855, Nov. 2012.

51. M. Noori and M. Ardakani, "On symbol mapping for binary physical-layer network coding with psk modulation," *IEEE Trans. Wireless Commun.*, vol. 11, no. 1, pp. 21–26, Jan. 2012.

52. M. Chen and A. Yener, "Multiuser two-way relaying: detection and interference management strategies," *IEEE Trans. Wireless Commun.*, vol. 8, no. 8, pp. 4296–4305, Aug. 2009.

53. M. Chen and A. Yener, "Power allocation for F/TDMA multiuser two-way relay networks," *IEEE Trans. Wireless Commun.*, vol. 9, no. 2, pp. 546–551, Feb. 2010.

54. W. Xu, X. Dong, and W.-S. Lu, "Joint precoding optimization for multiuser multi-antenna relaying downlinks using quadratic programming," *IEEE Trans. Commun.*, vol. 59, no. 5, pp. 1228–1235, May 2011.

55. H. Chung, N. Lee, B. Shim, and T. W. Oh, "Joint transceiver and relay beamforming design for multi-pair two-way relay systems," in *Proc. IEEE ICC*, Jun. 2012, pp. 3795–3799.

56. E. Yilmaz, R. Zakhour, D. Gesbert, and R. Knopp, “Multi-pair two-way relay channel with multiple antenna relay station,” in *Proc. IEEE ICC*, May 2010, pp. 1–5.

57. G. Amarasuriya, C. Tellambura, and M. Ardakani, “Performance analysis of pairwise amplify-and-forward multi-way relay networks,” *IEEE Wireless Commun. Lett.*, vol. 1, no. 5, pp. 524–527, Oct. 2012.

58. M. Noori, H. Bagheri, and M. Ardakani, “Low-latency data sharing in erasure multi-way relay channels,” *IEEE Trans. Commun.*, vol. 61, no. 10, pp. 4161–4172, Oct. 2013.

59. L. Ong, C. M. Kellett, and S. J. Johnson, “On the equal-rate capacity of the AWGN multiway relay channel,” *IEEE Trans. Inf. Theory*, vol. 58, no. 9, pp. 5761–5769, Sep. 2012.

60. L. Ong, S. J. Johnson, and C. M. Kellett, “The capacity region of multi-way relay channels over finite fields with full data exchange,” *IEEE Trans. Inf. Theory*, vol. 57, no. 5, pp. 3016–3031, May 2011.

61. G. Wang, W. Xiang, and J. Yuan, “Outage performance for compute-and-forward in generalized multi-way relay channels,” *IEEE Commun. Lett.*, vol. 16, no. 12, pp. 2099–2102, Dec. 2012.

62. B. Nazer and M. Gastpar, “Compute-and-forward: Harnessing interference through structured codes,” *IEEE Trans. Inf. Theory*, vol. 57, no. 10, pp. 6463–6486, Oct. 2011.

63. T. Cover and A. Gamal, “Capacity theorems for the relay channel,” *IEEE Trans. Inf. Theory*, vol. 25, no. 5, pp. 572–584, Sep. 1979.

64. A. Amah and A. Klein, “Non-regenerative multi-way relaying: Space-time analog network coding and repetition,” *IEEE Commun. Lett.*, vol. 15, no. 12, pp. 1362–1364, Dec. 2011.

65. S. Sharifian, B. Hashemitabar, and T. Gulliver, “Performance of complex field network coding in multi-way relay channels,” *IEEE Trans. Wireless Commun.*, vol. 13, no. 6, pp. 3100–3112, Jun. 2014.

66. S. Sharifian, B. Hashemitabar, and T. Gulliver, “QAM constellation design for complex field network coding in multi-way relay channels,” *IEEE Wireless Commun. Lett.*, vol. 2, no. 5, pp. 483–486, Oct. 2013.

67. R. R. Borujeny, M. Noori, and M. Ardakani, “On the achievable rates of pairwise multiway relay channels,” in *Proc. IEEE ISIT*, Jun. 2014, pp. 2714–2718.

68. U. Erez and R. Zamir, “Achieving 1/2 log (1+SNR) on the AWGN channel with lattice encoding and decoding,” *IEEE Trans. Inf. Theory*, vol. 50, no. 10, pp. 2293–2314, Oct. 2004.

69. C. Feng, D. Silva, and F. Kschischang, “An algebraic approach to physical-layer network coding,” *IEEE Trans. Inf. Theory*, vol. 59, no. 11, pp. 7576–7596, Nov. 2013.

70. R. Zamir, S. Shamai, and U. Erez, “Nested linear/lattice codes for structured multiterminal binning,” *IEEE Trans. Inf. Theory*, vol. 48, no. 6, pp. 1250–1276, Jun. 2002.

71. B. Nazer and M. Gastpar, “Lattice coding increases multicast rates for Gaussian multiple-access networks,” in *Proc. 45th Ann. Allerton Conf. Commun., Contr. Comput*, Sep. 2007.

72. M. Wilson, K. Narayanan, H. Pfister, and A. Sprintson, “Joint physical layer coding and network coding for bidirectional relaying,” *IEEE Trans. Inf. Theory*, vol. 56, no. 11, pp. 5641–5654, Nov. 2010.

73. W. Nam, S.-Y. Chung, and Y. H. Lee, “Capacity of the Gaussian two-way relay channel to within 1/2 bit,” *IEEE Trans. Inf. Theory*, vol. 56, no. 11, pp. 5488–5494, Nov. 2010.

74. W. Nam, S.-Y. Chung, and Y. H. Lee, "Nested lattice codes for Gaussian relay networks with interference," *IEEE Trans. Inf. Theory*, vol. 57, no. 12, pp. 7733–7745, Dec. 2011.

75. Y. Ma, T. Huang, J. Li, J. Yuan, Z. Lin, and B. Vucetic, "Novel nested convolutional lattice codes for multi-way relaying systems over fading channels," in *Proc. IEEE WCNC*, Apr. 2013, pp. 2671–2676.

76. T. Huang, J. Yuan, and Q. Sun, "Opportunistic pair-wise compute-and-forward in multi-way relay channels," in *Proc. IEEE ICC*, Jun. 2013, pp. 4614–4619.

77. B. Jiang, F. Gao, X. Gao, and A. Nallanathan, "Channel estimation and training design for two-way relay networks with power allocation," *IEEE Trans. Wireless Commun.*, vol. 9, no. 6, pp. 2022–2032, Jun. 2010.

78. X. Xie, M. Peng, B. Zhao, W. Wang, and Y. Hua, "Maximum a posteriori based channel estimation strategy for two-way relaying channels," *IEEE Trans. Wireless Commun.*, vol. 13, no. 1, pp. 450–463, Jan. 2014.

79. F. Gao, R. Zhang, and Y.-C. Liang, "Optimal channel estimation and training design for two-way relay networks," *IEEE Trans. Commun.*, vol. 57, no. 10, pp. 3024–3033, Oct. 2009.

80. F. Tabataba, P. Sadeghi, C. Hucher, and M. Pakravan, "Impact of channel estimation errors and power allocation on analog network coding and routing in two-way relaying," *IEEE Trans. Veh. Technol.*, vol. 61, no. 7, pp. 3223–3239, Sept. 2012.

81. A. Panah and R. Heath, "MIMO two-way amplify-and-forward relaying with imperfect receiver CSI," *IEEE Trans. Veh. Technol.*, vol. 59, no. 9, pp. 4377–4387, Nov. 2010.

82. Y. Jia and A. Vosoughi, "Outage probability and power allocation of two-way amplify-and-forward relaying with channel estimation errors," *IEEE Trans. Wireless Commun.*, vol. 11, no. 6, pp. 1985–1990, June 2012.

83. L. Yang, K. Qaraqe, E. Serpedin, and M.-S. Alouini, "Performance analysis of amplify-and-forward two-way relaying with co-channel interference and channel estimation error," *IEEE Trans. Commun.*, vol. 61, no. 6, pp. 2221–2231, June 2013.

84. J. Zhang and M. Gursoy, "An achievable rate region for imperfectly-known two-way relay fading channels," in *Proc. IEEE ISIT*, Jul. 2011, pp. 94–98.

85. J. Zhao, M. Kuhn, A. Wittneben, and G. Bauch, "Self-interference aided channel estimation in two-way relaying systems," in *Proc. IEEE GLOBECOM*, Nov. 2008, pp. 1–6.

86. T.-H. Pham, Y.-C. Liang, A. Nallanathan, and G. Krishna, "On the design of optimal training sequence for bi-directional relay networks," *IEEE Signal Process. Lett.*, vol. 16, no. 3, pp. 200–203, Mar. 2009.

87. S. Abdallah and I. N. Psaromiligkos, "Blind channel estimation for amplify-and-forward two-way relay networks employing M-PSK modulation," *IEEE Trans. Signal Process.*, vol. 60, no. 7, pp. 3604–3615, Jun. 2012.

88. S. Abdallah and I. Psaromiligkos, "Semi-blind channel estimation with superimposed training for ofdm-based AF two-way relaying," *IEEE Trans. Wireless Commun.*, vol. 13, no. 5, pp. 2468–2467, May 2014.

89. M. Chen and A. Yener, "Power allocation for multi-access two-way relaying," in *Proc. IEEE ICC*, Jun. 2009, pp. 1–5.

90. A. Vosoughi and Y. Jia, "How does channel estimation error affect average sum-rate in two-way amplify-and-forward relay networks?" *IEEE Trans. Wireless Commun.*, vol. 11, no. 5, pp. 1676–1687, May 2012.

91. C. Wang, T.-K. Liu, and X. Dong, "Impact of channel estimation error on the performance of amplify-and-forward two-way relaying," *IEEE Trans. Veh. Technol.*, vol. 61, no. 3, pp. 1197–1207, Mar. 2012.

92. Z. Zhao, Z. Ding, M. Peng, W. Wang, and K. K. Leung, "A special case of multi-way relay channel: When beamforming is not applicable," *IEEE Trans. Wireless Commun.*, vol. 10, no. 7, pp. 2046–2051, Jul. 2011.

93. Y. Song and N. Devroye, "Lattice codes for the Gaussian relay channel: Decode-and-forward and compress-and-forward," *IEEE Trans. Inf. Theory*, vol. 59, no. 8, pp. 4927–4948, Aug. 2013.

94. O. Ordentlich, U. Erez, and B. Nazer, "The approximate sum capacity of the symmetric Gaussian *k*-user interference channel," *IEEE Trans. Inf. Theory*, vol. 60, no. 6, pp. 3450–3482, Jun. 2014.

95. M. Nokleby and B. Nazer, "Amplify-and-compute: Function computation over layered networks," in *Proc. IEEE ISIT*, Jul. 2013, pp. 2314–2318.

96. Y. Tian and A. Yener, "Degrees of freedom for the MIMO multi-way relay channel," *IEEE Trans. Inf. Theory*, vol. 60, no. 5, pp. 2495–2511, May 2014.

97. T. M. Cover and J. A. Thomas, *Elements of Information Theory*. Wiley, 1991.

98. T. Cui and J. Kliewer, "Memoryless relay strategies for two-way relay channels: Performance analysis and optimization," in *Proc. IEEE ICC*, May 2008, pp. 1139–1143.

99. M. K. Simon and M.-S. Alouini, *Digital Communication over Fading Channels*. Wiley, 2000.

100. F. Tabataba, P. Sadeghi, and M. Pakravan, "Outage probability and power allocation of amplify and forward relaying with channel estimation errors," *IEEE Trans. Wireless Commun.*, vol. 10, no. 1, pp. 124–134, Jan. 2011.

101. G. Kramer, M. Gastpar, and P. Gupta, "Cooperative strategies and capacity theorems for relay networks," *IEEE Trans. Inf. Theory*, vol. 51, no. 9, pp. 3037–3063, Sep. 2005.

102. O. Amin, S. Ikki, and M. Uysal, "On the performance analysis of multirelay cooperative diversity systems with channel estimation errors," *IEEE Trans. Veh. Technol.*, vol. 60, no. 5, pp. 2050–2059, Jun. 2011.

103. C. Patel and G. Stuber, "Channel estimation for amplify and forward relay based cooperation diversity systems," *IEEE Trans. Wireless Commun.*, vol. 6, no. 6, pp. 2348–2356, Jun. 2007.

104. B. Hassibi and B. Hochwald, "How much training is needed in multiple-antenna wireless links?" *IEEE Trans. Inf. Theory*, vol. 49, no. 4, pp. 951–963, 2003.

105. K. Pappi, G. Karagiannidis, and R. Schober, "How sensitive is compute-and-forward to channel estimation errors?" in *Proc. IEEE ISIT*, Jul. 2013, pp. 3110–3114.

106. A. Nasir, H. Mehrpouyan, S. Durrani, S. Blostein, R. Kennedy, and B. Ottersten, "Transceiver design for distributed stbc based af cooperative networks in the presence of timing and frequency offsets," *IEEE Trans. Signal Process.*, vol. 61, no. 12, pp. 3143–3158, Jun. 2013.

107. L. Lu and S.-C. Liew, "Asynchronous physical-layer network coding," *IEEE Trans. Wireless Commun.*, vol. 11, no. 2, pp. 819–831, Feb. 2012.

108. X. Zhou, P. Sadeghi, T. A. Lamahewa, and S. Durrani, "Design guidelines for training-based mimo systems with feedback," *IEEE Trans. Signal Process.*, vol. 57, no. 10, pp. 4014–4026, Oct. 2009.

109. C. Hausl, O. Iscan, and F. Rossetto, "Resource allocation for asymmetric multi-way relay communication over orthogonal channels," *EURASIP Journal on Wireless Communications and Networking*, vol. 2012, no. 20, pp. 1–12, 2012.